NCDOT

*Final Report*

# Median Barrier Placement on Six-lane, 46-foot Median Divided Freeways

Prepared By

Howie Fang
Ning Li
Ning Tian

The University of North Carolina at Charlotte
Department of Mechanical Engineering & Engineering Science
Charlotte, NC 28223-0001

November 2010

**Technical Report Documentation Page**

| | | | |
|---|---|---|---|
| 1. Report No.<br>**FHWA/NC/2009-04** | 2. Government Accession No. | 3. Recipient's Catalog No. | |
| 4. Title and Subtitle<br>**Median Barrier Placement on Six-lane, 46-foot Median Divided Freeways** | | 5. Report Date<br>**November 2010** | |
| | | 6. Performing Organization Code | |
| 7. Author(s)<br>**Howie Fang, Ning Li, Ning Tian** | | 8. Performing Organization Report No. | |
| 9. Performing Organization Name and Address<br>**The University of North Carolina at Charlotte**<br>9201 University City Boulevard<br>Charlotte, NC 28223-0001 | | 10. Work Unit No. (TRAIS) | |
| | | 11. Contract or Grant No. | |
| 12. ***Sponsoring Agency Name and Address***<br>**North Carolina Department of Transportation**<br>**Research and Development Unit**<br>**1549 Mail Service Center**<br>**Raleigh, North Carolina 27601** | | 13. Type of Report and Period Covered<br>**Final Report**<br>**08/2008 – 11/2010** | |
| | | 14. Sponsoring Agency Code<br>**2009-04** | |
| Supplementary Notes: | | | |

16. Abstract


This report summarizes the research efforts of using finite element modeling and simulations to evaluate the performance of W-beam guardrails and cable median barriers on six-lane, 46-foot median divided freeways. A literature review is included on performance evaluation of W-beam guardrails and cable barriers as well as applications of finite element modeling and simulations in roadside safety research.

The three types of barriers evaluated in this project are the single-face W-beam, double-face W-beam (two designs), and generic low-tension cable barrier. All three types of barriers were evaluated at three impact speeds and three impact angles. Full-scale crash simulations were first performed on a single-face W-beam guardrail placed on the border of a 2.5:1 slope and the shoulder. Two designs of a double-face W-beam guardrail, which replaced the single-face W-beam at the same location, were then evaluated using simulations and compared to the single-face one. Finally, simulations were performed on vehicles impacting the cable median barrier placed on a 4:1 slope. The simulation results demonstrated the effects of sloped medians on vehicle redirection after contacting the cable median barriers or W-beam guardrails. A common issue for a sloped median is the increased potential of vehicle rollovers, particularly for large-size vehicles. The results will be used to update and validate the standard drawings and strategies for placement of median guardrails and cable barriers.

The use of finite element simulations is shown to be both effective and efficient, because they are nondestructive, repeatable, modifiable, and inexpensive. Furthermore, finite element simulations can be used to study crash scenarios that are impossible and/or extremely expensive to conduct physical crash testing. Finite element modeling and simulations are recommended for future investigations of other research issues.


| | | | |
|---|---|---|---|
| 17. Key Words<br>Cable barrier; W-beam; Median barrier; Roadside safety; Highway safety; Finite element method | | 18. Distribution Statement | |
| 19. Security Classif. (of this report)<br>Unclassified | 20. Security Classif. (of this page)<br>Unclassified | 21. No. of Pages<br>121 | 22. Price |

**Form DOT F 1700.7** (8-72) **Reproduction of completed page authorized**

# DISCLAIMER

The contents of this report reflect the views of the authors and not necessarily the views of the university. The authors are responsible for the facts and the accuracy of the data presented herein. The contents do not necessarily reflect the official views or policies of either the North Carolina Department of Transportation or the Federal Highway Administration. This report does not constitute a standard, specification, or regulation.

# ACKNOWLEDGMENTS

This study was supported by the North Carolina Department of Transportation (NCDOT) under Project No. 2009-04. The authors would like to thank NCDOT personnel from the *Roadway Design Unit*, *Division of Transportation Mobility & Safety*, *Highway Division 5*, *FHWA – NC Division*, and the *Research and Development Unit* for their support and cooperation during the grant period.

# EXECUTIVE SUMMARY

This report summarizes the research efforts of using finite element modeling and simulations to evaluate the performance of W-beam guardrails and generic low-tension cable median barriers (CMBs) on six-lane, 46-foot median divided freeways. A literature review is included on performance evaluation of W-beam guardrails and CMBs as well as applications of finite element modeling and simulations in roadside safety research. Full-scale crash simulations were performed on a single-face W-beam, two designs of double-face W-beam and a CMB under three impact speeds and three impact angles.

The results of finite element simulations showed that the single-face W-beam guardrail met the Test Level 3 (TL-3) requirements of the NCHRP Report 350, even on a 2.5:1 sloped median. At higher impact speeds and/or angles, vehicle rollover could occur with the single-face W-beam. The two designs of the double-face W-beam guardrail performed similarly to the single-face one in front-side impacts. In backside impacts, the two double-face W-beams were found to be able to redirect/retain the vehicle at all impact speeds and angles evaluated in this project. There was no significant performance difference between the two designs of the double-face W-beam.

Simulations were also performed on vehicles impacting the CMB placed on the 4:1 slope. The results of backside impacts showed that the vehicle would not land on top of the CMB; rather, it would impact the CMB right after or at the same time landing on the 4:1 slope. It was observed that the CMB could redirect the vehicle in most cases, but it was followed by vehicle rollovers except for the case of 25° backside impact at 62 mph (100 km/hr). The use of finite element simulations was shown to be both effective and efficient. Finite element modeling and simulations are recommended in future investigations of other research issues such as the placement of CMBs on 4:1 sloped medians.

# TABLE OF CONTENTS

## List of Tables

## List of Figures

# 1. Introduction

Median-involved crashes on high-speed, divided highways are predominately severe events in terms of injury severity, property damage, traffic impact, and the magnitude and duration of response required (BMI-SG 2004). Median barriers can be used to effectively prevent vehicles leaving the roadway from crossing the median and colliding with vehicles traveling in the opposite direction. Despite the dramatic increase in traffic volumes, the fatal crash rate on U.S. highways is only 20% of what it was 40 years ago. Part of the reason is attributed to the use of roadside barrier systems.

Over the years, different types of barriers have been developed and are classified into three categories: rigid, semi-rigid, and flexible systems. While all barriers serve the purpose of safely redirecting errant vehicles and preventing them from intruding into the oncoming traffic, they differ from each other in applicable site conditions as well as in their effects on impacting vehicles. Figure 1.1 shows several commonly used barrier systems including concrete barriers, W-beam and thrie-beam guardrails, and cable barriers.

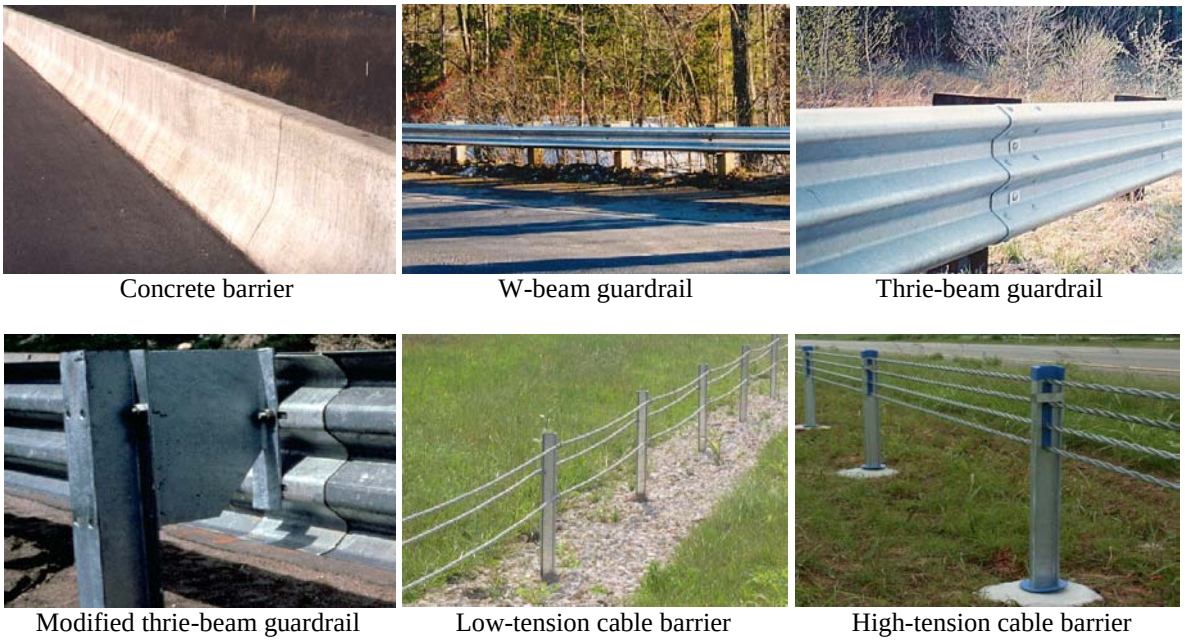


Fig. 1.1: Commonly used barrier systems.

Concrete barriers belong to the rigid category and have high initial cost yet require less maintenance; however, they are less forgiving in severe crashes. W-beam, thrie-beam, and modified thrie-beam guardrails are semi-rigid barriers that are more forgiving (or having less impact forces) but have larger deflections than concrete barriers. Cable barriers are flexible systems that are cost-effective and ideally suitable for retrofit designs on existing, relatively wide medians. Cable barriers are more forgiving then concrete barriers and W-beam guardrails, because the cables deflect laterally to absorb energy and reduce impact forces transmitted to the vehicle and occupants. The high flexibility of cable barriers, however,

requires the median to have sufficient width to allow for lateral deflections. For a single-run cable median barrier (CMB), the median is required to have a minimum width of 24 ft (7.32 m), with 12 ft (3.66 m) on each side of the barrier (AASHTO 2006).

## 1.1 Background

All barriers installed on U.S. highways are designed according to the Roadside Design Guide by the American Association of State Highway and Transportation Officials (AASHTO) (2006) and must be tested to satisfy the safety requirements specified by the NCHRP Report 350 (Ross et al. 1993), which was recently superseded by the new standard, Manual for Assessing Safety Hardware (MASH) (2009). However, the performance of in-service barrier systems may be different from those tested by the NCHRP Report 350 or MASH due to specific site conditions such as median slopes, superelevations, horizontal curvatures, etc. To this end, performance evaluation of in-service barriers for a given site condition is necessary for safety assurance.

According to the design specifications of the North Carolina Department of Transportation (NCDOT), forty-six feet is the minimum median width used for freeways without a concrete median barrier. It is the typical width used for non-freeway divided facilities on new location, and the standard median width used when widening existing two-lane roadways to a four-lane divided facility (NCDOT 2002). The median is required to have two 6-ft (1.83-m) shoulders and a 6:1 ditch slope. This 6:1 slope has been accepted as the desired slope to place CMBs and is the typical median condition for placing CMBs in North Carolina. Crash data collected in previous NCDOT projects on safety evaluations showed that cross median penetrations were reduced to 3.6% after the installation of CMBs (Troy 2007). This low penetration rate indicated that these median barrier treatments have resulted in a significant safety improvement by reducing the number of freeway head-on collisions.

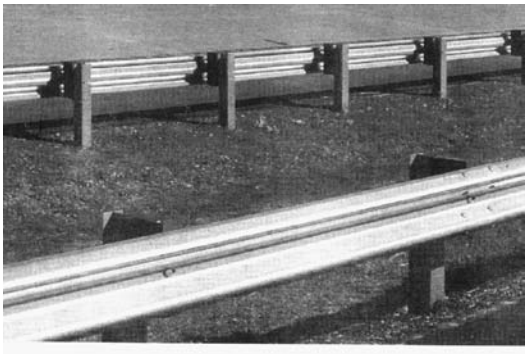

Fig. 1.2: Two lines of the single-face W-beam guardrail on a six-lane divided freeway.

For six-lane, 46-foot median divided freeways, the paved shoulder policy requires two 12-ft (3.66-m) median shoulders, which reduce the width of ditch from 34 ft (10.4 m) to 22 ft (6.7 m). For positive pavement drainage consideration, the median slopes should be changed to 4:1, which exceeds the optimal 6:1 slope for placing CMBs. As a practical solution, design engineers often place two lines of W-beam guardrail on the median shoulders (Fig. 1.2). While preventing cross-median crashes, the two lines of guardrail create great difficulty for vegetation maintenance operations (e.g. mowing). NCDOT engineers indicated that there was a strong need to

Fig. 1.3: A double-face W-beam guardrail.

investigate the possibility of placing a single line, double-face W-beam (Fig. 1.3) or other systems that would be at least equally safe as the current two-line system.

Another major concern on the six-lane, 46-foot median divided freeways is in areas with horizontal curves where superelevation is introduced. With two 12-ft (3.66-m) median shoulders, the median ditch slope may be required to exceed 4:1 on the high side of a horizontal curve. Figure 1.4 shows the typical placement of two lines of W-beam on a median with 2.5:1 and 4:1 ditch slopes. On this type of medians where cable barriers are used, the current placement is to set CMB at eight feet from the ditch centerline on the 4:1 slope as shown in Fig. 1.5 (NCDOT 2006). This treatment, however, has not been fully tested and thus deserves further investigation. The effects of median barriers on steeper slopes (e.g., 4:1 or 2.5:1) remain unknown and no guidelines are currently available.

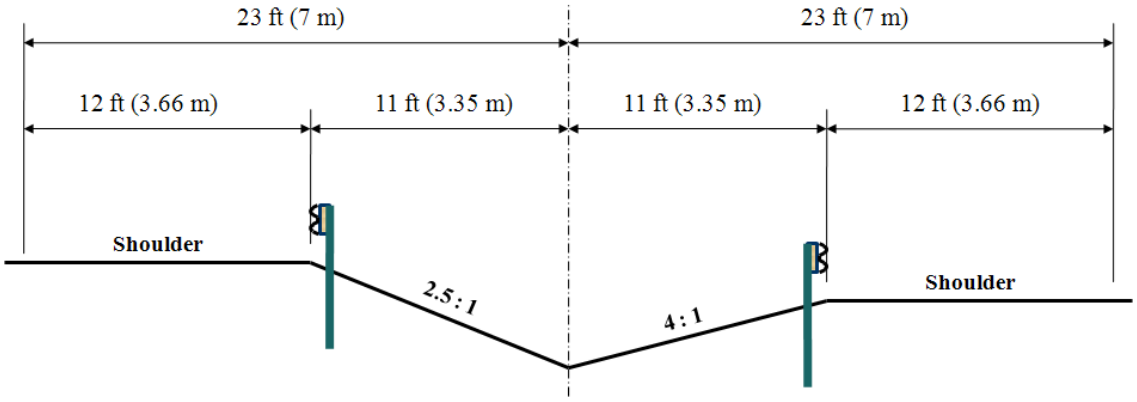


Fig. 1.4: Placement of two lines of W-beams on a 46-foot median with superelevation.

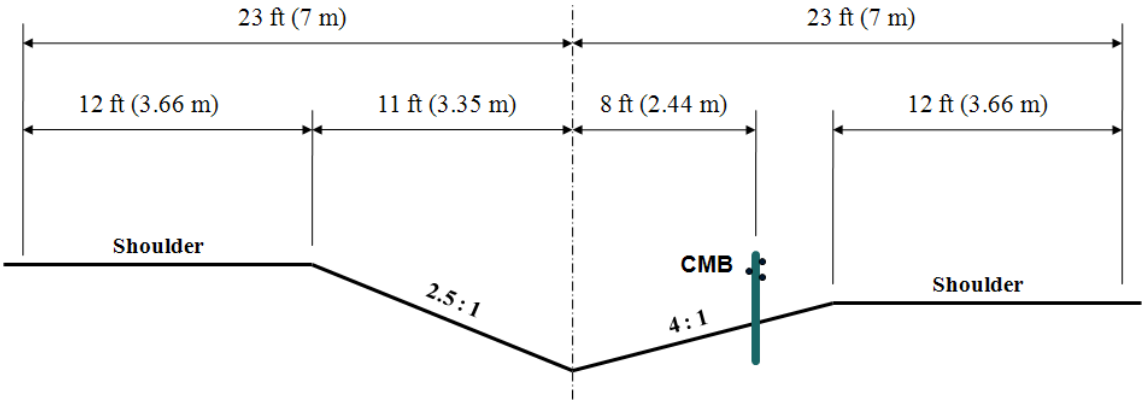


Fig. 1.5: Placement of the CMB on the 4:1 slope of a 46-foot median with superelevation.

With the rapid development of computer technology and parallel numerical codes, it is now possible to perform full-scale finite element (FE) simulations of vehicle crashes using commercial software such as LS-DYNA (LSTC 2007). Crash simulations using FE analysis are being increasingly used to design new roadside safety devices and evaluate the safety performance of current systems under different site and impact conditions. One particular benefit of using simulations is that we can assess the performance limits of roadside devices under conditions that full-scale physical crashing testing cannot be readily performed.

In this project, full-scale FE simulations were utilized to determine the feasibility of using a single line of double-face W-beam guardrail to replace the two lines of single-face W-beam. FE simulations were also used to evaluate the performance of a generic low-tension CMB placed on six-lane, 46-foot median divided freeways. Vehicle-barrier impacts were simulated under different combinations of impact speeds and angles.

## 1.2 Research Objectives and Tasks

The objectives of this project were to use full-scale FE simulations to: 1) investigate the placement of a single line of double-face W-beam guardrail on a six-lane, 46-foot median divided freeway with superelevation; and 2) evaluate the performance of a generic low-tension CMB placed eight feet from the ditch centerline on the 4:1 slope of a six-lane, 46-foot median divided freeway.

Full-scale FE simulations were employed as the major tool for evaluating the performance of the single-face W-beam, double-face W-beam, and the CMB on sloped medians. The following is a summary of the five major tasks for this project.

Task 1: Literature Review and Data Collection

The objective of this task was to review literature on crash testing, modeling, and simulations that were particularly related to W-beam guardrails and CMBs to assist model validation and crash simulations. Literature on median barrier placement with superelevation were also collected and reviewed. The following sources were used in literature search:

- AASHTO Technology Implementation Group (TIG) on CMBs
- Midwest Roadside Safety Facility (MwRSF)
- National Cooperative Highway Research Program (NCHRP) ongoing projects
- National Crash Analysis Center (NCAC)
- State DOT research reports
- Texas Transportation Institute (TTI)
- Transportation Research Board Roadside Safety Committee website
- Transportation Research Information Services (TRIS)
- Transportation Research Record (TRR) and other technical journals
- Worcester Polytechnic Institute (WPI)

Task 2: Finite Element Simulations of Single-face W-beam

In this task, the FE model of a single-face W-beam developed at NCAC was used to create the single-face W-beam according to NCDOT specifications. The FE model of a 2006 Ford F250 also developed at NCAC was validated and used in evaluating the performance of the single-face W-beam. These two FE models are shown in Fig. 1.6.

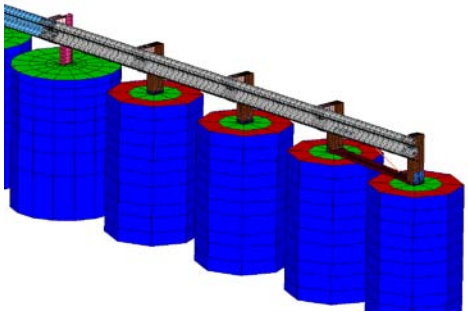

W-beam guardrail

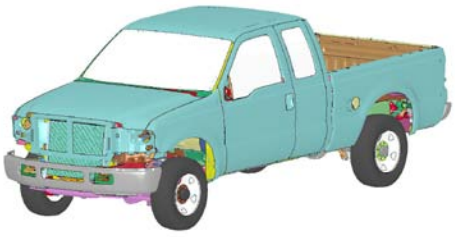

2006 Ford F250

Fig. 1.6: Finite element models of a single-face W-beam and a passenger truck.

For the single-face W-beam guardrail, only front-side impacts were simulated, because the results of preliminary simulations showed that, after impacting one line of the single-face W-beam, the vehicle did not reach and impact the other line from the backside (see Fig. 1.4 for the placement of the two lines of single-face W-beam). However, simulations of the single-face W-beam on both the 2.5:1 slope (or high-side) and 4:1 slope (or low-side) were performed, as shown in Fig. 1.7.

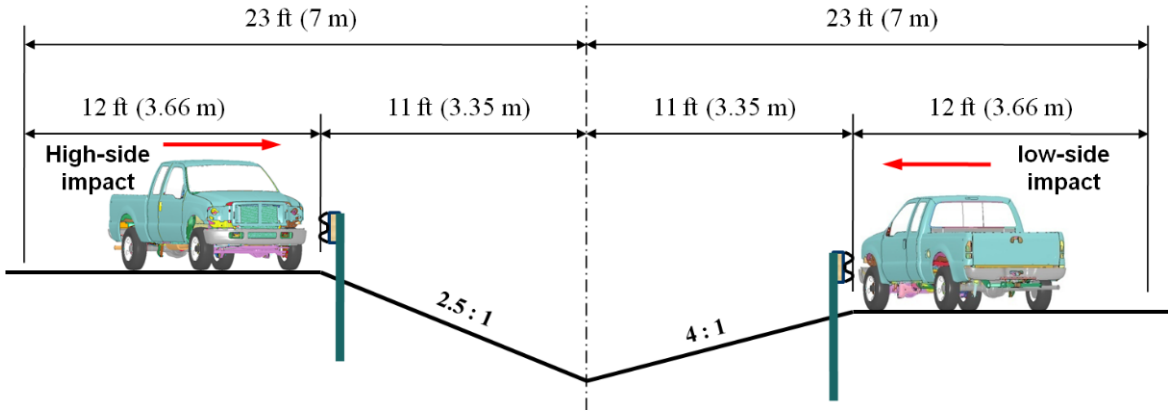


Fig. 1.7: Vehicle impacts with two lines of the single-face W-beam on a 46-foot median.

The standard impact condition of 62 mph (100 km/hr) at 25º specified by the NCHRP Report 350 was first used. FE simulations were then performed at higher impact speeds, 70 and 75 mph (112.6 and 120.7 km/hr), and larger angles, 30º and 35º. The FE models were also validated in this task to improve the numerical stability of the simulations. Simulation results of the single-face W-beam were used as a baseline to evaluate the performance of the double-face W-beam.

Task 3: Investigation of Placement of Double-face W-beam

The FE models of two designs of the double-face W-beam were generated in this task and evaluated under both front-side and backside impacts by the Ford F250 (see Fig. 1.8).

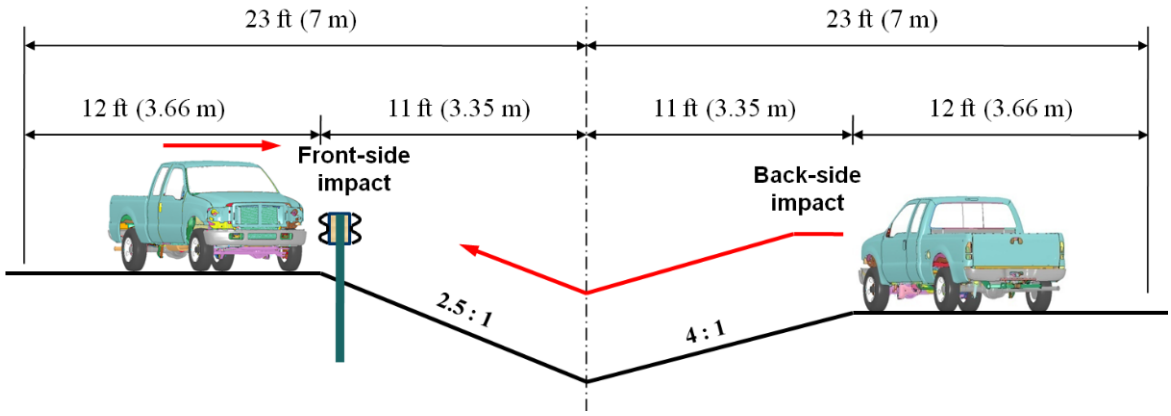


Fig. 1.8: Front-side and backside impacts with the double-face W-beam on a 46-foot median.

In the first design of the double-face W-beam, the backside rail was placed at the same height as front-side rail. The height of the backside rail was lowered in the second design based on the engineering practice in other states. Both designs of the double-face W-beam were evaluated under the same impact conditions as those used for the single-face W-beam. The performance of the two double-face W-beam guardrails was evaluated and compared, and both designs were compared to the single-face W-beam.

Task 4: Performance Evaluation of CMBs

The performance of the CMB on a six-lane, 46-foot median divided freeway with superelevation was evaluated in this Task. The CMB was placed eight feet from the centerline on the low side of the median (with a 4:1 ditch slope), as shown in Fig. 1.9. There was a strong concern on situations in which the vehicles left the high-side shoulder and impact the CMB from the backside. In these cases, there was a possibility that the vehicle might override (i.e., land on top of) the CMB and cause a straight-through penetration.

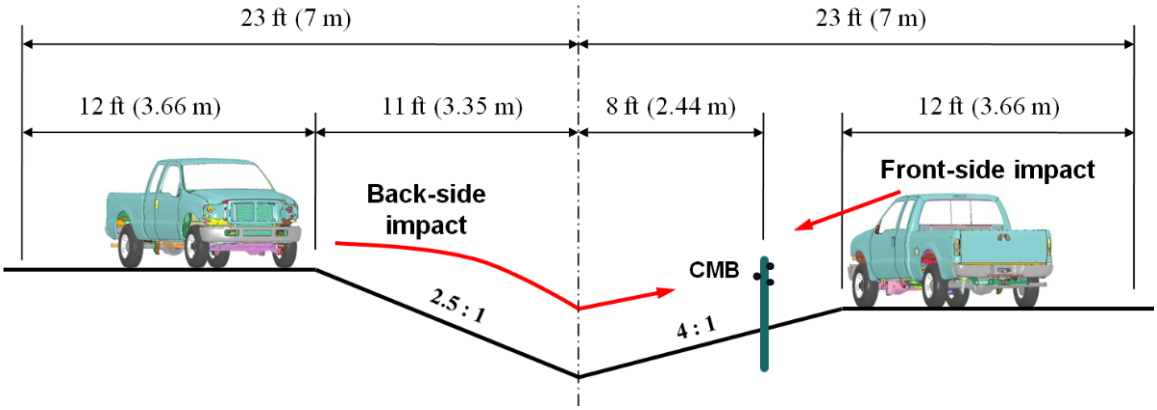


Fig. 1.9: Front-side and backside impacts with the CMB on a 46-foot median.

The simulation model of the CMB was taken from NCDOT Research Project 2008-10, "*Finite Element Evaluation of Two Retrofit Options to Enhance the Performance of Cable Median Barriers*." Due to the change of median slopes, i.e. from 6:1 to 4:1 and 2.5:1, the vehicle-barrier impact simulations were re-run to obtain the CMB performance under the

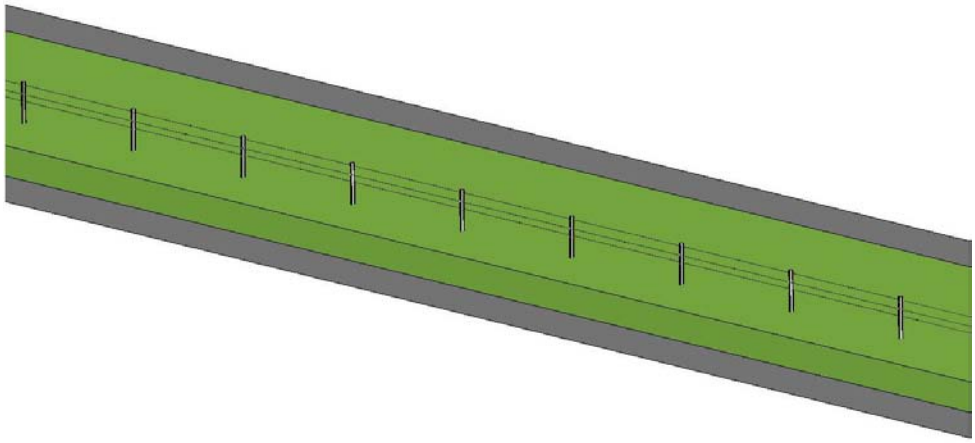

Fig. 1.10: Finite element model of an NCDOT CMB.

median conditions. In addition, simulations in project NCDOT 2008-10 on the current design of NCDOT CMBs were mainly based on a 1996 Dodge Neon model, which was much smaller than the Ford F250 used in this project.

In this task, both front-side and backside impacts were simulated under three impact speeds, 62, 70 and 75 mph (100, 112.6 and 120.7 km/hr), and three impact angles, 25º, 30º and 35º. There were a total of 18 simulations, nine for front-side and nine for backside impacts.

Task 5: Final Report

This final report provides a comprehensive summary of research activities, findings, and outcomes for this project. It synthesizes literature review, FE modeling efforts, simulation results, a recommended guideline for the placement of double-face W-beams, if deemed feasible, and the performance evaluation of CMBs placed on six-lane, 46 foot median divided freeways with superelevation.

# 2. Literature Review

Median barriers have been developed and used on U.S. highway for decades. Presently, the W-beam guardrails and cable barriers are widely used across the U.S. In this section, we provide a comprehensive summary of studies related to W-beams guardrail, CMBs, and other barrier systems. The topics cover performance evaluation (in-service and crash testing) and the application of FE modeling and simulations to highway safety research.

## 2.1 Performance Evaluation of Median Barriers

Early in the 1960's, New York State pioneered the development of weak-post barrier systems through analytical models and full-scale vehicle crash testing. In 1965, the state guardrail and median barrier standards were changed to include only weak-post barriers. In the early 1970's, a study by Zweden and Bryden (1977) was performed to evaluate the field performance of the older strong-post barriers and newly developed weak-post barriers based on New York State accident data collected from 1967 to 1970. Statistical analysis was performed to compare the performance of the investigated barriers based on occupant injury, vehicular responses, and after impact maintenance. This study generated a number of significant conclusions on the performance of weak- and strong-post barriers. Although there was no significant difference in fatality rates between the two barriers, weak-post barriers exhibited a combined fatality/serious injury rate significantly lower than that for strong-post barriers. The resulting occupant injury appeared to be linked to barrier stiffness since the two barriers (both strong and weak post versions) had lower injury severity rates, while the stiffer median barriers had the highest injury rates. With respect to barrier penetration, the weak-post barriers demonstrated a lower penetration rate than the strong-post barriers (with the exception of the W-beam), which may be due to the lack of consistency between early strong-post barrier designs. The study also indicated that barrier penetrations for the weak-post systems typically resulted from a low rail height. Barrier end terminals (first or last 50 feet of the barrier) were observed to have higher penetration rates than their midsection counterparts and resulted in higher serious injury rates. Barrier damage was linked to their stiffness; however, weak-post barriers on average were less expensive to repair than strong-post barriers despite the former's longer damage lengths.

In the early 1980's, there were significant changes in vehicle designs that led to a significant increase in the number of smaller and lighter vehicles on highways. A study (Hiss and Bryden1992) was initiated in 1983 by the New York State DOT to determine how impact severity on traffic barriers was affected by vehicle sizes and weights, barrier types and mounting heights, and roadway features. Several conclusions were drawn regarding the performance of cable, W-beam, and box-beam guardrails. For example, injuries were found insensitive for cable guardrails to rail heights over 610 mm (24 in.). For cable and W-beam median barriers, however, the sample sizes were too small to assess their performance due to their limited use and exposure to possible accidents.

Ross et al. (1984) investigated the impact performance of longitudinal barriers when placed on sloped terrain using both crash tests and the highway vehicle object simulation model (HVOSM) computer program. In the study, they determined typical conditions to place longitudinal barriers on sloped terrain and evaluated the impact behavior of widely used

barrier systems. Guidelines were developed for the selection and placement of barriers on sloped terrain. It was found from the study that W-beam and thrie-beam barriers were more sensitive to the effects of sloped terrain than cable barriers.

In the study conducted by Ross et al. (1993), uniform procedures were developed for evaluating the safety performance of candidate roadside hardware, including longitudinal barriers, crash cushions, breakaway supports, truck-mounted attenuators and work zone traffic control devices. The report from this study, the NCHRP Report 350, has been adopted as the standard guideline for evaluating the safety performance of roadside safety devices. The evaluation of devices is facilitated through three main criteria: 1) structural adequacy; 2) occupant risk; and 3) post-impact trajectory. Structural adequacy refers to how well the device performs its intended task (i.e. a guardrail preventing a vehicle from striking a shielded object). The occupant risk criteria attempts to quantify the potential for severe occupant injury. The post-impact vehicle trajectory ensures that the device will not cause subsequent harm (i.e. a vehicle being redirected back into traffic). The guideline recognizes the infinite number of roadside hardware installations and crash configurations; therefore, standardized installation configurations and practical worst-case impact scenarios are used to provide a basis of comparing the performance of similar devices. Of particular note is the multi-service level concept that provides six different test levels to allow for more or less stringent performance evaluation (ideally depending on the ultimate usage/placement of the hardware).

With respect to cross-median crashes, the NCHRP Report 350 is the standard by which median barriers are tested. Although the report specifies six different test levels, the warrants for devices meeting an individual test level is outside the scope of the document and left to the judgment of the transportation agency implementing the hardware. Generally, however, devices tested to the lower test levels (1 and 2) are used on lower volume, lower speed roadways, while devices tested to higher levels (3 to 6) are typically used on larger volume, higher speed roadways. Note that the 2000P test vehicle is used to evaluate the strength and redirecting capabilities of longitudinal barriers up to and including test level 3. All impacts are performed at 25° and at 50, 70, and 100 km/hour for test levels 1, 2 and 3, respectively. This guideline is currently under revision by the FHWA.

In the early 1990's, the Traffic Engineering Branch of NCDOT conducted a study (Lynch et al. 1993) of accidents on North Carolina's interstate highways in which vehicles crossed the median and entered the opposing travel lanes. The study analyzed accidents that occurred during the time period from April 1, 1988 through October 31, 1991. The objectives of this study were to identify interstate locations with unusually high cross-median accidents, to determine possible safety improvements, to develop a priority listing of these locations with recommended improvements, and to develop a model for identifying potentially dangerous locations on North Carolina interstate highways. Data collected in the study showed that 751 cross-median crashes took place in North Carolina, resulting in 105 fatalities. These crashes represented three percent of total crashes but 32% of total fatalities on interstate highways during the study period. One of the outcomes of this study was the recommendation to construct median barriers at 24 sections of interstate highways in North Carolina.

In a subsequent safety study, Hunter et al. (2001) evaluated three-strand cable median barriers installed on a 14.5-km (9-mile) stretch on Interstate 40, a freeway in North Carolina. Data extracted from the Highway Safety Information System (HSIS) were from 1990 to 1997 and a before-after comparison was made by developing several regression models that used a reference population (e.g. all freeway locations without CMBs) to predict the number of accidents at the locations with CMB treatments. The predicted number of accidents was then compared to the actual number of collisions at sites with CMBs. Although a statistically significant increase was found in the total number of crashes on the sections after the installation of CMBs, a significant reduction was also found in the number of serious and fatal collisions. These safety studies by NCDOT "provided a great deal of momentum" towards the installation of more barriers in North Carolina (Stasburg and Crawley 2005), with three-strand cable barriers the most commonly used median barriers. North Carolina currently has approximately 885 km (550 miles) of low-tension CMBs, which has reduced the cross-median penetrations to 3.6% by year 2006 (Troy 2007). This low penetration rate indicated that these median barrier treatments have resulted in a significant safety improvement by reducing the number of freeway head-on collisions.

Following three fatalities from a cross-median accident in 1996, Oregon DOT installed a CMB system along sections of I-5 to reduce the potential of future occurrences. The study conducted by Sposito and Johnston (1999) evaluated the cost-effectiveness of this system at preventing cross-median crashes. Based on a comparison of frequency/severity data from pre- and post-barrier installation, the CMBs were found to reduce both the fatality rate and susceptibility to cross-median collisions. The study also indicated that minor accidents had increased from 0.7 to 3.8 injury accidents per year since the barrier installation. Based on a cost-analysis incorporating the maintenance cost, the annual cost of the CMBs was found to always be less than that of concrete median barriers. The report showed that the cost-effectiveness of CMBs for reducing cross-median crashes was in agreement with similar studies performed in North Carolina, Iowa, and New York.

In the early 1990's, the Washington DOT (WSDOT) became interested in installing the U.S. generic low-tension CMBs on medians wider than 9.75 m (32 ft). Subsequently, the WSDOT sponsored crash tests to evaluate the performance of this barrier system in accordance with the NCHRP Report 350 (Albin et al. 2001). In the first test (Bullard and Menges 1996), a 1991 Ford Festiva impacted the CMB at a speed of 62 mph (100 km/hr) and an angle of 20.4 degrees. In the second test (Bullard and Menges 2000), a 1995 Chevrolet 2500 pickup truck impacted the CMB at a speed of 101.3 km/hr (63 mph) and an angle of 24.8 degrees. In both tests, the vehicles were contained by the cables and brought to a stop with relatively minor damage; the occupant risk values were within the preferred limits set by the NCHRP Report 350 (Albin 2001).

Cable barriers in Washington State successfully restrained 95 percent of errant vehicles without involving a second vehicle (WSDOT 2006). In comparison, only 67 to 75 percent of crashes with W-beam guardrails and concrete barriers successfully restrained errant vehicles without involving a second vehicle. This means that vehicles striking concrete barriers and beam guardrails are more likely to involve a second vehicle in a collision and thus have higher risk of injury. Despite the statewide success of CMBs, however, the public had

significant concerns on the increasing number of crashes and cross-median collisions on I-5 in Marysville, WA. As a result, the WSDOT (2006) conducted a comprehensive review of traffic safety on I-5 in Marysville from 1999 through 2004. Researchers of this study found that these cross-median penetrations occurred where the cable barrier was placed within 1.52 m (5 ft) from the bottom of the ditch. The front suspensions were compressed when the vehicle traversed through the bottom of the ditch and continued up the slope. Consequently, the vehicle's front profile was lowered and unable to engage with the cables, particularly the bottom cable; this resulted in an under-riding on the CMB.

Following the investigation on I-5 in Marysville, the WSDOT installed a high-tension CMB system about 3.66 m (12 ft) from the southbound lanes and 0.61 m (2 ft) past the slope breakpoint. The existing low-tension CMBs (about 16 feet from the northbound lane) were also kept on this 12.2-m (40-ft) median. Unfortunately, on February 13, 2007, the two lines of CMBs failed to retain an errant SUV, which overrode the high-tension CMBs, penetrated the low-tension CMBs, and collided onto a charter bus traveling in the opposite direction (MacDonald and Batiste 2007). There are a number of reasons for the penetrations, including:

- Specific road conditions: transitioning from rural to urban surrounds, low congestion to higher congestion, higher speeds to lower speeds, and widely spaced interchanges to closely spaced interchanges
- Driver's high blood alcohol level (0.07, right below the 0.08 limit) and failure of braking before and during the impacts
- High vehicle bumper and high impact speed
- Placement of high-tension CMBs, which was 0.61 m (2 ft) from the slope breakpoint and effectively reduced the cable heights by 38.1 mm (1.5 in.)
- Mechanical failure of the anchor of the low-tension CMBs

While recommending the continuous use of CMBs, a few suggestions were also made for future research and/or further investigation including placement of CMBs on sloped medians and CMB anchor design (MacDonald and Batiste 2007).

On observation of cross-median collisions (CMCs) that happened where median barriers were not warranted by the Pennsylvania DOT design policy, Donnell et al. (2002) reviewed the methods used to assess median safety on interstates and expressways in Pennsylvania. A critical literature review and assessment of median safety practices in various state DOTs were conducted, and qualitatively assessed median safety practices were used to provide input for quantitative data collection. Negative binomial regression models were used to model CMC frequencies on earth-divided highways. The qualitative results from the study suggested that three-strand cable barriers, strong-post W-beam guardrail, or concrete barriers were recommended median barriers in appropriate site conditions. Quantitative results showed that CMCs were rare events and that nearly 15% involved fatalities and 72% involved nonfatal injuries. Additional findings included that CMC rates at earth-divided highways decreased as the median width increased, that CMCs appeared more likely to occur downstream of interchange entrance ramps, and that CMCs were more likely to involve adverse pavement surface conditions (wet or icy) than other crashes.

In a project funded by the New Jersey DOT, Gabler et al. (2005) evaluated the post-impact performance of two median barrier systems in New Jersey: a three-strand cable median barrier system and a modified thrie-beam median barrier system. FE modeling was adopted as a major means for the investigation. The project also included field investigation of crashes into the subject barriers and a survey of the median barrier experience of other state DOTs. This study concluded that three-strand cable barriers were capable of containing and redirecting passenger vehicles, that cable barriers were effective at reducing the incidence of cross-median collisions in wider medians, and that cable barriers reduced the overall collision severity despite typically increasing the total number of accidents.

Ray and McGinnis (1997) provided a synthesis of information regarding the use of guardrails and median barriers in the U.S. and their performance with respect to the testing standards specified by the NCHRP Report 350. Comprehensive background information is provided for the evolution of testing procedures, selection and placement procedures, and in-service evaluation of longitudinal and median barriers. The notable advantages of steel-post cable guiderails/median barriers, as indicated in the report, are their compliance to test level 3 of the NCHRP Report 350, inexpensive installation, minimized sight distance problems, reduced occupant forces in the event of a collision, and reduced snow drifting/accumulation. Disadvantages of this system include periodic monitoring of cable tension, a large clear area for barrier deflection, and increased barrier damage in the event of a collision.

Using data collected from Connecticut, Iowa, and North Carolina from 1997 to 1999, Ray and Weir (2001) performed an in-service performance evaluation of four guardrail systems: the G1 cable guiderail, G2 weak-post W-beam guardrail, and the G4(1S) and G4(1W) strong-post W-beam guardrails. The study particularly focused on estimating the number of unreported collisions and the true distribution of vehicle occupant injuries. The collision performance was measured in terms of collision characteristics, occupant injury, and barrier damage. Within the sample size limitations of the data collected in the study, no statistically significant difference was found on the performance of the guardrails in the three states, and there was no difference between the performance of G1 and G2 and between G1 and G4(1W). However, occupant injuries were found less common in collisions with a G1 cable guardrail than in collisions with G4(1S) or both G4 types combined.

Ray et al. (2003) reviewed literature on in-service evaluation studies and identified previously effective methods. The in-service performance of common barriers and terminals was examined by collecting data in the following three areas: crash, maintenance, and inventory information. A procedure manual for planning and conducting in-service evaluations of roadside hardware was developed based on the methods used and the lessons learned in the evaluation study. The manual was subsequently used as a guide for an in-service evaluation project performed in Washington State by a different research team and modified based on their experiences and recommendations.

In the work by Bligh and Mak (1999), they evaluated the crashworthiness of roadside features across vehicle platforms. The impact performances of roadside safety features are typically evaluated through full-scale crash testing with two vehicles selected from the extremes of the passenger vehicle fleet in terms of weight and size. The implicit assumption

was that if a roadside safety device successfully passed the test requirements for vehicles at the extremes for the fleet, it would perform satisfactorily for all other vehicles in between. Since many vehicle parameters could influence the performance during impacts, this assumption may or may not be valid. The safety performances of roadside features for various passenger car platforms and light-truck subclasses were evaluated in the study, which consisted of evaluations of the frequency and severity of roadside crashes for these generic platforms and subclasses by using recent crash data from the Fatal Accident Report System, the General Estimates System, and the Highway Safety Information System.

A new median barrier guideline (Miaou et al. 2005; Bligh et al. 2006) for Texas was developed to assist highway engineers evaluating median barrier needs with the intention of achieving the highest practical level of median safety. In this work, statistical crash models for various types of median-related crashes were developed based on an analysis of crash data in Texas. Based on the estimates from the frequency and severity models and crash costs used by TxDOT, an economic analysis of the median barrier need was performed. Guidelines for installing median barriers on divided, access-controlled freeways were developed as a function of average annual daily traffic (AADT) and median width. Guidance to assist engineers evaluating median barriers needed on existing highway facilities was also developed based on the mean cross-median crash rate.

Based on a review of previous research and testing of cable barrier systems, Alberson et al. (2003) developed a new terminal to improve the lateral deflection, maintenance, and crash performance of the generic low-tension cable barriers. By replacing the single, large concrete anchorage block with three specially designed posts, the new terminal eliminates spring connectors and is expected to withstand higher tensile loads. Full-scale crash testing on the new terminal showed reduced lateral cable deflections and suggested a performance improvement. This newly developed cable guardrail terminal was expected to (partially) address the issue of cable heights in backside hits by changing the cable heights in the terminal section. A recommendation was made on further investigation of cable heights in the length-of-need sections in relation to vehicle profiles.

Recently, Alberson et al. (2007) completed a study in which preliminary guidelines were developed for the selection of cable barrier systems. The project reviewed cable barrier installations in the U.S. and possibly overseas including the generic low-tension cables and five proprietary high tension cable systems. A survey was also conducted in the study to identify experiences, practices, and design and construction standards for cable barrier systems in various states. The study indicated a continuously increased usage of cable barrier systems with a total of 2647 km (1645 miles) of installation. As expected, the severity of accidents was found to decrease at locations where CMBs were installed while the total number of accidents was found to increase. The study indicated that placement of the systems is key to minimizing the number of accidents and maximizing the performance of the systems, and that these issues are sometimes at odds and deserve further research.

Placement of median barriers has been and will continue to be an area that deserves more research work. The placement of median barriers on sloped median also imposes a significant challenge to retaining the performance when placed on flat terrains. The performance tests

specified by the NCHRP Report 350 are all based on flat terrain conditions. Terrain conditions can have a significant effect on the barrier's impact performance (AASHTO 2006). The slopes in the median can affect the performance of the barrier as the locations the vehicle impacting the barrier may be significantly different from those on flat terrain.

In the NCHRP Project 17-14, "Improved Guidelines for Median Safety," researchers attempted to develop guidelines for using median barrier and selecting median widths and slopes (BMI-SG 2004). Unfortunately, collection of data needed for this project proved to be very expensive, and the data limitations hampered the strength of the recommendations. The project results have not been incorporated into practice, but should be very beneficial to future research.

To avoid some of the obstacles that NCHRP Project 17-14 faced, the NCHRP Project 22-21 (NCHRP ongoing) focuses on typical cross-section designs for a construction or reconstruction project rather than the exact cross-section design at a particular point. The typical cross-section designs are determined fairly early in the design process before adjustments are made to account for variations along the alignment (e.g., horizontal and vertical curves, interchanges and intersections, and special drainage requirements). The Project 22-21 was started on January 24, 2006 and was still ongoing as of August, 2010.

The NCHRP Project 22-22, "Placement of Traffic Barriers on Roadside and Median Slopes," (NCHRP pending) has been planned and the project results are to be incorporated into the final product of NCHRP Project 22-21. An analysis performed in the 1970s indicated that most guardrails do not perform well when placed on 1:6 or steeper slopes. Since that time, the vehicle fleet has changed dramatically with a significant increase in the popularity of light trucks and sport utility vehicles. In addition, there has been a significant change in the design of roadside barriers in recent decades. It is unclear how these changes affect the behavior of longitudinal barriers placed on slopes. Information from the Fatality Analysis Reporting System (FARS) database of the National Highway Traffic Safety Administration (NHTSA) indicated that some cross-median crashes have occurred where median barriers were in place. A full-scale crash test also showed that a passenger vehicle could penetrate a cable barrier on the backside of a depressed median. With the dramatic increase in use of barriers in depressed medians, a more detailed study of the performance of barriers in depressed medians is needed to achieve acceptable safety performance.

During the TRB AFB20 (Committee on Roadside Safety Design) 2007 Summer Meeting, placement of cable median barriers on sloped medians was considered one of the most important and urgent issues for roadside safety research. Research work was suggested to consider both safety and maintenance aspects, impact angles, impact speeds, critical impact point(s), cable heights/spacing, post spacing and deflections, soil conditions, etc.

## 2.2 Crash Modeling and Simulations

Mackerle (2003) provided a bibliography that had 271 references published between 1998 and 2002 on crash simulations using FE analysis (FEA) and impact-induced injuries. This bibliography categorized the references into four different topic areas: 1) Crash and impact simulations where occupants are not included; 2) Impact-induced injuries; 3) Human

surrogates; and 4) Injury protection. Topics in the first area include crashworthiness of aircrafts and helicopters, automobiles, and vehicle rail structures. The second area of research utilizes two major types of models for humans, the crash dummy and real human body models. Research topics in this area are mainly on biomechanics and impact analyses for various human injuries. Topics on human surrogates focus on the development FE models of hybrid and other types of human dummies. These dummy models are used to obtain dynamic responses of the whole human bodies during impacts, which are difficult to measure experimentally. In the area of injury protection, FE techniques are utilized to analyze and simulate injury protection systems such as seat belt, air bags, and collapsible structures to reduce serious or fatal injuries. The references included in Mackerle's bibliography are generally useful to the work on FE crash simulations; however, only a few references under injury protection are related to roadside safety and none is related to CMB simulations.

Most publically available FE models of vehicles and roadside safety structures were developed at the FHWA National Crash Analysis Center (NCAC), George Washington University. Since the 1990's, significant efforts have been put on the development of FE crash models that are available as LS-DYNA input files from NCAC's website (NCAC web1). A list of references on these modeling efforts and simulation work performed at NCAC is also available from NCAC's website (NCAC web2).

The modeling and simulation efforts at NCAC can be found in several representative works. Marzougui et al. (2000) developed the FE model of an F-shaped portable concrete barrier (PCB) and validated the model with full-scale crash test data. With the proven fidelity and accuracy of the modeling methodology, the models of two modified PCB designs were created and used in FE simulations to evaluate their safety performance. A third design was then developed based on the simulation results and its performance was analyzed. In the work by Zaouk et al. (2000a, 2000b), a detailed FE model of a 1996 Plymouth Neon was developed. The three dimensional geometric data of each component was obtained by using a passive digitizing arm and then imported into a preprocessor for mesh generation, parts connection, and material properties. Tensile tests were conducted on specimen to obtain the material properties of the various sheet metal components. The body-in-white model was used in the simulation of a frontal impact and the results were compared with test data to evaluate the accuracy and validity of the model. Kan et al. (2001) developed an integrated FE model that included the vehicular structure, interior components, an occupant (Hybrid III dummy), and an airbag for crashworthiness evaluation. The integrated model was then used in a case study to demonstrate the potential benefit of the integrated simulation and analysis approach, which would further improve the engineering practice with cost savings and producing more accurate and consistent analysis results.

Marzougui et al. (2004) developed a detailed suspension model and incorporated it into the previously developed FE model of a Chevrolet C2500 pickup truck (Zaouk et al. 1997). Pendulum tests were conducted at the Federal Outdoor Impact Laboratory (FOIL) of FHWA and compared with simulation results of deformations, displacements and accelerations at various locations. Crash simulations were performed using the upgraded vehicle model and the results were compared with crash data from previously conducted full-scale tests.

Mohan et al. (2005) developed a detailed FE model for the three-strand low-tension cable barriers. The model addressed the important issues with cable modeling for crash simulations by defining soil and post, post and hook-bolt, cable and hook-bolt, and cable and vehicle interactions. The CMB model was then combined with the FE model of a Chevrolet C2500 pickup truck and used in the simulation of CMBs placed on a flat terrain. The simulation results were compared to data from a full-scale crash test with the same setup. Cable pullout and soli-post dynamic deflections from the simulation were found to correlate well with the crash test. Angular displacements of the pickup truck in the simulation were similar to those in the crash test. Recorded test data such as maximum dynamic deflection allowed by the cable barriers and the vehicle's acceleration at the center of gravity compared well with the simulation results.

To facilitate the use of FE simulation to evaluate roadside safety structures at higher test levels specified by the NCHRP Report 350, Mohan et al. (2007) improved and validated a previously developed model of a 1996 Ford F800 single unit truck. This 8172-kg (18,000-lb) truck was the one used by NCHRP Report 350 as the standard vehicle for test level 4. Simulations were performed using the improved model and the results were compared with those from a full-scale crash test. The global kinematics and acceleration time histories of the truck from simulation correlated well with the crash test. Mohan et al. also suggested further improving the normal forces on non-impacted tires so as to correlate well on the vehicle's yaw by considering frictions between the tire and barrier and between the tires and ground.

In the most recent work by Marzougui et al. (2007a), they investigated penetration of low-tension CMBs placed on flat and sloped medians using FEA and vehicle dynamics analysis coupled with full-scale crash testing. The FE model of a Chevrolet C2500 pickup truck was used in the simulation of CMBs placed on a flat terrain and the results showed that the vehicle was retained by the barriers. The FE model of a Ford Crown Victoria was used in the simulation of CMBs placed on a 6:1 median and 1.22 m (4 ft) from the ditch centerline. The Victoria was found to under-ride the CMBs with almost no resistance from the cables. The simulation results using the Victoria model were confirmed by full-scale crash tests (No. 04010 and 04011) performed at the FHWA/FOIL. A conclusion from the simulation results was that the sloped terrain caused the vehicle to be relatively lower than the cable and hence reduced the effectiveness of the CMBs. In both simulations, the impact speed and angle were 62 mph (100 km/hr) and 25°, respectively.

Marzougui et al. (2007a) also performed vehicle dynamics analysis using these two models along with the model of a small sedan, Mitsubishi Mirage, to further investigate the effect of sloped (6:1) terrains on the CMB performance. It was determined that suspensions of mid-sized vehicles tended to be fully compressed due to dynamic forces imposed by the terrain, speed, and angle when the vehicle started up the slope on the opposite side of the median. These conditions are likely to place the nose of the vehicle below the lowest cable and hence allow for under-riding the barrier. Future work recommended by Marzougui et al. (2007a) was to further analyze alternative designs and barrier placement retrofits to improve the CMB performance on sloped terrains. Their suggested retrofits involved adding a fourth cable, using a closer post spacing, using a stronger cable/post connection, and incorporating ties to connect the three cables.

In the study of Marzougui et al. (2007b), they developed a FE W-beam model and validated it using full-scale crash testing. The model was shown to give an accurate representation of the real system by comparing the roll and yaw angles. Using the validated model, they performed four simulations of a passenger truck impacting the W-beam with different rail heights. The simulation results showed that the effectiveness of the barrier to redirect a vehicle could be compromised when the rail height was lower than recommended.

Researchers from the roadside safety group at Worcester Polytechnic Institute (WPI) utilized FE models in a number of roadside safety studies. Ray (1996a) analyzed data of full-scale crash tests and developed a criterion using statistical parameters to assess the repeatability of full-scale crash test and to evaluate simulation results compared to crash data. Ray (1996b) reviewed the history of using FEA in roadside safety research, and presented the vehicle, occupant, and roadside hardware models that had been developed to date. Ray and Patzner (1997) developed a nonlinear FE model of a modified eccentric loader breakaway cable terminal (MELT) and used it in simulating a full-scale crash test involving a small passenger car. Simulation results were analyzed and compared to crash data, and the FE model were recommended to be used in the evaluation of new design alternatives. Plaxico et al. (1997) developed a 3D FE model of a modified thrie-beam and simulated the impact of a compact automobile on this guardrail. The computational model was then calibrated with data from an actual field test that was previously conducted as part of a full-scale crash test program carried out under the auspices of FHWA. Plaxico et al. (1998) developed the FE model of a breakaway timber post and soil system used in the breakaway cable terminal (BCT) and the modified eccentric loader BCT. Simulation results were compared and found to correlate well to data from physical tests. Patzner et al. (1999) examined the effects of post strength and soil strength on the overall performance of the MELT terminal system using a nonlinear FE model. A matrix of twelve simulations of particular full-scale crash test scenarios was used to establish the combinations of post and soil strengths that produce favorable results. The parametric study showed that certain combinations of soil and post strengths increased the hazardous possibilities of wheel snagging, pocketing, or rail penetration, while other combinations produced more favorable results.

In the work of Plaxico et al. (2000), the impact performance of two strong-post W-beam guardrails, the G4 (2W) and G4 (1W), were compared. After validating the FE model of the G4 (W2) guardrail with data of a full-scale crash test, the FE model of the G4 (1W) guardrail was developed. The two guardrails were compared with respect to deflection, vehicle redirection, and occupant risk factors. The two systems were found to perform similarly in collisions and both to satisfy the requirements of the NCHRP Report 350 for the test 3-11 conditions. Using LS-DYNA simulations and laboratory experiments, Plaxico et al. (2003) investigated the failure mechanism of the bolted connection of a W-beam rail to a guardrail post, which could have a significant effect on the performance of a guardrail system. A computationally efficient and accurate FE model of the rail-to-post connection was developed to be used in analysis of guardrail system performance using LS-DYNA. Orengo et al. (2003) presented a method to model tire deflation in LS-DYNA simulations along with examples to use the model. Deflated tires have significant different behaviors from those of inflated tires, as observed in real world crashes and in full-scale crash tests. Vehicles' kinematics is strongly coupled to the behaviors of deflated tires; therefore, modeling such

behaviors is critical to roadside hardware simulations. Ray et al. (2004) used LS-DYNA simulations to determine if an extruded aluminum bridge rail will pass the full-scale crash tests for test levels three and four conditions of the NCHRP Report 350. The simulation results, which were supported by a subsequent AASHTO LRFD analysis, indicated a high likelihood of passing the crash tests.

FE simulations have also been used by researchers at the Midwest Roadside Safety Facility (MwRSF). Reid (1996) utilized FEA in the study of material property influence on automobile crash structures and attempted to develop crashworthiness guidelines for design engineers. In one of his later works, Reid (1998) demonstrated through two simple examples the potential modeling issues that could be easily overlooked in FE impact simulations: contact definition and damping. He also suggested ways to check for modeling errors and to make improvements. In the work of Reid and Bielenberg (1999), FE simulations were performed for a bullnose median barrier crashed by a 2000-kg (4405-lb) pickup truck to determine the cause of failure and to evaluate a potential solution to the problem. Reid and Coon (2002) presented details on the development of the hook-bolt model used in the CMBs. In a collaborative work to improve the FE model of a Chevrolet C2500 pickup truck (Reid and Marzougui 2002; Tiso et al. 2002), structural modeling methods were introduced for model improvement through refining meshes, using better material models, adding details to simplified components, and improving connections between components. Suspension modeling, which is critical to the correct vehicle dynamic responses, was also investigated in this collaborative work and a new model was successfully developed with significant improvements.

To educate roadside safety engineers and promote the use of simulation, Reid (2004) summarized ten years of the simulation efforts at MwRSF on the development of new roadside safety appurtenances. More recently, Reid and Hiser (2004) studied the friction effects, particularly between solid elements, on component connections and interactions in crash modeling and analysis. In their work on modeling bolted connections that allowed for slippage, Reid and Hiser (2005) investigated two modeling techniques that are based on discrete-spring clamping and stressed clamping model with deformable elements, respectively. The simulation results for both models compared well with test data, with the stressed clamping model with deformable mesh having better accuracy accompanied by significantly increased computational cost. Hiser and Reid (2005) also investigated improved FE modeling methods for slip base structures, which could have a considerable potential for reducing the amount of crash resistance and thus occupant injury when struck by errant vehicles. They developed and evaluated two bolt preloading methods, with one using discrete spring elements and the other using pre-stressed solid elements. Similar to their findings in the work of modeling hook-bolts, they found that the method using solid elements was more accurate than that using discrete spring elements when the impact conditions became more severe. As a result, the model using pre-stressed solid elements was incorporated into the FE model of a cable guardrail system. The results showed that the slip base model was acceptable in both end-on impact and length-of-need impact simulations.

In the study by Reid et al. (2009), they investigated the potential of increasing the suggested flare rates for strong post W-beams to reduce guardrail installation lengths, which would

result in decreased guardrail construction and maintenance costs, and reduce the impact frequency. Both computer simulation and full-scale crash tests were used in the evaluation of increased flare rates up to, and including, 5:1. Simulation results indicated that the conventional G4 (1S) guardrail modified to incorporate a routed wood block could not successfully meet NCHRP Report 350 crash test criteria when installed at any steeper flare rates than the 15:1 recommended in the Roadside Design Guide. Their study also showed that the Midwest Guardrail System (MGS) could meet NCHRP Report 350 impact criteria when installed at a 5:1 flare rate, yet with greater impact severities during testing than anticipated. Reid et al. also indicated that whenever roadside or median slopes are relatively flat (10:1 or flatter), increasing the flare rate on guardrail installations becomes practical and has some major advantages including significantly reducing guardrail lengths and associated costs. The study, however, did not give any indications of W-beam performance on steeper slopes.

FE simulations were also found in the work of other researchers in roadside safety Research. Whitworth et al. (2004) evaluated the crashworthiness of a modified W-beam guardrail using detailed FE models of the guardrail and a Chevrolet C2500 pickup truck. The simulation results were compared and found in good agreement with crash test data in terms of roll and yaw angles. Simulations were also performed to evaluate the effect of certain guardrail design parameters, such as rail mounting height and routed/non-routed blockouts, on the crashworthiness and safety performance of the system. In the work of Bligh et al. (2004), FEA was utilized to develop new roadside features to address three roadside safety issues. An alternative to the popular T6 tubular W-beam bridge rail was developed to address problems with vehicle instability observed in full-scale crash testing. A retrofit connection to TxDOT's grid-slot portable concrete barrier was developed to limit dynamic barrier deflections to levels that are more practical for work zone deployment. Finally, crashworthy mow strip configurations were developed for use when vegetation control around guard fence systems is desired to reduce the cost and risk associated with hand mowing. In a project funded by the New Jersey DOT, Gabler et al. (2005) evaluated the post-impact performance of two median barrier systems in New Jersey: a three-strand cable median barrier system and a modified thrie-beam median barrier system. FE modeling was adopted as a major means for the investigation. The project also included field investigation of crashes into the subject barriers and a survey of the median barrier experience of other state DOTs. This study concluded that the three-strand cable barriers were capable of containing and redirecting passenger vehicles, that cable barriers were effective at reducing the incidence of cross-median collisions in wider medians, and that cable barriers reduced the overall collision severity despite typically increasing the total number of accidents.

Computer simulations are also used by international researchers on roadside safety research. Using LS-DYNA simulations, Atahan (2002) analyzed a strong-post W-bean system that was failed in a previously conducted full-scale crash test. After identifying the cause of failure and incorporating necessary improvements, a new W-beam system was developed and showed improved performance based on simulation results. Atahan (2003) studied the impact performance of G2 steel weak-post W-beams installed at the slope-break point on non-level terrains using LS-DYNA simulations. His results showed that there was a risk of increased vehicle instability when the roadside slope adjacent to the W-beam guardrail became steeper

than 6:1. Atahan and Cansiz (2005) investigated the failure of a bridge rail-to-guardrail transition design in a full-scale crash test in which the vehicle rolled over the guardrail. They used full-scale LS-DYNA simulations to replicate the crash tests and identified the cause of the failure attributed to the low height of the W-beam rails. In the work by Atahan (2007), LS-DYNA simulation was used to study the crashworthiness behavior of a bridge rail-to-guardrail transition structure under 8,000 kg of impact load. This work demonstrated the effectiveness of FE simulations for its replications of the actual dynamic interactions and mechanics of the crash. Atahan also pointed out that the use of a real soil model other than the simplified spring soil model could improve the accuracy of FE simulations but would significantly increase the computational costs.

FE simulation, particularly with LS-DYNA, has been increasingly used in roadside safety research. In addition to the abovementioned references, FHWA recently published several manuals on using LS-DYNA material models and evaluation of these models (Lewis 2004; Murray et al. 2005; Murray 2007; Reid et al. 2004). These references can also be useful in the crash modeling work using LS-DYNA.

# 3. Finite Element Modeling of Vehicle and Barriers

The simulation work of this project included: 1) the vehicle impacting a single-face W-beam guardrail; 2) the vehicle impacting a double-face W-beam guardrail (two designs); and 3) the vehicle impacting a generic low-tension CMB. The FE models of the vehicle, single-face W-beam, and CMB were obtained from NCAC and modified to correct modeling issues and suit the needs of this project, e.g., to adjust to NCDOT designs and accommodate median slopes. The FE models of two designs of the double-face W-beam were generated based on the model of the single-face W-beam used in this project.

In all simulation cases, the vehicle left the shoulder with prescribed speeds; therefore, vehicle trajectories were included in these simulations. The impact speed was defined in the vehicle's travel direction, and the impact angle was defined as one between the vehicle's travel direction and the longitudinal direction of the barrier. Both front-side and backside impacts were simulated in this project. The vehicle's initial impact point on the W-beam or CMB was in the middle of the effective barrier length and midway between the two adjacent posts.

### 3.1 FE Model of a 2006 Ford F250 Passenger Truck

The vehicle model used in this project was a 2006 Ford F250 passenger truck, which has a curb weight of 5,504 lb (2,499 kg), overall length of 226.4 in. (5.75 m), overall width of 79.9 in. (2.03 m), overall height of 76.5 in. (1.94 m), and ground clearance of 8.3 in. (211 mm). The FE model of the F250 was originally developed at NCAC and validated using frontal-impact tests that were conducted on flat terrain according to the Federal Motor Vehicle Safety Standards and Regulations.

Simulations of the vehicles crashing onto roadside barriers imposed significant challenges to the numerical models. For example, in the simulation of a crash on a sloped median, robust and reliable suspension models were required to ensure the correct dynamic behavior of the vehicle. Before running simulations for this project, FE simulations of the Ford F250 traversing a 46-ft (14-m) sloped median were performed to validate the suspension models. Figure 3.1 shows the results after correcting several modeling issues on the suspensions and other parts of the vehicle. The new suspension models did not have the unrealistic titling found in the old ones.

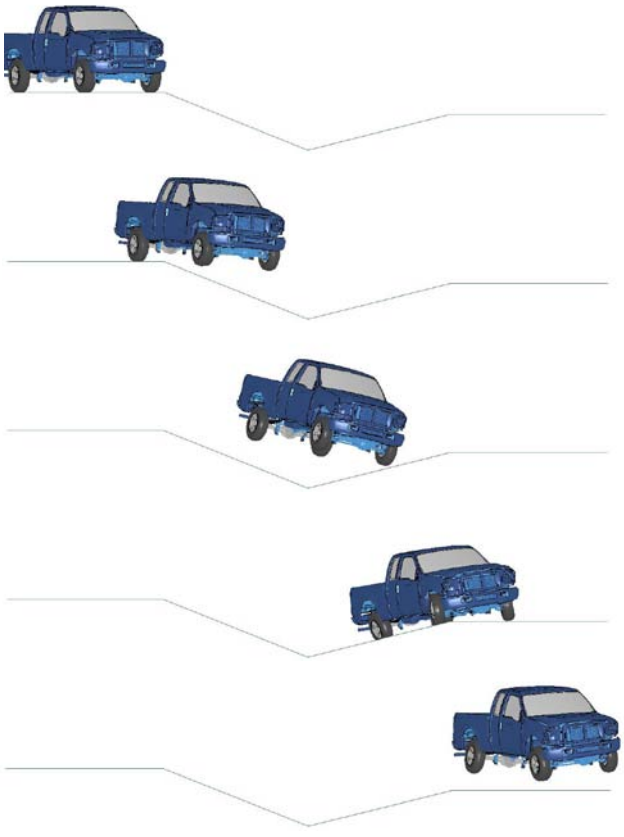

Fig. 3.1: Finite element simulation of the Ford F250 traversing a 46-foot median.

### 3.2 FE Model of the Single-face W-beam

The single-face W-beam guardrail was used as a baseline to compare the performance of the double-face W-beams. In the FE model of the single-face W-beam developed at NCAC, the top surface of the soil around each post was flat; this model could be used for a W-beam guardrail installed on a flat terrain but was not appropriate for that on a sloped median, as in the case of this project. Consequently, the single-face W-beam model was modified with a new soil model to accommodate the slopes of the ditch. Figure 3.2 shows the modified single-face W-beam models placed on a 4:1 and a 2.5:1 slope. The length of the single-face W-beam used in this project was 174.9 ft (53.3 m).

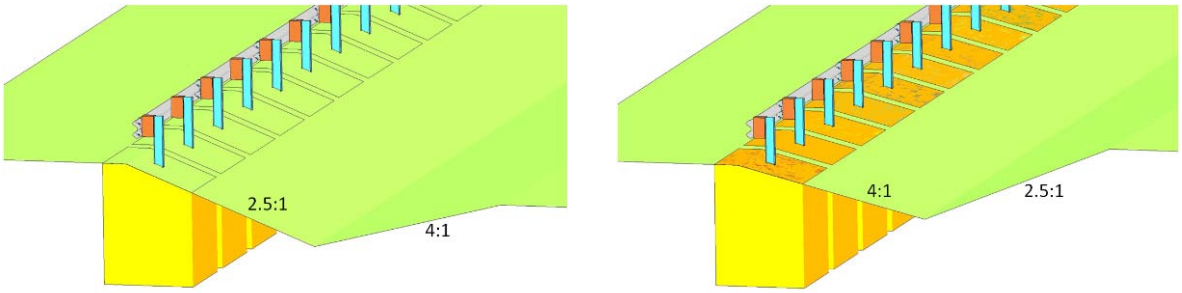


W-beam on a 2.5:1 slope W-beam on a 4:1 slope

Fig. 3.2: The modified W-beam models on a sloped median.

In addition to modifications on the soil model, other modeling issues were found in the original W-beam model and fixed in the modified model to improve numerical stability and accuracy of the simulations. Figure 3.3 compares a terminal wood post in the original and modified models in a crash simulation. In the original model, the steel plate penetrated into the wood post due to improperly defined contacts between the two and resulted in a shock wave in the post. This and other contact issues such as initial penetrations due to mismatched geometries in the original model were all corrected in the modified model.

The modified W-beam model was compared to the original model using crash simulations of a cubic block impacting the W-beam. The comparison was performed to ensure there was no significant difference between the two models due to modifications on the soil model. Simulation results using both models are shown in Fig. 3.4, which includes six snapshots taken at the same time instances from each of the two models. It can be seen that there is no significant difference between the two models under impact of the massive block. The displacements, deformations, and stresses of the rails and posts around the impact areas were also compared; they conformed to the observations from Fig. 3.4.

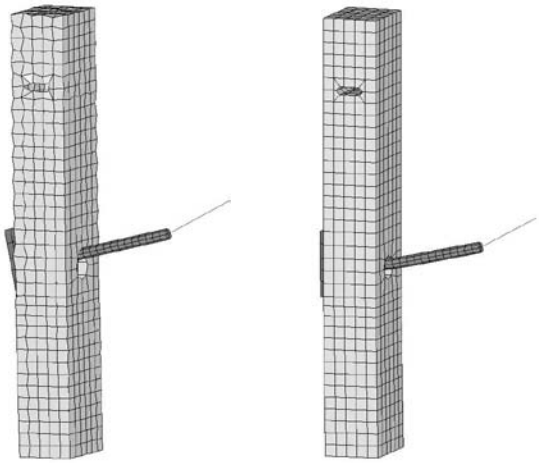

Original model Modified model

Fig. 3.3: Responses of the terminal posts in the original and modified W-beam models.

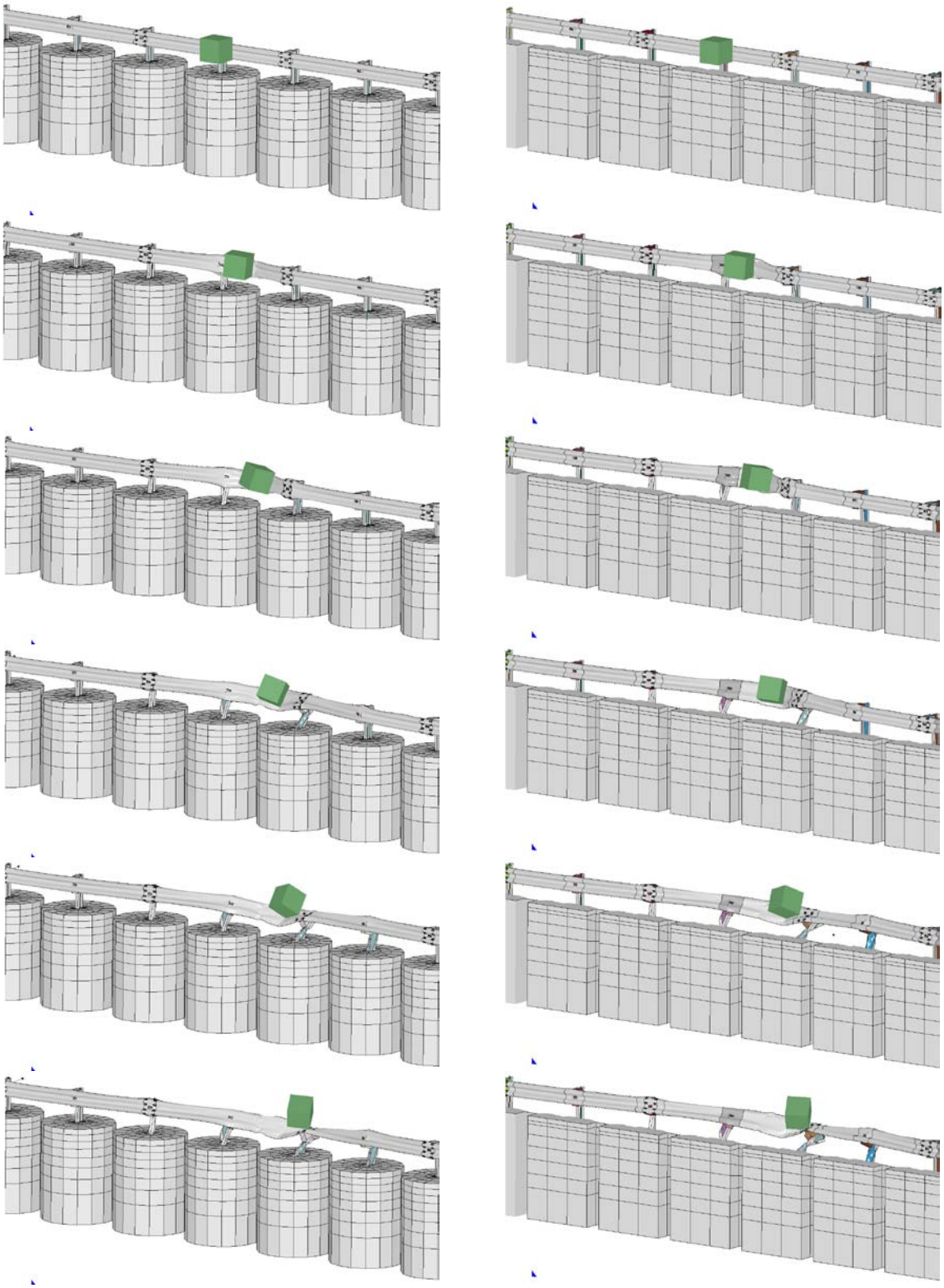

Original model Modified model

Fig. 3.4: Comparison of the original and modified W-beam models under impact of a mass block.

## 3.3 FE Model of the Double-face W-beam

The FE model of the double-face W-beam guardrail was developed based on the single-face W-beam model by adding a rail and woodblocks on the opposite side of the posts. Figure 3.5 shows the FE model of a double-face W-beam placed on the 2.5:1 slope of a 46-ft median.

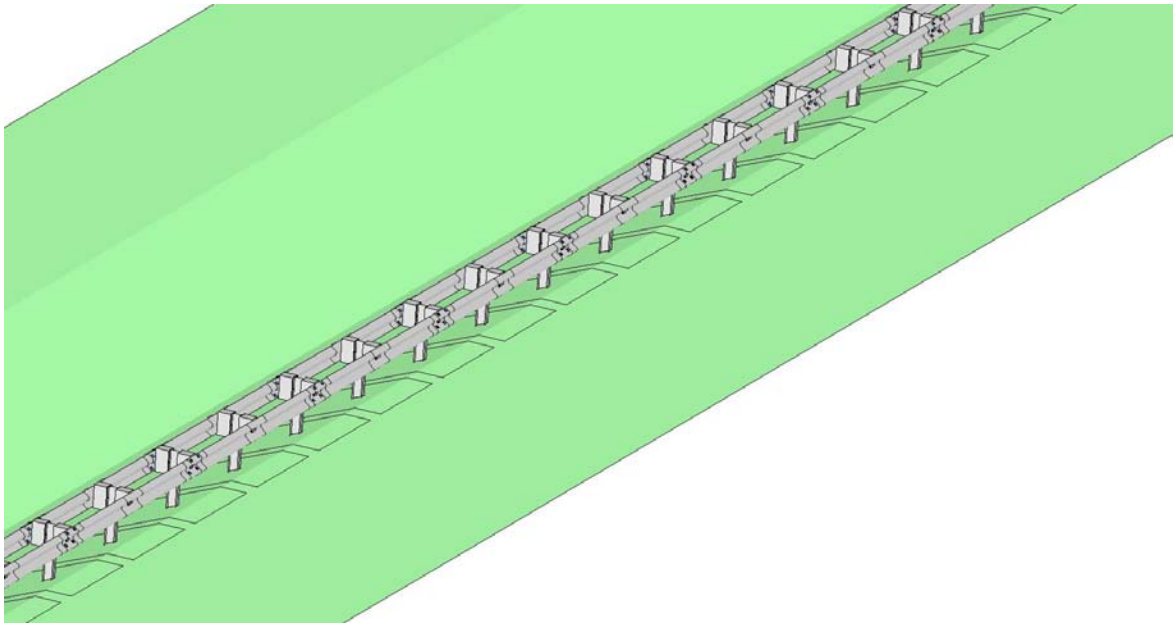

Fig. 3.5: The finite element model of the double-face W-beam placed on the 2.5:1 slope of a 46-ft median.

Two designs of the double-face W-beam were considered in this project: Design #1 – the rails on both sides of the posts had the same height; and Design #2 – the backside rail, i.e., the one facing the ditch centerline, was 7.1 in. (0.18 m) lower than the front-side rail. Figure 3.6 shows the FE models of the two designs of the double-face W-beam, both with a length of 174.9 ft (53.3 m), same as the single-face W-beam.

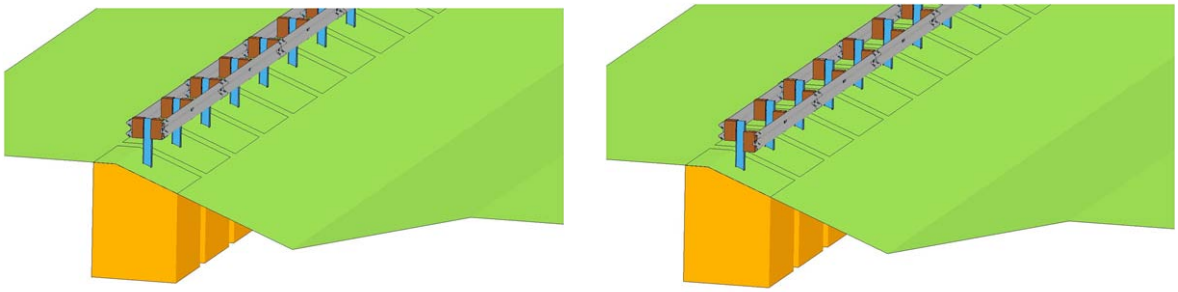

Design #1 Design #2

Fig. 3.6: The finite element models of two designs of the double-face W-beam.

## 3.4 FE Model of the Cable Median Barrier

The CMB studied in this project was based on the current NCDOT design as shown in Fig. 3.7. Figure 3.8 shows the FE model of this CMB placed on the 4:1 slope of a 46-ft median. In

this model, the effective length of the CMB was approximately 400 ft (122 m). The contacts between cables and other components were upgraded to beam-based contacts in the new CMB model to improve the numerical accuracy and stability.

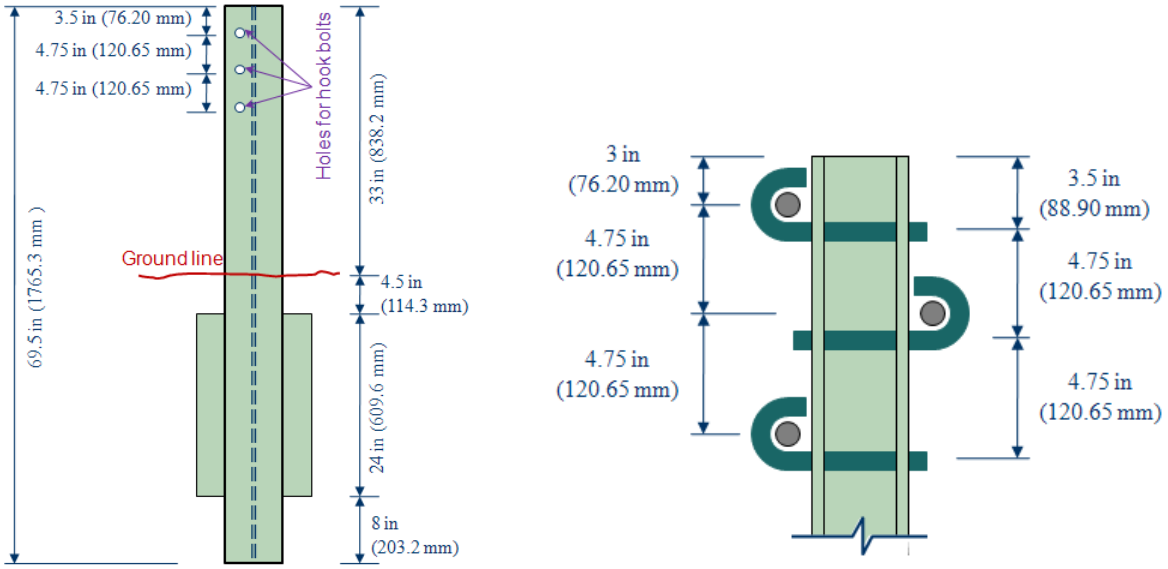


Fig. 3.7: Post geometry and cable positions of the CMB in the current NCDOT design.

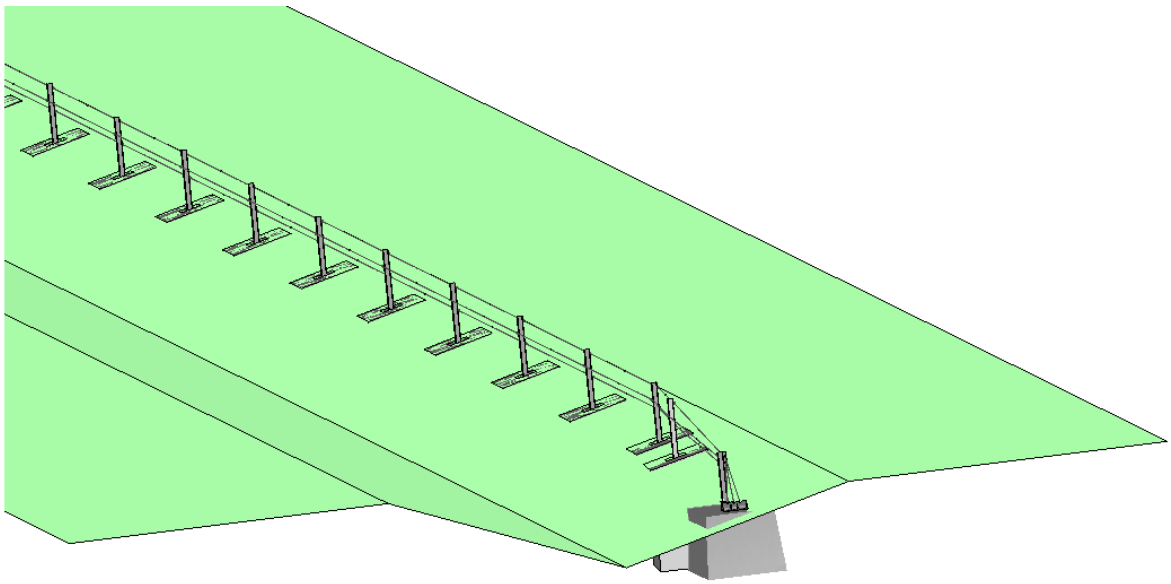

Fig. 3.8: The finite element model of the CMB placed on the 4:1 slope of a 46-ft median.

# 4. Simulation Results and Analysis

In this section, the results of FE simulations for the single-face W-beam guardrail are first presented. Simulation results of two designs of the double-face W-beam are then discussed and compared to the single-face W-beam for performance evaluation. Finally, the performance of the CMB placed on the 4:1 median is evaluated based on simulation results.

## 4.1 The Single-face W-beam

According to NCDOT design specifications, there were two lines of the single-face W-beam installed on the 46-foot median, one on each side of the ditch as illustrated in Fig. 1.4. The results of preliminary simulations showed that the vehicle, after impacting one line of the W-beam, would not cross the ditch and impact the other W-beam from the backside. This indicated that only simulations of front-side impacts were needed for the single-face W-beam. Furthermore, the case of impacting the W-beam on the 2.5:1 slope was shown to be more severe than on the 4:1 slope; therefore, the single-face W-beam on the 2.5:1 slope was evaluated under all combinations of impact speeds and angles. The single-face W-beam on the 4:1 slope was evaluated only for the 25° impacts at 62 and 70 mph (100 and 112.6 km/hr) to demonstrate impact severity compared to the cases on the 2.5:1 slope.

For the single-face W-beam on the 2.5:1 slope, simulations were performed for crashes at three impact speeds and three impact angles. Table 4.1 shows the simulation matrix and gives a summary of the simulation results.

Table 4.1: Simulation results of the single-face W-beam on the 2.5:1 slope

| **W-beam Location** | **Impact Angle** | **Impact Speed** | | |
|---|---|---|---|---|
| | | 62 mph (100 km/hr ) | 70 mph (112.6 km/hr) | 75 mph (120.7 km/hr) |
| Along the border of shoulder and the 2.5:1 slope | 25° | Vehicle redirected on the shoulder | Vehicle redirected with a tendency of rollover | Vehicle redirected with a tendency of rollover |
| | 30° | Vehicle redirected with a tendency of rollover | Vehicle rolled over towards the ditch | Vehicle rolled over towards the ditch |
| | 35° | Vehicle redirected with a tendency of rollover | Vehicle rolled over towards the ditch | Vehicle rolled over towards the ditch |

Under the 25° impact at 62 mph (100 km/hr), the single-face W-beam could redirect the vehicle on the shoulder, an indication of satisfying the Test Level 3 (TL-3) requirements of NCHRP Report 350 even under a large-vehicle impact. For 25° impacts at higher speeds, however, the vehicle showed a tendency of rollover towards the median after being redirected. As the impact angle increased, the rollover tendency also increased and rollovers occurred at impact speeds larger than 62 mph (100 km/hr). It was observed from simulation results that the rollover was more sensitive to impact angles than impact speeds. Figures 4.1 to 4.27 show the vehicle's displacement paths, detailed views of vehicle-barrier interactions, and time histories of traversal displacements and velocities for all the cases in Table 4.1. In the figures of vehicle's displacement paths, the W-beam is shown in its undeformed shape. In the time-history figures, the displacements and velocities were measured at two points on the longitudinal centerline of the vehicle: one on the hood and the other on the bed of the truck.

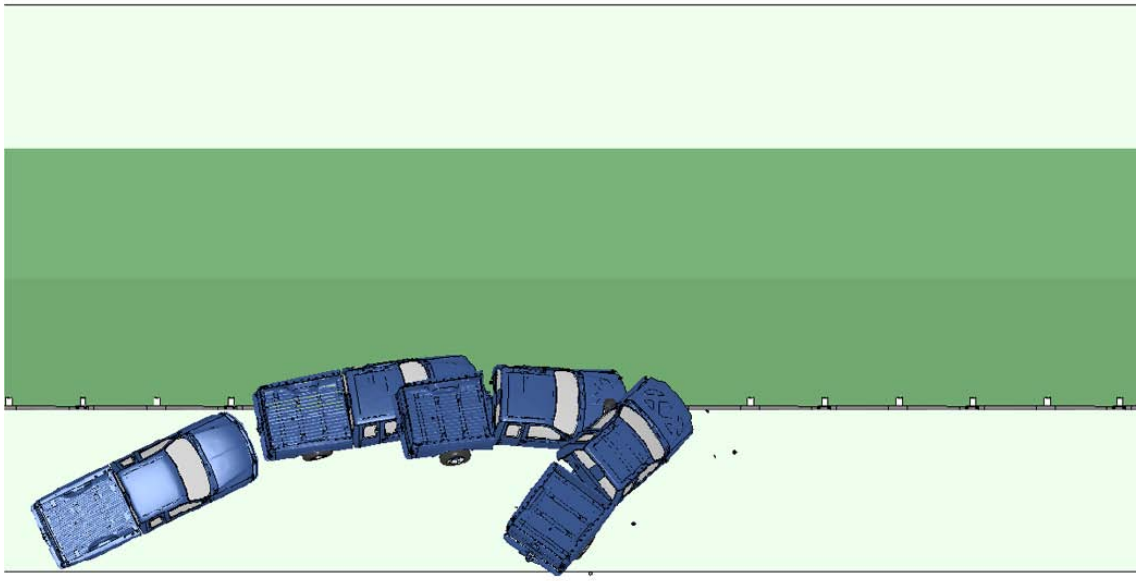

Fig. 4.1: Vehicle impact on the single-face W-beam on the 2.5:1 slope at 62 mph and 25°.

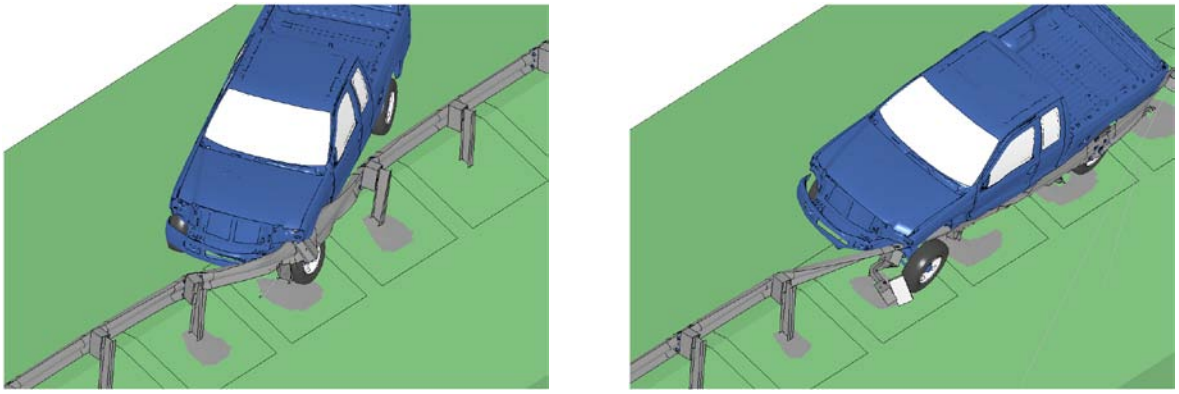

Fig. 4.2: Two instances of vehicle impacting the single-face W-beam on the 2.5:1 slope at 62 mph and 25°.

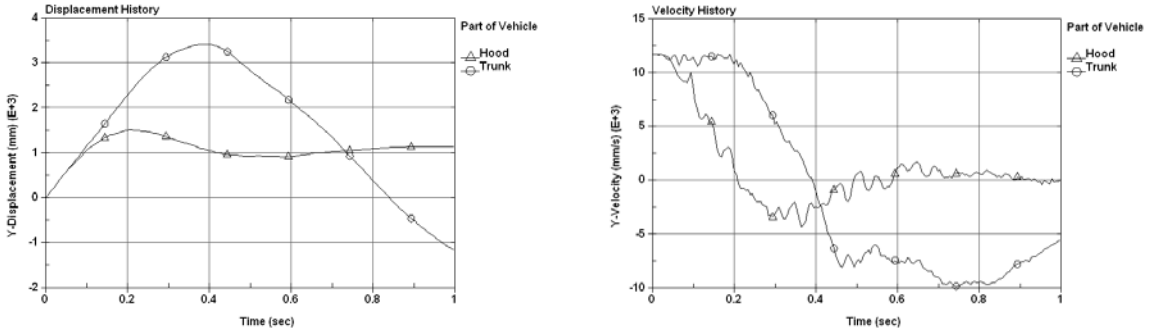


Traversal displacements Traversal velocities

Fig. 4.3: Time histories of traversal displacements and velocities of the vehicle impacting the single-face W-beam on the 2.5:1 slope at 62 mph and 25° ('trunk' means 'bed' on the truck).

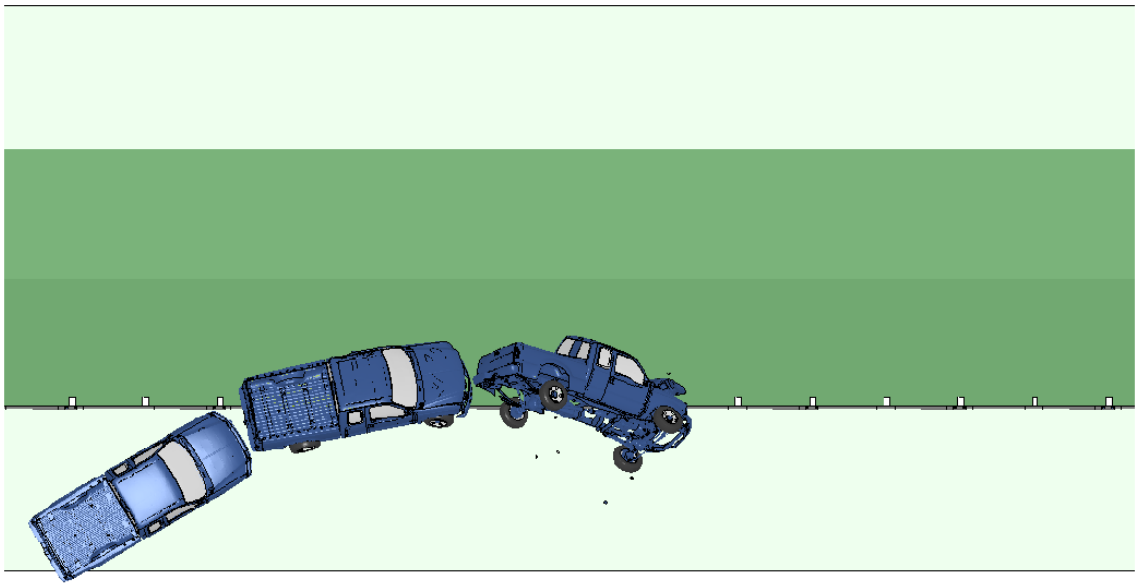

Fig. 4.4: Vehicle impact on the single-face W-beam on the 2.5:1 slope at 62 mph and 30°.

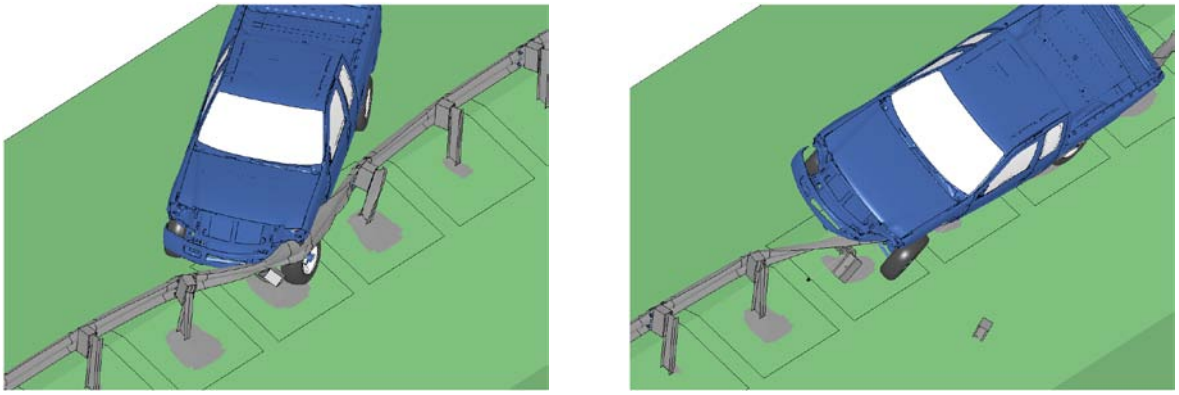

Fig. 4.5: Two instances of vehicle impacting the single-face W-beam on the 2.5:1 slope at 62 mph and 30°.

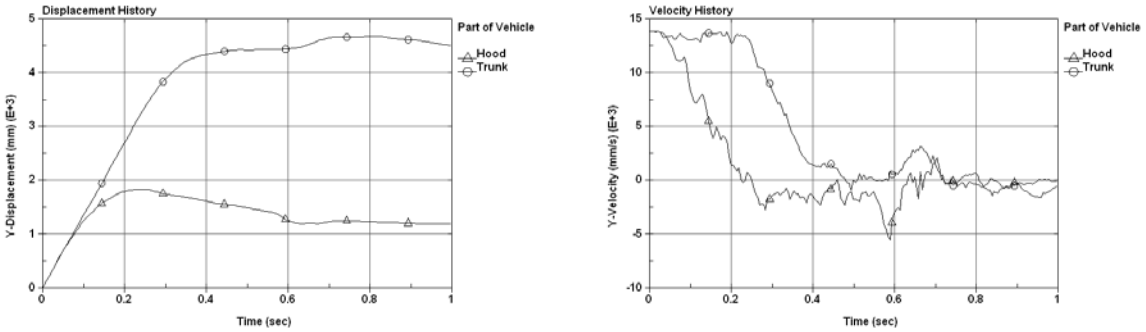


Traversal displacements Traversal velocities

Fig. 4.6: Time histories of traversal displacements and velocities of the vehicle impacting the single-face W-beam on the 2.5:1 slope at 62 mph and 30° ('trunk' means 'bed' on the truck).

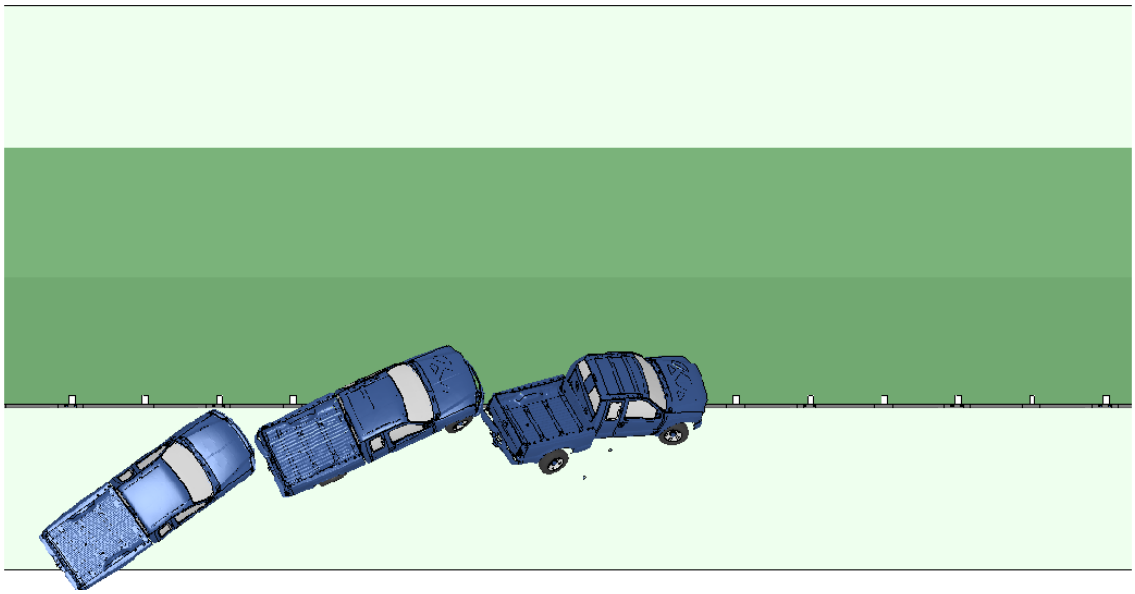

Fig. 4.7: Vehicle impact on the single-face W-beam on the 2.5:1 slope at 62 mph and 35°.

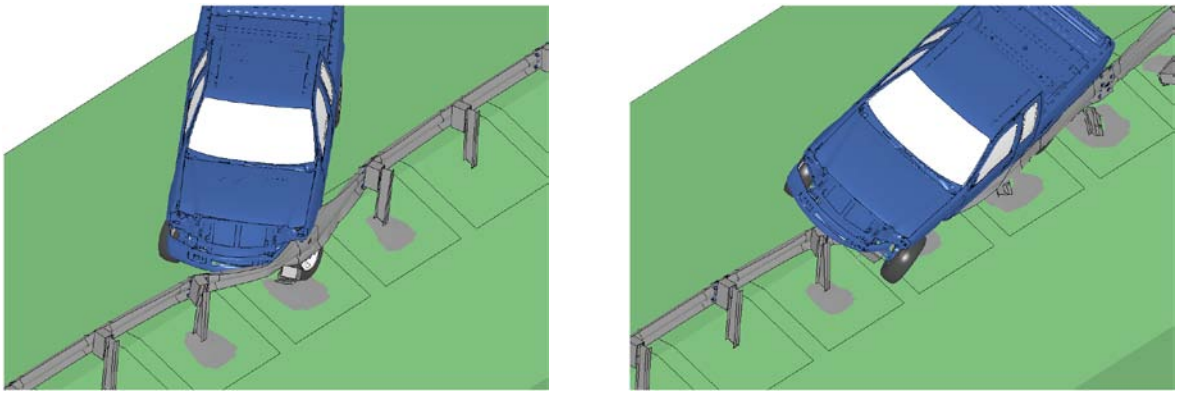

Fig. 4.8: Two instances of vehicle impacting the single-face W-beam on the 2.5:1 slope at 62 mph and 35°.

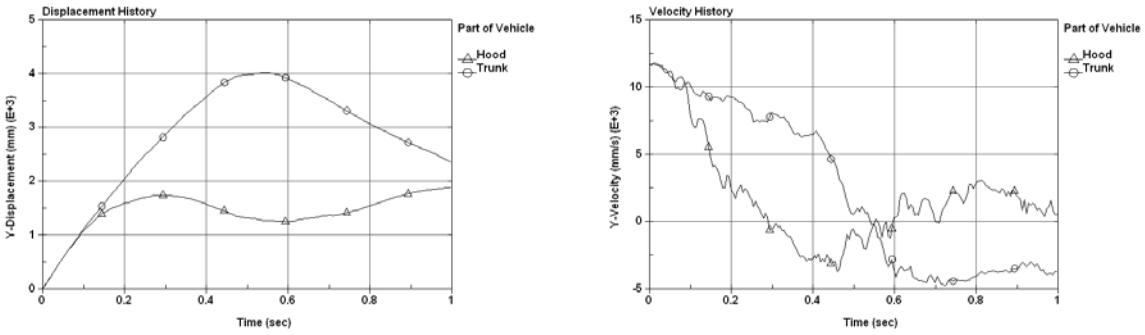


Traversal displacements Traversal velocities

Fig. 4.9: Time histories of traversal displacements and velocities of the vehicle impacting the single-face W-beam on the 2.5:1 slope at 62 mph and 35° ('trunk' means 'bed' on the truck).

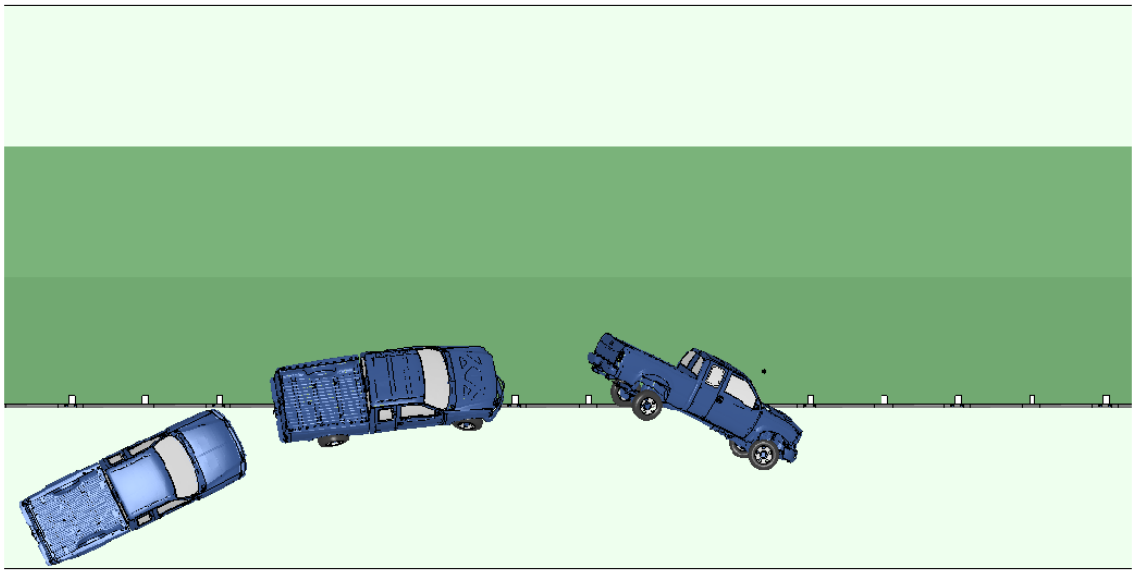

Fig. 4.10: Vehicle impact on the single-face W-beam on the 2.5:1 slope at 70 mph and 25°.

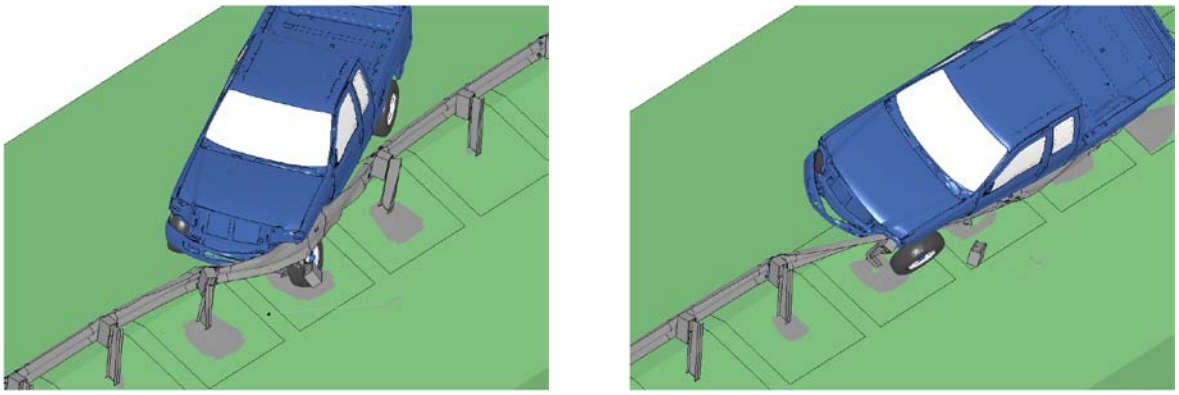

Fig. 4.11: Two instances of vehicle impacting the single-face W-beam on the 2.5:1 slope at 70 mph and 25°.

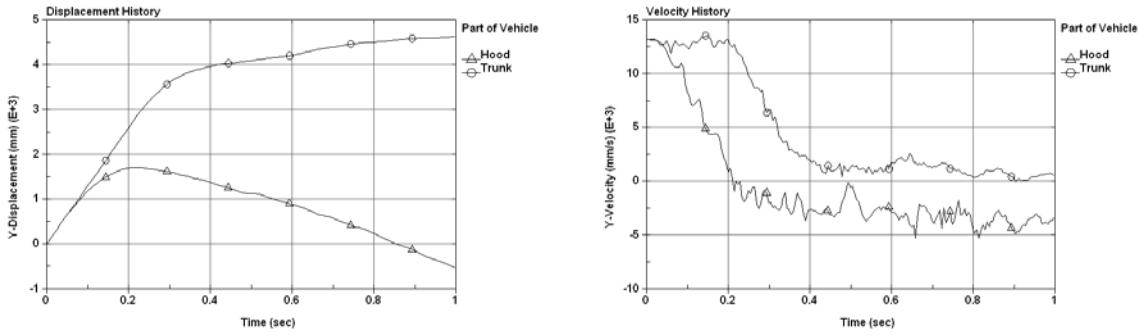


Traversal displacements Traversal velocities

Fig. 4.12: Time histories of traversal displacements and velocities of the vehicle impacting the single-face W-beam on 2.5:1 slope at 70 mph and 25° ('trunk' means 'bed' on the truck).

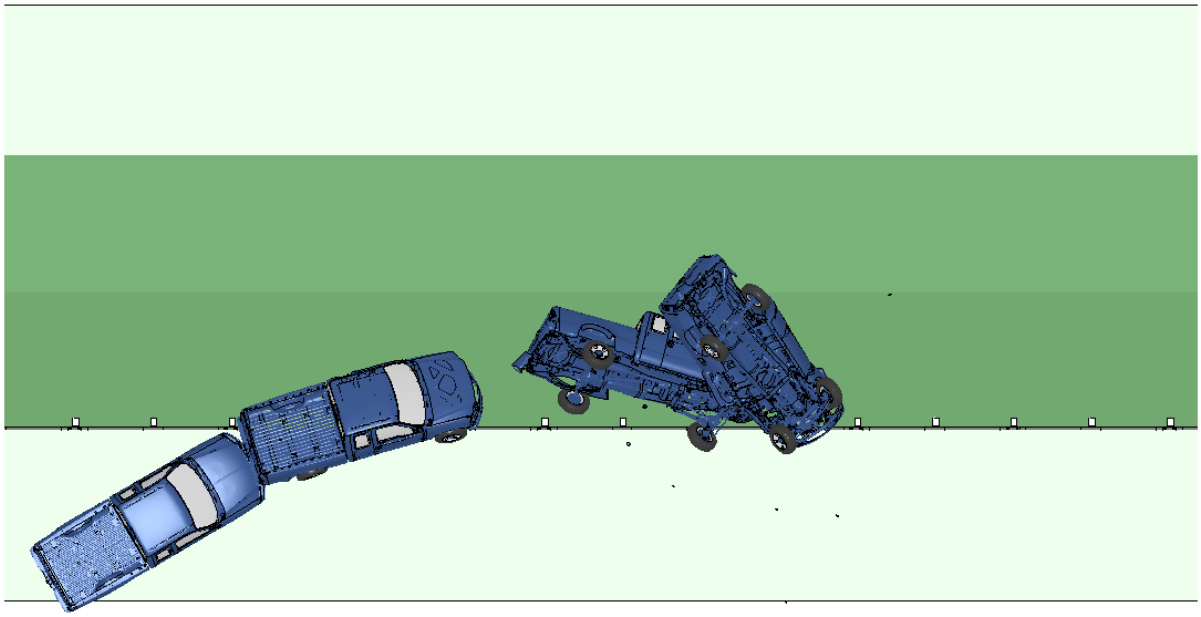

Fig. 4.13: Vehicle impact on the single-face W-beam on the 2.5:1 slope at 70 mph and 30°.

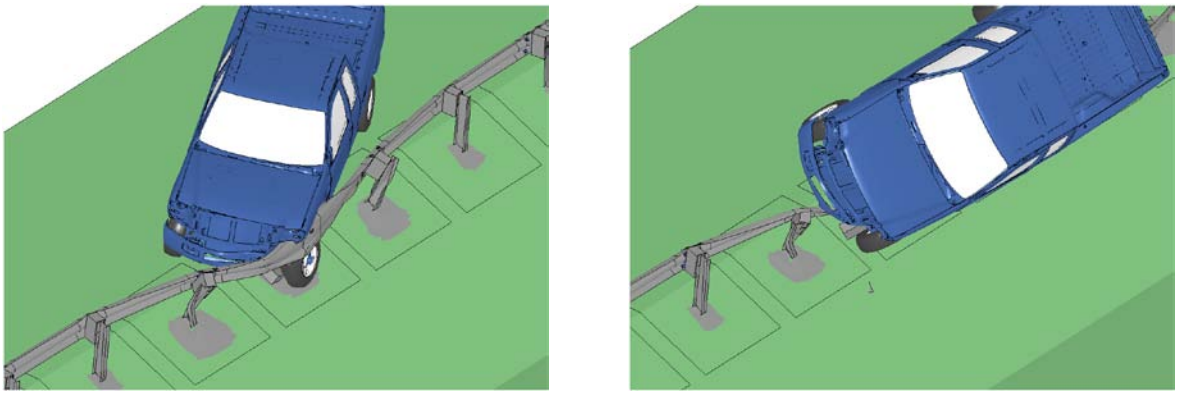

Fig. 4.14: Two instances of vehicle impacting the single-face W-beam on the 2.5:1 slope at 70 mph and 30°.

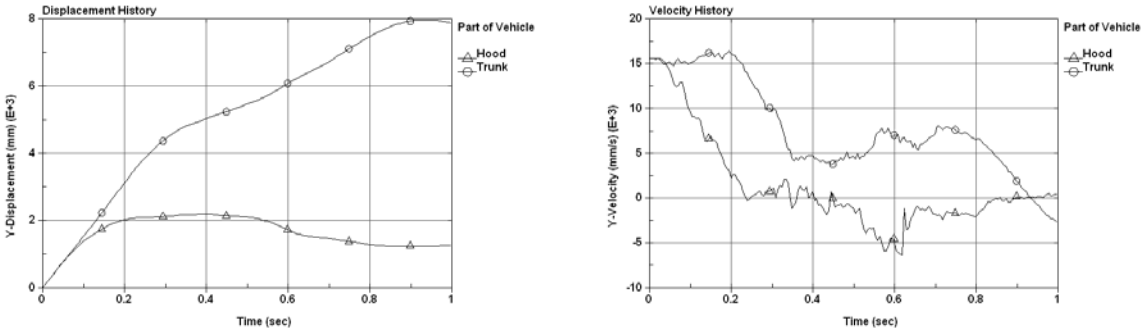


Traversal displacements Traversal velocities

Fig. 4.15: Time histories of traversal displacements and velocities of the vehicle impacting the single-face W-beam on the 2.5:1 slope at 70 mph and 30° ('trunk' means 'bed' on the truck).

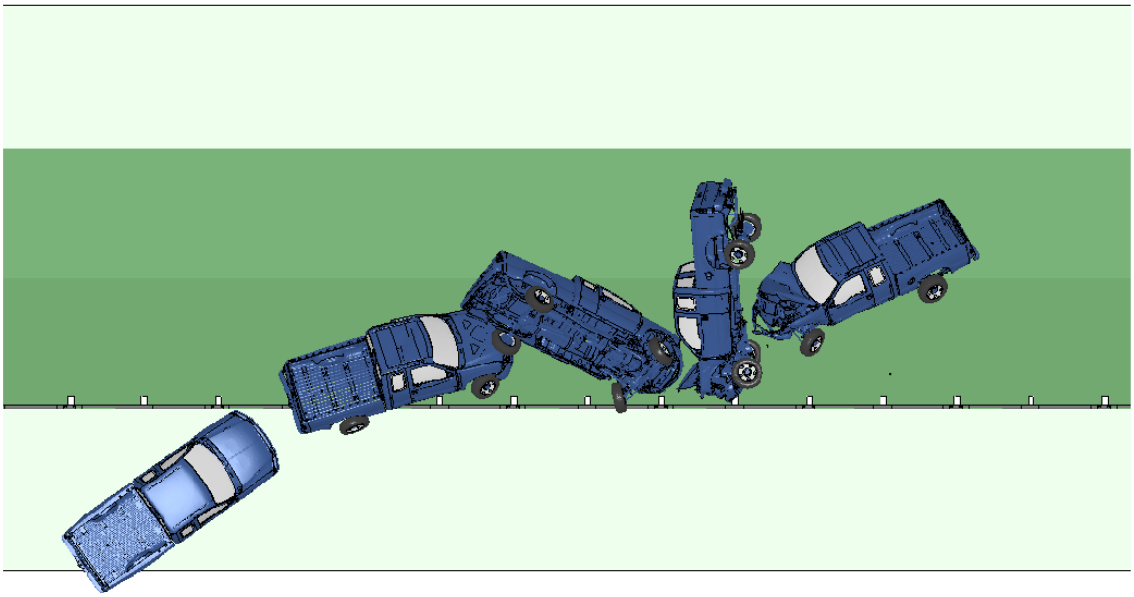

Fig. 4.16: Vehicle impact on the single-face W-beam on the 2.5:1 slope at 70 mph and 35°.

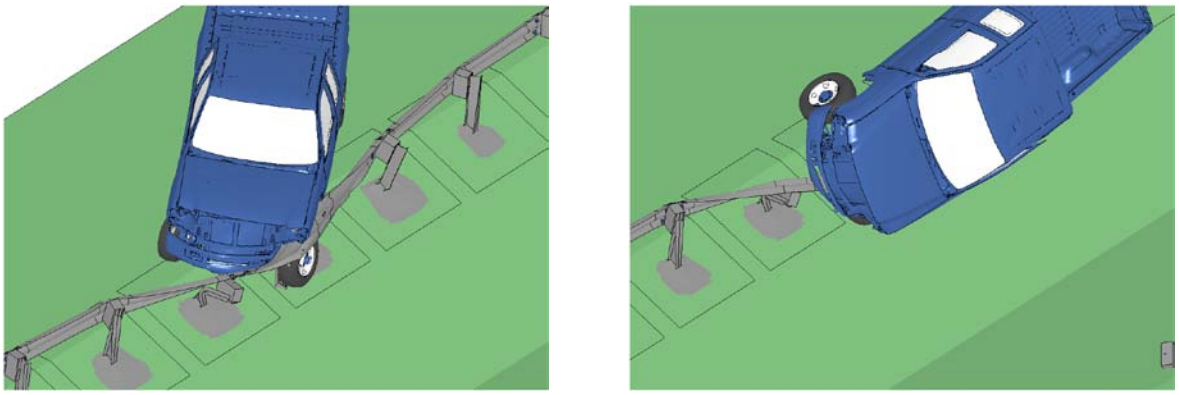

Fig. 4.17: Two instances of vehicle impacting the single-face W-beam on the 2.5:1 slope at 70 mph and 35°.

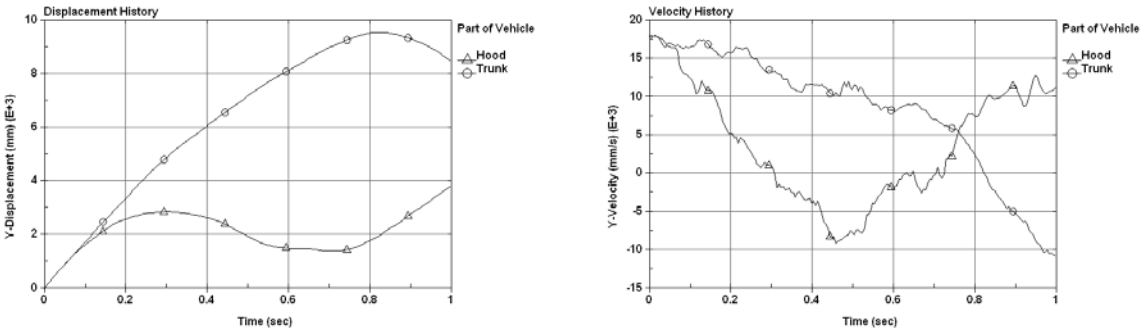


Traversal displacements Traversal velocities

Fig. 4.18: Time histories of traversal displacements and velocities of the vehicle impacting the single-face W-beam on the 2.5:1 slope at 70 mph and 35° ('trunk' means 'bed' on the truck).

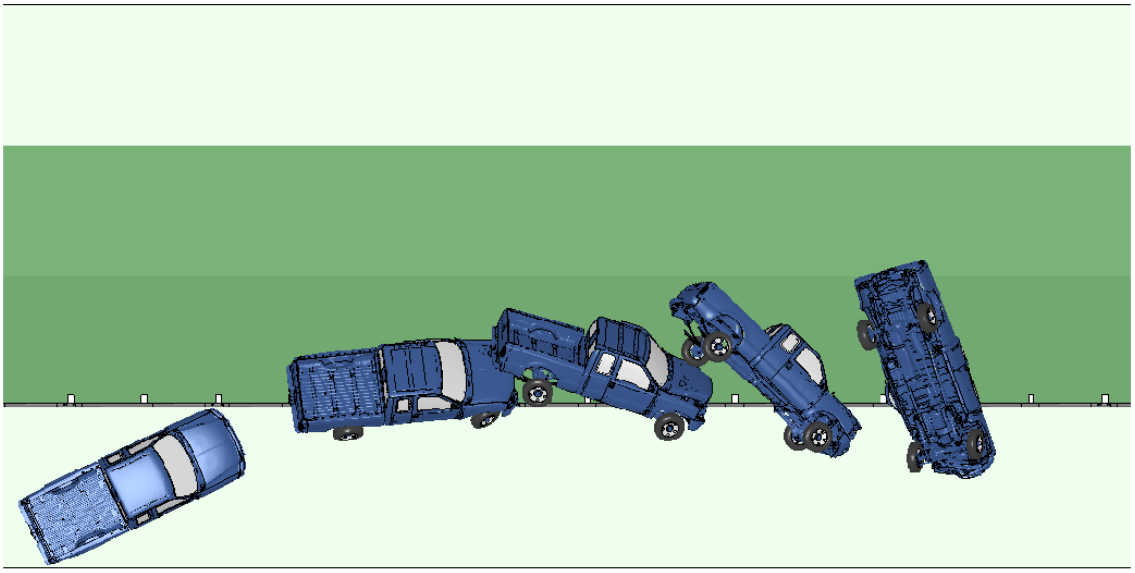

Fig. 4.19: Vehicle impact on the single-face W-beam on the 2.5:1 slope at 75 mph and 25°.

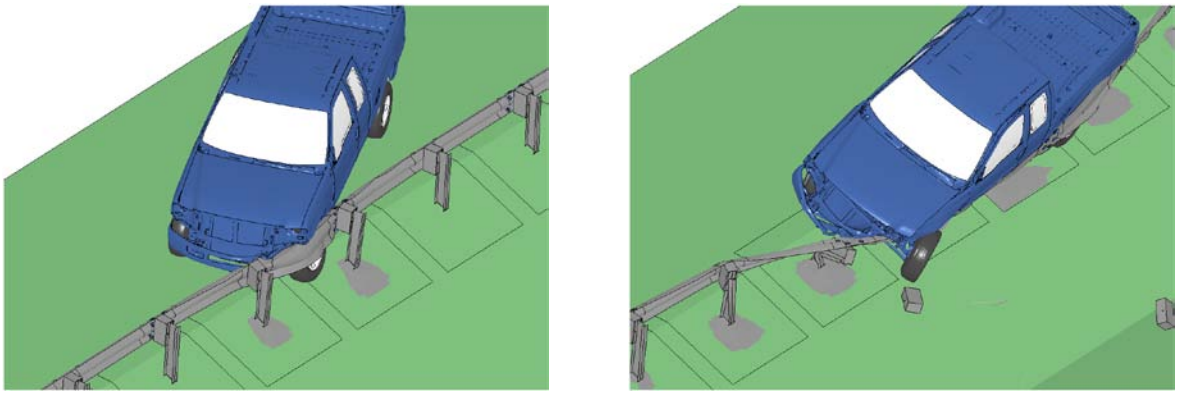

Fig. 4.20: Two instances of vehicle impacting the single-face W-beam on the 2.5:1 slope at 75 mph and 25°.

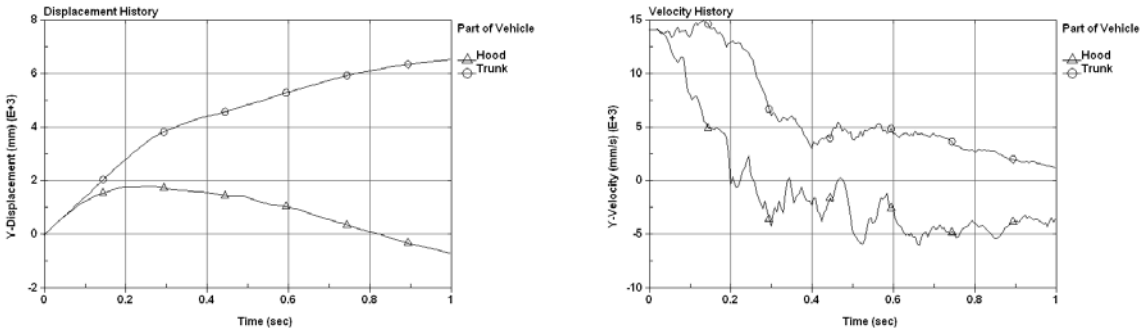


Traversal displacements Traversal velocities

Fig. 4.21: Time histories of traversal displacements and velocities of the vehicle impacting the single-face W-beam on the 2.5:1 slope at 75 mph and 25° ('trunk' means 'bed' on the truck).

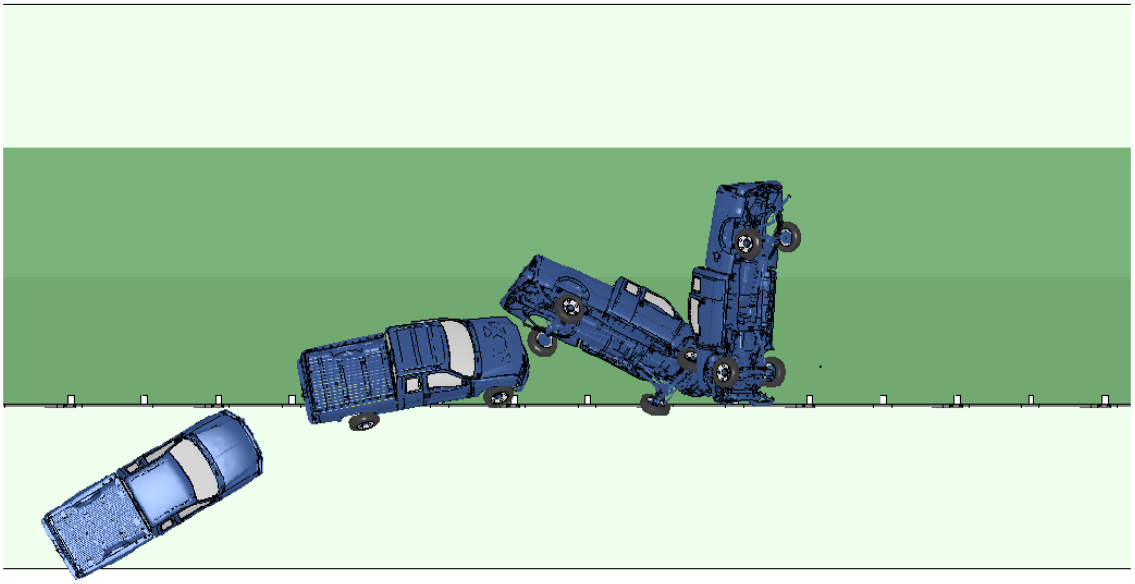

Fig. 4.22: Vehicle impact on the single-face W-beam on the 2.5:1 slope at 75 mph and 30°.

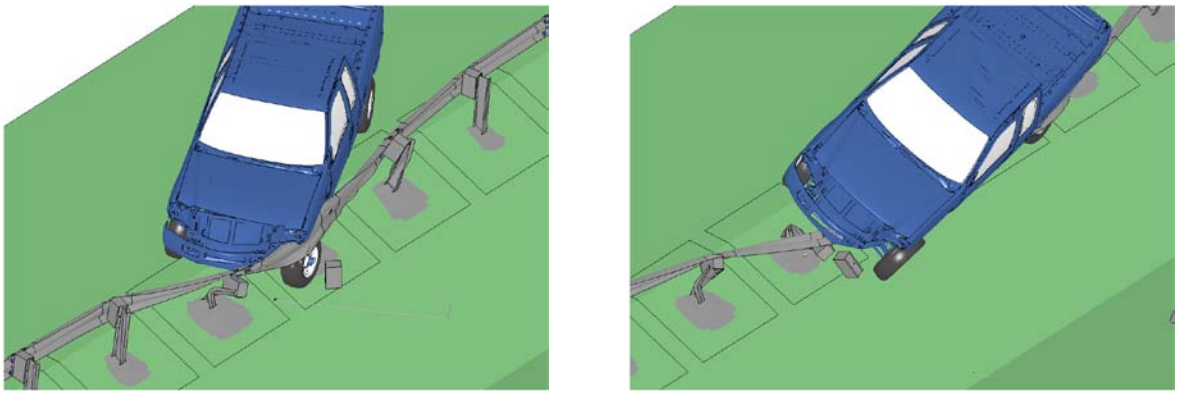

Fig. 4.23: Two instances of vehicle impacting the single-face W-beam on the 2.5:1 slope at 75 mph and 30°.

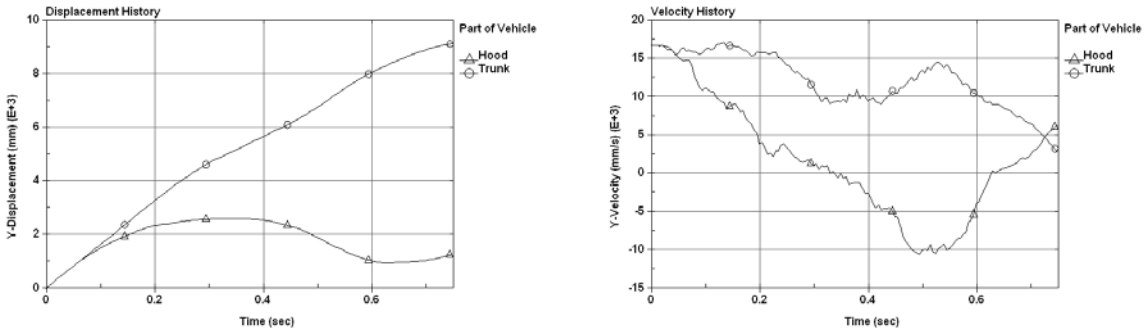


Traversal displacements Traversal velocities

Fig. 4.24: Time histories of traversal displacements and velocities of the vehicle impacting the single-face W-beam on the 2.5:1 slope at 75 mph and 30° (‘trunk’ means ‘bed’ on the truck).

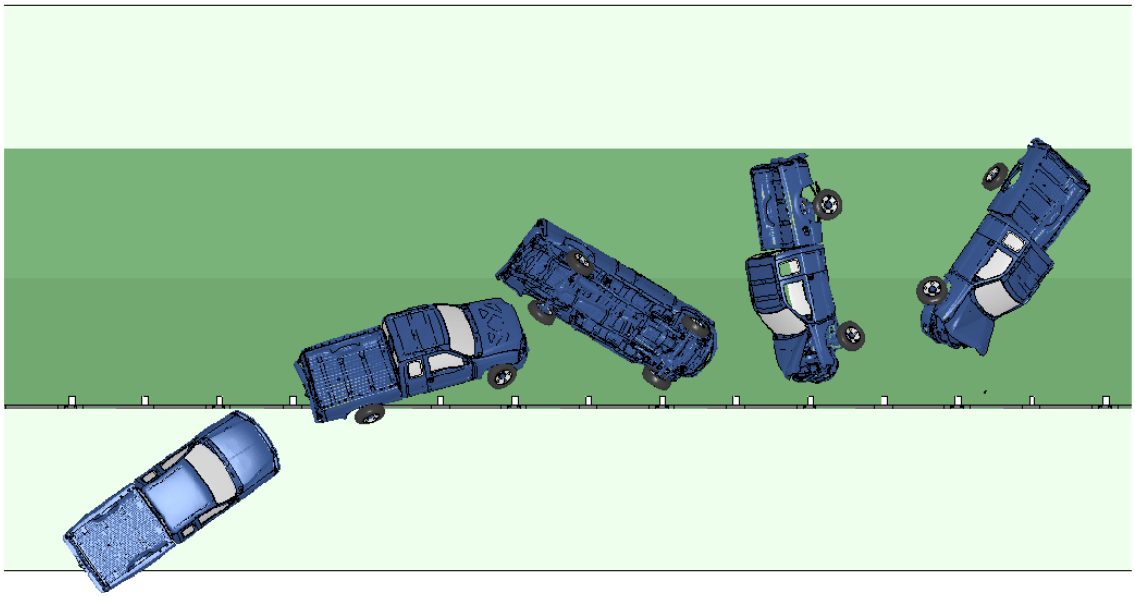

Fig. 4.25: Vehicle impact on the single-face W-beam on the 2.5:1 slope at 75 mph and 35°.

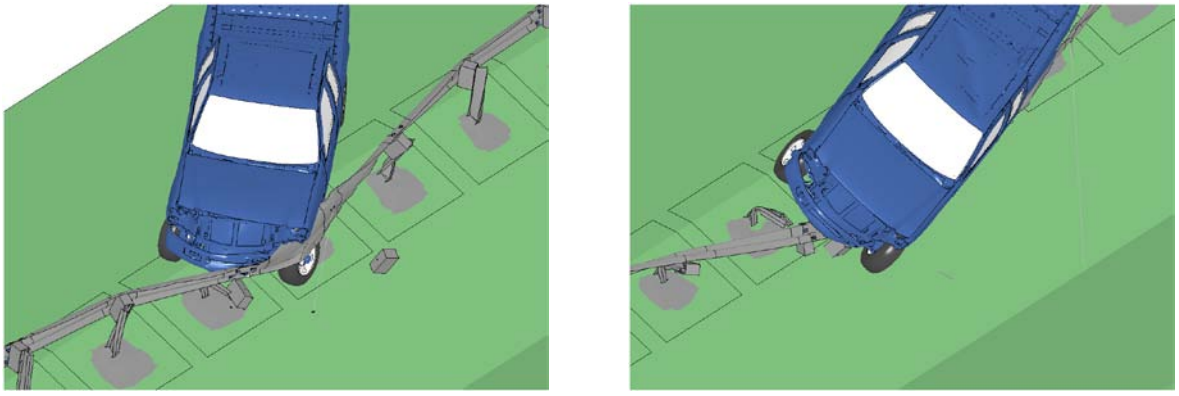

Fig. 4.26: Two instances of vehicle impacting the single-face W-beam on the 2.5:1 slope at 75 mph and 35°.

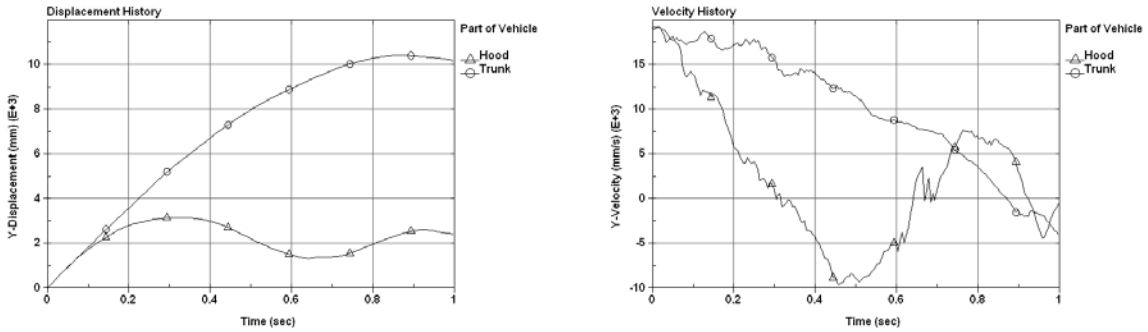


Traversal displacements Traversal velocities

Fig. 4.27: Time histories of traversal displacements and velocities of the vehicle impacting the single-face W-beam on the 2.5:1 slope at 75 mph and 35° ('trunk' means 'bed' on the truck).

In a graph of traversal displacements, the difference between displacements at the hood and bed of the truck served as an indication of vehicle rotations and redirections. For example, the increasing difference before 0.4 sec in Fig. 4.27 indicated a redirection of the vehicle, because the bed displaced more than the hood from their respective initial locations. The displacement curves mainly showed vehicle's horizontal spins and did not give a clear indication of vehicle rollover. The curves of traversal velocities were used to determine if a redirection was safe or temporary. For example, if the vehicle was redirected but the traversal velocity remained large, the redirection would likely be followed by a rollover.

For the single-face W-beam installed on the 4:1 slope, two impact scenarios were evaluated: 62 and 70 mph (100 and 112.6 km/hr), both at a 25° angle. The vehicle's responses were similar to but less severe than the corresponding cases on the 2.5:1 slope. The vehicle was shown being redirected in both cases. The results of these two cases are shown in Figs. 4.28 to 4.33.

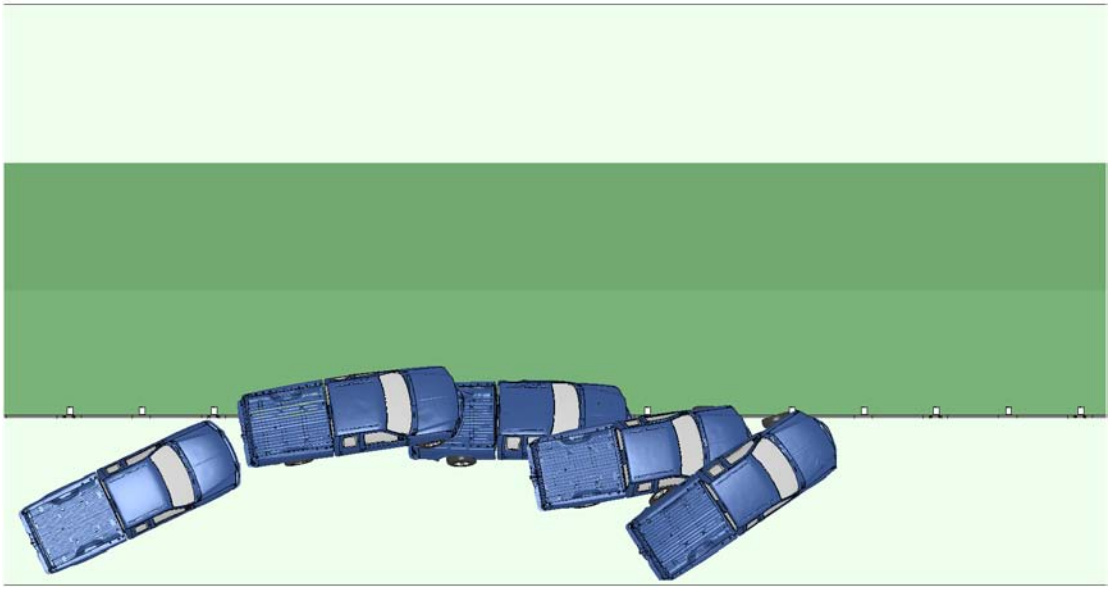

Fig. 4.28: Vehicle impact on the single-face W-beam on the 4:1 slope at 62 mph and 25°.

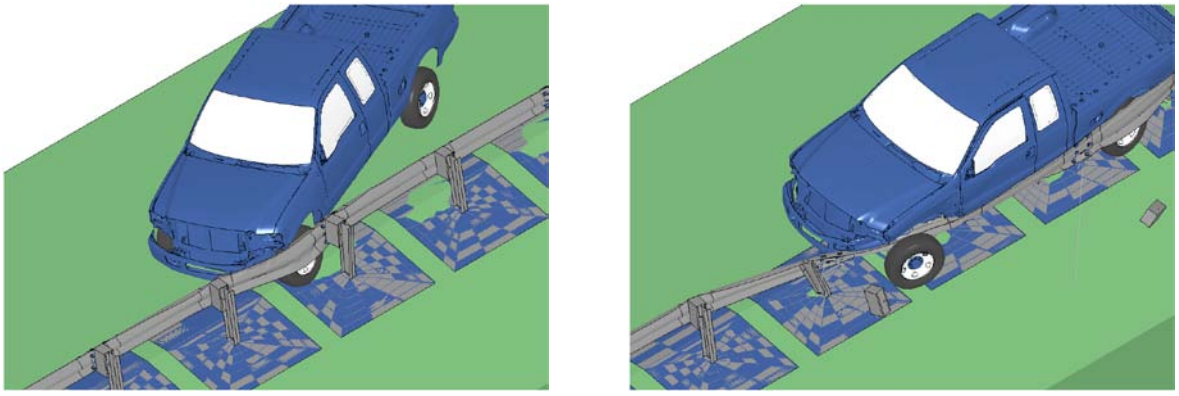

Fig. 4.29: Two instances of vehicle the impacting single-face W-beam on the 4:1 slope at 62 mph and 25°.

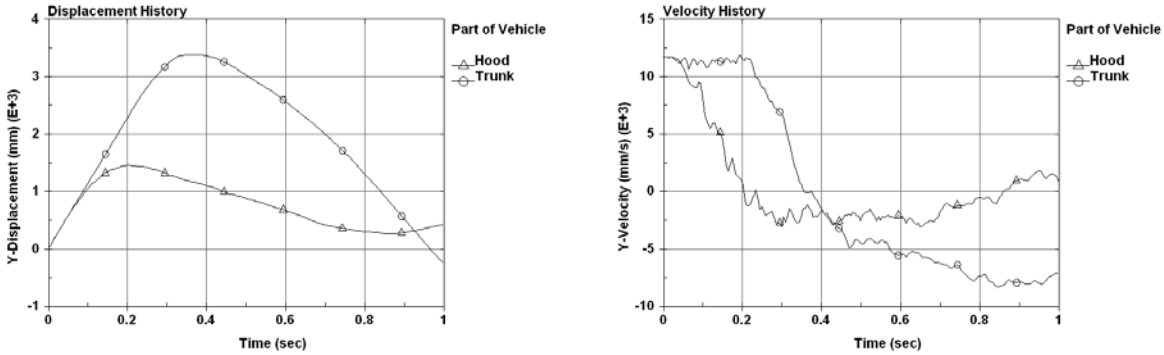


Traversal displacements Traversal velocities

Fig. 4.30: Time histories of traversal displacements and velocities of the vehicle impacting the single-face W-beam on the 4:1 slope at 62 mph and 25° ('trunk' means 'bed' on the truck).

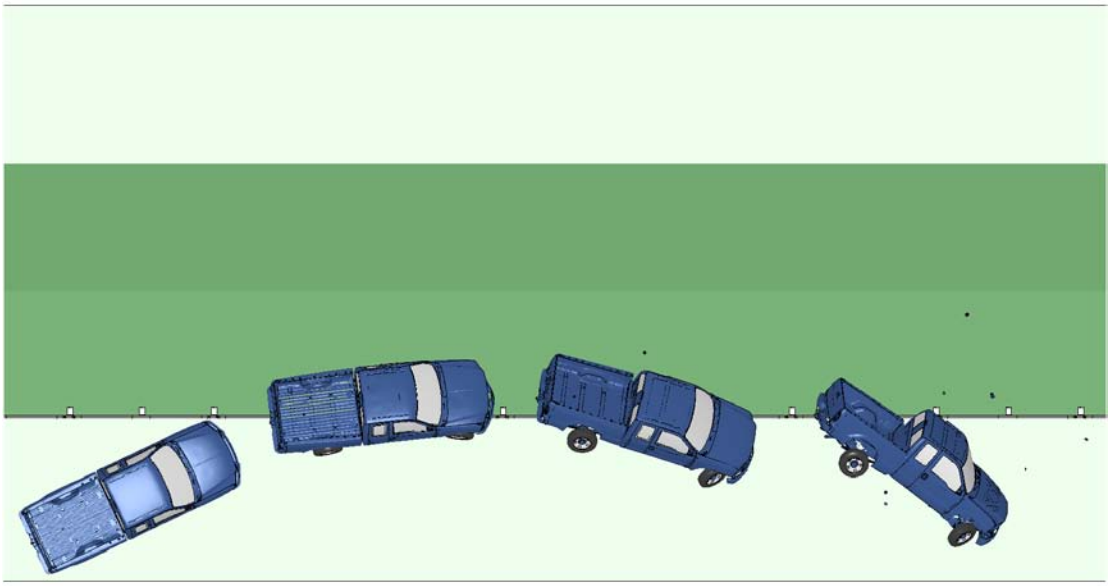

Fig. 4.31: Vehicle impact on the single-face W-beam on the 4:1 slope at 70 mph and 25°.

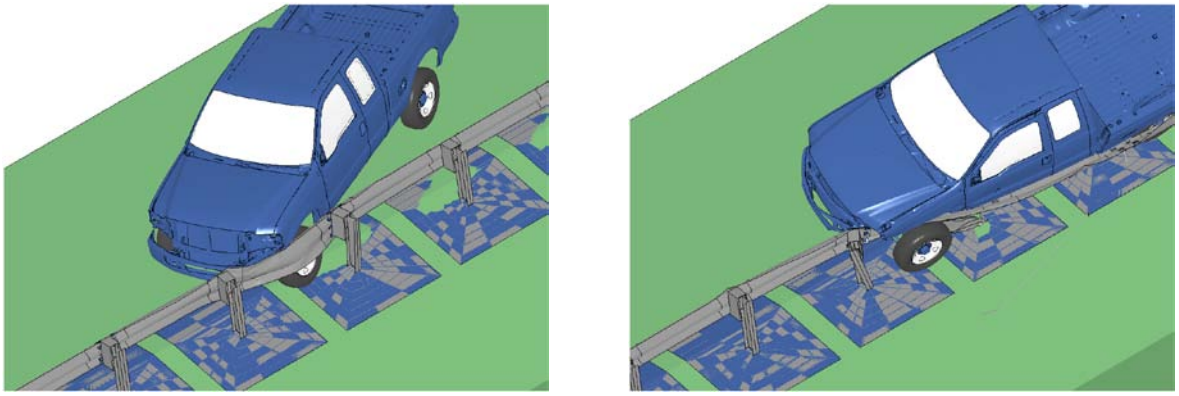

Fig. 4.32: Two instances of vehicle impacting the single-face W-beam on the 4:1 slope at 70 mph and 25°.

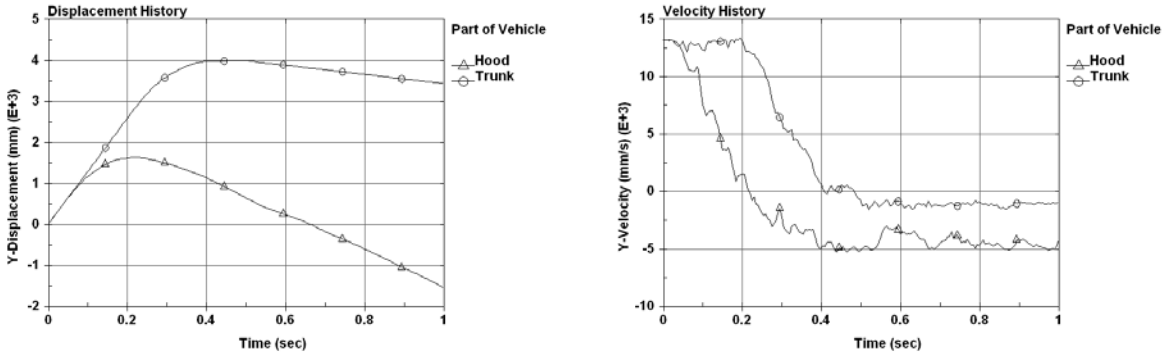


Traversal displacements Traversal velocities

Fig. 4.33: Time histories of traversal displacements and velocities of the vehicle impacting the single-face W-beam on the 4:1 slope at 70 mph and 25° ('trunk' means 'bed' on the truck).

## 4.2 The Double-face W-beam

In this project, a single line of double-face W-beam guardrail was used to replace the two lines of single-face W-beam. The double-face W-beam was installed on the 2.5:1 slope, with the front rail surface aligned with the borderline between the slope and its adjacent shoulder. The double-face W-beam was subject to impacts from both sides.

### *4.2.1 Design #1: Double-face W-beam with Same Rail Heights*

In Design #1 of the double-face W-beam, both front-side and backside rails had the same height measured from the top of rail to the shoulder ground. Simulation results of Design #1 are summarized in Table 4.2 for both front-side and backside impacts.

Table 4.2: Simulation results of the double-face W-beam, Design #1

| **Impact Side** | **Impact Angle** | **Impact Speed** | | |
|---|---|---|---|---|
| | | 62 mph (100 km/hr ) | 70 mph (112.6 km/hr) | 75 mph (120.7 km/hr) |
| Front | 25° | Vehicle redirected on the shoulder | Vehicle redirected on the shoulder | Vehicle redirected on the shoulder |
| | 30° | Vehicle redirected with a tendency of rollover towards the ditch | Vehicle redirected followed by rollover towards the ditch | Vehicle redirected followed by a rollover towards the ditch |
| | 35° | Vehicle redirected followed by a rollover towards the ditch | Vehicle rolled over towards the ditch | Vehicle rolled over towards the ditch |
| Back | 25° | Vehicle redirected in the ditch | Vehicle redirected in the ditch | Vehicle redirected in the ditch |
| | 30° | Vehicle not redirected but retained in the ditch | Vehicle redirected in the ditch | Vehicle redirected in the ditch |
| | 35° | Vehicle redirected in the ditch | Vehicle redirected in the ditch | Vehicle redirected in the ditch |

In low-angle (i.e., 25°) front-side impacts, the double-face W-beam was found to perform better than the single-face W-beam. For example, in all three 25° impacts, the vehicle did not have a rollover or the tendency of rollover after being redirected. Recall in the cases of the

single-face W-beam, the vehicle tended to roll over in 25° impacts at 70 and 75 mph (112.6 and 120.7 km/hr). The added backside rail increased the stiffness and strength of the W-beam, which in turn helped vehicle redirection and reduced the tendency of vehicle rollover. For 30° front-side impacts, the vehicle was redirected and exhibited a tendency of rollover in the cases of 62 and 70 mph (100 and 112.6 km/hr). At 30° and 75 mph (120.7 km/hr), the vehicle was redirected but rolled over towards the ditch. For 35° front-side impact at 62 mph (100 km/hr), the vehicle was redirected and then rolled over towards the ditch. For the other two cases of 35° front-side impacts, the vehicle simply rolled over towards the ditch. The simulation results showed that vehicle rollover was more sensitive to impact angles than impact speeds. This observation is the same as that on the single-face W-beam. Figures 4.34 to 4.60 show the vehicle's displacement paths, detailed views of vehicle-barrier interactions, and time histories of the vehicle's traversal displacements and velocities for all front-side impacts.

For all backside impacts (see Figs. 4.61 to 4.87), the double-face W-beam was able to redirect and/or retain the vehicle within the ditch. At 62 mph (100 km/hr), the vehicle was redirected for the 25° and 35° impacts, and was retained on the ditch slope for the 30° impact with no redirection. In this 30° impact, the vehicle was locked with the post upon impact at the left corner and thus was not redirected. In addition, the vehicle's impact speed was reduced compared to the initial velocity after going up a 2.5:1 slope. This was shown by the simulation results in which the vehicle was actually bounced back with near-zero velocity on the hood (see Figs. 4.64 and 4.66). In the case of 35° and 75 mph (120.7 km/hr), the vehicle was redirected and retained on the slope. In general, Design #1 of the double-face W-beam performed better than the single-face W-beam.

### *4.2.2 Design #2: Double-face W-beam with Different Rail Heights*

Table 4.3 summarizes the simulation results of Design #2 of the double-face W-beam in which the backside rail is 7.1 in. (0.18 m) lower than the front-side rail.

Table 4.3: Simulation results of the double-face W-beam, Design #2

| **Impact Side** | **Impact Angle** | **Impact Speed** | | |
|---|---|---|---|---|
| | | 62 mph (100 km/hr ) | 70 mph (112.6 km/hr) | 75 mph (120.7 km/hr) |
| Front | 25° | Vehicle redirected on the shoulder | Vehicle redirected on the shoulder | Vehicle redirected on the shoulder |
| | 30° | Vehicle redirected on the shoulder | Vehicle redirected followed by a rollover towards the ditch | Vehicle redirected followed by a rollover towards the ditch |
| | 35° | Vehicle rolled over towards the ditch | Vehicle rolled over towards the ditch | Vehicle rolled over towards the ditch |
| Back | 25° | Vehicle redirected in the ditch | Vehicle redirected in the ditch | Vehicle redirected in the ditch |
| | 30° | Vehicle not redirected but retained in the ditch | Vehicle redirected in the ditch | Vehicle redirected in the ditch |
| | 35° | Vehicle not redirected but retained in the ditch | Vehicle redirected in the ditch | Vehicle redirected in the ditch |

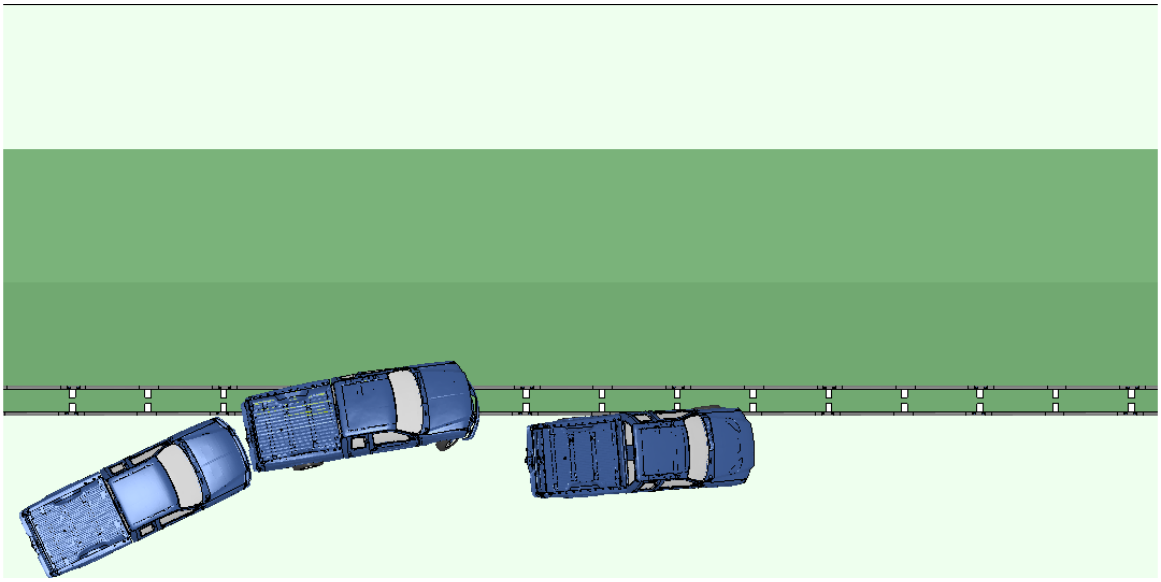

Fig. 4.34: Front-side impact on the double-face W-beam (Design #1) at 62 mph and 25°.

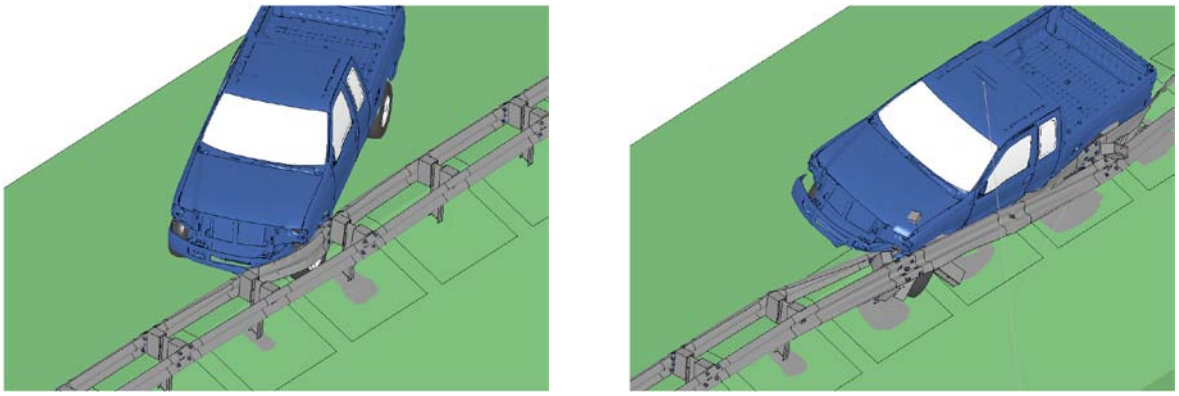

Fig. 4.35: Two instances of front-side impact on the double-face W-beam (Design #1) at 62 mph and 25°.

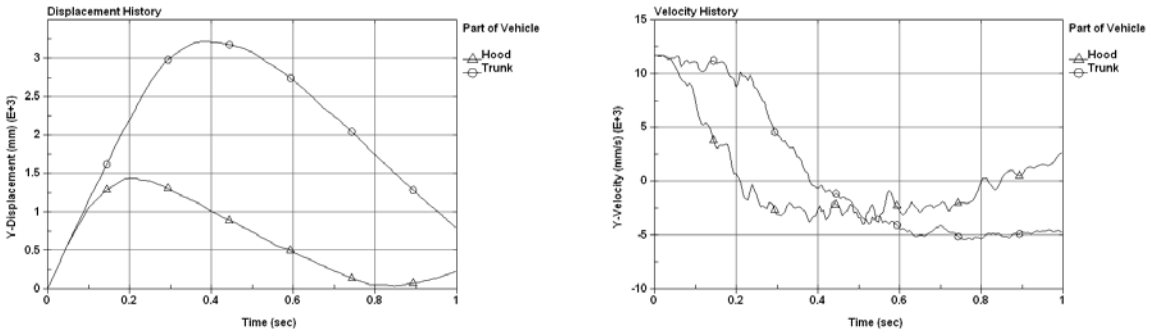


Traversal displacements Traversal velocities

Fig. 4.36: Time histories of traversal displacements and velocities of front-side impact on the double-face W-beam (Design #1) at 62 mph and 25° (‘trunk’ means ‘bed’ on the truck).

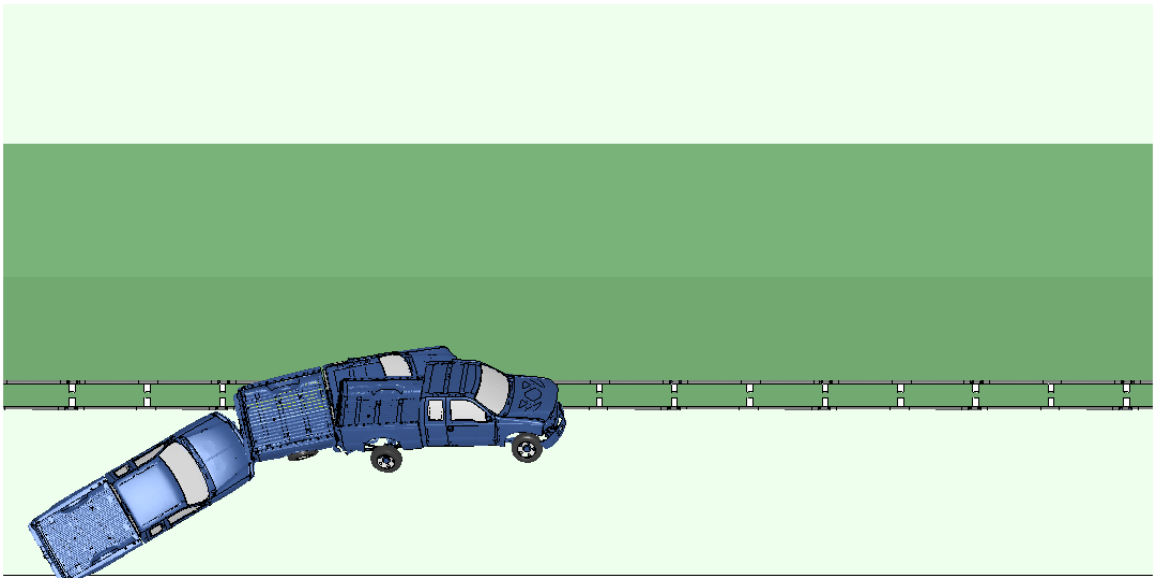

Fig. 4.37: Front-side impact on the double-face W-beam (Design #1) at 62 mph and 30°.

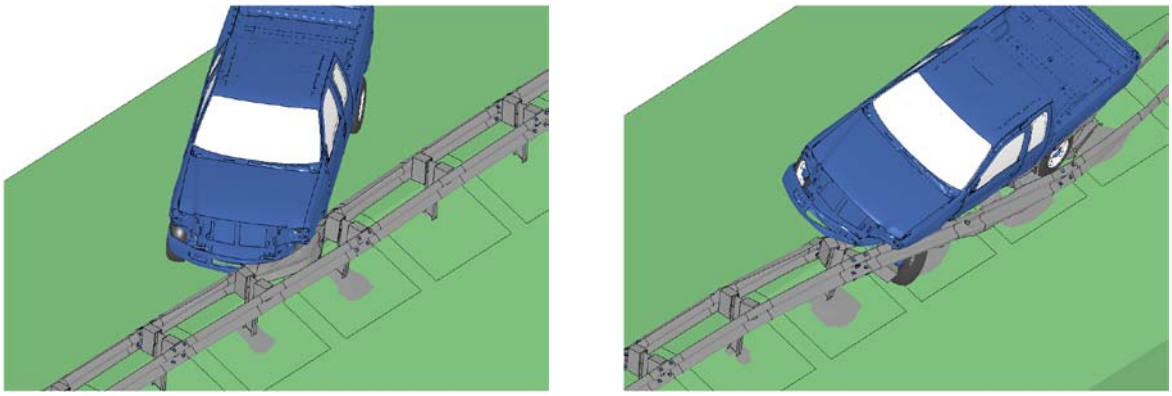

Fig. 4.38: Two instances of front-side impact on the double-face W-beam (Design #1) at 62 mph and 30°.

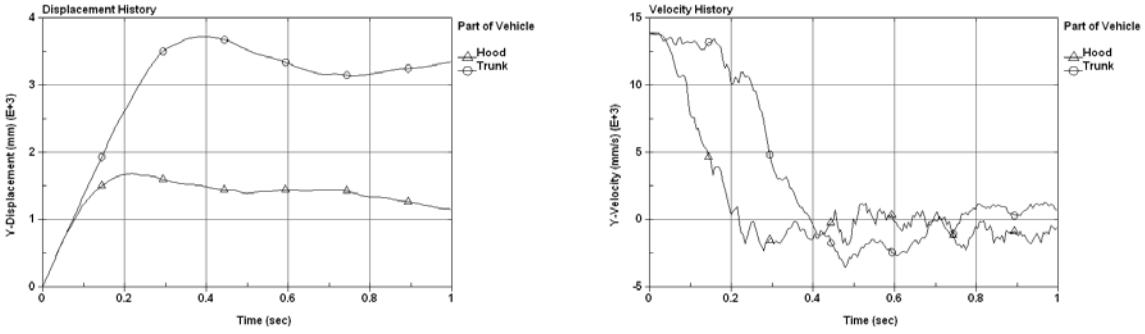


Traversal displacements Traversal velocities

Fig. 4.39: Time histories of traversal displacements and velocities of front-side impact on the double-face W-beam (Design #1) at 62 mph and 30° (‘trunk’ means ‘bed’ on the truck).

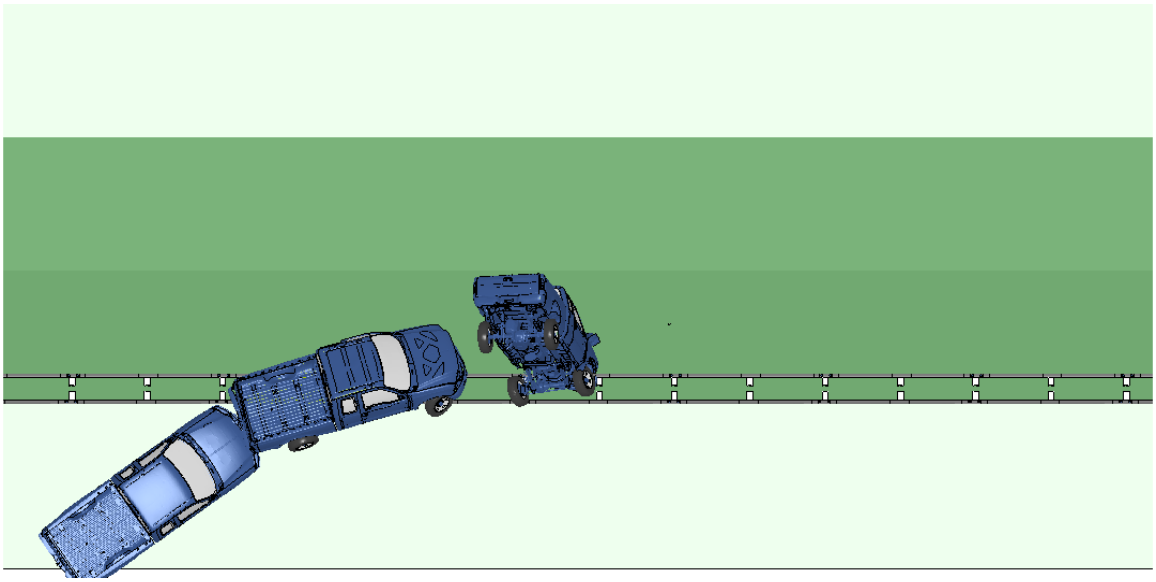

Fig. 4.40: Front-side impact on the double-face W-beam (Design #1) at 62 mph and 35°.

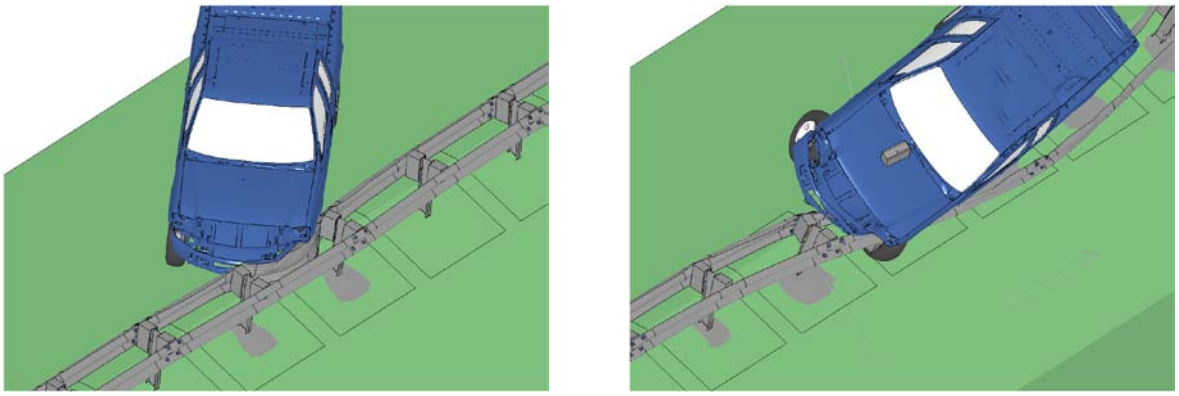

Fig. 4.41: Two instances of front-side impact on the double-face W-beam (Design #1) at 62 mph and 35°.

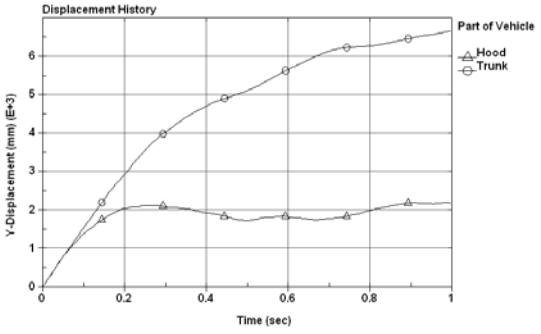


Traversal displacements

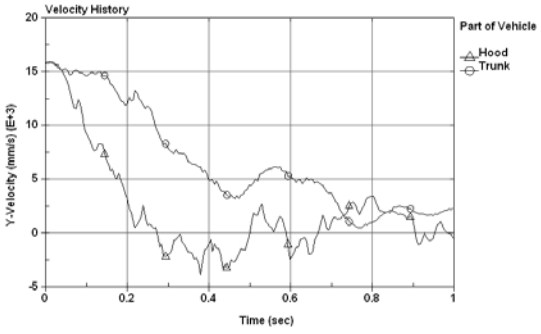


Traversal velocities

Fig. 4.42: Time histories of traversal displacements and velocities of front-side impact on the double-face W-beam (Design #1) at 62 mph and 35° (‘trunk’ means ‘bed’ on the truck).

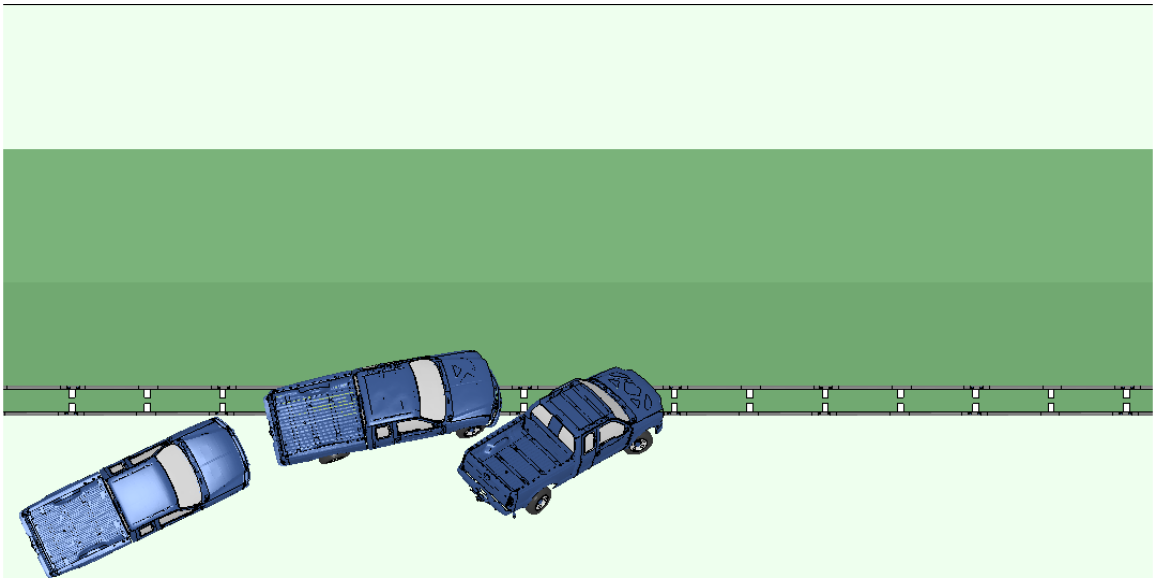

Fig. 4.43: Front-side impact on the double-face W-beam (Design #1) at 70 mph and 25°.

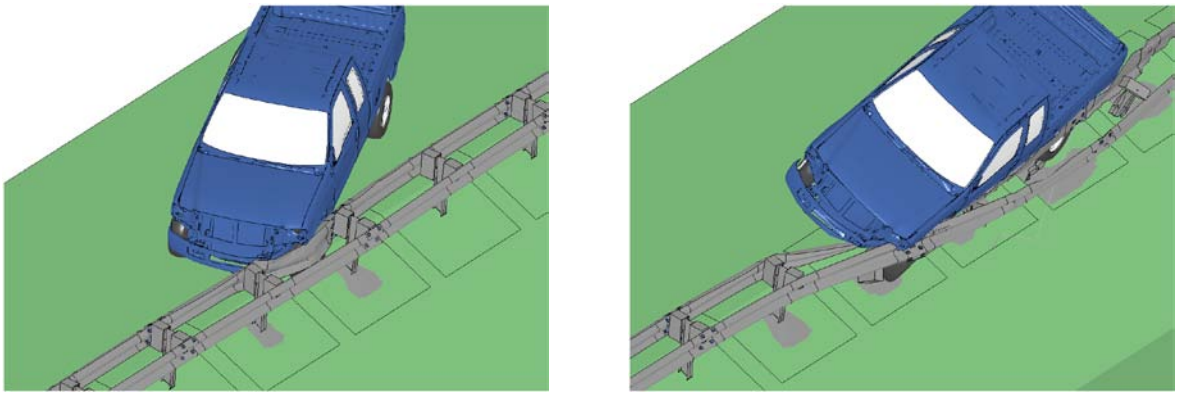

Fig. 4.44: Two instances of front-side impact on the double-face W-beam (Design #1) at 70 mph and 25°.

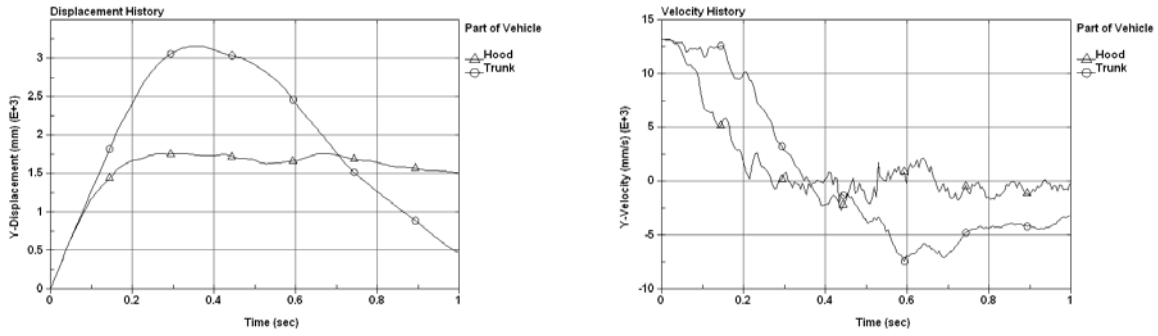


Traversal displacements Traversal velocities

Fig. 4.45: Time histories of traversal displacements and velocities of front-side impact on the double-face W-beam (Design #1) at 70 mph and 25° (‘trunk’ means ‘bed’ on the truck).

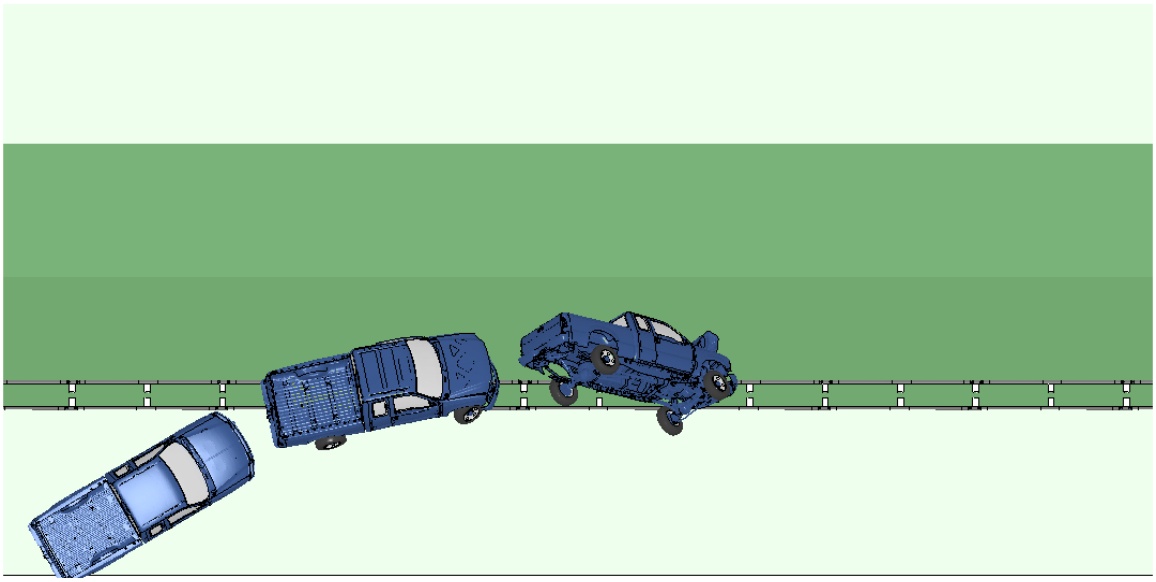

Fig. 4.46: Front-side impact on the double-face W-beam (Design #1) at 70 mph and 30°.

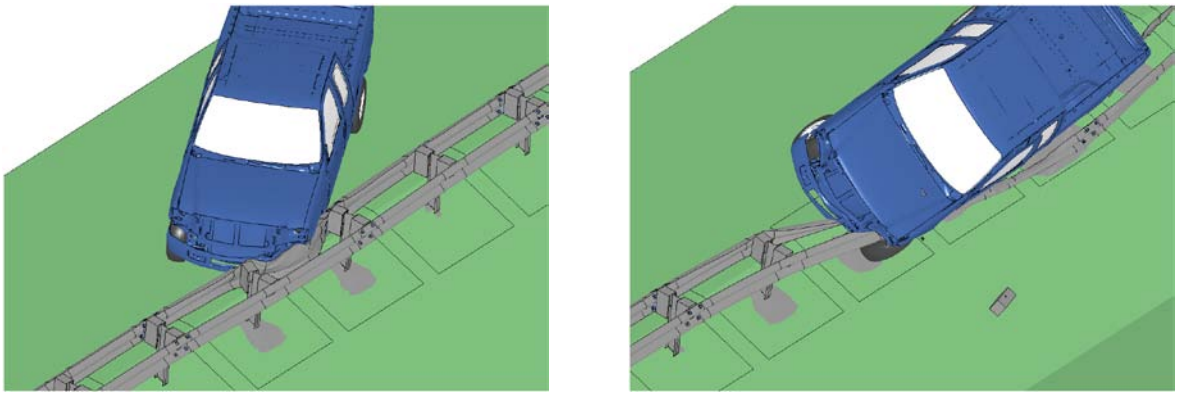

Fig. 4.47: Two instances of front-side impact on the double-face W-beam (Design #1) at 70 mph and 30°.

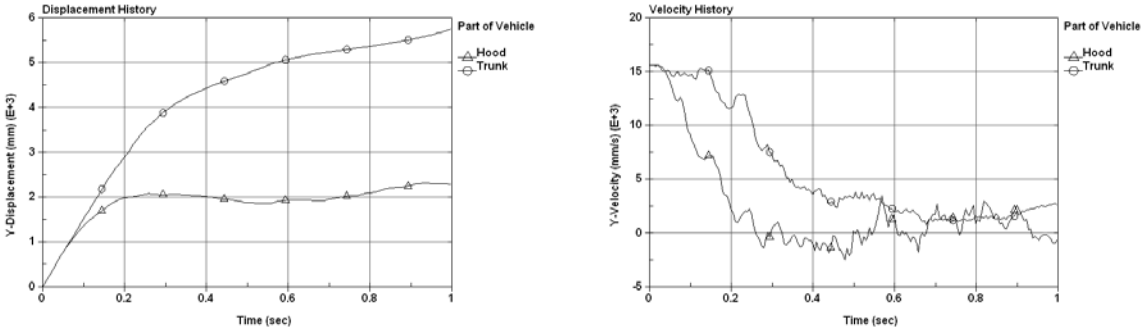


Traversal displacements Traversal velocities

Fig. 4.48: Time histories of traversal displacements and velocities of front-side impact on the double-face W-beam (Design #1) at 70 mph and 30° (‘trunk’ means ‘bed’ on the truck).

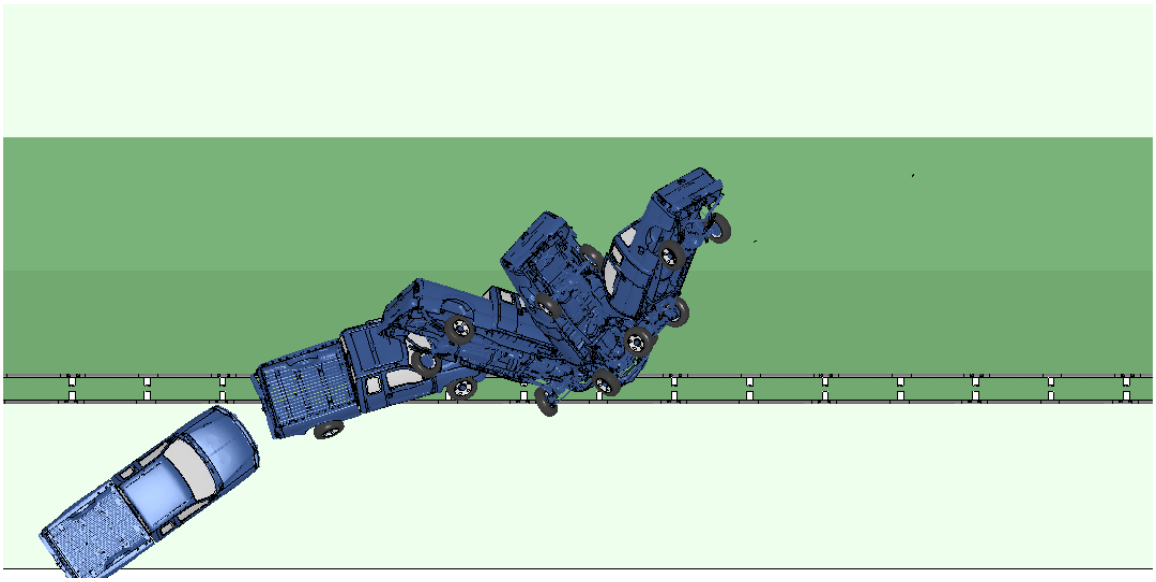

Fig. 4.49: Front-side impact on the double-face W-beam (Design #1) at 70 mph and 35°.

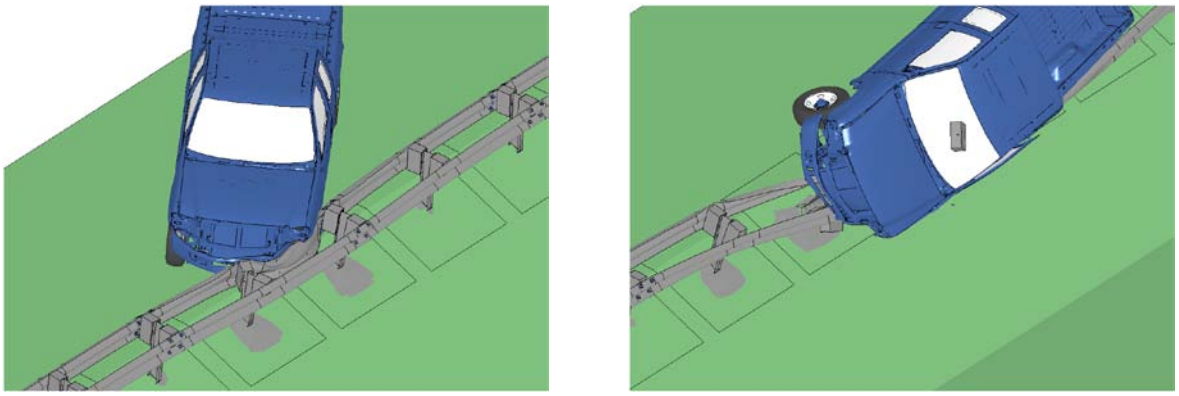

Fig. 4.50: Two instances of front-side impact on the double-face W-beam (Design #1) at 70 mph and 35°.

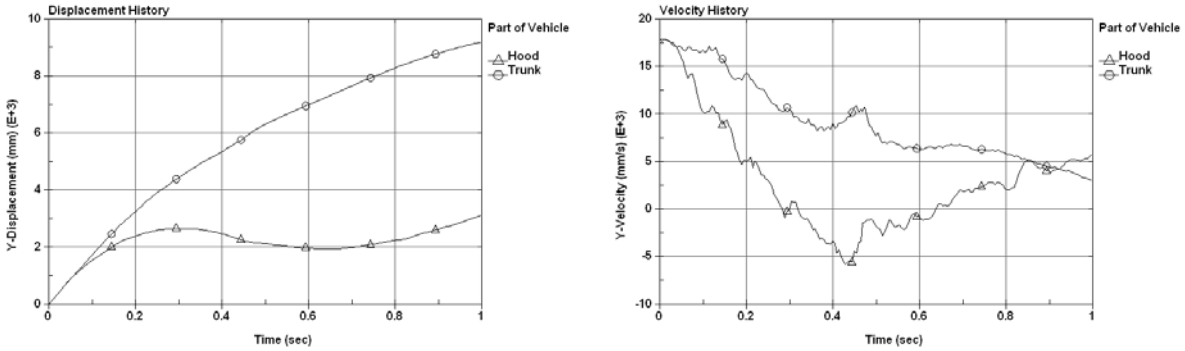


Traversal displacements Traversal velocities

Fig. 4.51: Time histories of traversal displacements and velocities of front-side impact on the double-face W-beam (Design #1) at 70 mph and 35° (‘trunk’ means ‘bed’ on the truck).

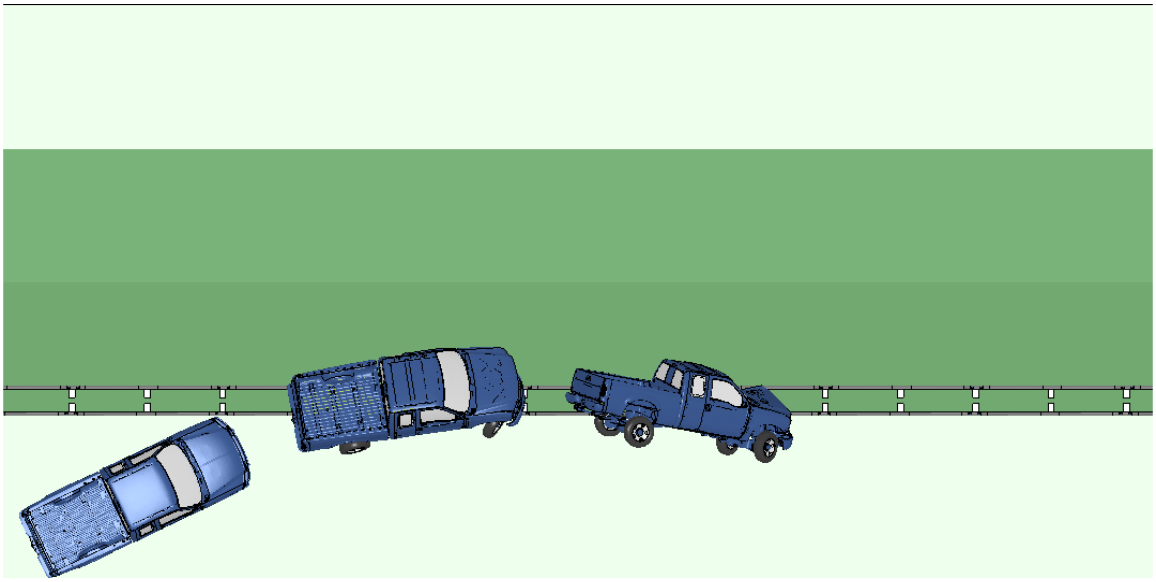

Fig. 4.52: Front-side impact on the double-face W-beam (Design #1) at 75 mph and 25°.

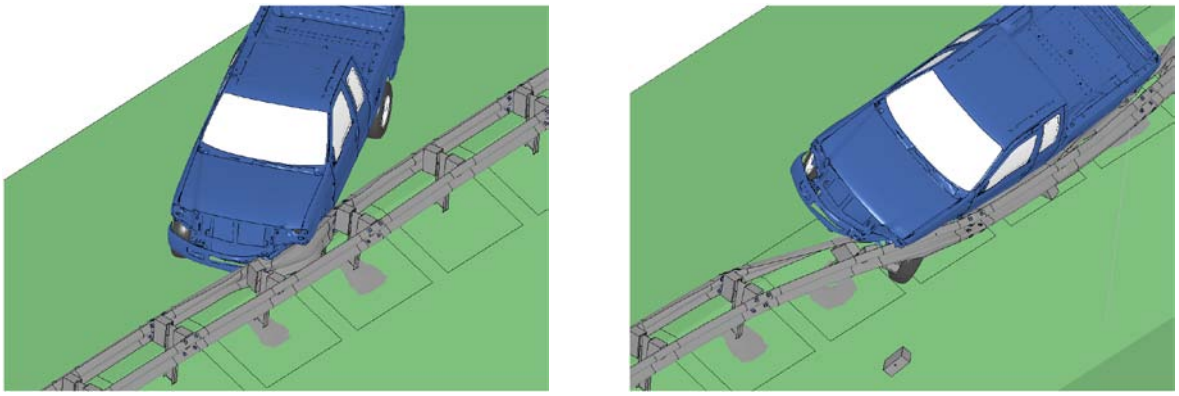

Fig. 4.53: Two instances of front-side impact on the double-face W-beam (Design #1) at 75 mph and 25°.

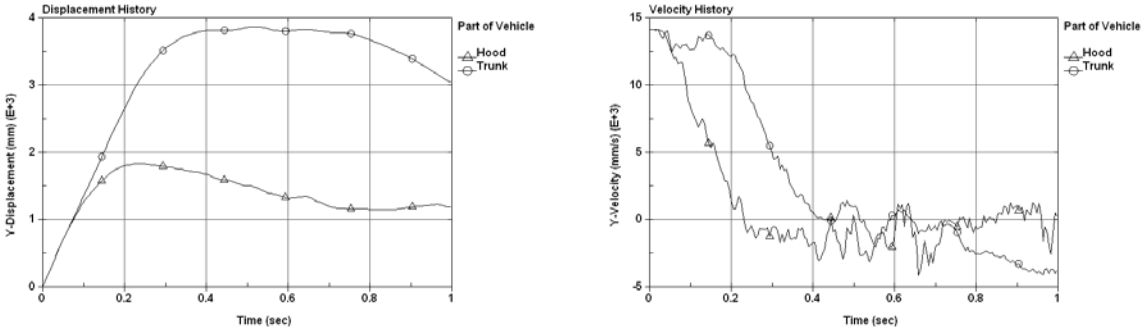


Traversal displacements Traversal velocities

Fig. 4.54: Time histories of traversal displacements and velocities of front-side impact on the double-face W-beam (Design #1) at 75 mph and 25° (‘trunk’ means ‘bed’ on the truck).

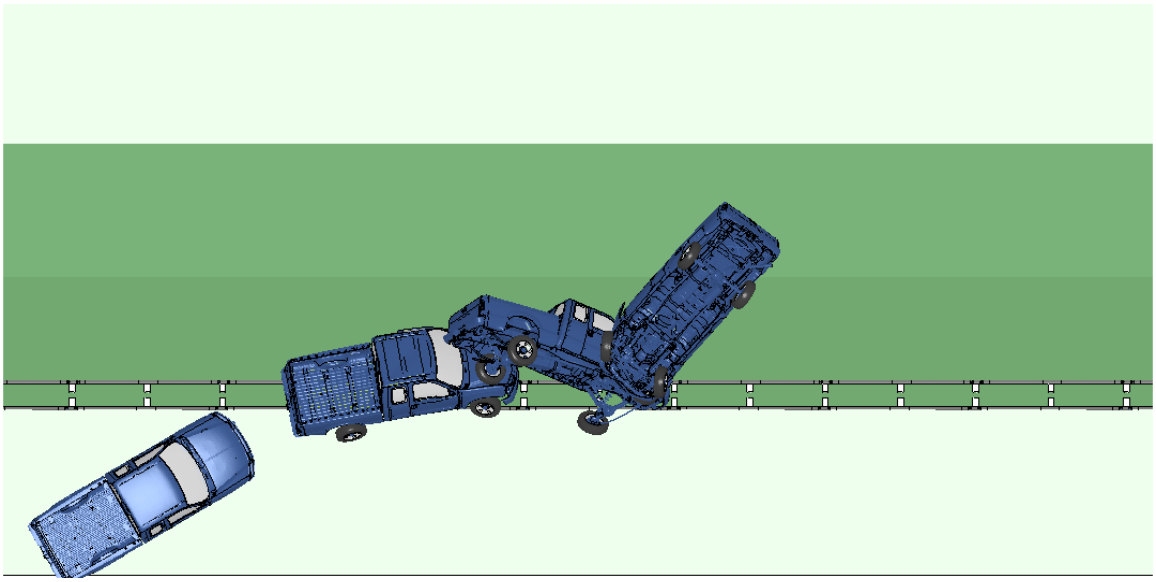

Fig. 4.55: Front-side impact on the double-face W-beam (Design #1) at 75 mph and 30°.

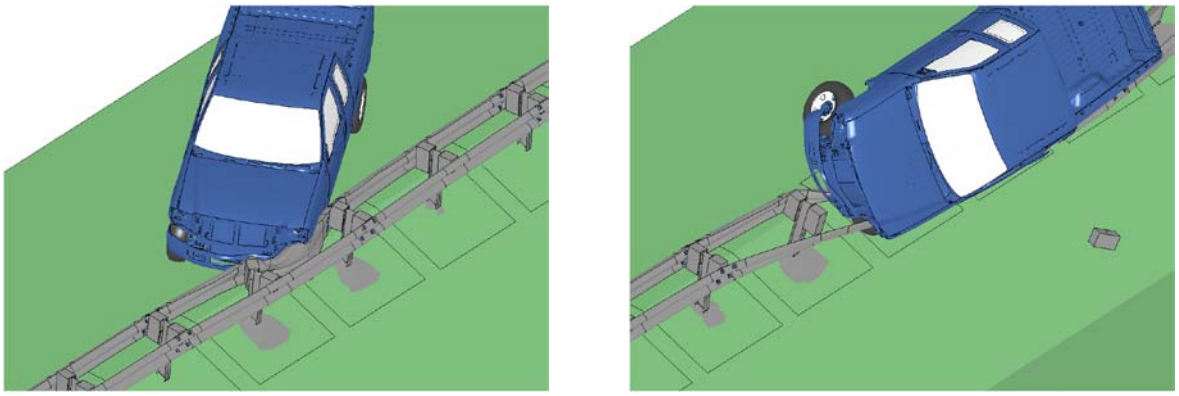

Fig. 4.56: Two instances of front-side impact on the double-face W-beam (Design #1) at 75 mph and 30°.

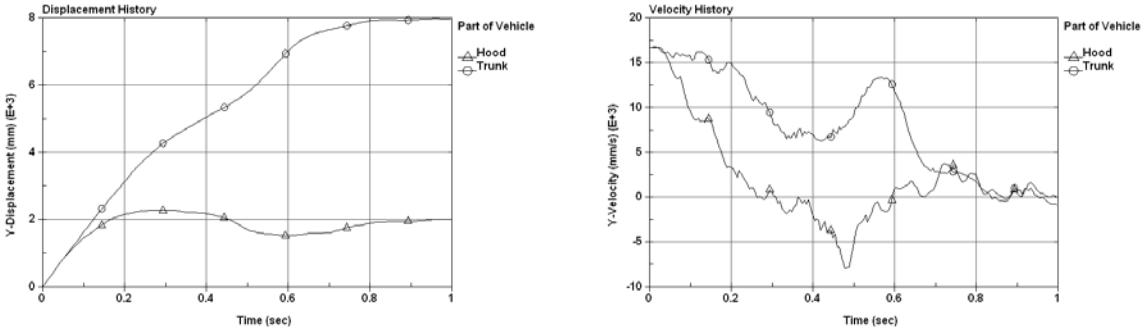


Traversal displacements Traversal velocities

Fig. 4.57: Time histories of traversal displacements and velocities of front-side impact on the double-face W-beam (Design #1) at 75 mph and 30° ('trunk' means 'bed' on the truck).

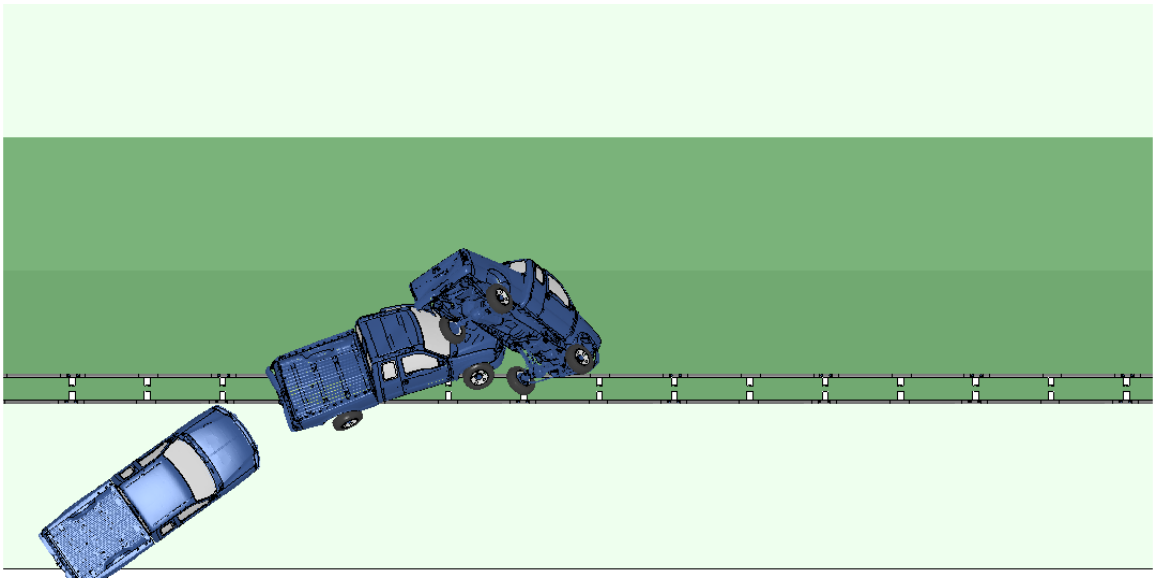

Fig. 4.58: Front-side impact on the double-face W-beam (Design #1) at 75 mph and 35°.

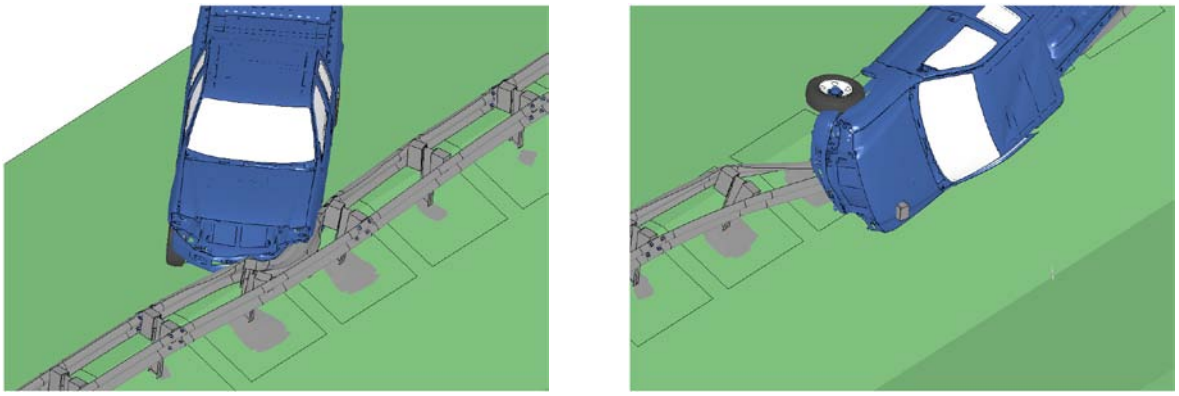

Fig. 4.59: Two instances of front-side impact on the double-face W-beam (Design #1) at 75 mph and 35°.

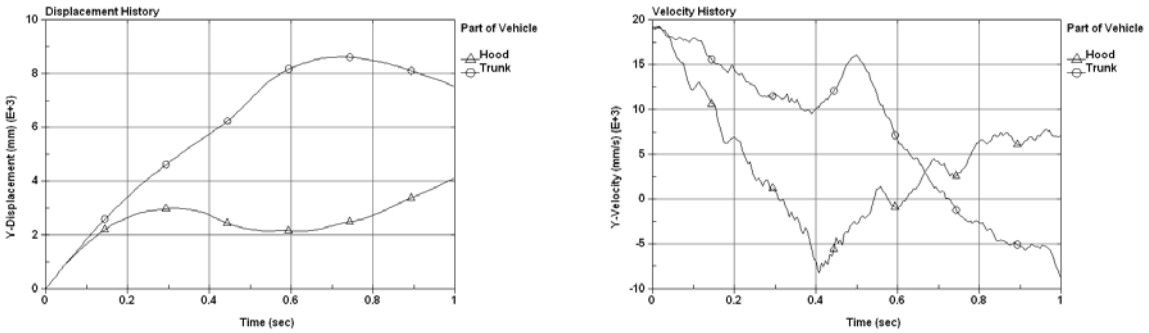


Traversal displacements Traversal velocities

Fig. 4.60: Time histories of traversal displacements and velocities of front-side impact on the double-face W-beam (Design #1) at 75 mph and 35° (‘trunk’ means ‘bed’ on the truck).

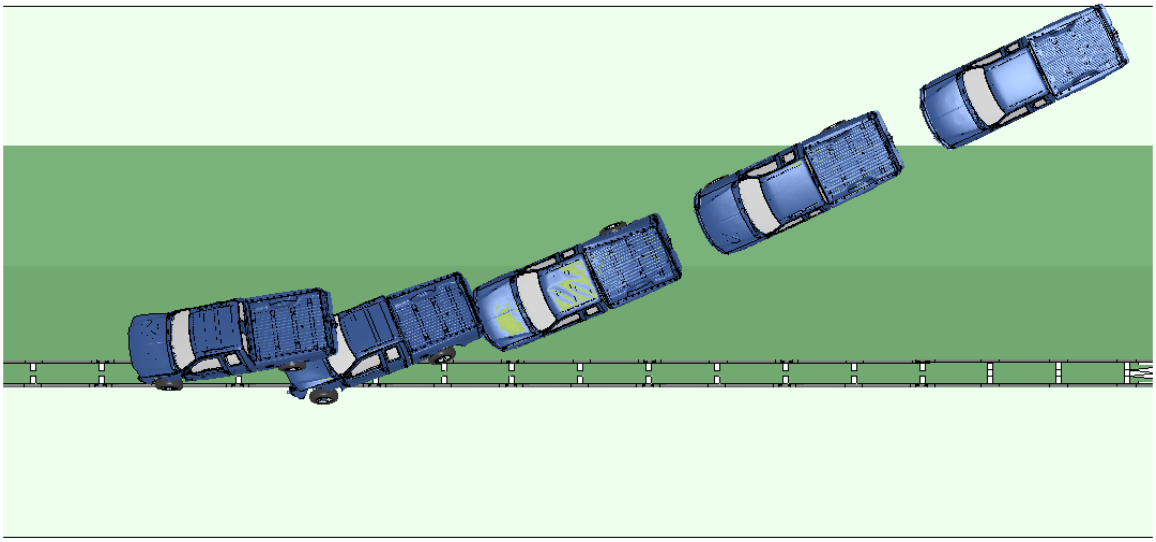

Fig. 4.61: Backside impact on the double-face W-beam (Design #1) at 62 mph and 25°.

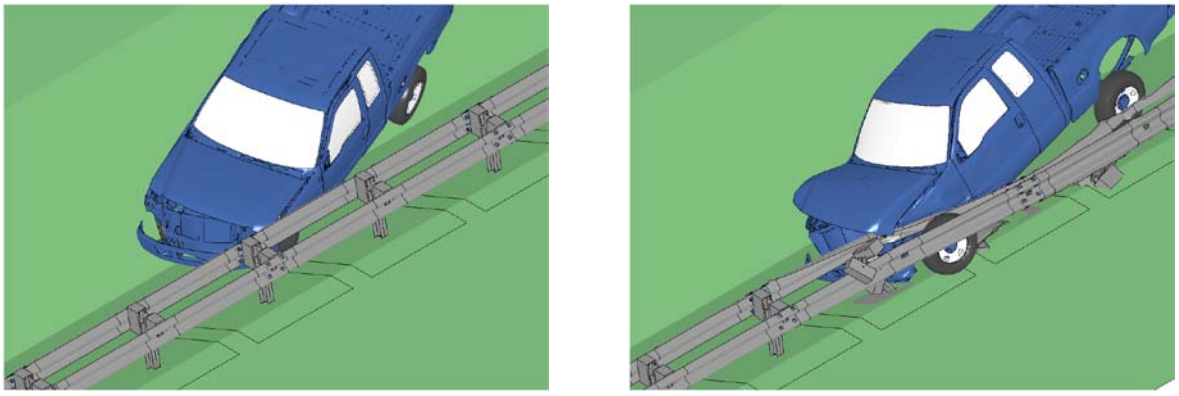

Fig. 4.62: Two instances of backside impact on the double-face W-beam (Design #1) at 62 mph and 25°.

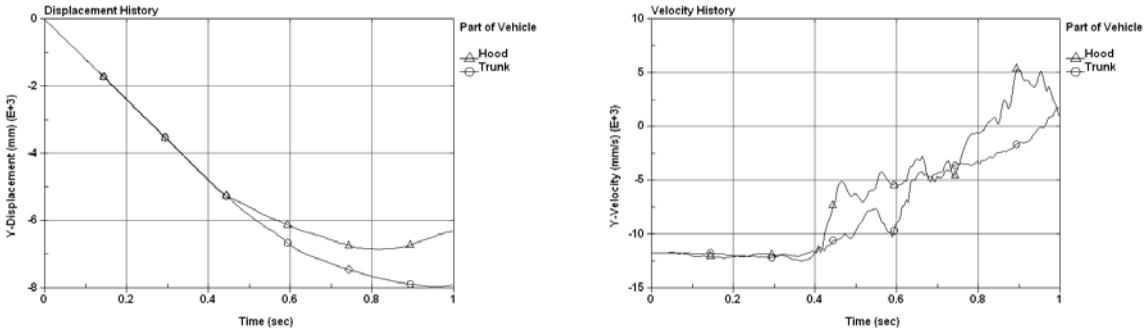


Traversal displacements Traversal velocities

Fig. 4.63: Time histories of traversal displacements and velocities of backside impact on the double-face W-beam (Design #1) at 62 mph and 25° (‘trunk’ means ‘bed’ on the truck).

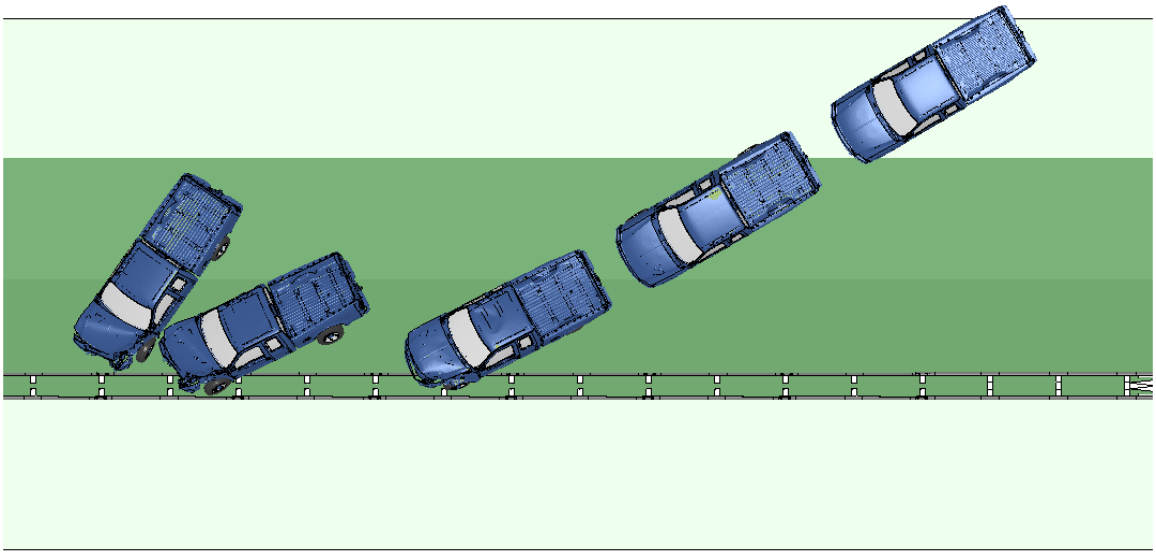

Fig. 4.64: Backside impact on the double-face W-beam (Design #1) at 62 mph and 30°.

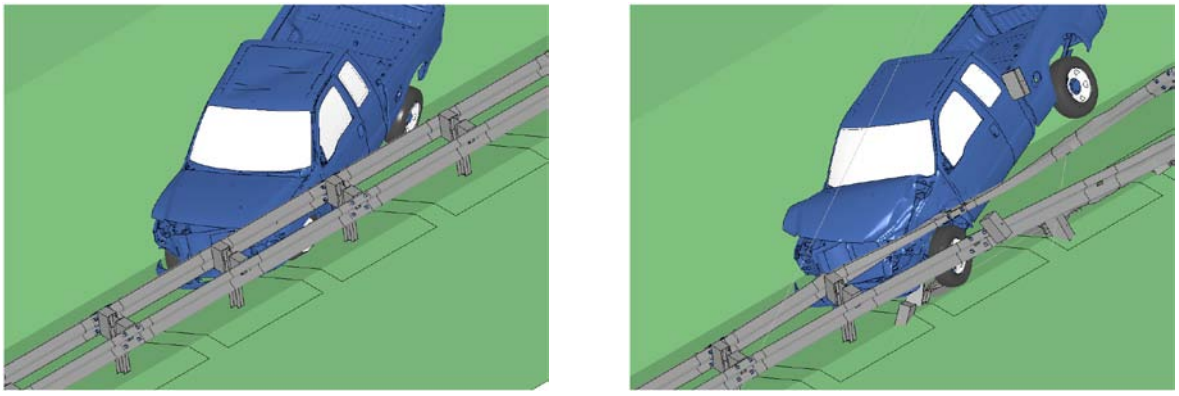

Fig. 4.65: Two instances of backside impact on the double-face W-beam (Design #1) at 62 mph and 30°.

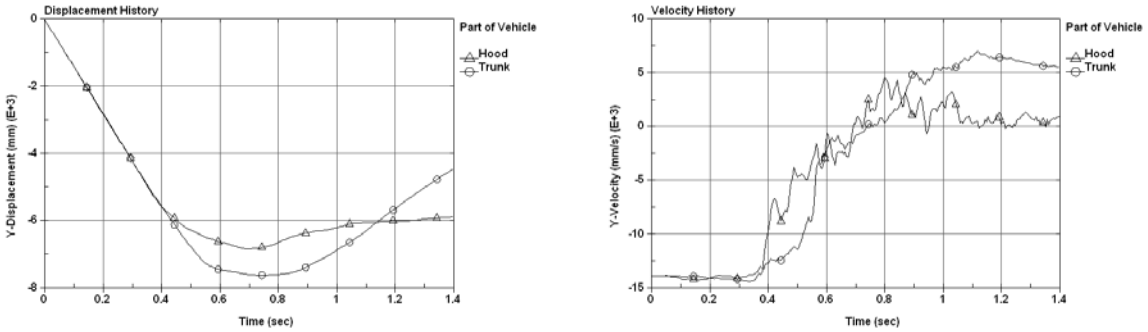


Traversal displacements Traversal velocities

Fig. 4.66: Time histories of traversal displacements and velocities of backside impact on the double-face W-beam (Design #1) at 62 mph and 30° (‘trunk’ means ‘bed’ on the truck).

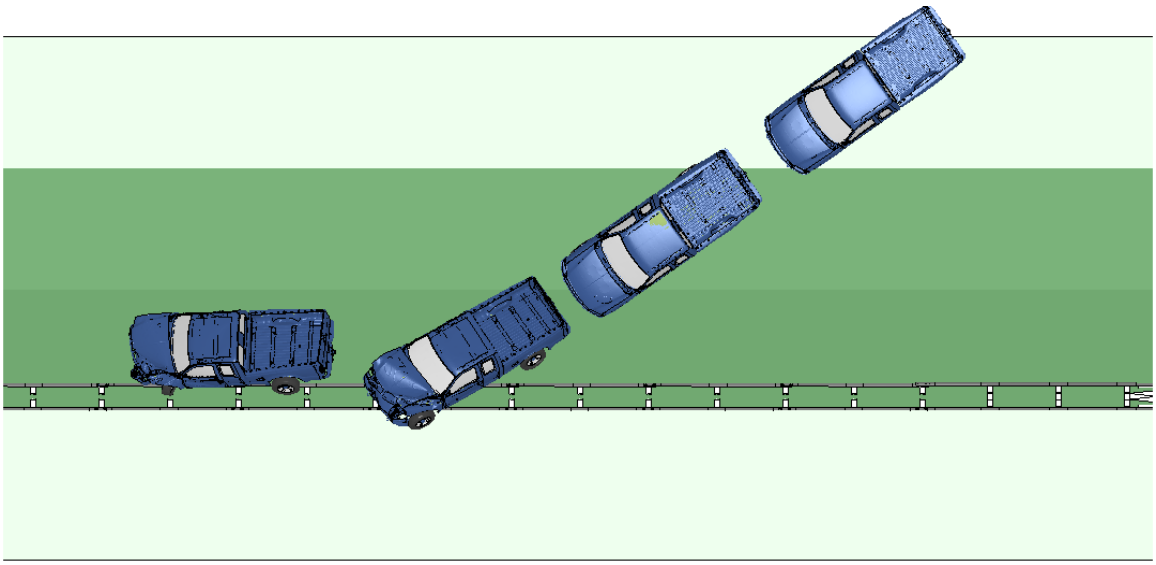

Fig. 4.67: Backside impact on the double-face W-beam (Design #1) at 62 mph and 35°.

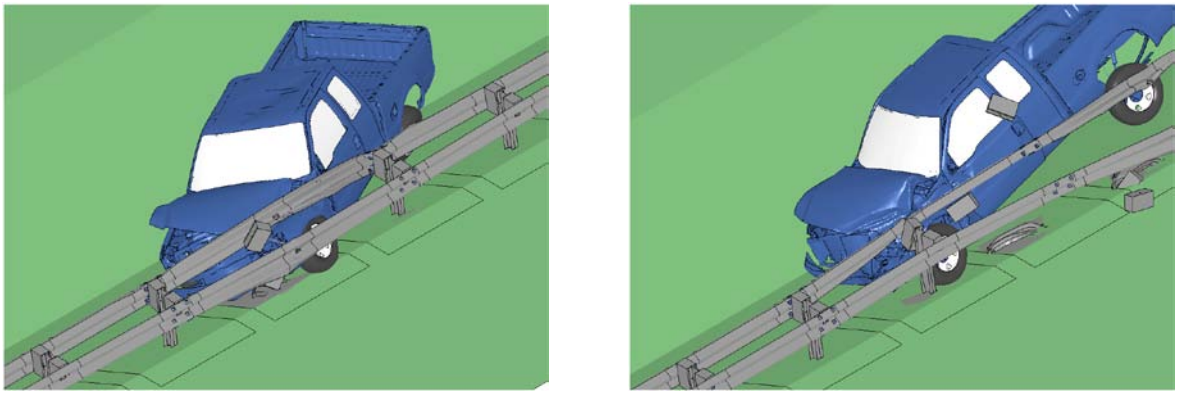

Fig. 4.68: Two instances of backside impact on the double-face W-beam (Design #1) at 62 mph and 35°.

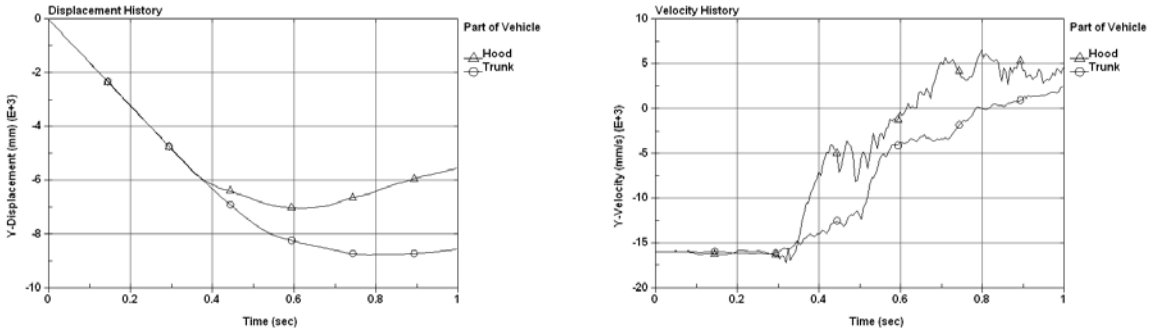


Traversal displacements Traversal velocities

Fig. 4.69: Time histories of traversal displacements and velocities of backside impact on the double-face W-beam (Design #1) at 62 mph and 35° (‘trunk’ means ‘bed’ on the truck).

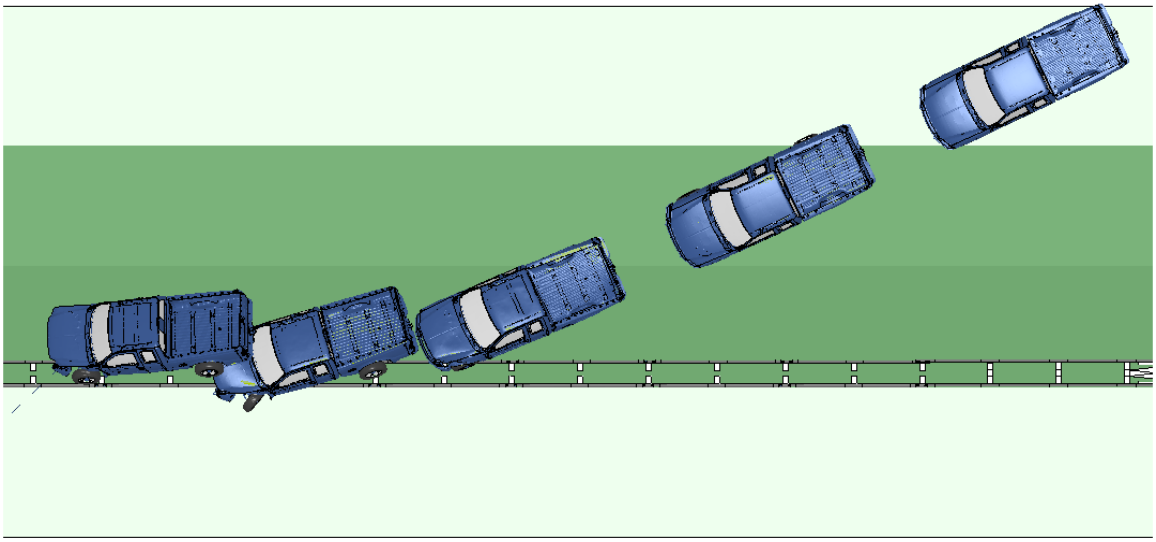

Fig. 4.70: Backside impact on the double-face W-beam (Design #1) at 70 mph and 25°.

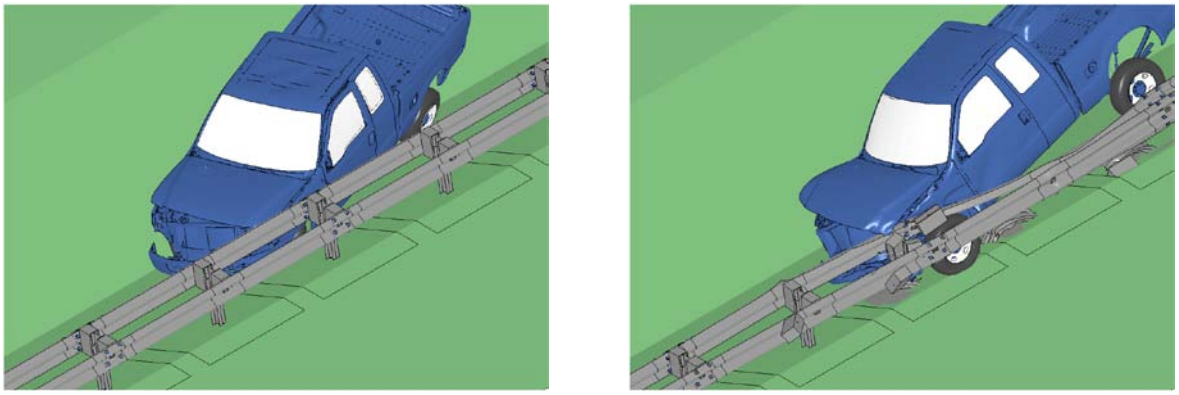

Fig. 4.71: Two instances of backside impact on the double-face W-beam (Design #1) at 70 mph and 25°.

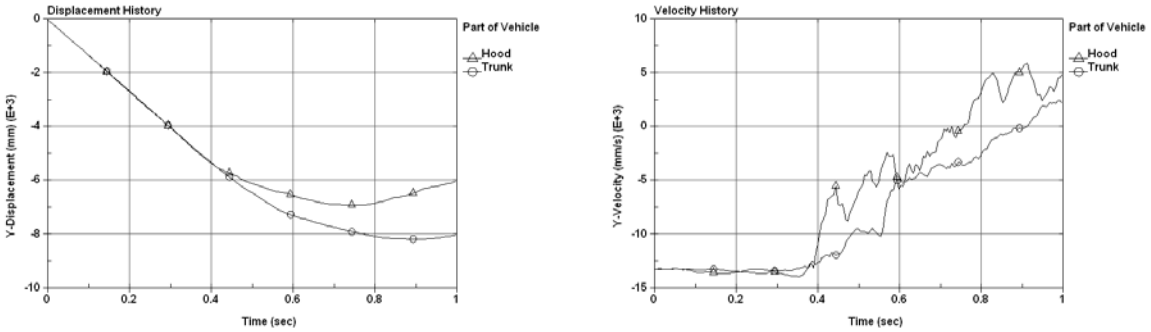


Traversal displacements Traversal velocities

Fig. 4.72: Time histories of traversal displacements and velocities of backside impact on the double-face W-beam (Design #1) at 70 mph and 25° (‘trunk’ means ‘bed’ on the truck).

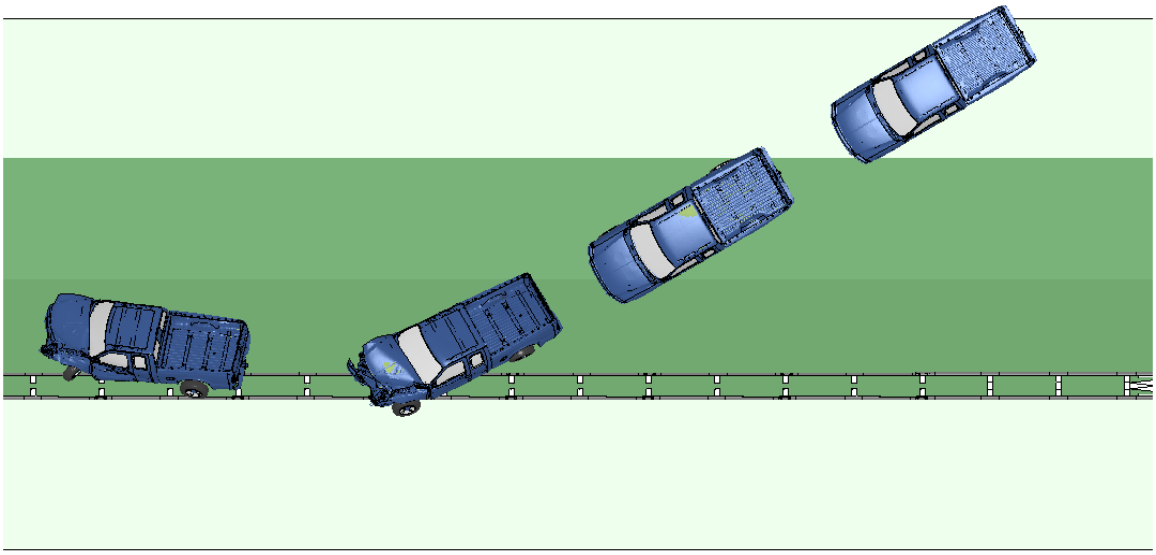

Fig. 4.73: Backside impact on the double-face W-beam (Design #1) at 70 mph and 30°.

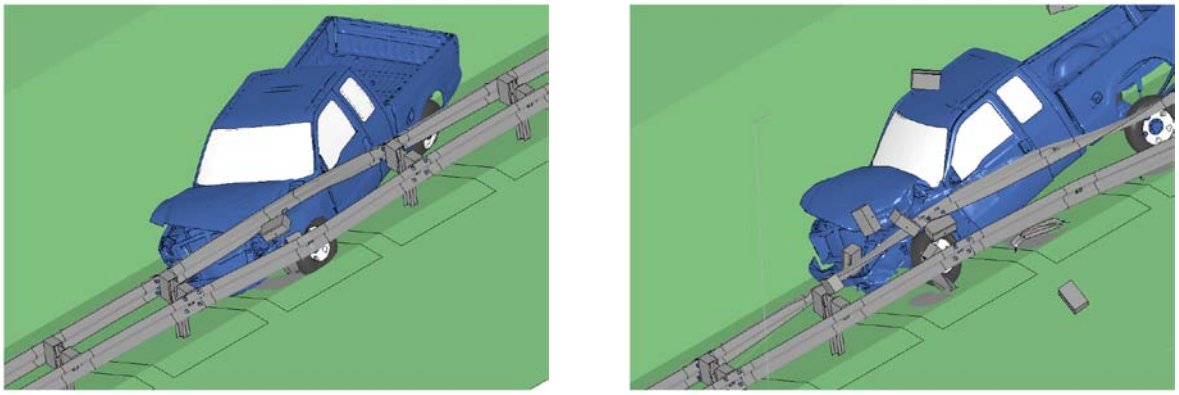

Fig. 4.74: Two instances of backside impact on the double-face W-beam (Design #1) at 70 mph and 30°.

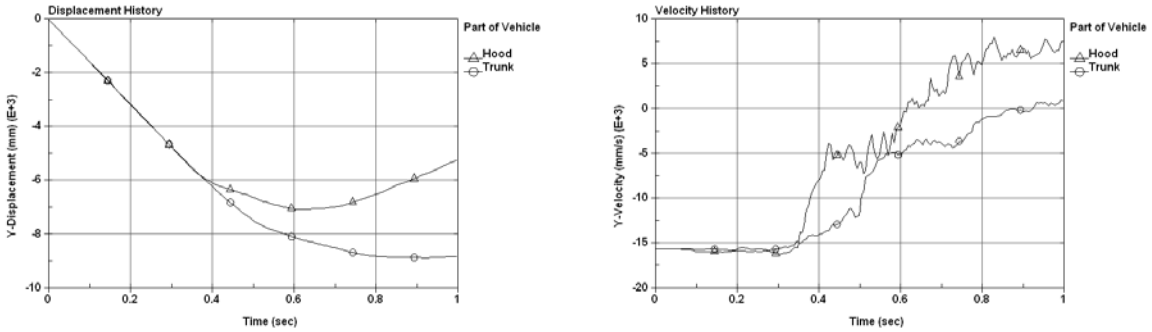


Traversal displacements Traversal velocities

Fig. 4.75: Time histories of traversal displacements and velocities of backside impact on the double-face W-beam (Design #1) at 70 mph and 30° (‘trunk’ means ‘bed’ on the truck).

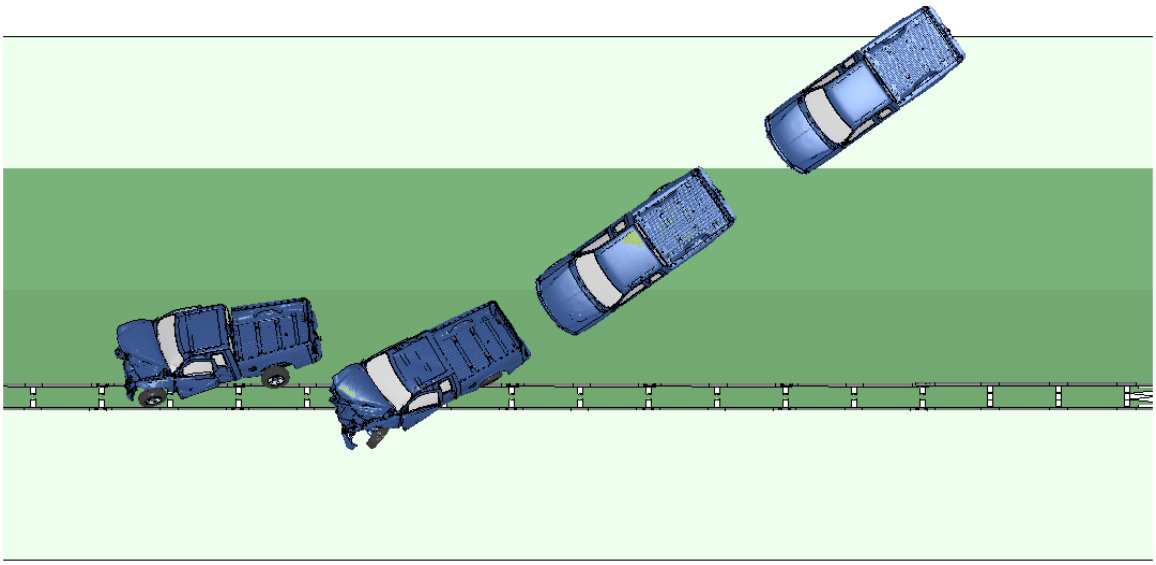

Fig. 4.76: Backside impact on the double-face W-beam (Design #1) at 70 mph and 35°.

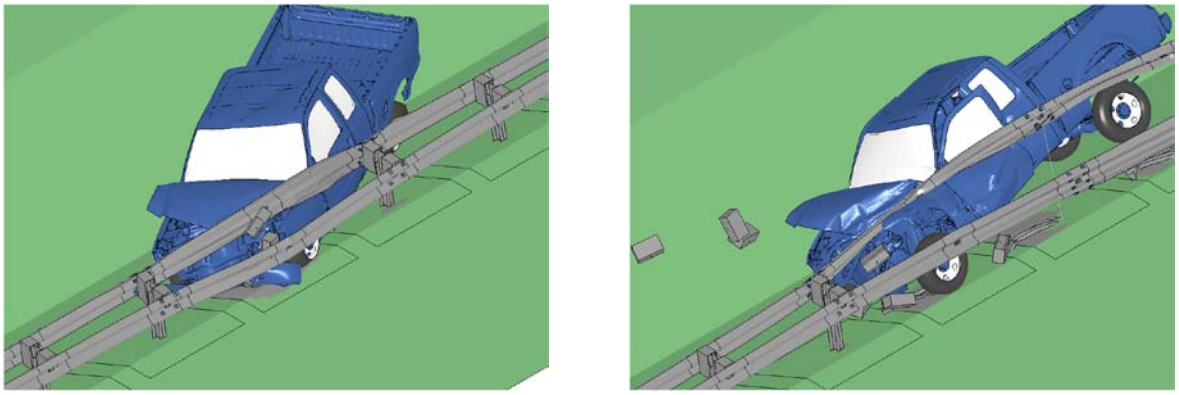

Fig. 4.77: Two instances of backside impact on the double-face W-beam (Design #1) at 70 mph and 35°.

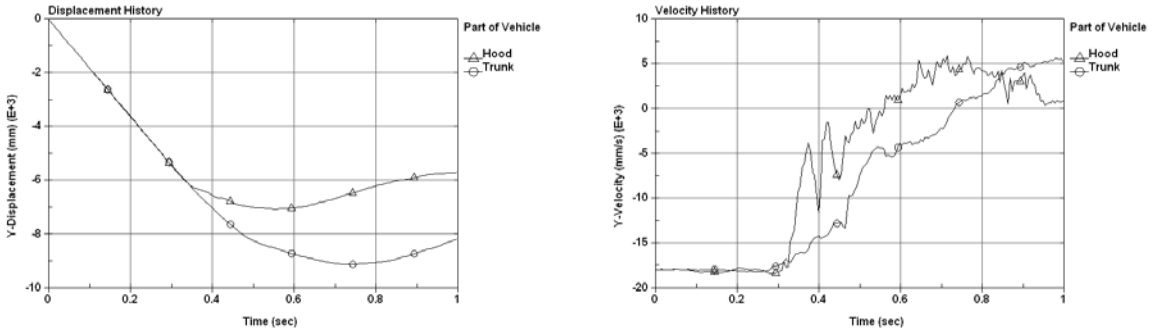


Traversal displacements Traversal velocities

Fig. 4.78: Time histories of traversal displacements and velocities of backside impact on the double-face W-beam (Design #1) at 70 mph and 35° (‘trunk’ means ‘bed’ on the truck).

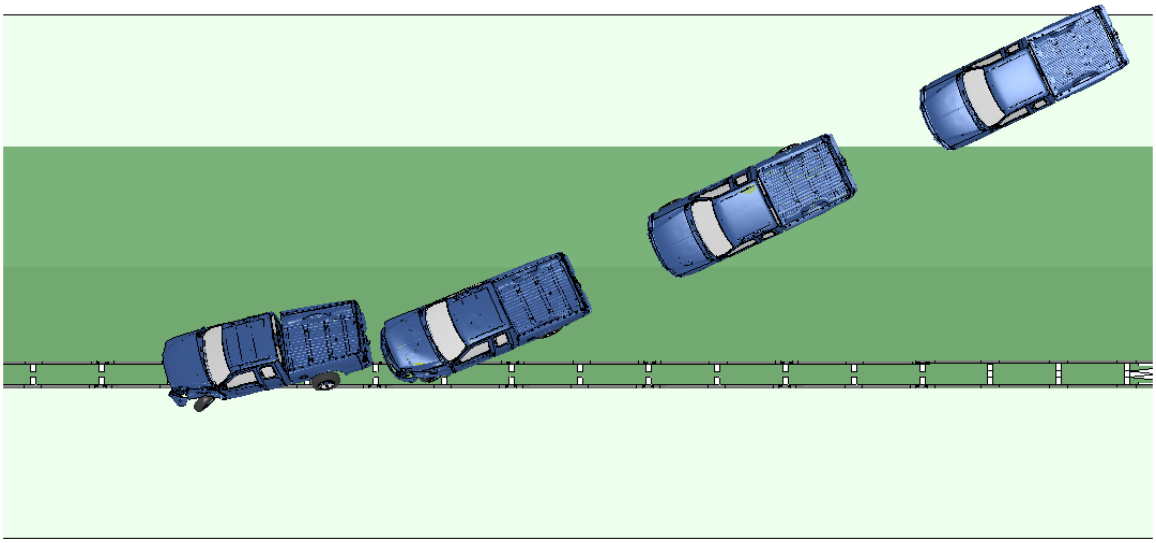

Fig. 4.79: Backside impact on the double-face W-beam (Design #1) at 75 mph and 25°.

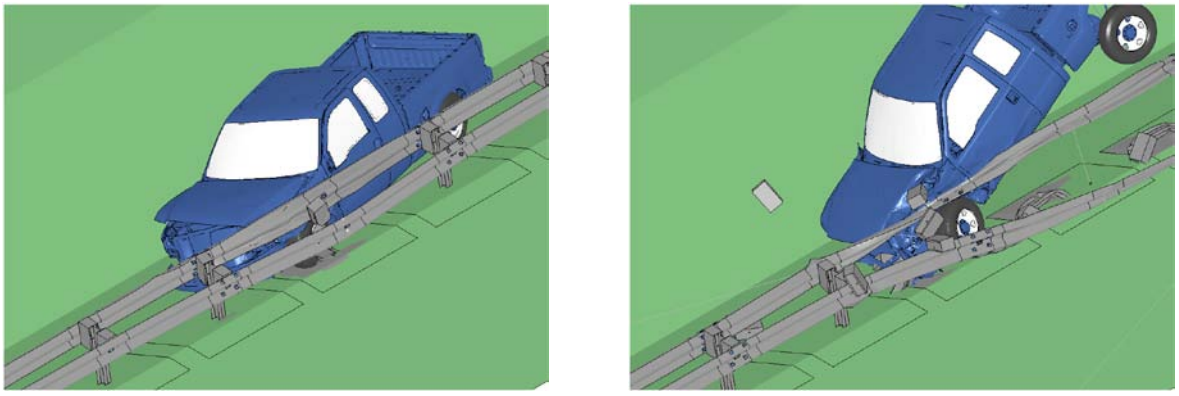

Fig. 4.80: Two instances of backside impact on the double-face W-beam (Design #1) at 75 mph and 25°.

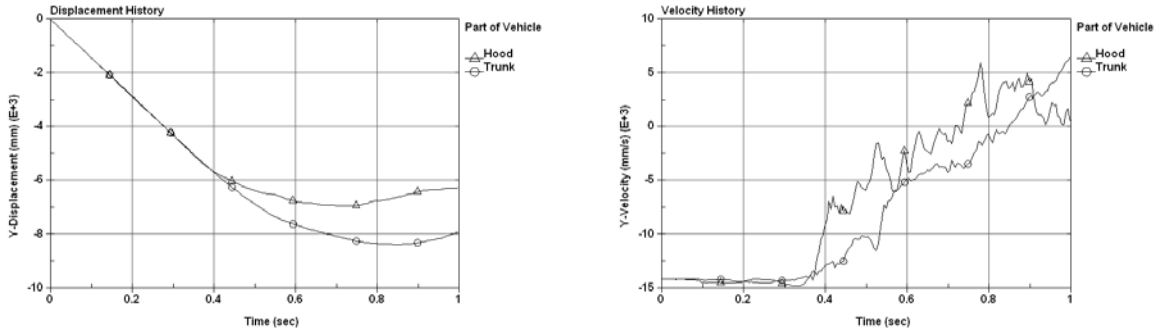


Traversal displacements Traversal velocities

Fig. 4.81: Time histories of traversal displacements and velocities of backside impact on the double-face W-beam (Design #1) at 75 mph and 25° (‘trunk’ means ‘bed’ on the truck).

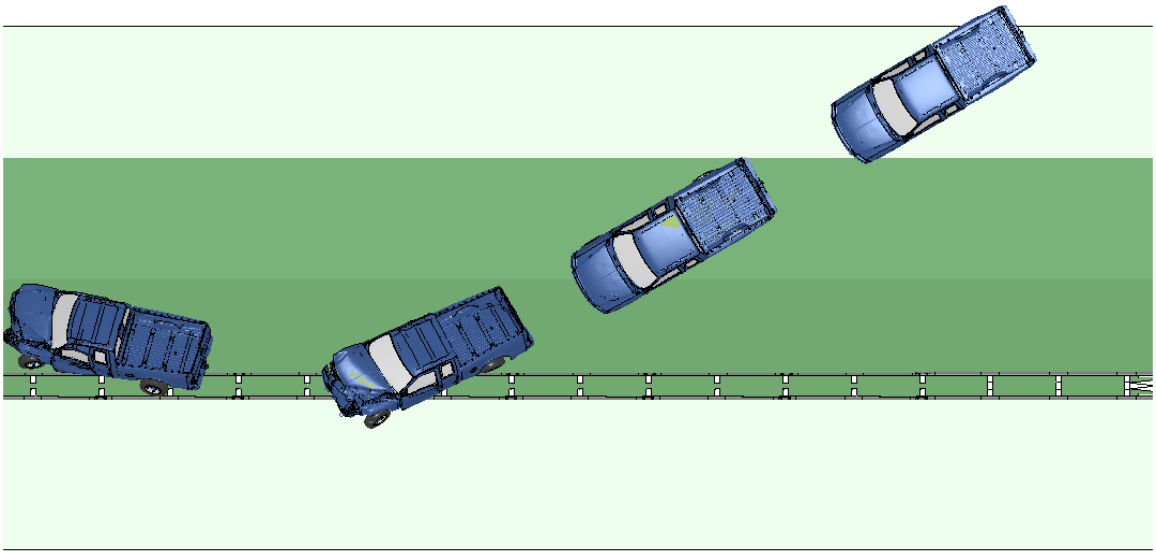

Fig. 4.82: Backside impact on the double-face W-beam (Design #1) at 75 mph and 30°.

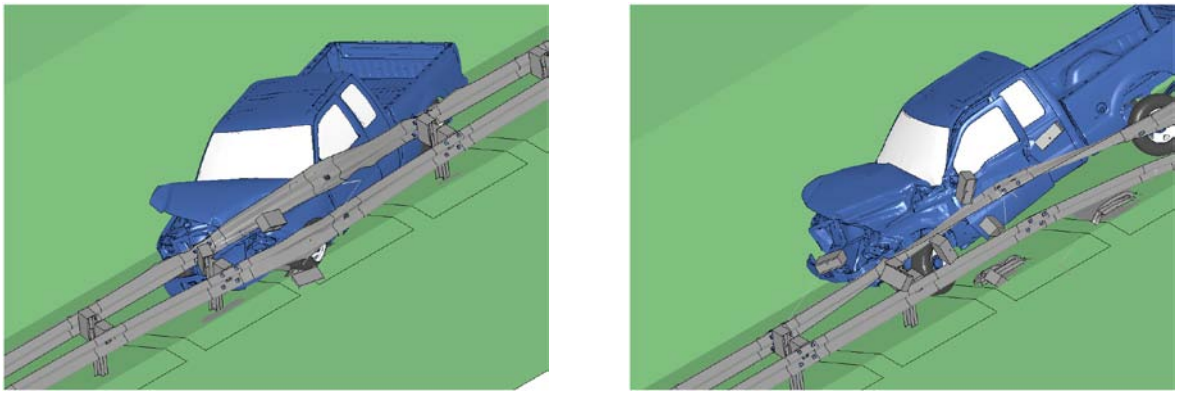

Fig. 4.83: Two instances of backside impact on the double-face W-beam (Design #1) at 75 mph and 30°.

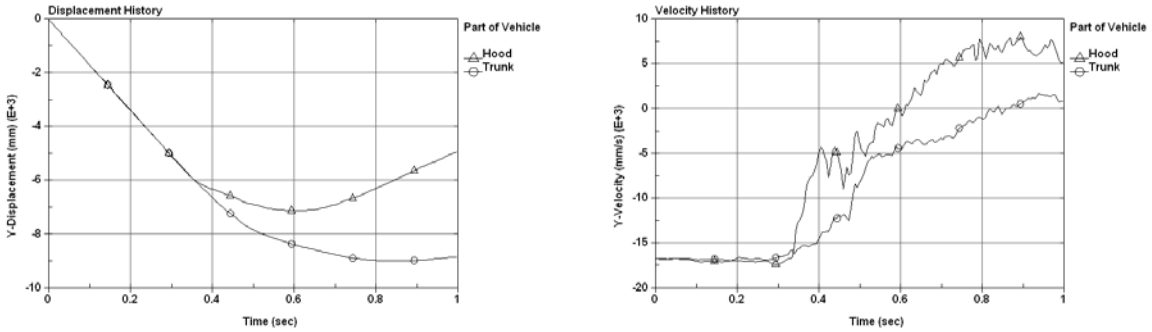


Traversal displacements Traversal velocities

Fig. 4.84: Time histories of traversal displacements and velocities of backside impact on the double-face W-beam (Design #1) at 75 mph and 30° (‘trunk’ means ‘bed’ on the truck).

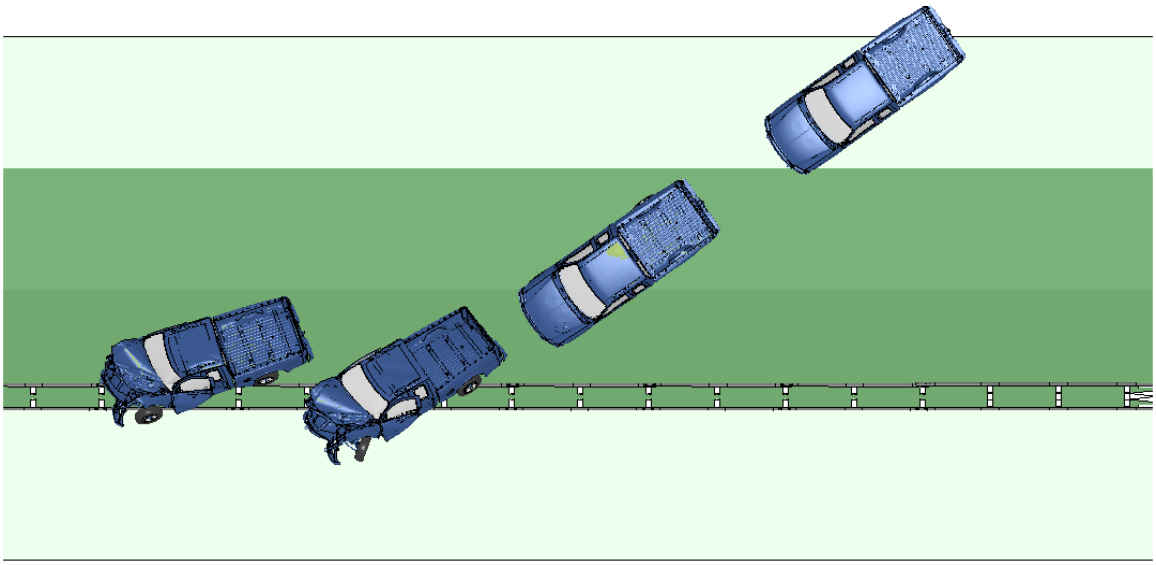

Fig. 4.85: Backside impact on the double-face W-beam (Design #1) at 75 mph and 35°.

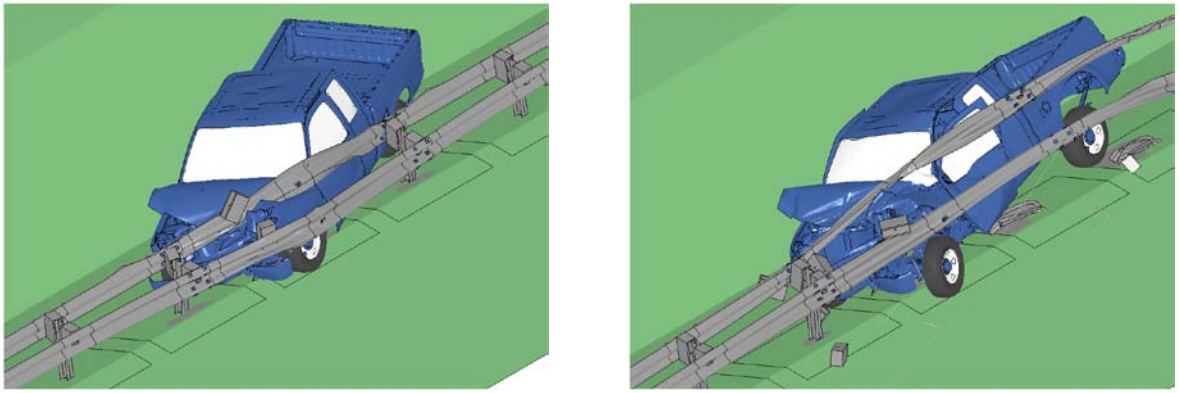

Fig. 4.86: Two instances of backside impact on the double-face W-beam (Design #1) at 75 mph and 35°.

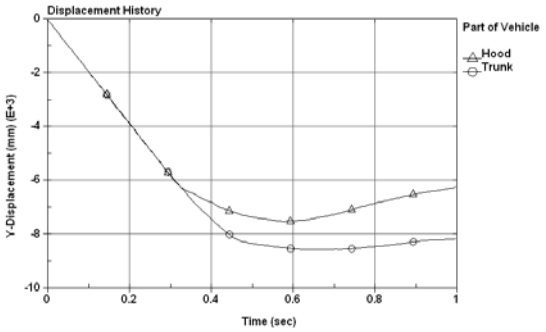


Traversal displacements

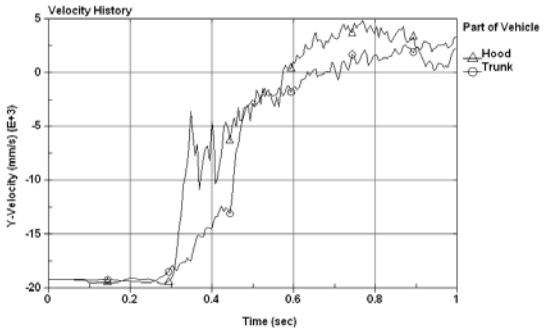


Traversal velocities

Fig. 4.87: Time histories of traversal displacements and velocities of backside impact on the double-face W-beam (Design #1) at 75 mph and 35° (‘trunk’ means ‘bed’ on the truck).

The simulation results showed that Design #2 of the double-face W-beam had a similar performance to Design #1 under both front-side and backside impacts of the Ford F250. Compared to Design #1, the lowered backside rail in Design #2 had more interactions with the vehicle and thus performed more effectively. The vehicle's response in backside impacts, i.e., vehicle rotations, appeared to be slightly less severe than those in Design #1.

For front-side impacts, the lowered backside rail did not degrade the performance of the W-beam. In the 25° impact at 62 mph (100 km/hr), the vehicle was redirected and safely retained on the shoulder. In the other two cases of 25° impacts, the vehicle was successfully redirected on the shoulder. In 30° impacts, the vehicle was redirected at all three speeds, but rollover followed the redirection in the cases of 70 and 75 mph (112.6 and 120.7 km/hr). For 35° impacts, the vehicle rolled over towards the median for all the three speeds due to the severity of the impacts.

In backside impacts, the vehicle was successfully redirected for all cases except for 30° and 35° impacts at 62 mph (100 km/hr) in which the vehicle was redirected and safely retained in the ditch. This is similar to the corresponding cases for Design #1.

Simulation results of all front-side impacts for Design #2 of the double-face W-beam are shown in Figs. 4.88 to 4.114. The figures for each case include the vehicle's displacement paths, detailed views of vehicle-barrier interactions, and time histories of the vehicle's traversal displacements and velocities for. Figures 4.115 to 4.141 show the results of all back-side impacts for Design #2.

### 4.3 Comparison of the Single- and Double-face W-beams

The single-face W-beam was installed on the borderline between the 2.5:1 slope and the adjacent shoulder. Due to this large slope, the vehicle was shown to have a tendency of rollover towards the median when the impact speeds were higher than 62 mph (100 km/hr). This was also true for the single-face W-beam on the 4:1 slope. For the two lines of single-face W-beam, the simulation results indicated that after impacting one rail from the front-side, the vehicle was unlikely to impact the other rail from the backside. The reason was that the vehicle either was redirected or rolled over towards the ditch after impacting the first line of W-beam and that it would not go up the slope to reach the second line from backside.

For small-angle (i.e., 25°) front-side impacts, the two designs of double-face W-beam performed similarly and slightly better than the single-face W-beam. The two rails increased the stiffness and strength of the W-beam, provided better retention to the vehicle, and reduced the tendency/potential of vehicle rollover. For large-angle (i.e., 30° and 35°) front-side impacts, the two designs of the double-face W-beam produced better vehicle redirection but did not improve much on vehicle rollover.

Assuming the two lines of single-face W-beam are subject to equal number of impacts, then half of the front-side impacts on the single-face W-beam would become backside impacts on the double-face W-beam. Since the two designs of double-face W-beam performed very well in backside impacts, they can be considered to replace the two lines of single-face W-beam with no reduction on the performance in front-side impacts.

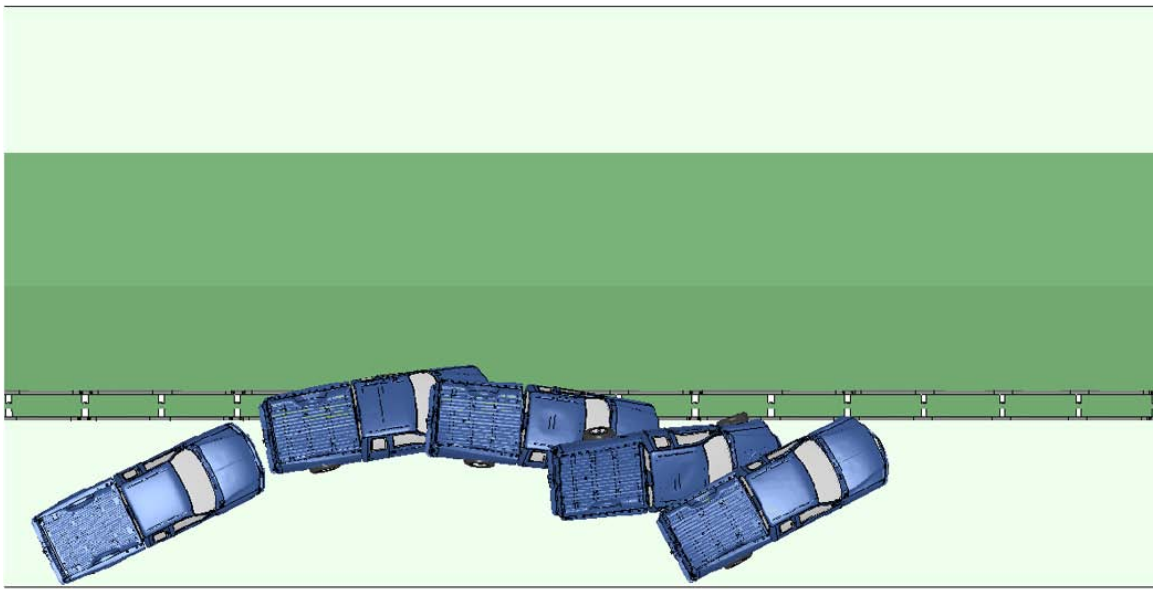

Fig. 4.88: Front-side impact on the double-face W-beam (Design #2) at 62 mph and 25°.

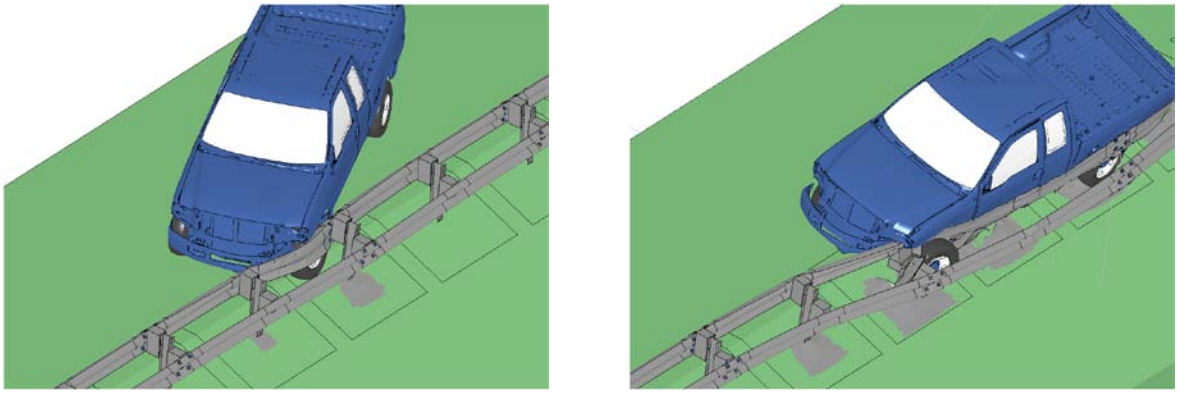

Fig. 4.89: Two instances of front-side impact on the double-face W-beam (Design #2) at 62 mph and 25°.

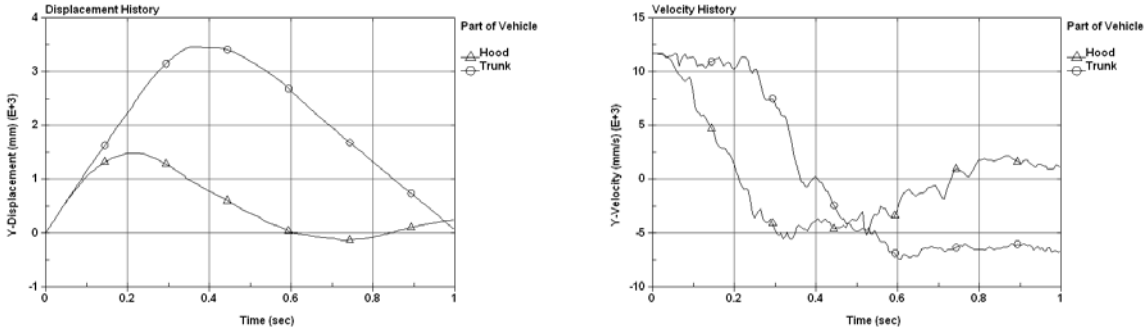


Traversal displacements Traversal velocities

Fig. 4.90: Time histories of traversal displacements and velocities of front-side impact on the double-face W-beam (Design #2) at 62 mph and 25° ('trunk' means 'bed' on the truck).

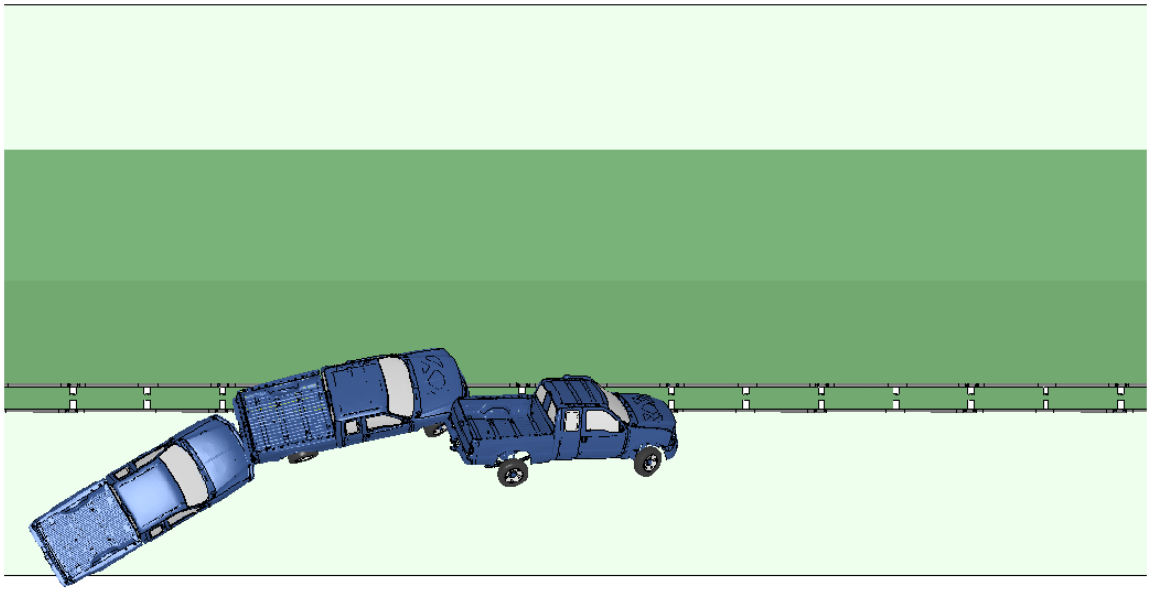

Fig. 4.91: Front-side impact on the double-face W-beam (Design #2) at 62 mph and 30°.

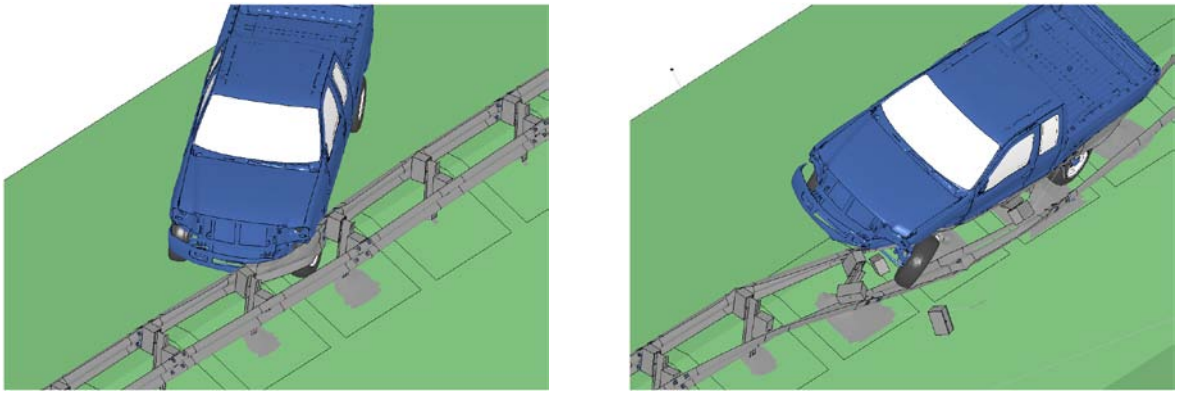

Fig. 4.92: Two instances of front-side impact on the double-face W-beam (Design #2) at 62 mph and 30°.

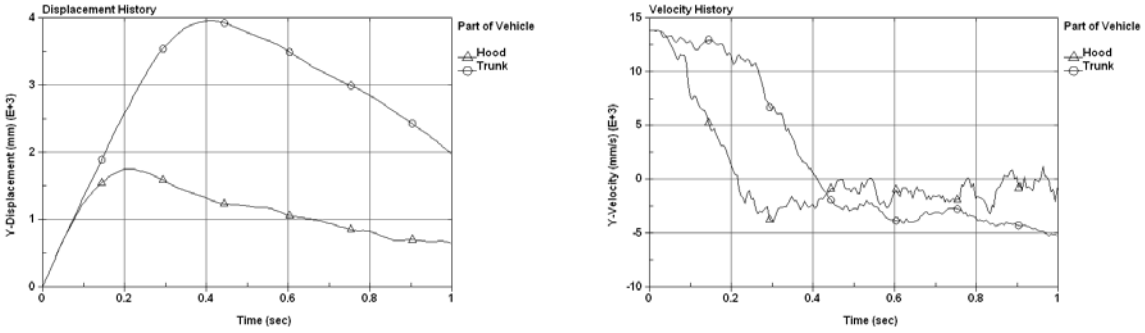


Traversal displacements Traversal velocities

Fig. 4.93: Time histories of traversal displacements and velocities of front-side impact on the double-face W-beam (Design #2) at 62 mph and 30° (‘trunk’ means ‘bed’ on the truck).

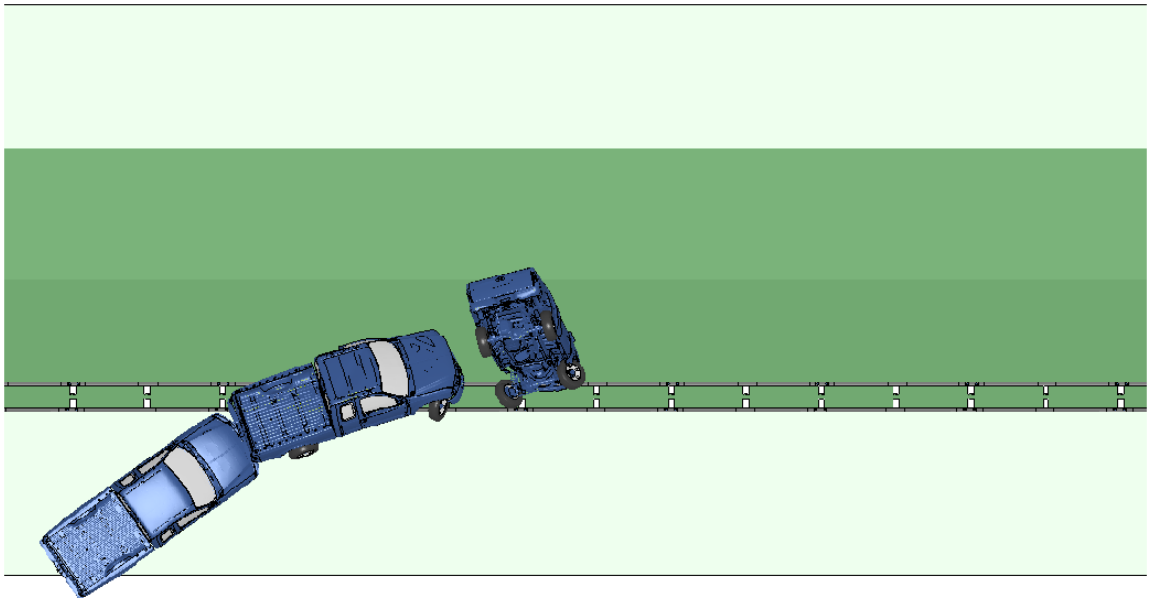

Fig. 4.94: Front-side impact on the double-face W-beam (Design #2) at 62 mph and 35°.

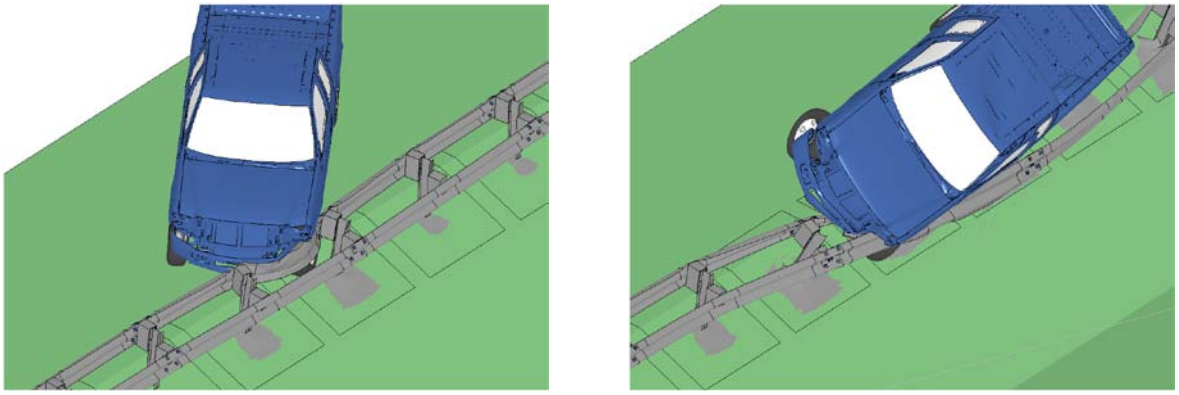

Fig. 4.95: Two instances of front-side impact on the double-face W-beam (Design #2) at 62 mph and 35°.

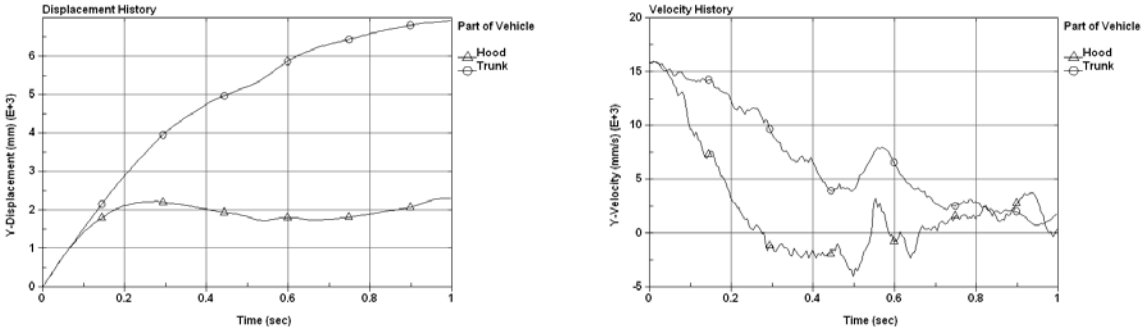


Traversal displacements Traversal velocities

Fig. 4.96: Time histories of traversal displacements and velocities of front-side impact on the double-face W-beam (Design #2) at 62 mph and 35° (‘trunk’ means ‘bed’ on the truck).

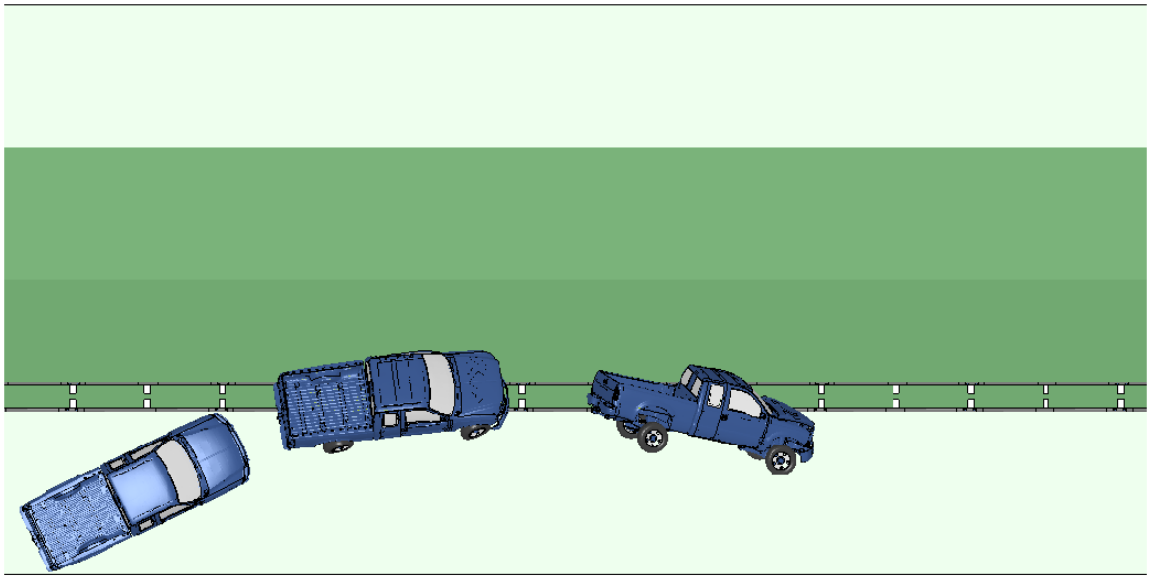

Fig. 4.97: Front-side impact on the double-face W-beam (Design #2) at 70 mph and 25°.

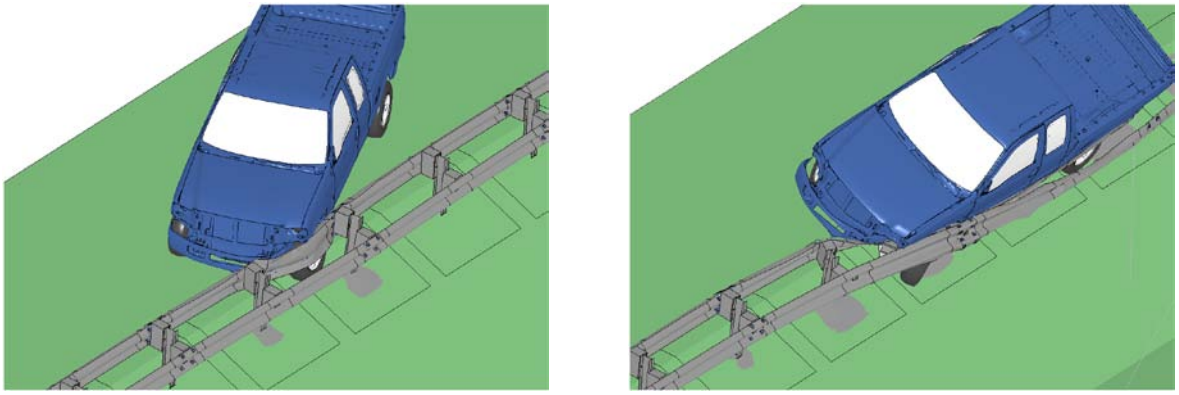

Fig. 4.98: Two instances of front-side impact on the double-face W-beam (Design #2) at 70 mph and 25°.

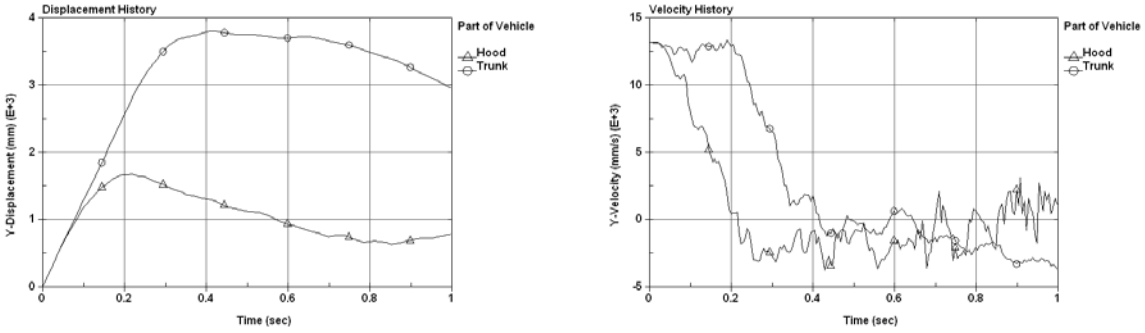


Traversal displacements Traversal velocities

Fig. 4.99: Time histories of traversal displacements and velocities of front-side impact on the double-face W-beam (Design #2) at 70 mph and 25° ('trunk' means 'bed' on the truck).

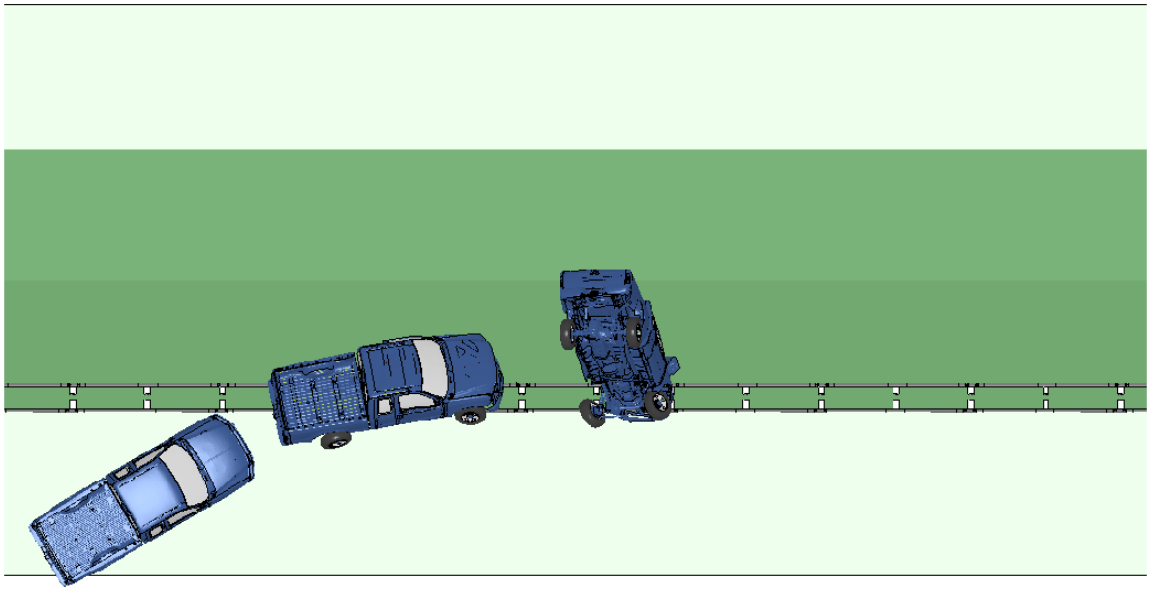

Fig. 4.100: Front-side impact on the double-face W-beam (Design #2) at 70 mph and 30°.

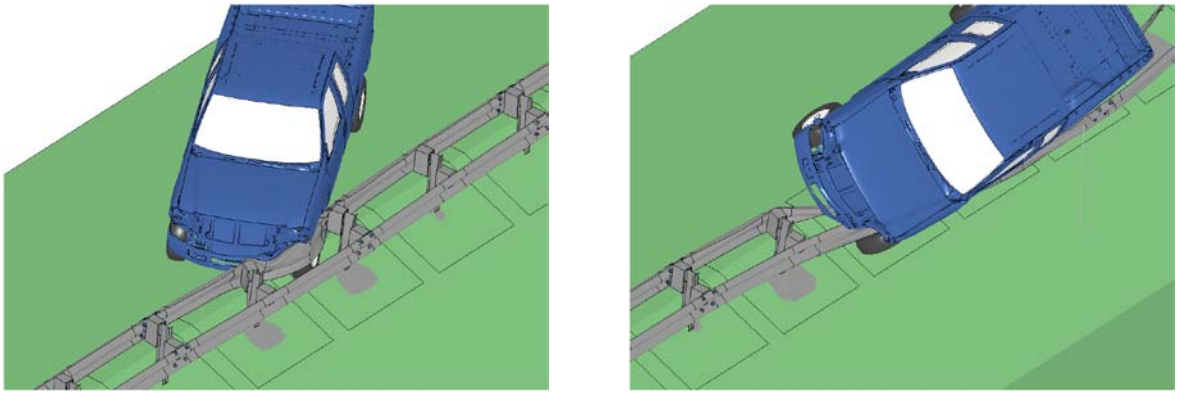

Fig. 4.101: Two instances of front-side impact on the double-face W-beam (Design #2) at 70 mph and 30°.

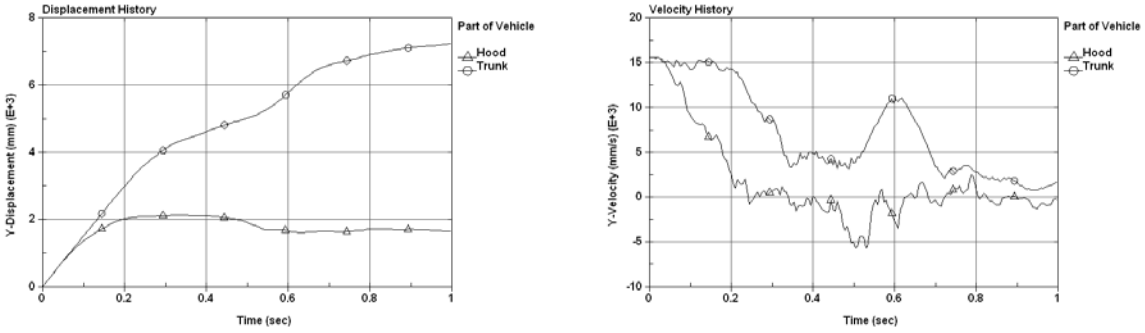


Traversal displacements Traversal velocities

Fig. 4.102: Time histories of traversal displacements and velocities of front-side impact on the double-face W-beam (Design #2) at 70 mph and 30° (‘trunk’ means ‘bed’ on the truck).

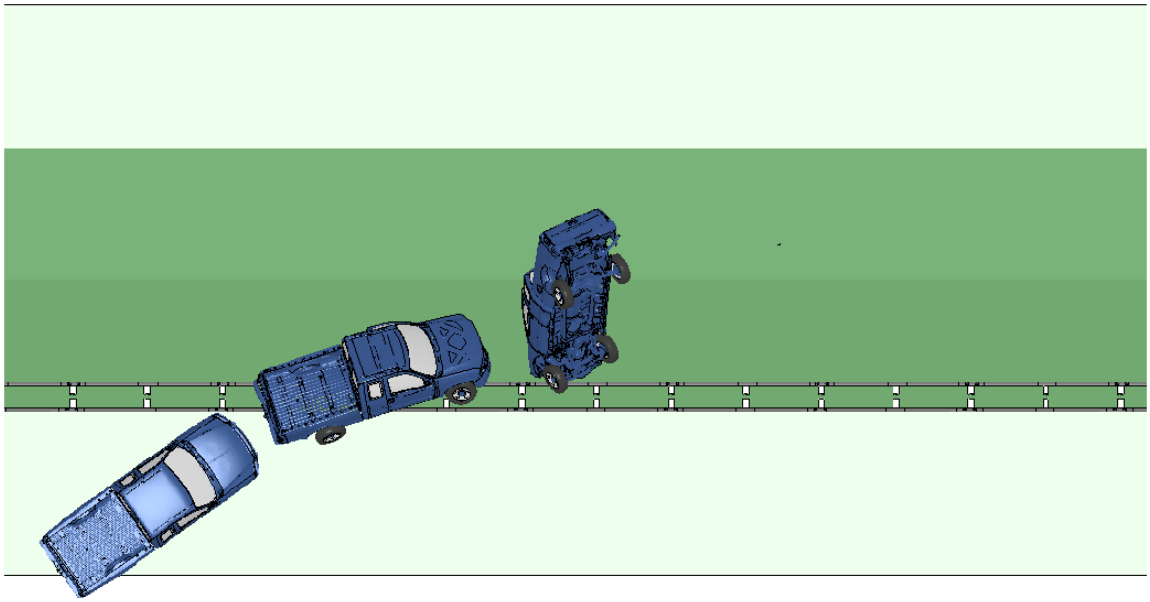

Fig. 4.103: Front-side impact on the double-face W-beam (Design #2) at 70 mph and 35°.

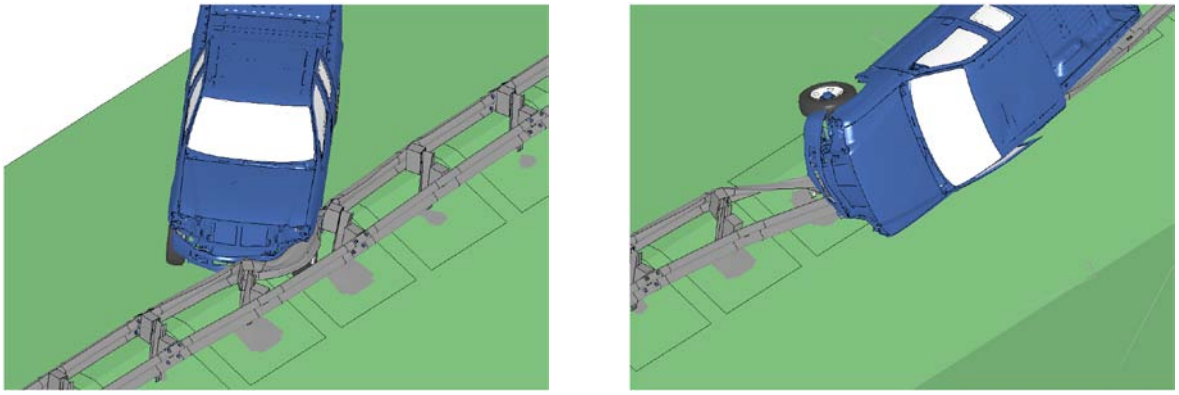

Fig. 4.104: Two instances of front-side impact on the double-face W-beam (Design #2) at 70 mph and 35°.

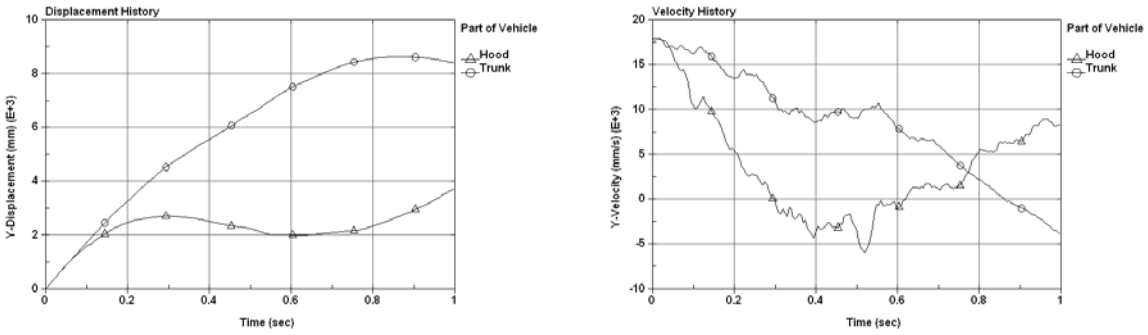


Traversal displacements Traversal velocities

Fig. 4.105: Time histories of traversal displacements and velocities of front-side impact on the double-face W-beam (Design #2) at 70 mph and 35° (‘trunk’ means ‘bed’ on the truck).

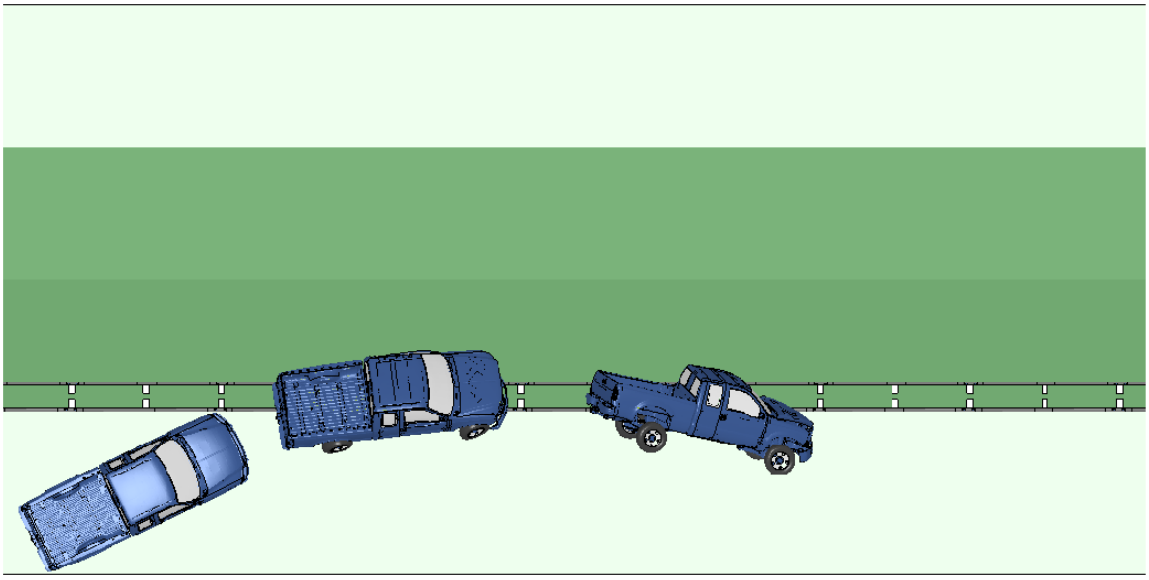

Fig. 4.106: Front-side impact on the double-face W-beam (Design #2) at 75 mph and 25°.

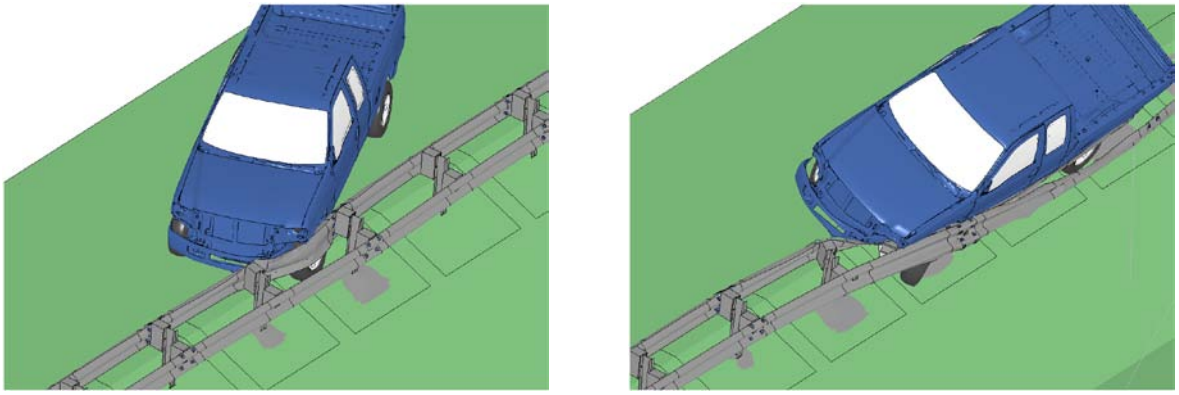

Fig. 4.107: Two instances of front-side impact on the double-face W-beam (Design #2) at 75 mph and 25°.

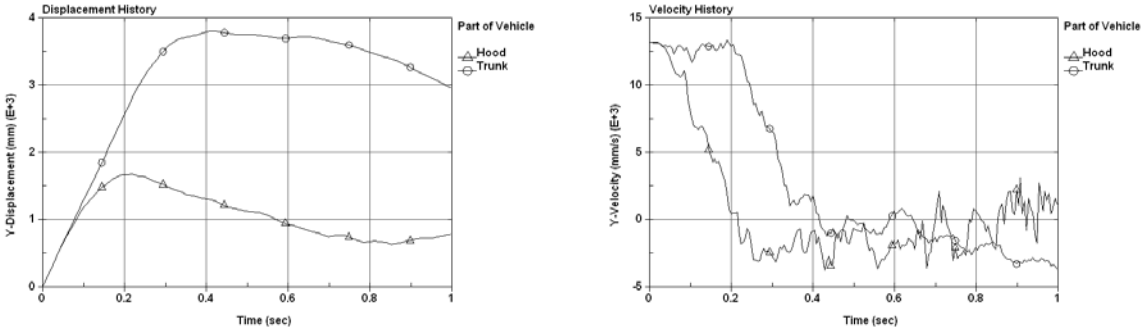


Traversal displacements Traversal velocities

Fig. 4.108: Time histories of traversal displacements and velocities of front-side impact on the double-face W-beam (Design #2) at 75 mph and 25° (‘trunk’ means ‘bed’ on the truck).

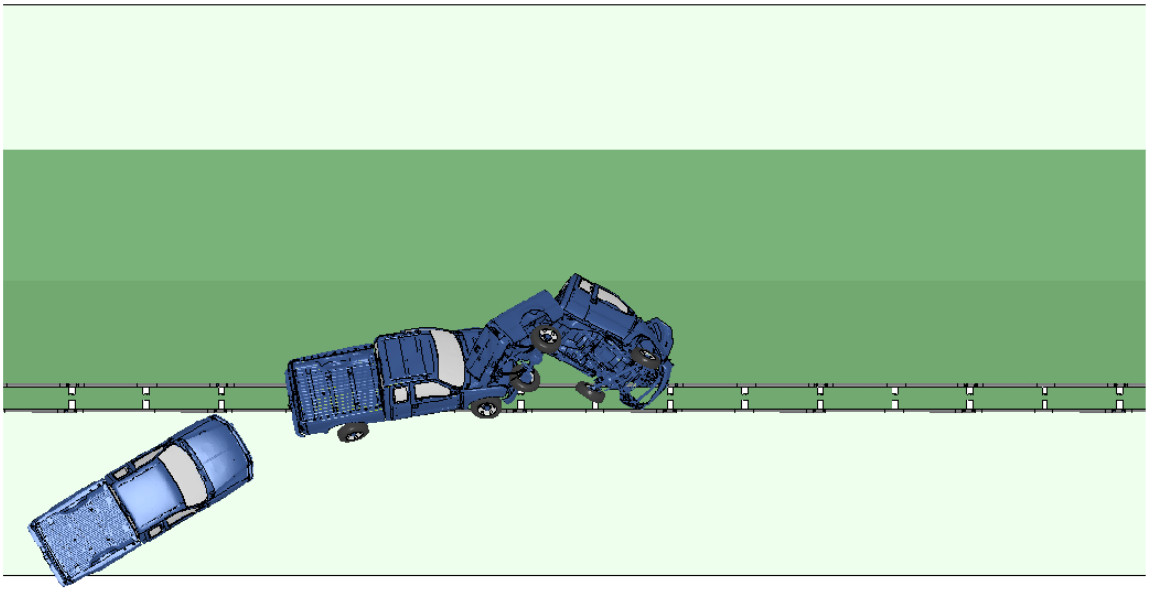

Fig. 4.109: Front-side impact on the double-face W-beam (Design #2) at 75 mph and 30°.

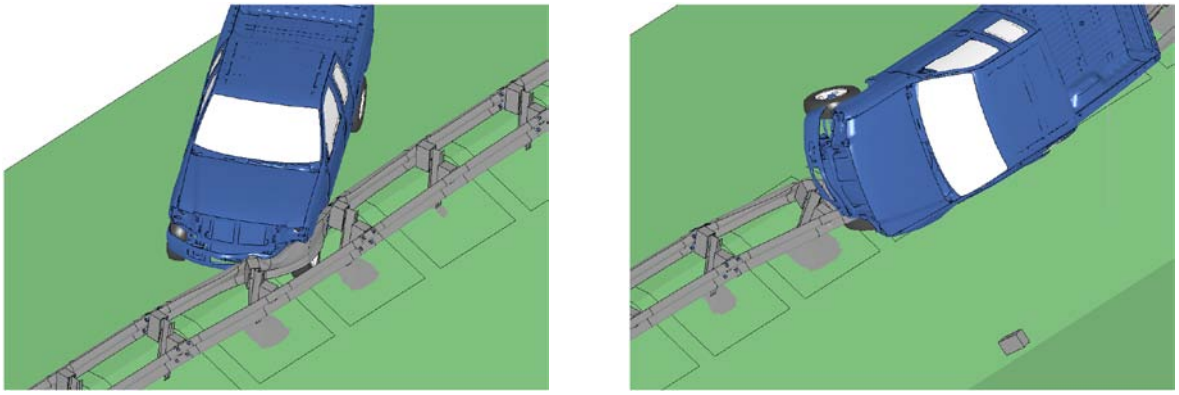

Fig. 4.110: Two instances of front-side impact on the double-face W-beam (Design #2) at 75 mph and 30°.

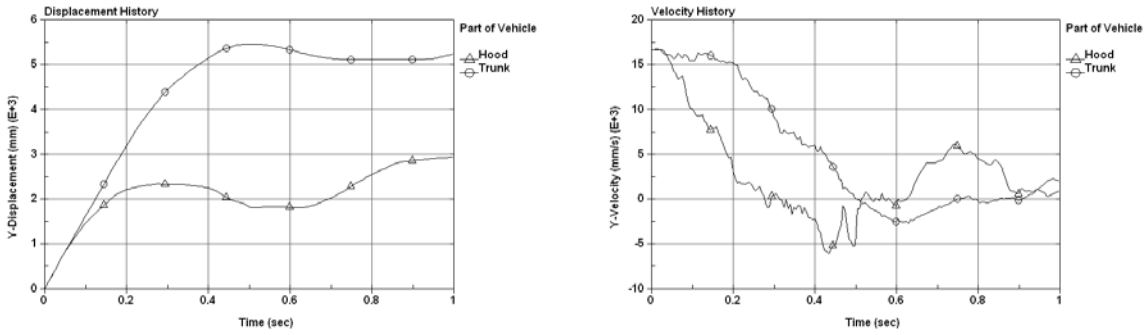


Traversal displacements Traversal velocities

Fig. 4.111: Time histories of traversal displacements and velocities of front-side impact on the double-face W-beam (Design #2) at 75 mph and 30° (‘trunk’ means ‘bed’ on the truck).

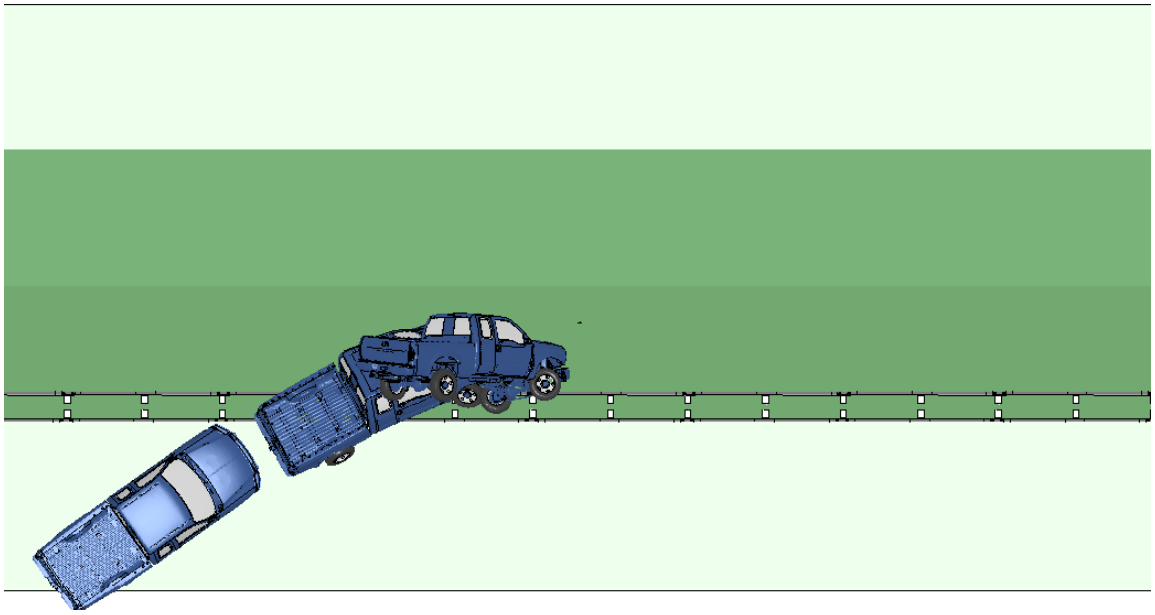

Fig. 4.112: Front-side impact on the double-face W-beam (Design #2) at 75 mph and 35°.

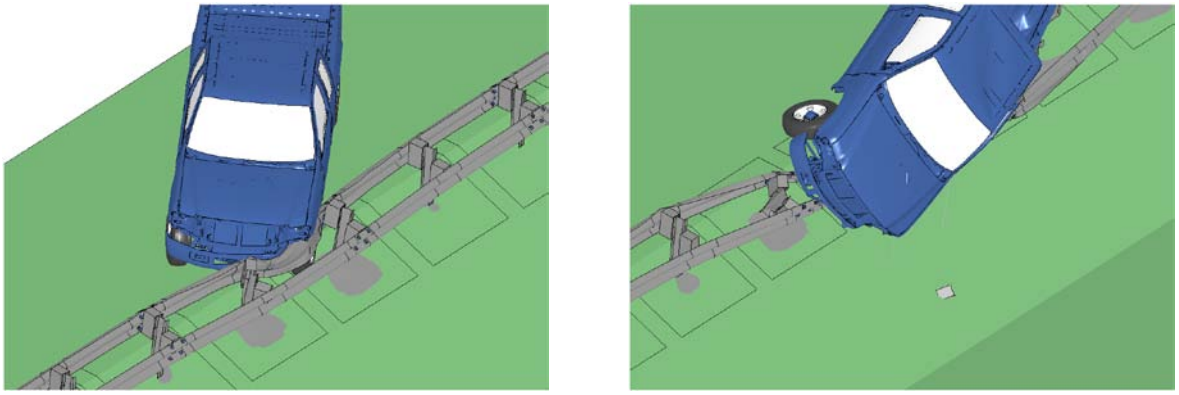

Fig. 4.113: Two instances of front-side impact on the double-face W-beam (Design #2) at 75 mph and 35°.

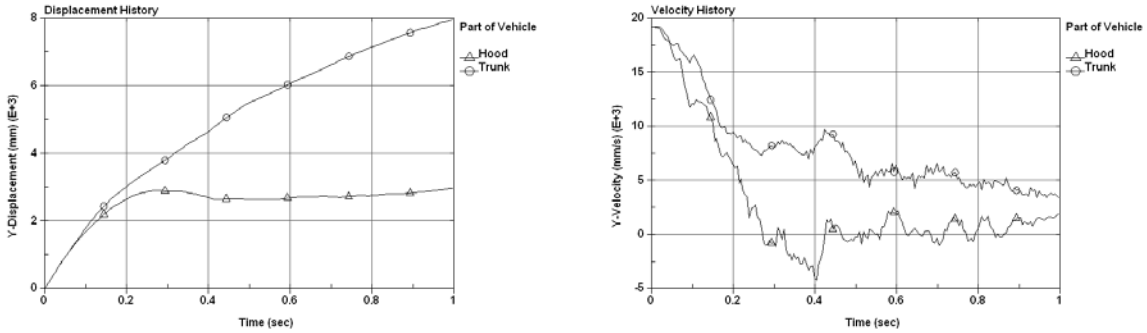


Traversal displacements Traversal velocities

Fig. 4.114: Time histories of traversal displacements and velocities of front-side impact on the double-face W-beam (Design #2) at 75 mph and 35° ('trunk' means 'bed' on the truck).

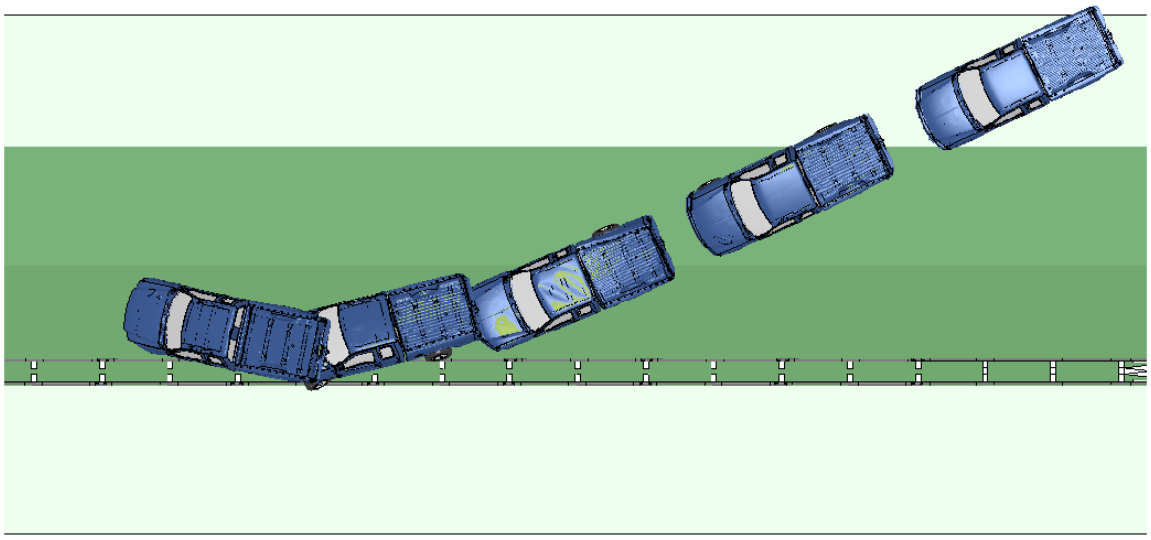

Fig. 4.115: Backside impact on the double-face W-beam (Design #2) at 62 mph and 25°.

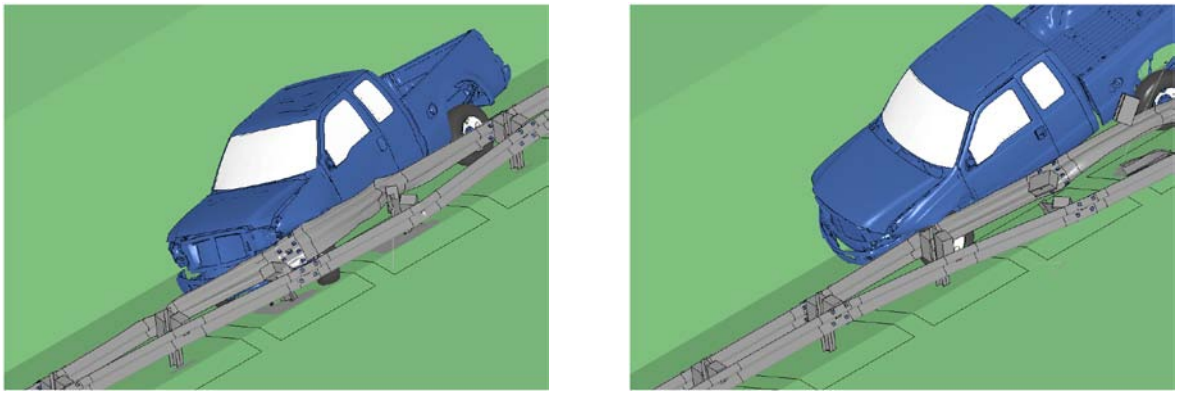

Fig. 4.116: Two instances of backside impact on the double-face W-beam (Design #2) at 62 mph and 25°.

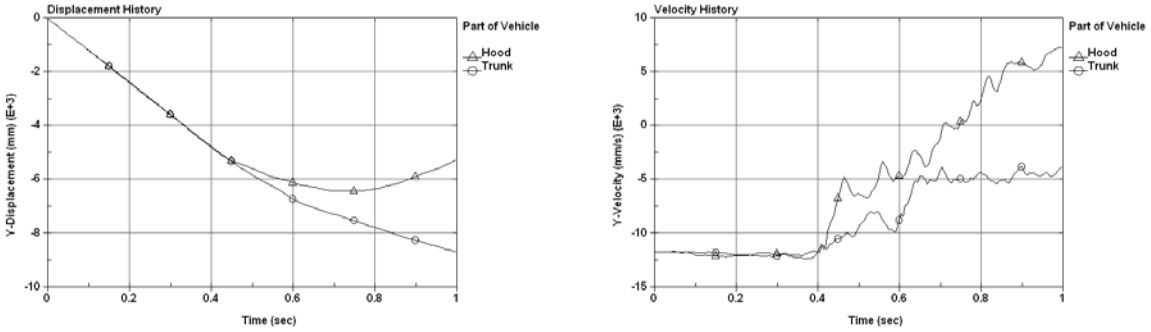


Traversal displacements Traversal velocities

Fig. 4.117: Time histories of traversal displacements and velocities of backside impact on the double-face W-beam (Design #2) at 62 mph and 25° (‘trunk’ means ‘bed’ on the truck).

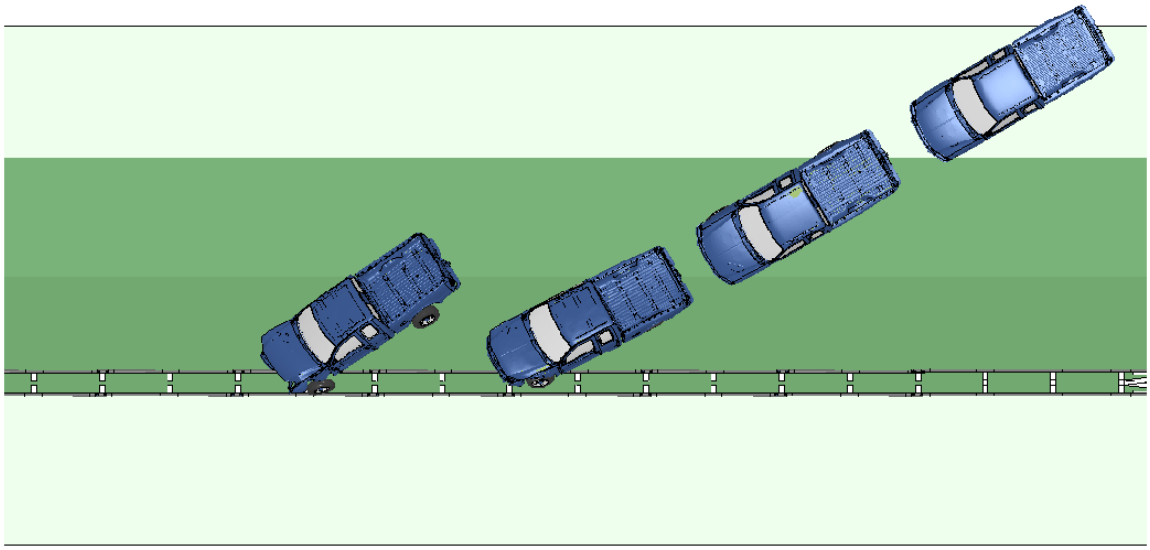

Fig. 4.118: Backside impact on the double-face W-beam (Design #2) at 62 mph and 30°.

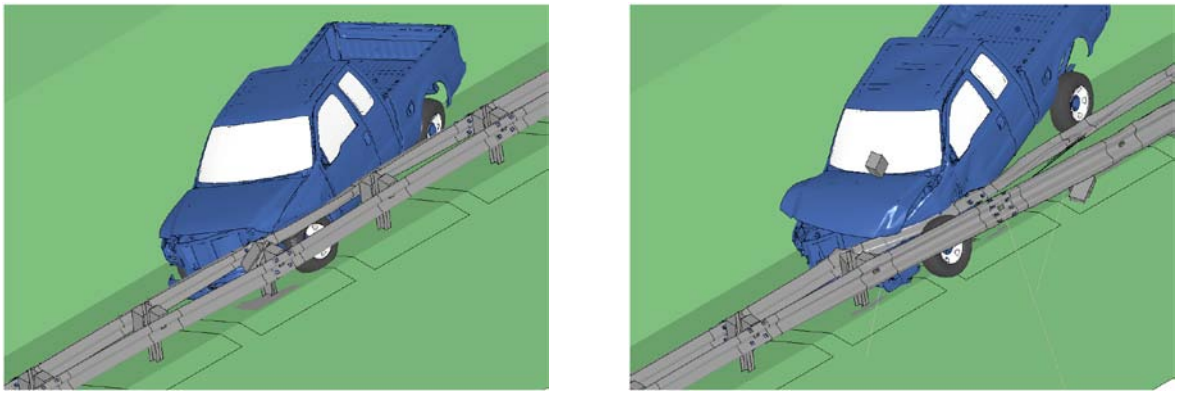

Fig. 4.119: Two instances of backside impact on the double-face W-beam (Design #2) at 62 mph and 30°.

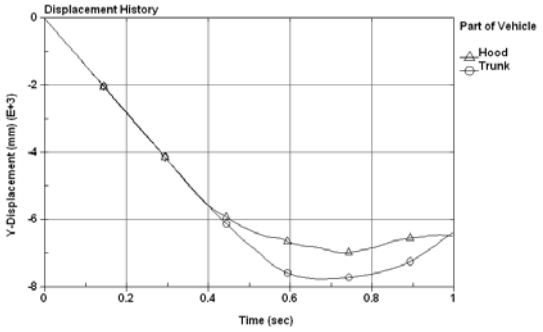


Traversal displacements

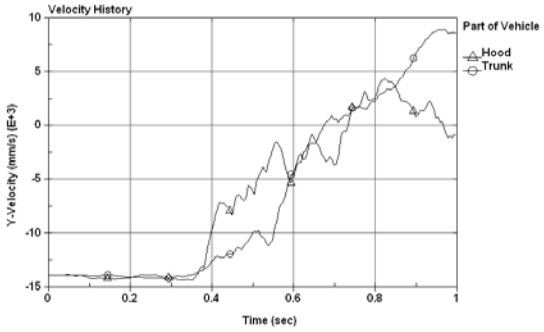


Traversal velocities

Fig. 4.120: Time histories of traversal displacements and velocities of backside impact on the double-face W-beam (Design #2) at 62 mph and 30° (‘trunk’ means ‘bed’ on the truck).

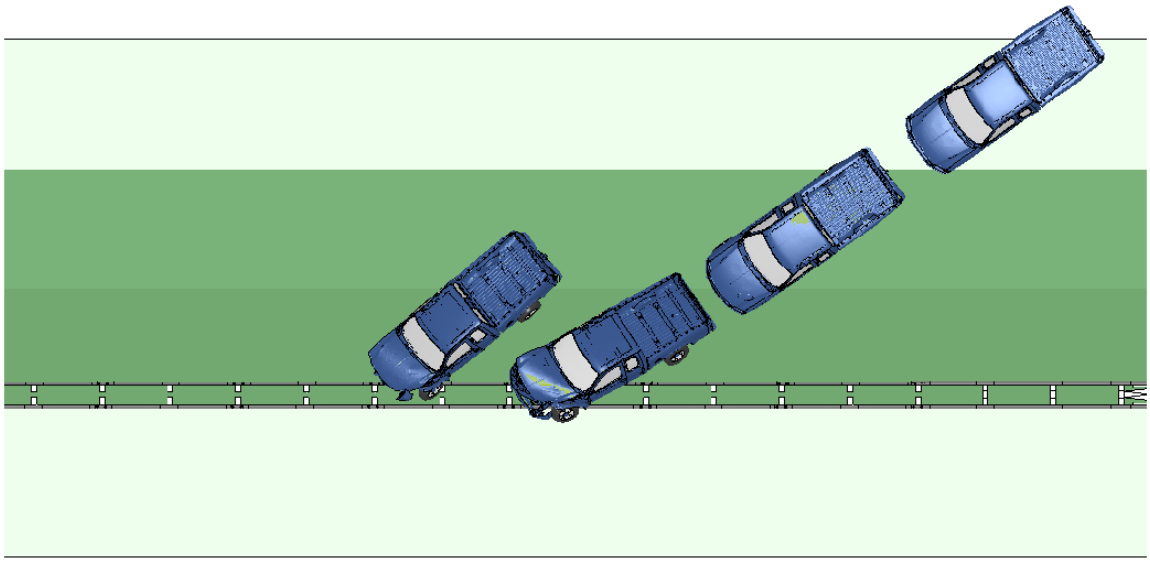

Fig. 4.121: Backside impact on the double-face W-beam (Design #2) at 62 mph and 35°.

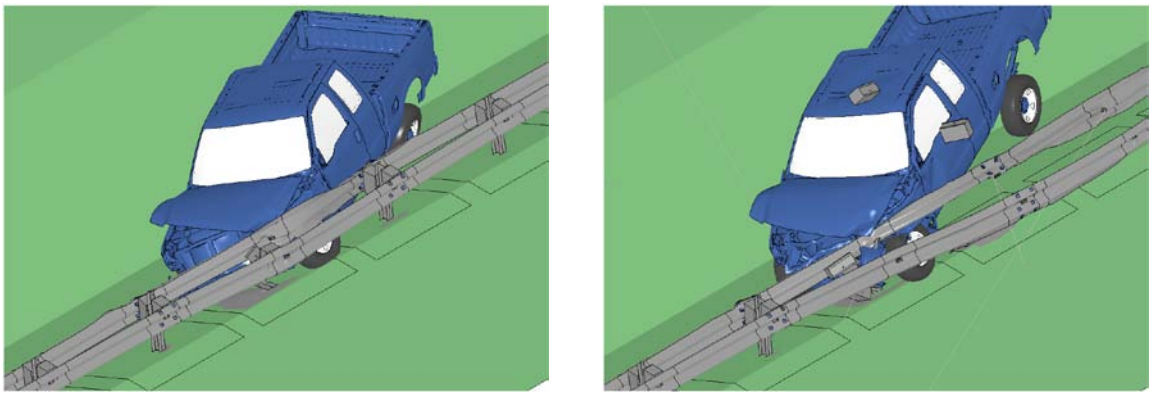

Fig. 4.122: Two instances of backside impact on the double-face W-beam (Design #2) at 62 mph and 35°.

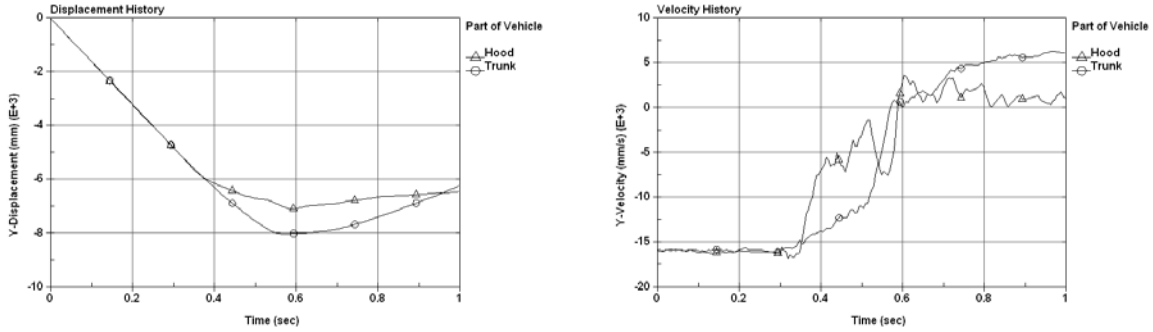


Traversal displacements Traversal velocities

Fig. 4.123: Time histories of traversal displacements and velocities of backside impact on the double-face W-beam (Design #2) at 62 mph and 35° (‘trunk’ means ‘bed’ on the truck).

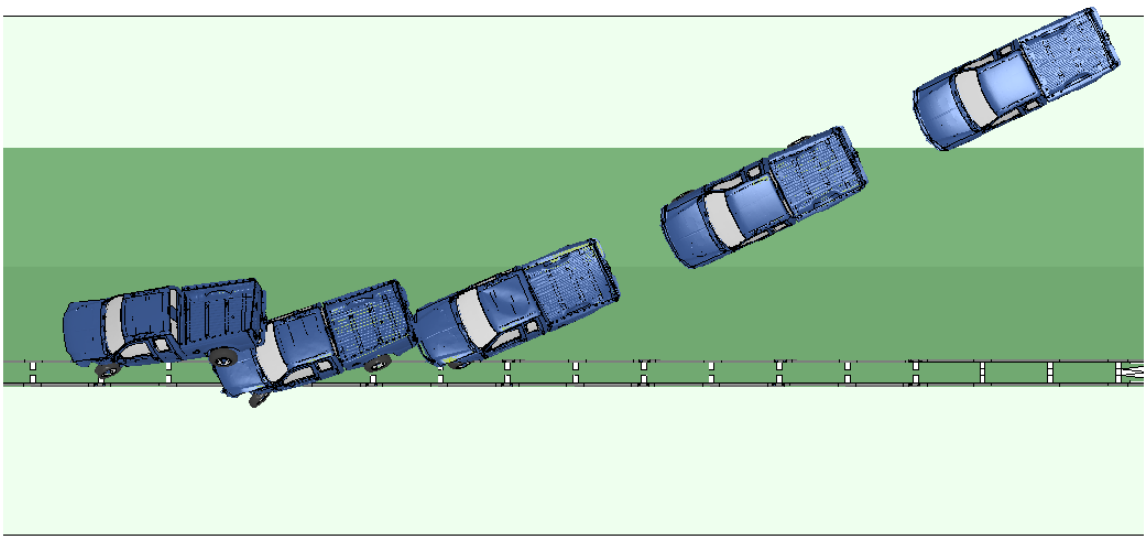

Fig. 4.124: Backside impact on the double-face W-beam (Design #2) at 70 mph and 25°.

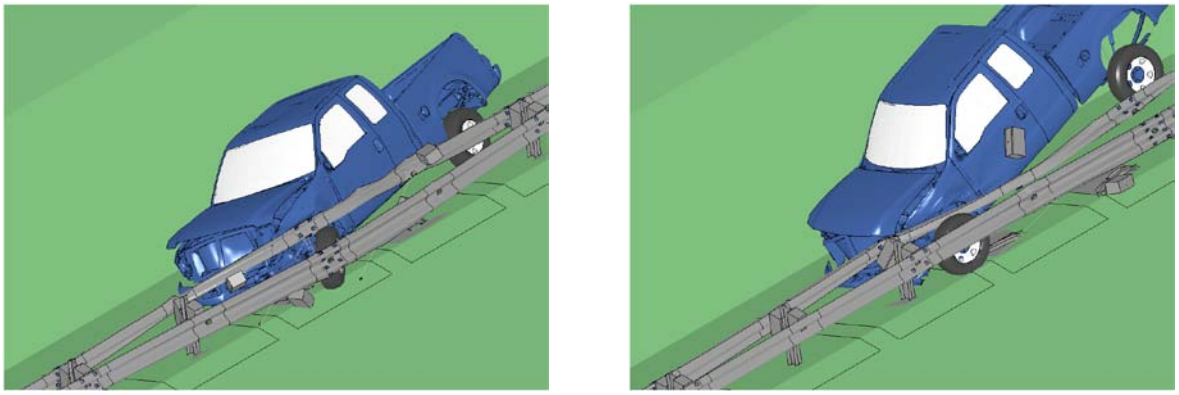

Fig. 4.125: Two instances of backside impact on the double-face W-beam (Design #2) at 70 mph and 25°.

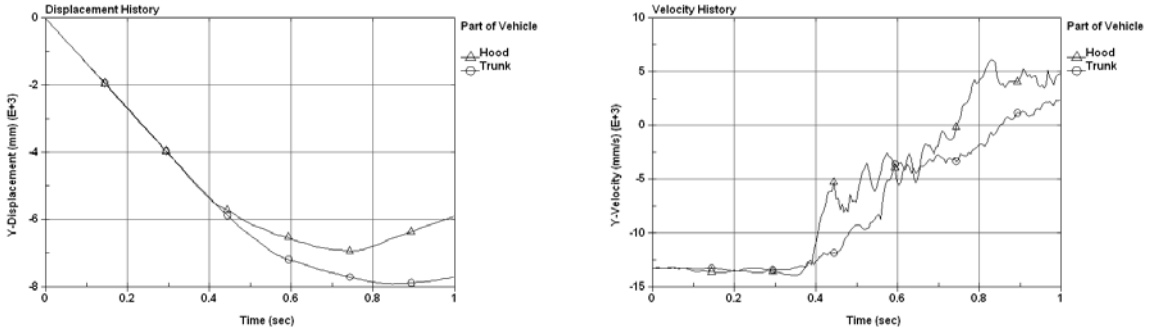


Traversal displacements Traversal velocities

Fig. 4.126: Time histories of traversal displacements and velocities of backside impact on the double-face W-beam (Design #2) at 70 mph and 25° (‘trunk’ means ‘bed’ on the truck).

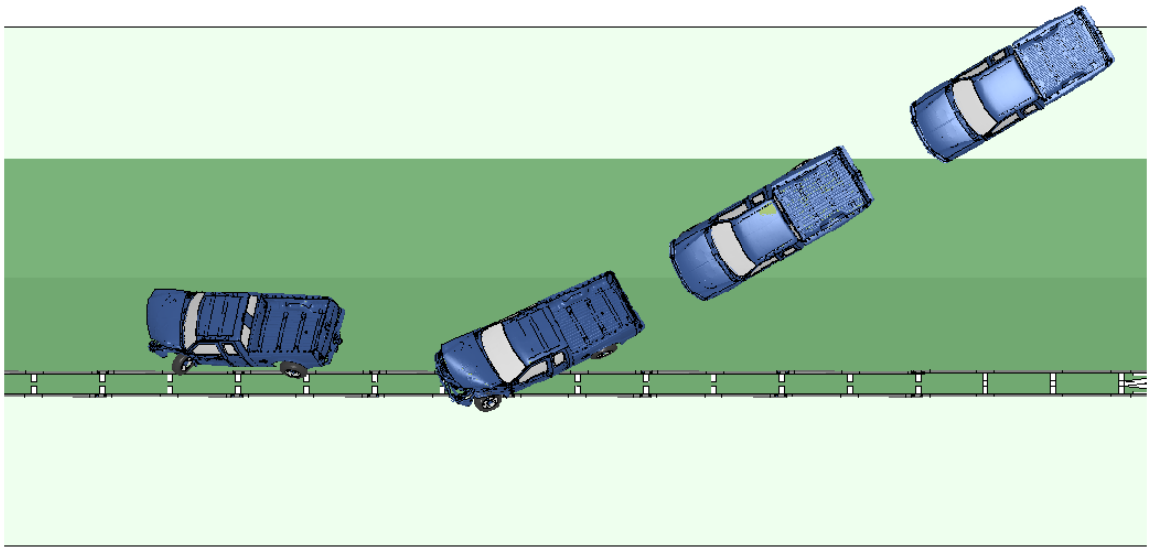

Fig. 4.127: Backside impact on the double-face W-beam (Design #2) at 70 mph and 30°.

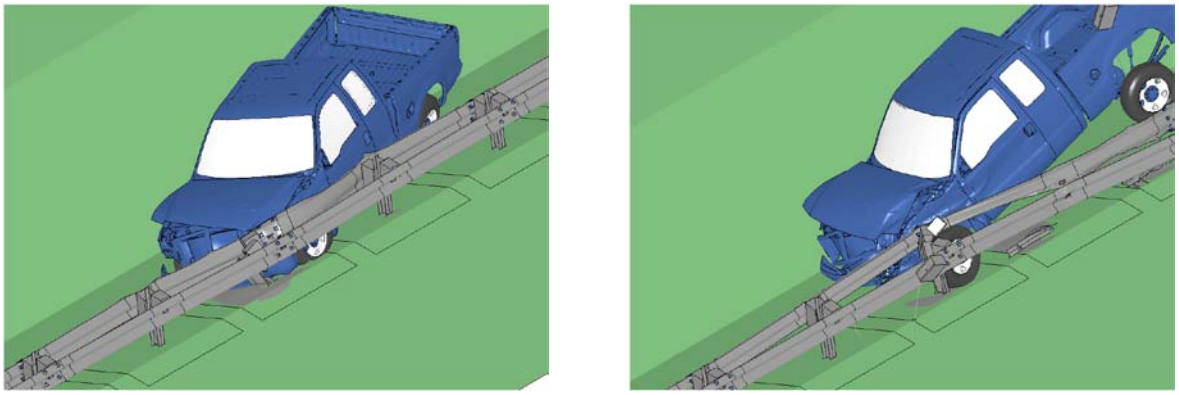

Fig. 4.128: Two instances of backside impact on the double-face W-beam (Design #2) at 70 mph and 30°.

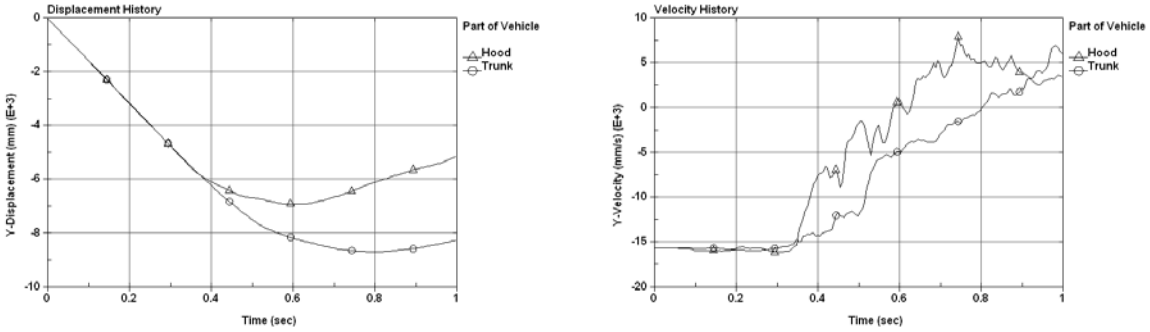


Traversal displacements Traversal velocities

Fig. 4.129: Time histories of traversal displacements and velocities of backside impact on the double-face W-beam (Design #2) at 70 mph and 30° (‘trunk’ means ‘bed’ on the truck).

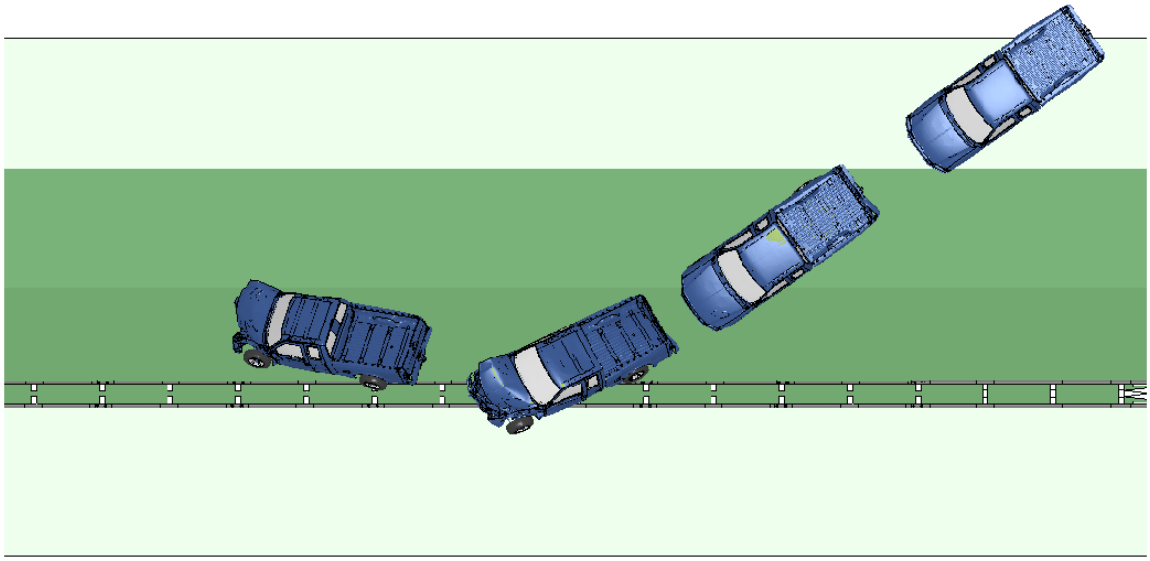

Fig. 4.130: Backside impact on the double-face W-beam (Design #2) at 70 mph and 35°.

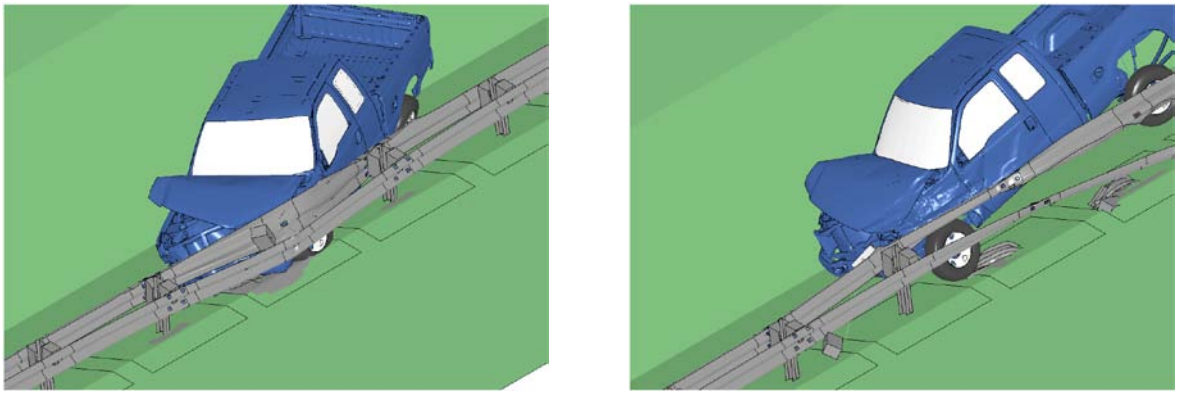

Fig. 4.131: Two instances of backside impact on the double-face W-beam (Design #2) at 70 mph and 35°.

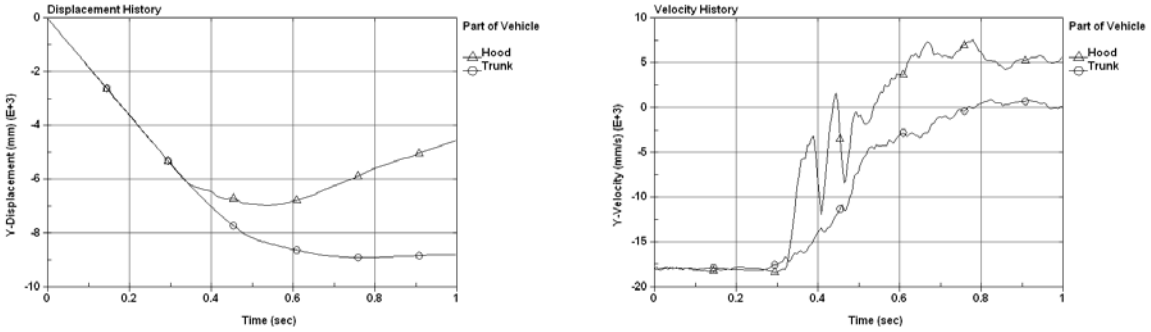


Traversal displacements Traversal velocities

Fig. 4.132: Time histories of traversal displacements and velocities of backside impact on the double-face W-beam (Design #2) at 70 mph and 35° (‘trunk’ means ‘bed’ on the truck).

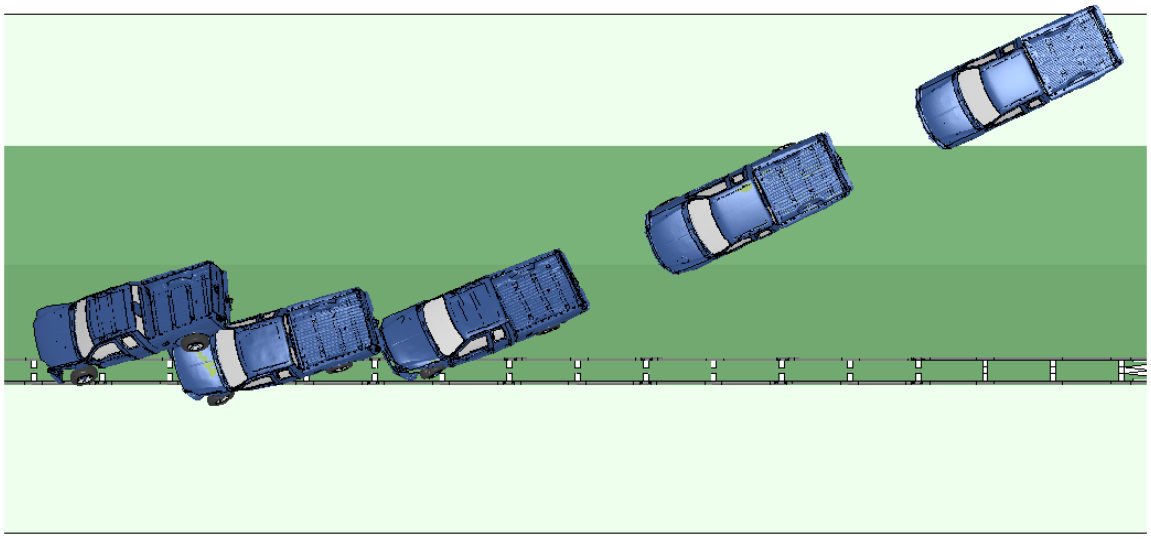

Fig. 4.133: Backside impact on the double-face W-beam (Design #2) at 75 mph and 25°.

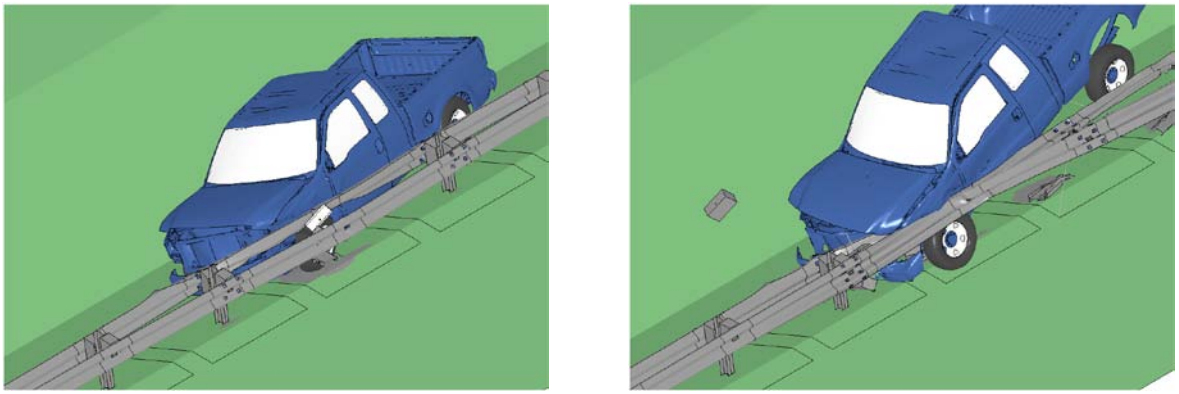

Fig. 4.134: Two instances of backside impact on the double-face W-beam (Design #2) at 75 mph and 25°.

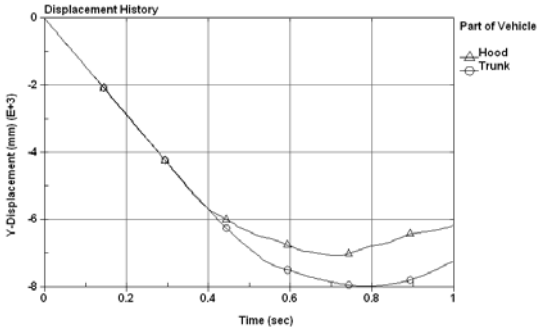


Traversal displacements

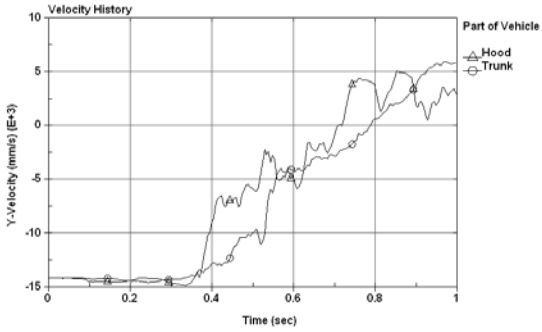


Traversal velocities

Fig. 4.135: Time histories of traversal displacements and velocities of backside impact on the double-face W-beam (Design #2) at 75 mph and 25° (‘trunk’ means ‘bed’ on the truck).

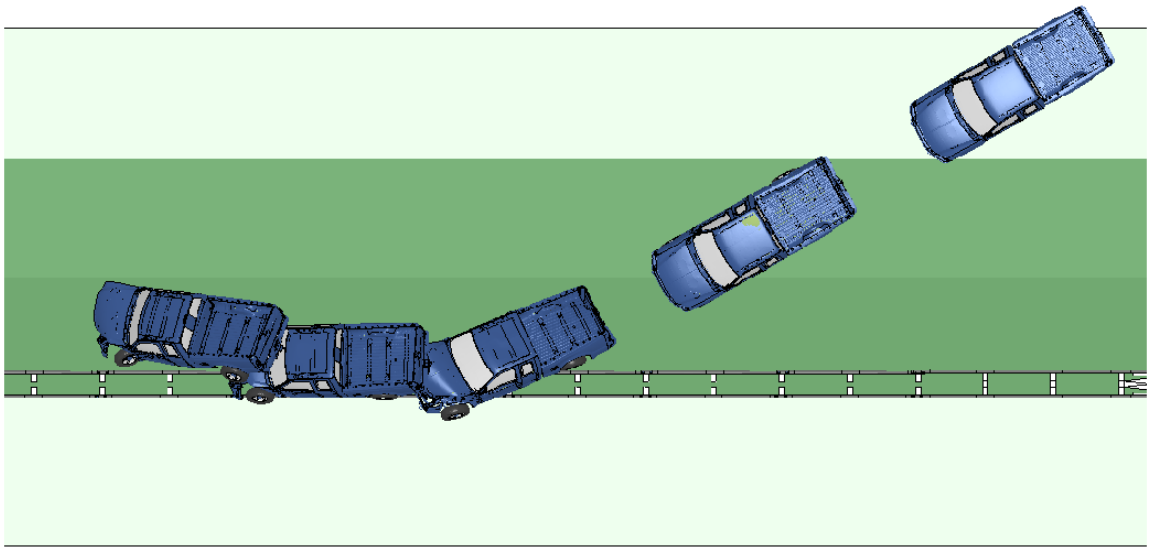

Fig. 4.136: Backside impact on the double-face W-beam (Design #2) at 75 mph and 30°.

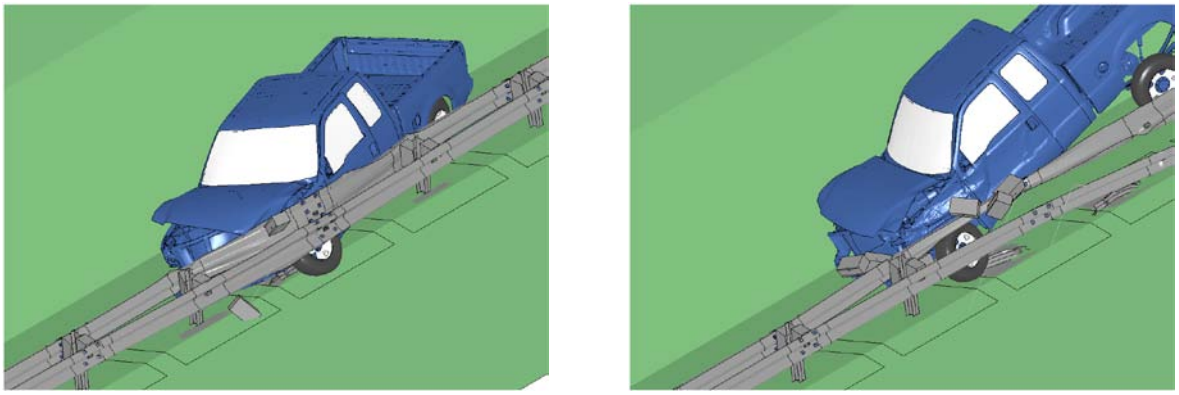

Fig. 4.137: Two instances of backside impact on the double-face W-beam (Design #2) at 75 mph and 30°.

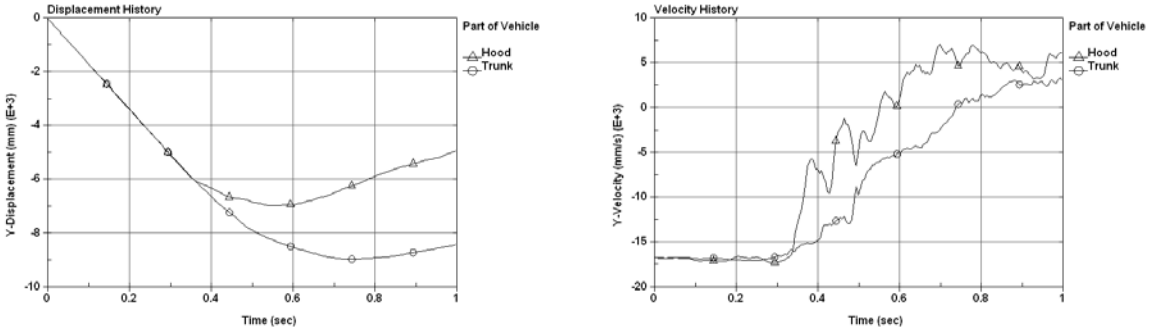


Traversal displacements Traversal velocities

Fig. 4.138: Time histories of traversal displacements and velocities of backside impact on the double-face W-beam (Design #2) at 75 mph and 30° (‘trunk’ means ‘bed’ on the truck).

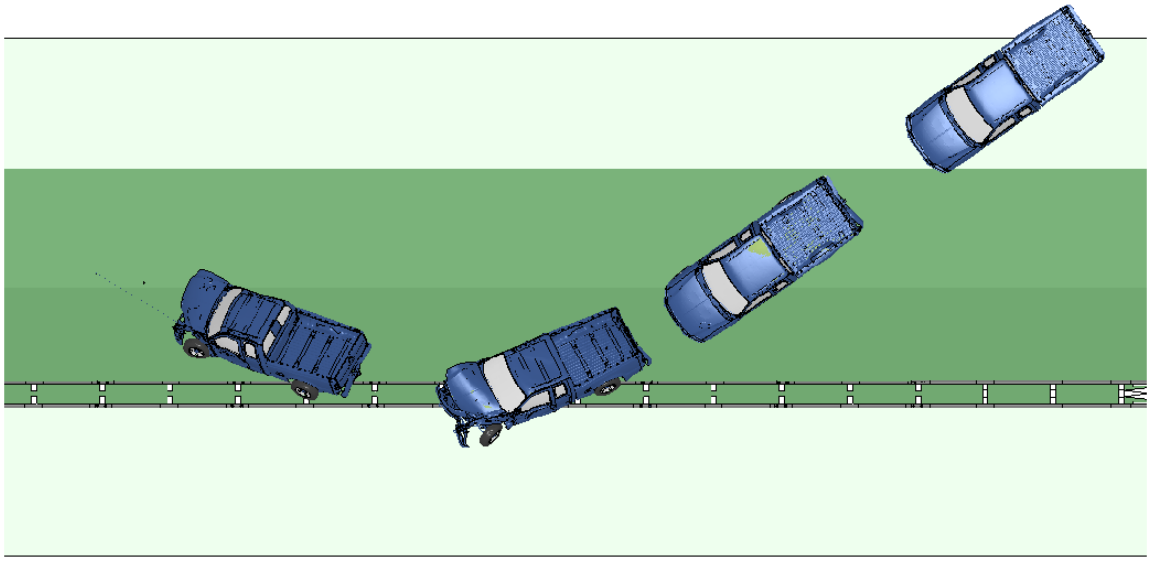

Fig. 4.139: Backside impact on the double-face W-beam (Design #2) at 75 mph and 35°.

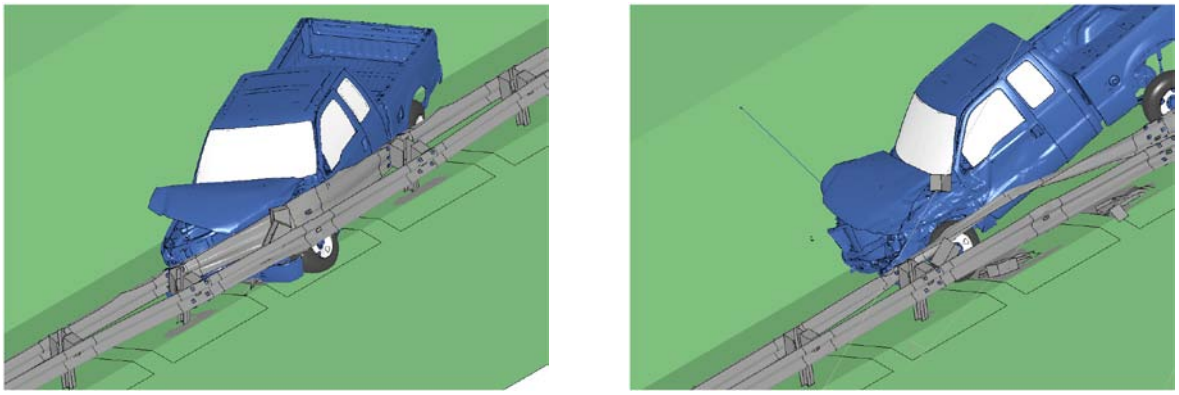

Fig. 4.140: Two instances of backside impact on the double-face W-beam (Design #2) at 75 mph and 35°.

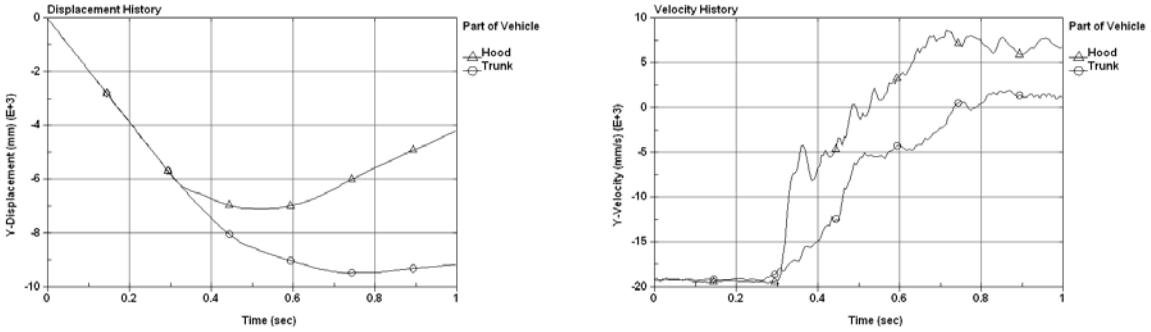


Traversal displacements Traversal velocities

Fig. 4.141: Time histories of traversal displacements and velocities of backside impact on the double-face W-beam (Design #2) at 75 mph and 35° (‘trunk’ means ‘bed’ on the truck).

## 4.4 The Cable Median Barrier

In this project, the CMB was installed 8 ft (2.44 m) from the ditch centerline on the 4:1 slope. Simulations were performed for the CMB under the impacts of the Ford F250 from both front-side and backside. In both front-side and backside impacts, the vehicle was launched from the shoulder with prescribed speeds and angles. The simulation results are summarized in Table 4.4 for both front-side and backside impacts.

Table 4.4: Simulation results of the cable median barrier

| **Impact Side** | **Impact Angle** | **Impact Speed** | | |
|---|---|---|---|---|
| | | 62 mph (100 km/hr ) | 70 mph (112.6 km/hr) | 75 mph (120.7 km/hr) |
| Front | 25° | Vehicle redirected followed by a rollover towards the 2.5:1 slope | Vehicle redirected followed by a rollover towards the 2.5:1 slope | Vehicle redirected followed by a rollover towards the 2.5:1 slope |
| | 30° | Vehicle redirected followed by a rollover towards the 2.5:1 slope | Vehicle redirected followed by a rollover towards the 2.5:1 slope | Vehicle redirected without rollover |
| | 35° | Vehicle redirected followed by a rollover towards the 4:1 slope | Vehicle redirected followed by a rollover towards the 4:1 slope | Vehicle redirected followed by a rollover towards the 4:1 slope |
| Back | 25° | Vehicle redirected on the shoulder | Vehicle redirected on the shoulder followed by a rollover | Vehicle redirected on the shoulder followed by a rollover |
| | 30° | Vehicle redirected on the shoulder followed by a rollover | Vehicle redirected on the shoulder followed by a rollover | Vehicle not redirected |
| | 35° | Vehicle redirected on the shoulder followed by a rollover | Vehicle redirected on the shoulder followed by a rollover | Vehicle not redirected |

In all cases of front-side impacts, the vehicle was engaged with one or two cables and was retained in the median. Due to the large vehicle mass, high central gravity, and relatively large median slope (4:1), the vehicle rolled over on the median in all cases except for the 30° impact at 75 mph (120.7 km/hr). In all of the 25° and 30° impacts, the vehicle was first redirected after impacting the CMB and going down the 4:1 slope. The vehicle then rolled over towards the uphill 2.5:1 slope. In the cases of 35° impacts, the vehicle was not fully redirected at the bottom of the ditch and, upon going up the 2.5:1 slope, rolled over backwards towards the 4:1 slope. Note that the vehicle traveled a shorter distance in the 35° cases from the initial impact point to the bottom of the ditch. Consequently, the vehicle maintained a relatively large traversal velocity that allowed it to go up the 2.5 slope without being fully redirected. Without the full redirection, the vehicle did not roll over towards the 2.5:1 slope. While being redirected on the 2.5:1 slope by the cables, the vehicle turned back towards the 4:1 slope, resulting in a rollover in the 35° impacts at all three speeds.

The simulation results of all front-side impacts are shown in Figs. 4.142 to 4.168, including the vehicle's displacement paths, detailed views of vehicle-CMB interactions, and time histories of the vehicle's traversal displacements and velocities.

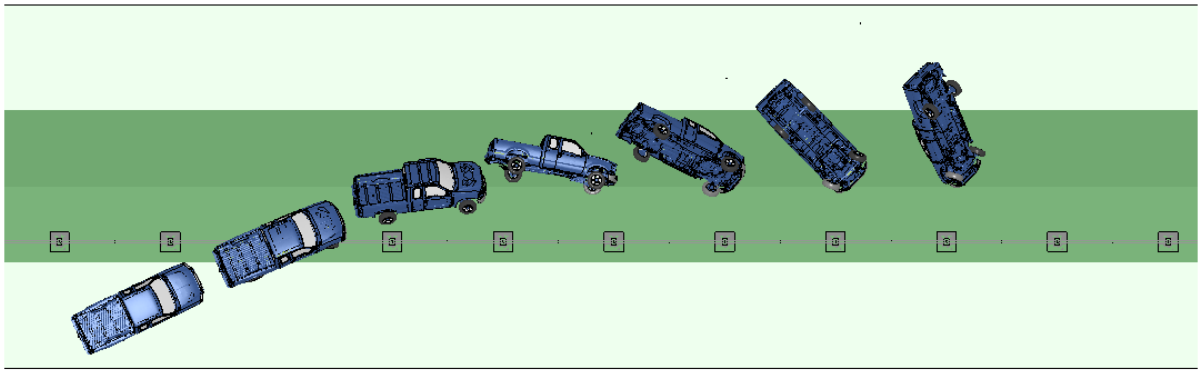

Fig. 4.142: Front-side impact on CMB at 62 mph and 25°.

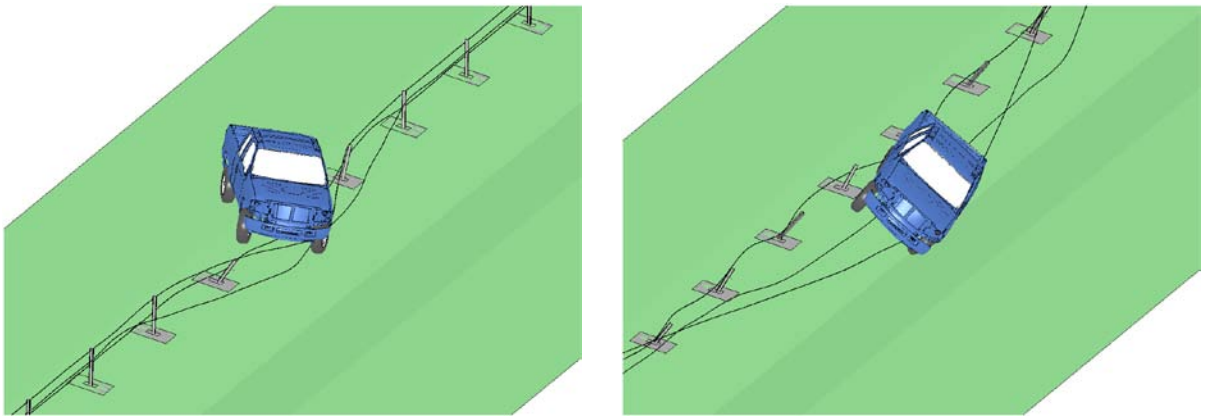

Fig. 4.143: Two instances of vehicle impacting CMB from front-side at 62 mph and 25°.

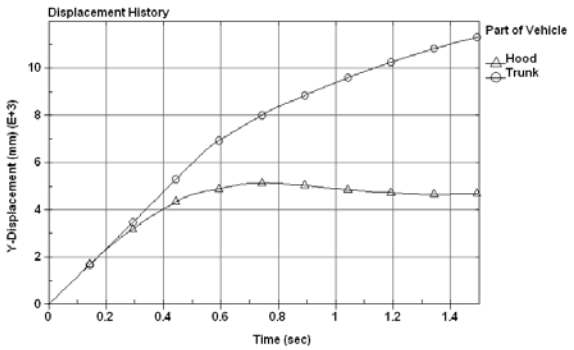


Traversal displacements

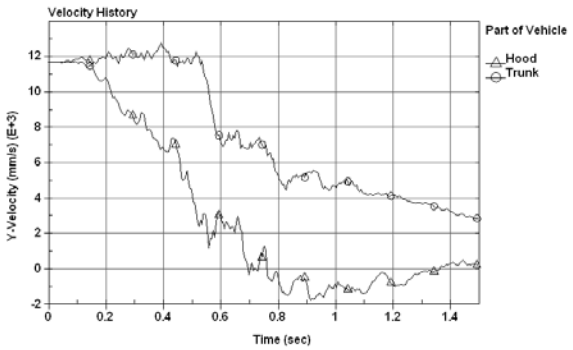


Traversal velocities

Fig. 4.144: Time histories of traversal displacements and velocities of the vehicle impacting the CMB from front-side at 62 mph and 25° ('trunk' means 'bed' on the truck).

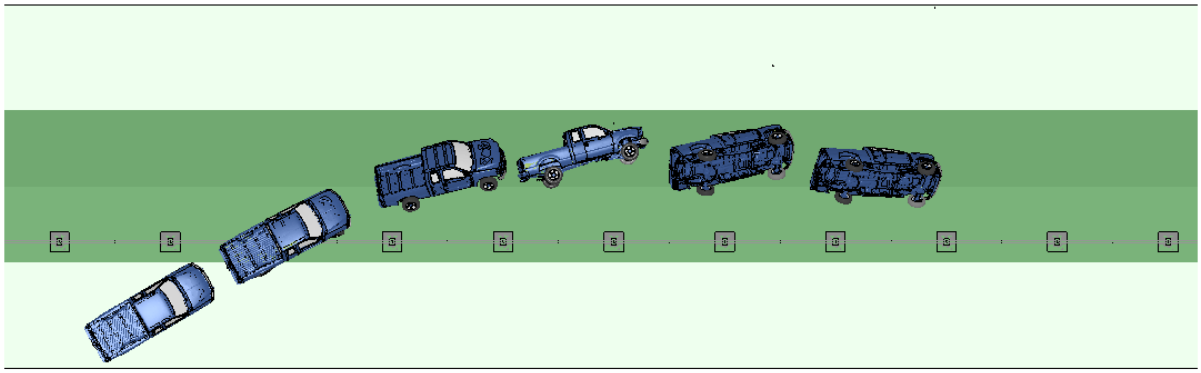

Fig. 4.145: Front-side impact on CMB at 62 mph and 30°.

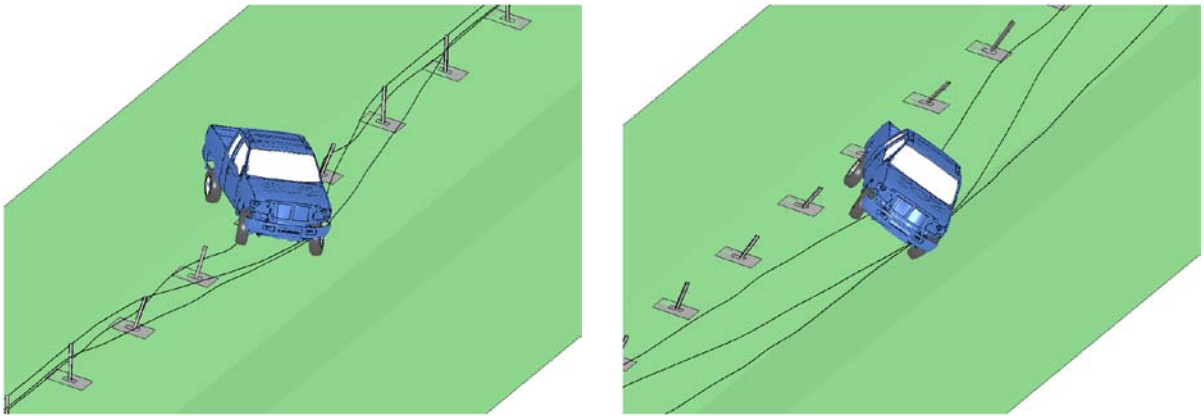

Fig. 4.146: Two instances of vehicle impacting CMB from front-side at 62 mph and 30°.

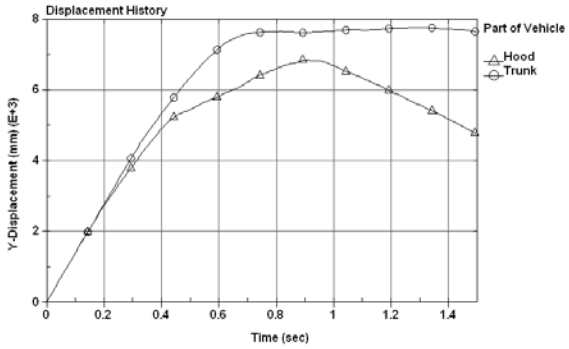


Traversal displacements

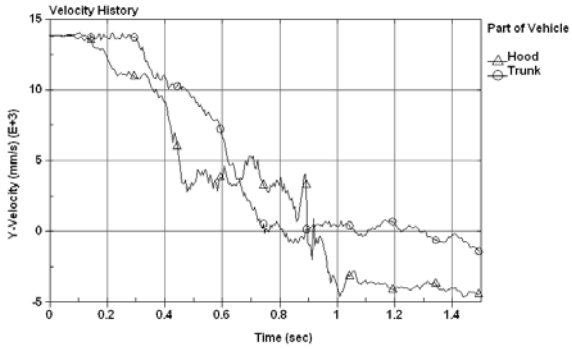


Traversal velocities

Fig. 4.147: Time histories of traversal displacements and velocities of the vehicle impacting the CMB from front-side at 62 mph and 30° ('trunk' means 'bed' on the truck).

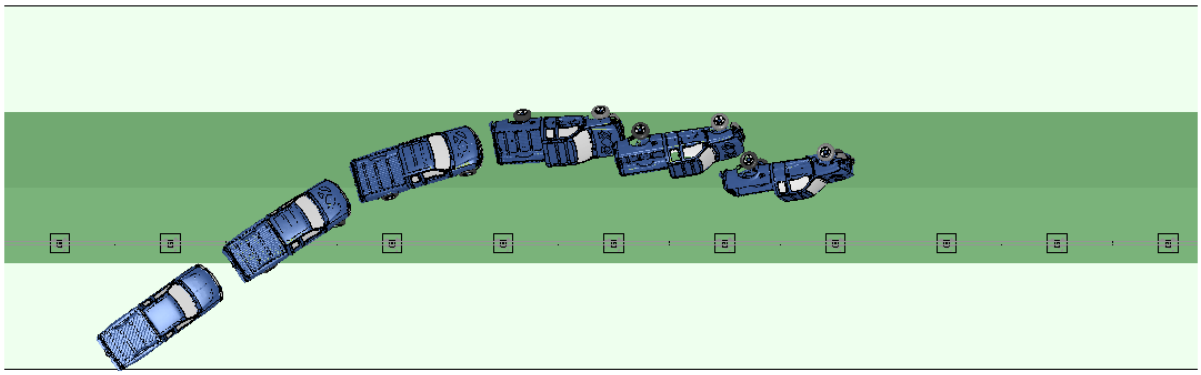

Fig. 4.148: Front-side impact on CMB at 62 mph and 35°.

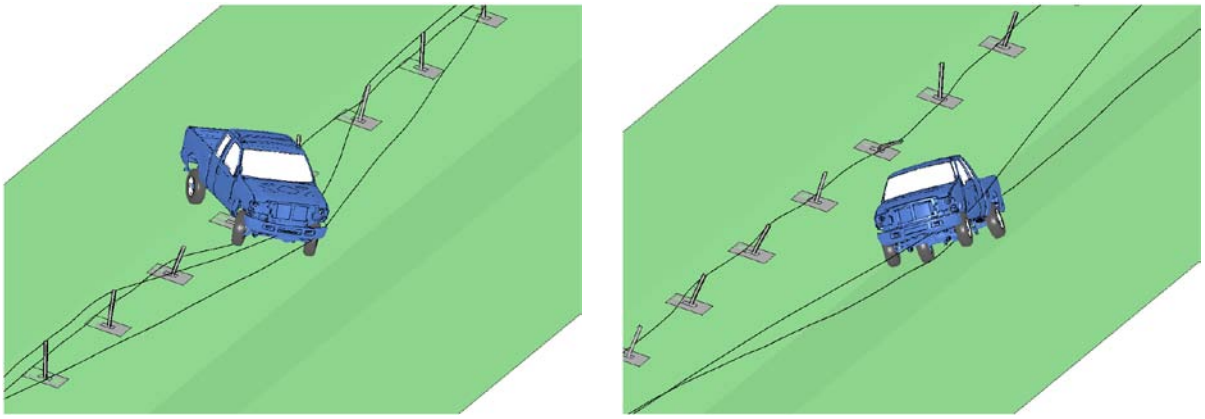

Fig. 4.149: Two instances of vehicle impacting CMB from front-side at 62 mph and 35°.

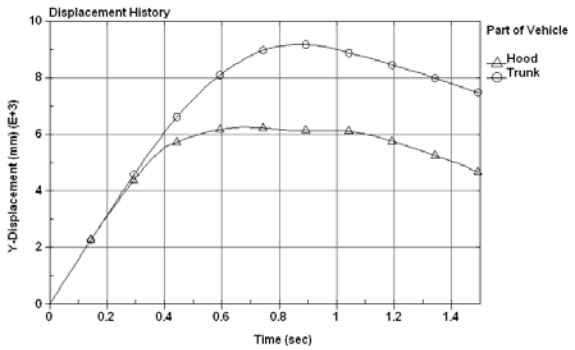


Traversal displacements

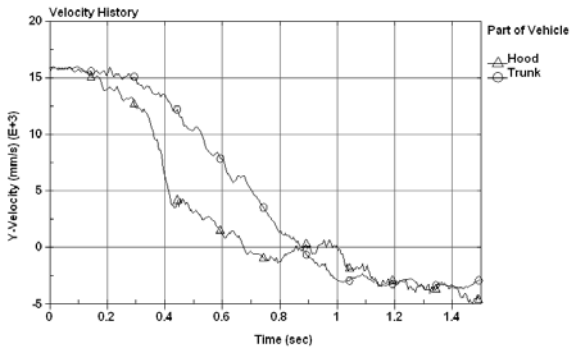


Traversal velocities

Fig. 4.150: Time histories of traversal displacements and velocities of the vehicle impacting the CMB from front-side at 62 mph and 35° (‘trunk’ means ‘bed’ on the truck).

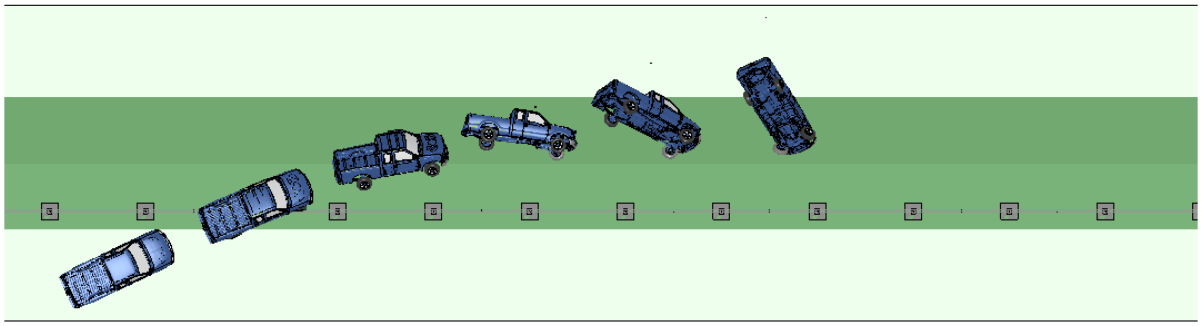

Fig. 4.151: Front-side impact on CMB at 70 mph and 25°.

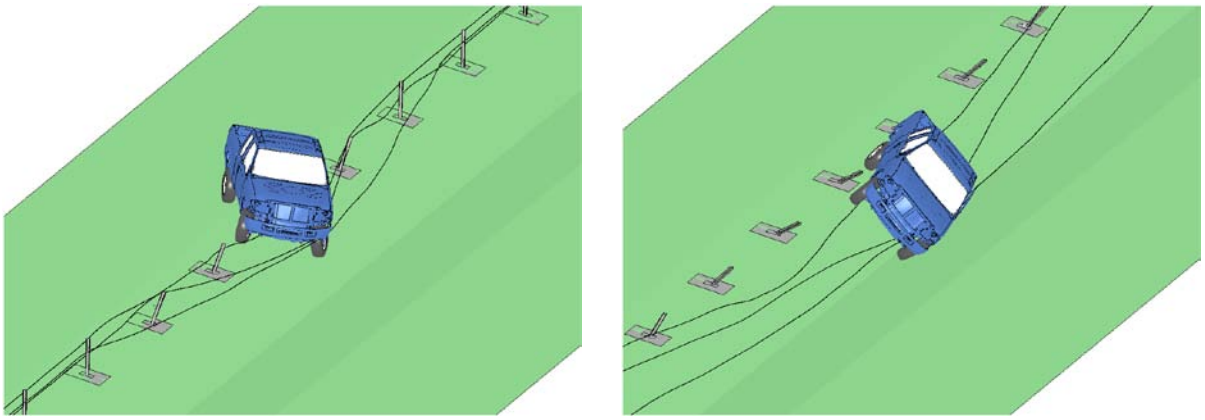

Fig. 4.152: Two instances of vehicle impacting CMB from front-side at 70 mph and 25°.

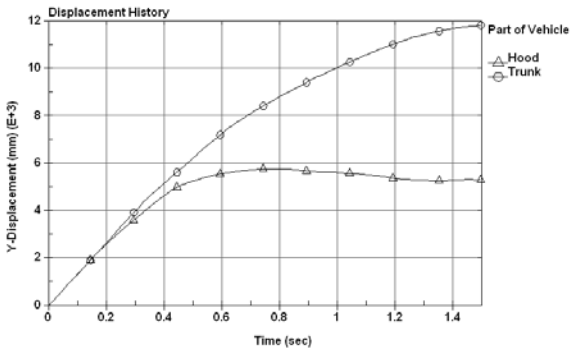


Traversal displacements

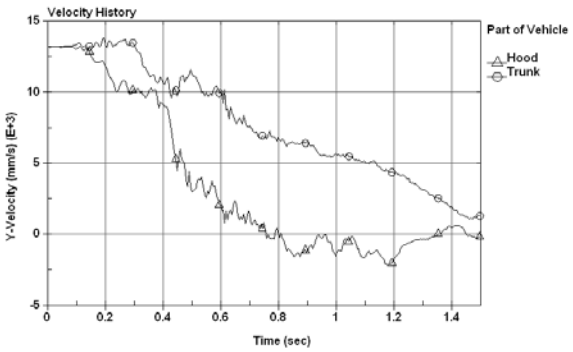


Traversal velocities

Fig. 4.153: Time histories of traversal displacements and velocities of the vehicle impacting the CMB from front-side at 70 mph and 25° (‘trunk’ means ‘bed’ on the truck).

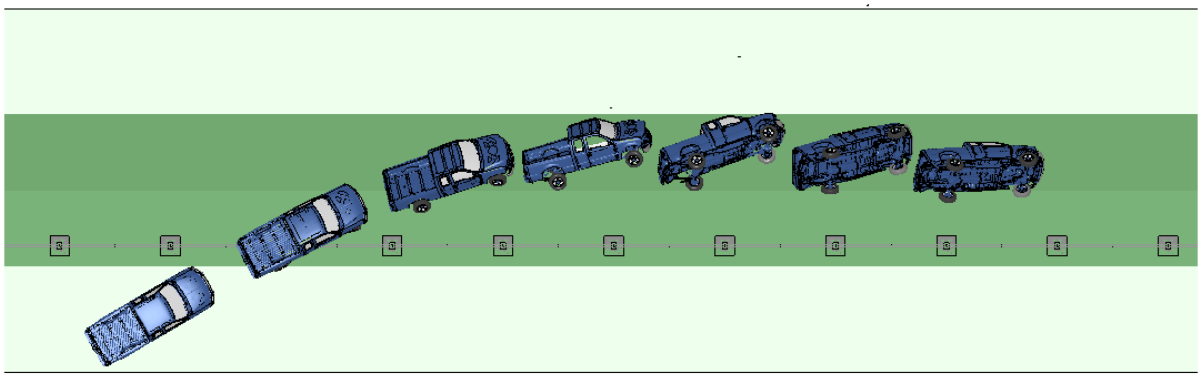

Fig. 4.154: Front-side impact on CMB at 70 mph and 30°.

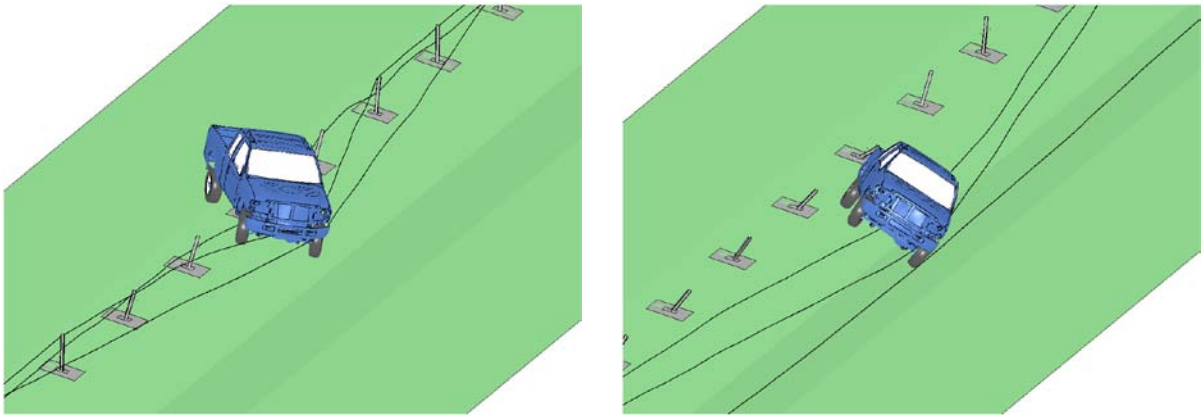

Fig. 4.155: Two instances of vehicle impacting CMB from front-side at 70 mph and 30°.

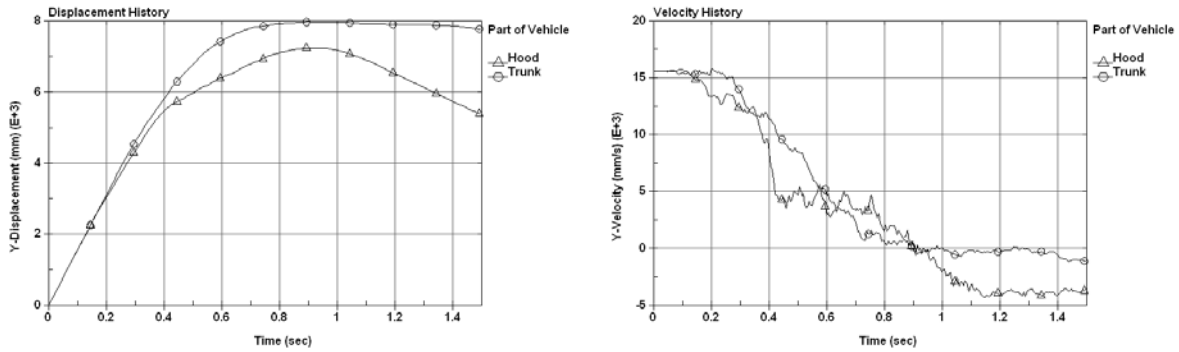


Traversal displacements Traversal velocities

Fig. 4.156: Time histories of traversal displacements and velocities of the vehicle impacting the CMB from front-side at 70 mph and 30° ('trunk' means 'bed' on the truck).

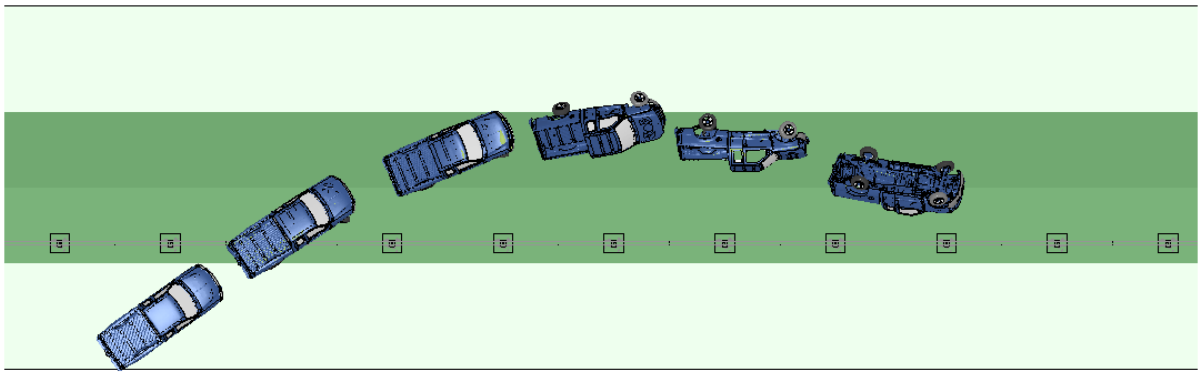

Fig. 4.157: Front-side impact on CMB at 70 mph and 35°.

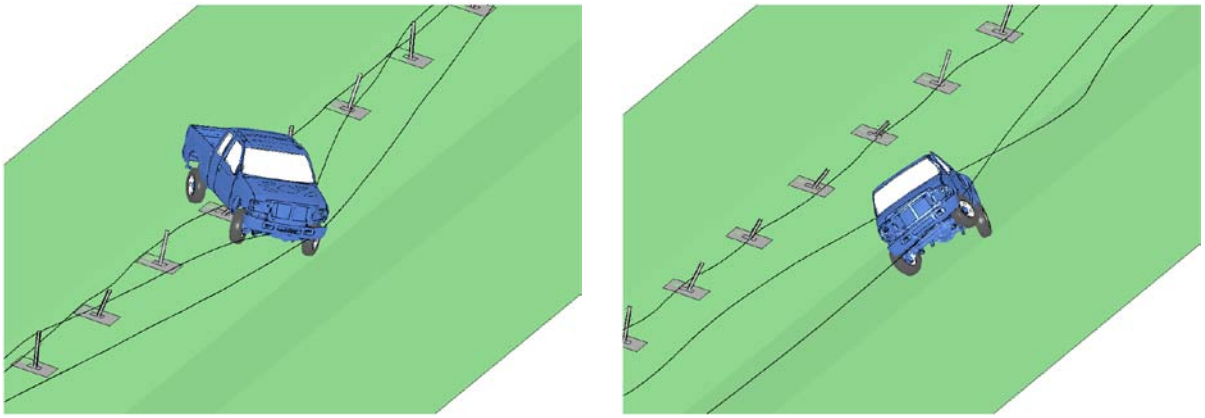

Fig. 4.158: Two instances of vehicle impacting CMB from front-side at 70 mph and 35°.

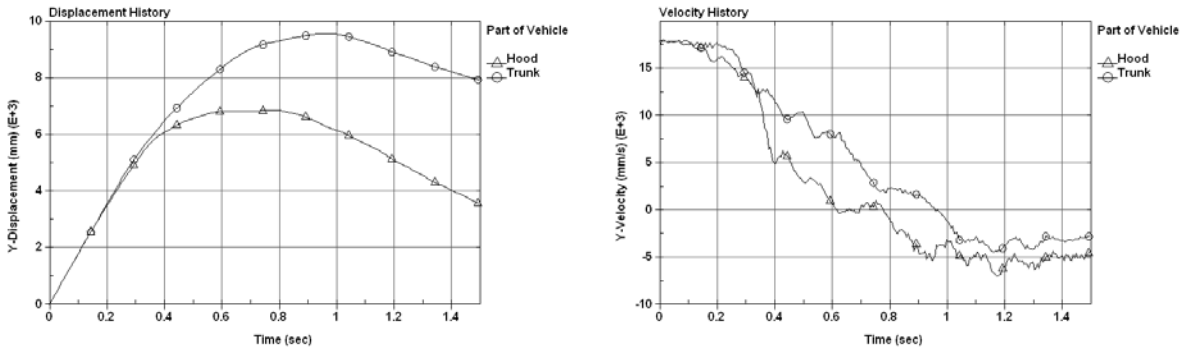


Traversal displacements Traversal velocities

Fig. 4.159: Time histories of traversal displacements and velocities of the vehicle impacting the CMB from front-side at 70 mph and 35° ('trunk' means 'bed' on the truck).

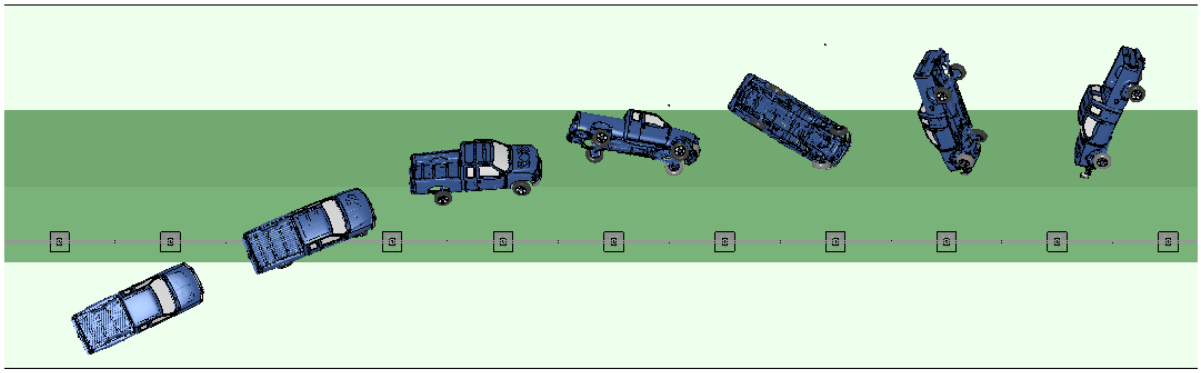

Fig. 4.160: Front-side impact on CMB at 75 mph and 25°.

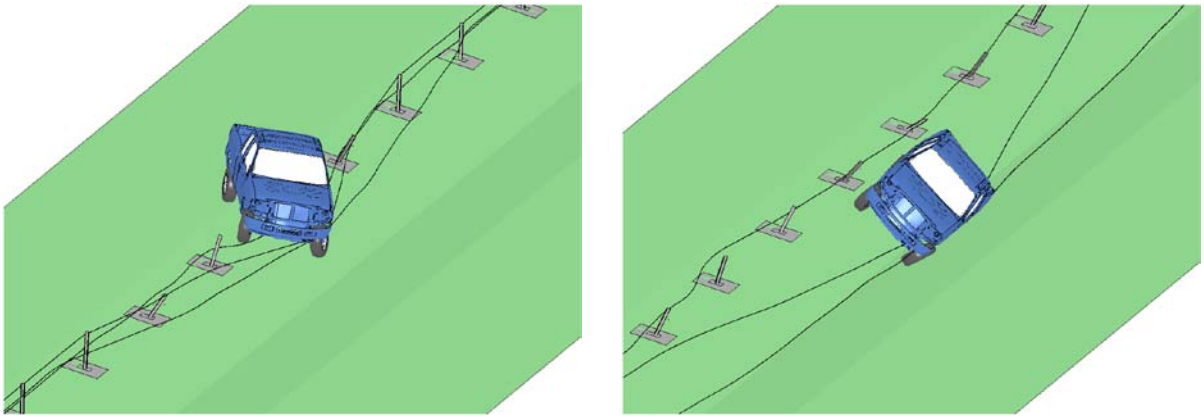

Fig. 4.161: Two instances of vehicle impacting CMB from front-side at 75 mph and 25°.

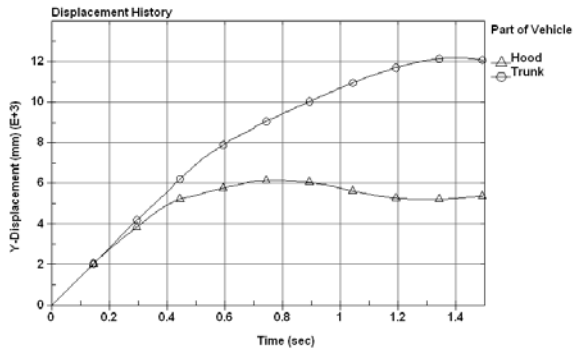


Traversal displacements

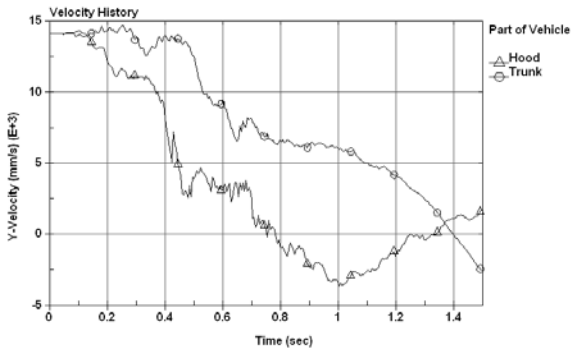


Traversal velocities

Fig. 4.162: Time histories of traversal displacements and velocities of the vehicle impacting the CMB from front-side at 75 mph and 25° ('trunk' means 'bed' on the truck).

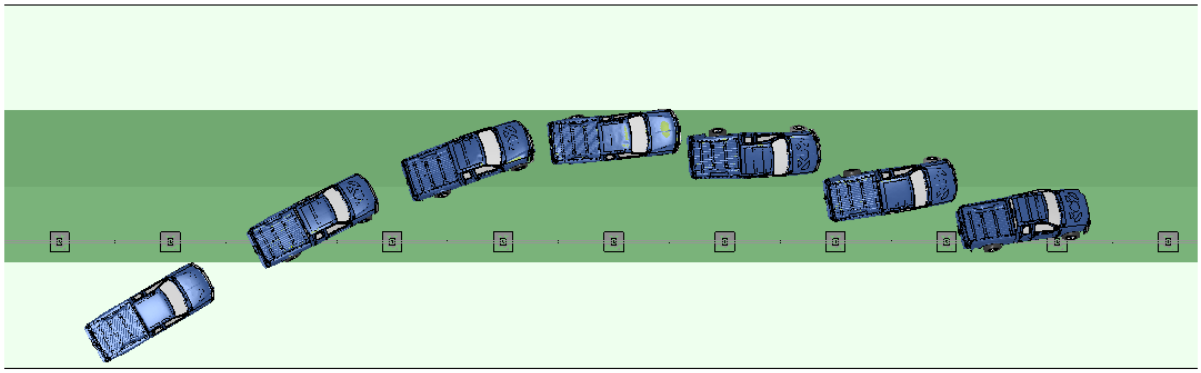

Fig. 4.163: Front-side impact on CMB at 75 mph and 30°.

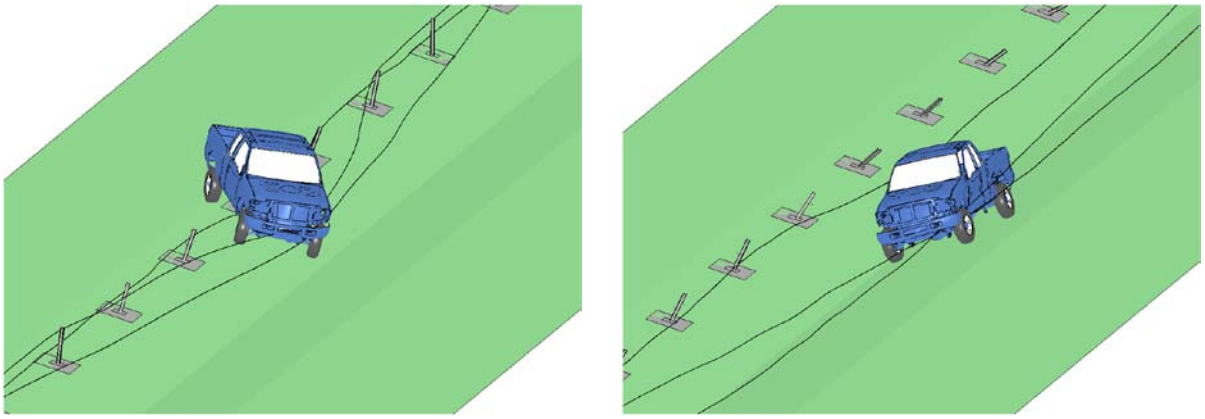

Fig. 4.164: Two instances of vehicle impacting CMB from front-side at 75 mph and 30°.

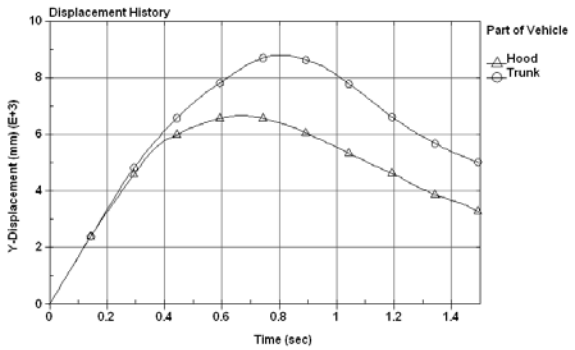


Traversal displacements

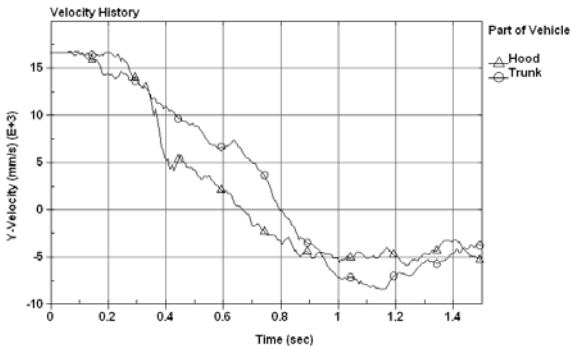


Traversal velocities

Fig. 4.165: Time histories of traversal displacements and velocities of the vehicle impacting the CMB from front-side at 75 mph and 30° ('trunk' means 'bed' on the truck).

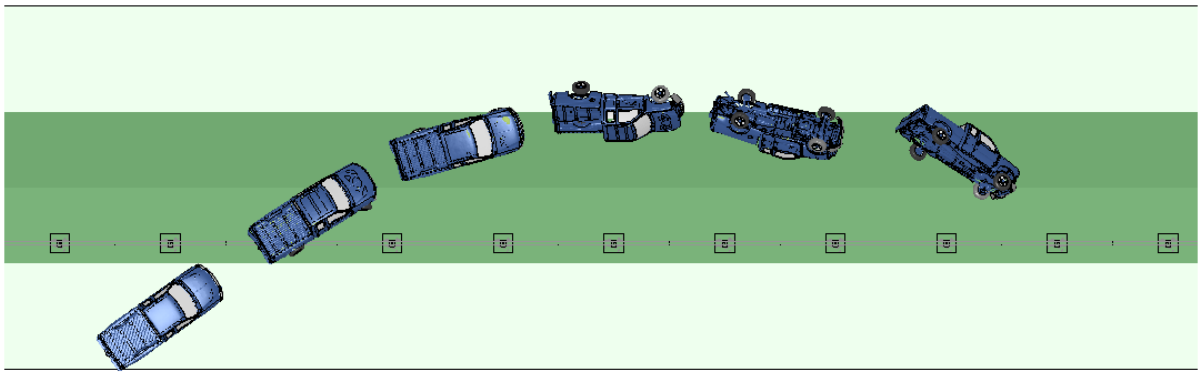

Fig. 4.166: Front-side impact on CMB at 75 mph and 35°.

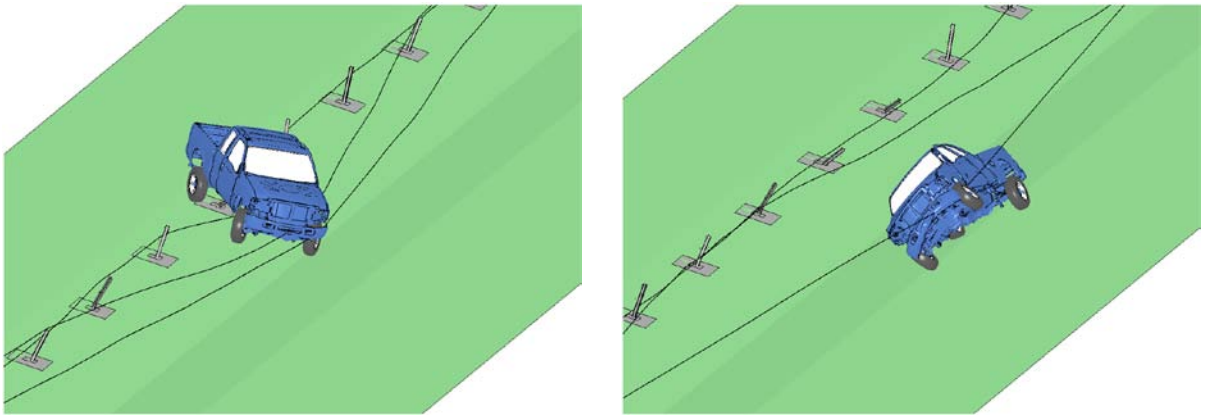

Fig. 4.167: Two instances of vehicle impacting CMB from front-side at 75 mph and 35°.

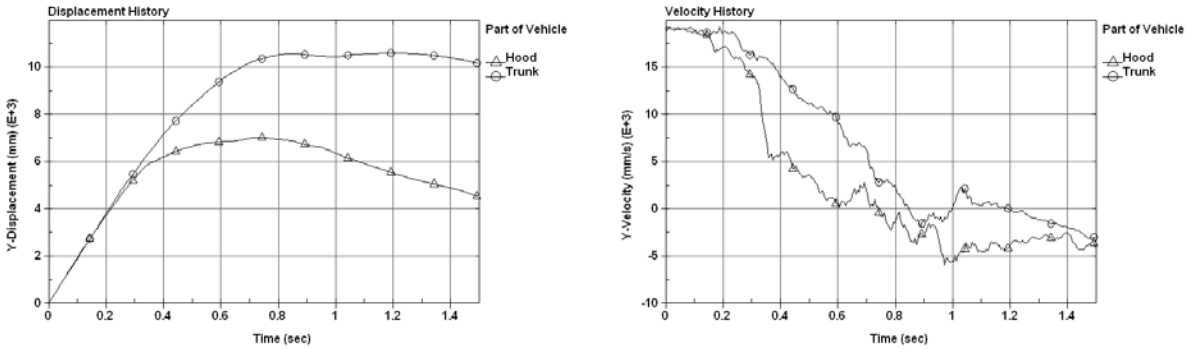


Traversal displacements Traversal velocities

Fig. 4.168: Time histories of traversal displacements and velocities of the vehicle impacting the CMB from front-side at 75 mph and 35° (‘trunk’ means ‘bed’ on the truck).

In all backside-impact simulations, the vehicle left the shoulder next to the 2.5:1 slope with prescribed speeds and angles. The simulation results showed that in all these cases, the vehicle landed on the 4:1 slope, either immediately followed by or at the same time impacting the CMB from the backside. The vehicle did not land on top of the CMB, which was a major concern and would cause a straight-through penetration. Due to the airborne trajectory, the vehicle bounced up after hitting the ground and thus engaged with the cable(s) on the lower part of its body. This low-position engagement and the large traversal velocities were the main reason for the vehicle rollover that occurred in most cases of backside impacts.

The 25° backside impact at 62 mph (100 km/hr) was the only one in which the vehicle was safely redirected on the shoulder next to the opposing travel lanes. This indicated that the CMB actually outperformed the TL-3 requirements specified by the NCHRP Report 350, because the impacting vehicle, Ford F250, had a larger mass than the TL-3 testing vehicle in addition to the unfavorable median conditions (i.e., the large median slopes). In the two most severe cases, the 30° and 35° impacts at 75 mph (120.7 km/hr), the vehicle was weakly engaged with the cables and was not redirected. In all the other backside impacts, the vehicle was first redirected and then rolled over towards the oncoming traffic lanes. The simulation results of all backside impacts are shown in Figs. 4.169 to 4.195, including the vehicle's displacement paths, detailed views of vehicle-CMB interactions, and time histories of the vehicle's traversal displacements and velocities.

Recall that the CMB was able to redirect the vehicle in the 25° front-side impact at 62 mph (100 km/hr) even though a rollover followed the redirection. This rollover was mainly caused by the median slope, large vehicle size and mass, and the vehicle's airborne trajectory before impacting the CMB. Considering the successful redirection in the 25° backside impact at 62 mph (100 km/hr), the CMB actually outperformed the TL-3 requirements of the NCHRP Report 350. For impacts at higher speeds and larger angles, the observed vehicle rollover may become a practical concern and deserve further investigation for improvement. The simulation results of this study suggested that the passenger truck was rollover-prone after impacting the CMB and landing on the sloped median. Therefore, an investigation of the placement of CMB on larger slopes may provide an insight of CMB performance and help to reduce the occurrence of rollovers. It was also observed that vehicle rollover was closely related to impact angles and median slopes. To this end, installing CMB on a flatter median is always preferred when site conditions along with other considerations permit.

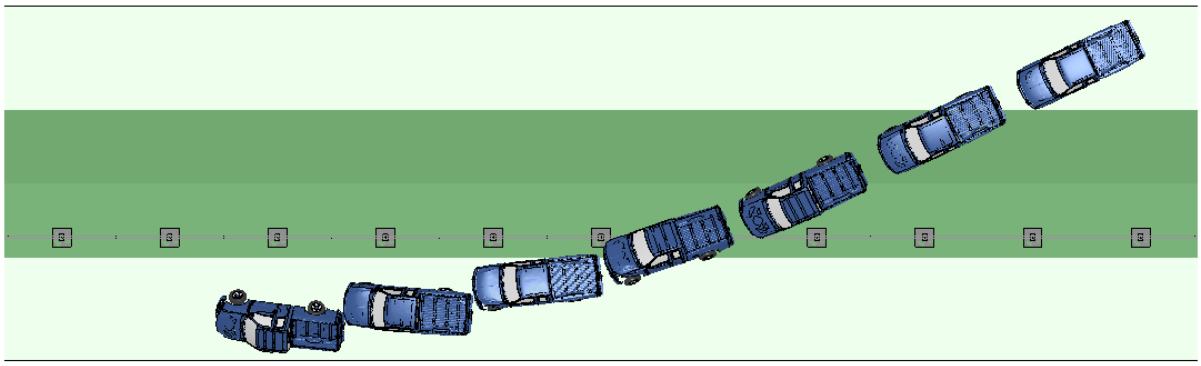

Fig. 4.169: Backside impact on CMB at 62 mph and 25°.

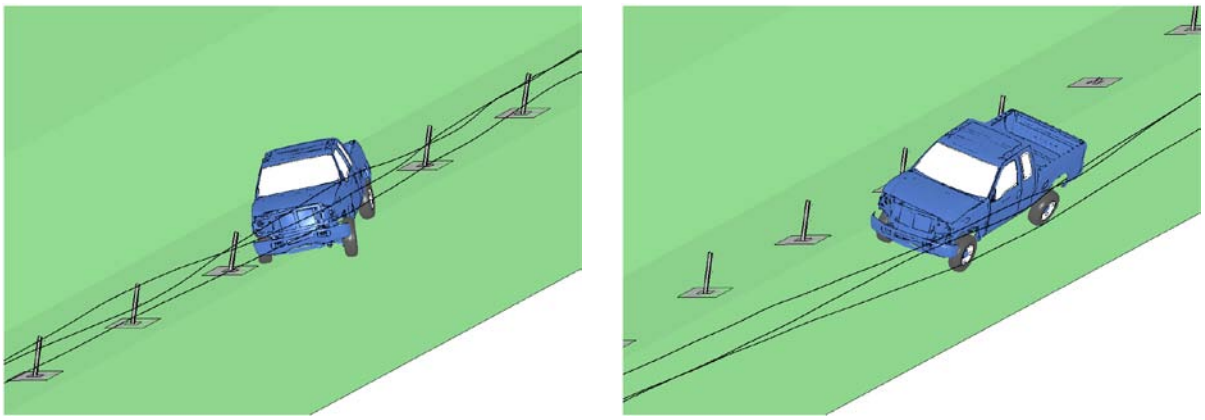

Fig. 4.170: Two instances of vehicle impacting CMB from backside at 62 mph and 25°.

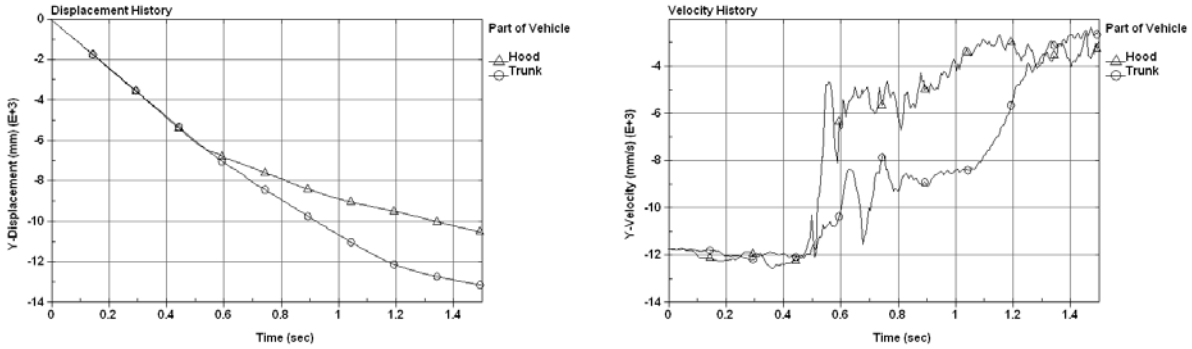


Traversal displacements Traversal velocities

Fig. 4.171: Time histories of traversal displacements and velocities of the vehicle impacting the CMB from backside at 62 mph and 25° (‘trunk’ means ‘bed’ on the truck).

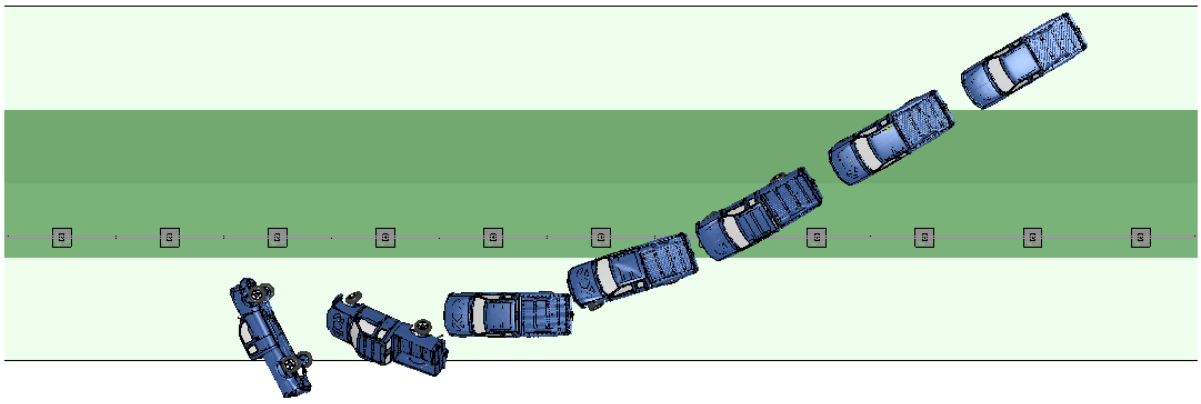

Fig. 4.172: Backside impact on CMB at 62 mph and 30°.

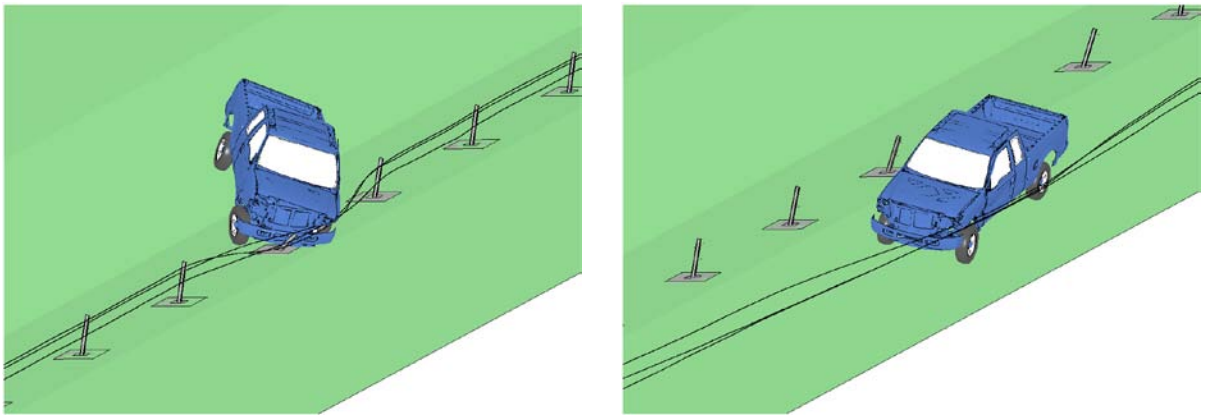

Fig. 4.173: Two instances of vehicle impacting CMB from backside at 62 mph and 30°.

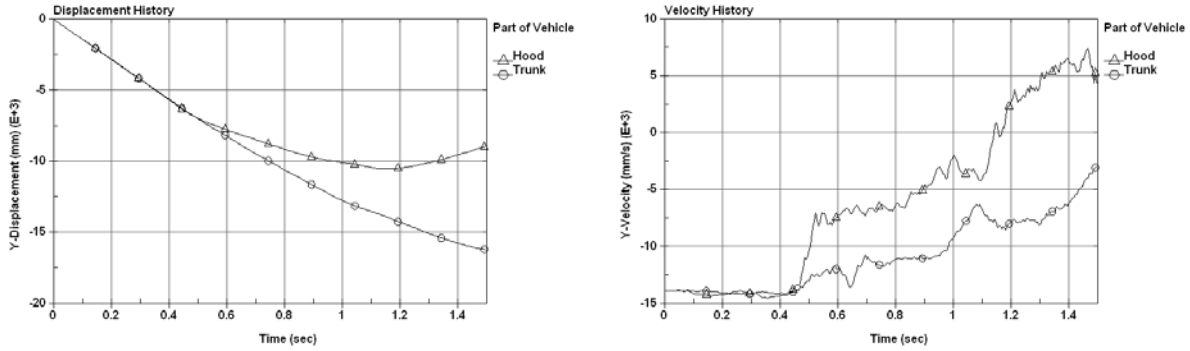


Traversal displacements Traversal velocities

Fig. 4.174: Time histories of traversal displacements and velocities of the vehicle impacting the CMB from backside at 62 mph and 30° ('trunk' means 'bed' on the truck).

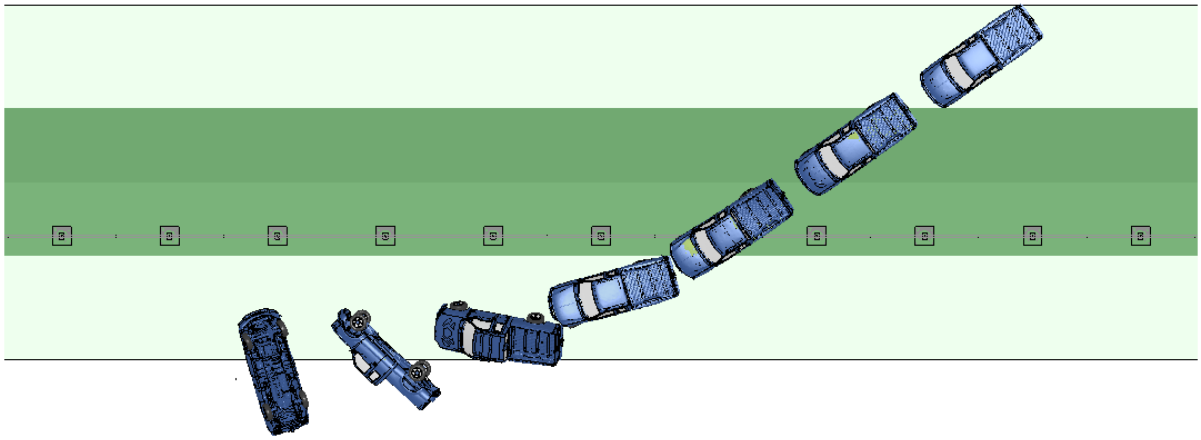

Fig. 4.175: Backside impact on CMB at 62 mph and 35°.

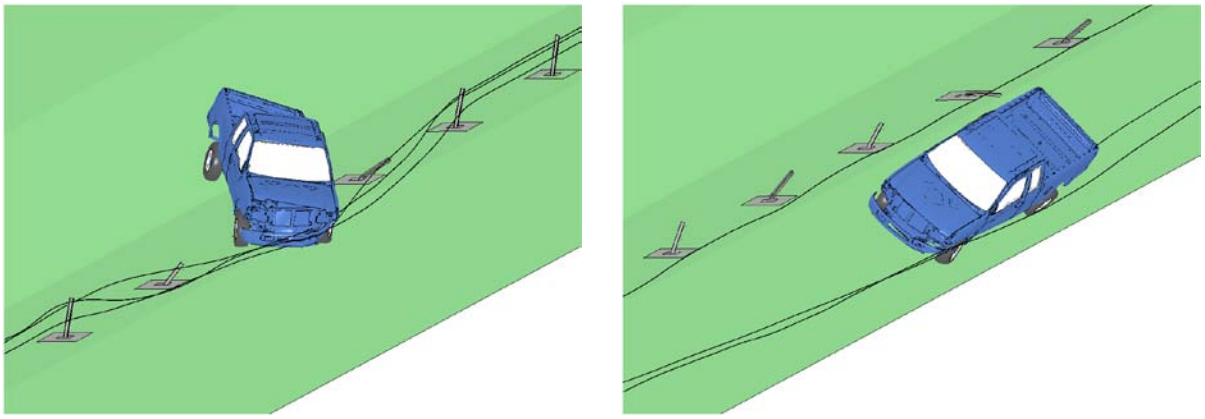

Fig. 4.176: Two instances of vehicle impacting CMB from backside at 62 mph and 35°.

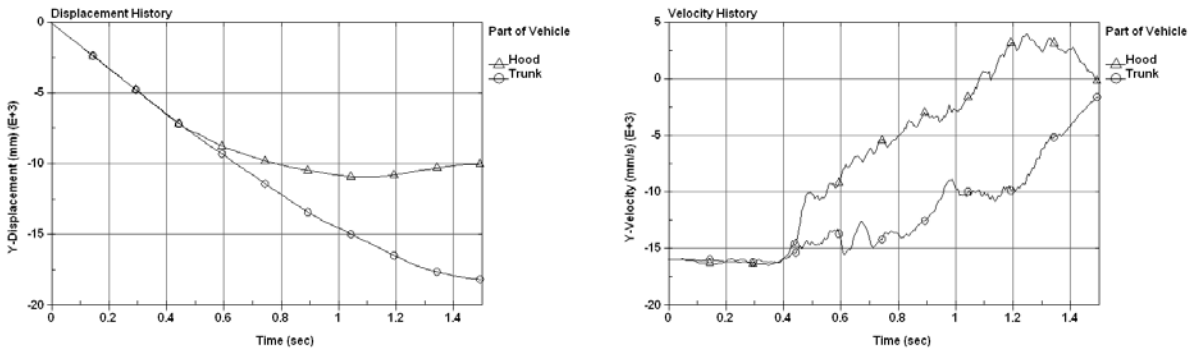


Traversal displacements Traversal velocities

Fig. 4.177: Time histories of traversal displacements and velocities of the vehicle impacting the CMB from backside at 62 mph and 35° ('trunk' means 'bed' on the truck).

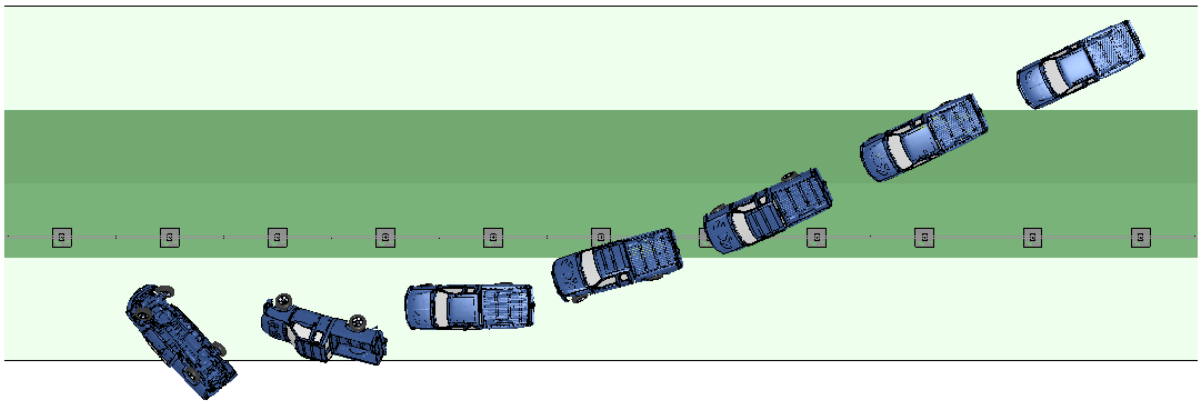

Fig. 4.178: Backside impact on CMB at 70 mph and 25°.

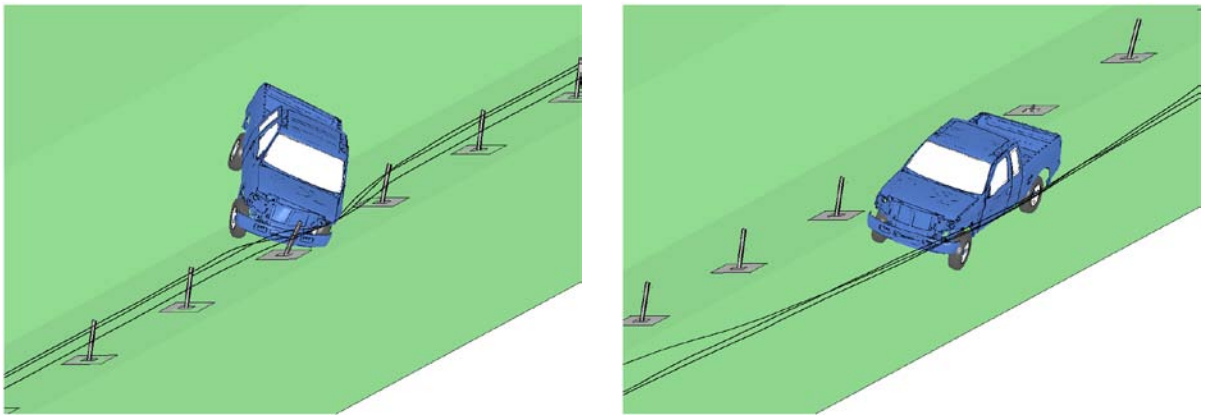

Fig. 4.179: Two instances of vehicle impacting CMB from backside at 70 mph and 25°.

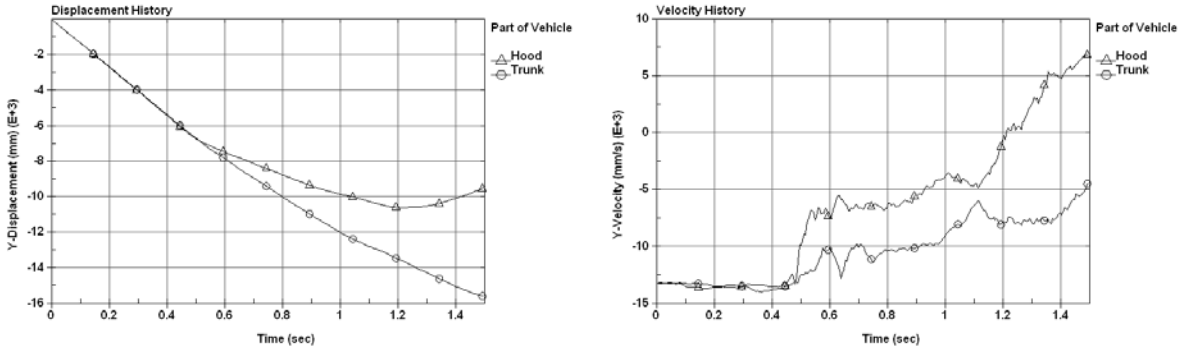


Traversal displacements Traversal velocities

Fig. 4.180: Time histories of traversal displacements and velocities of the vehicle impacting the CMB from backside at 70 mph and 25° ('trunk' means 'bed' on the truck).

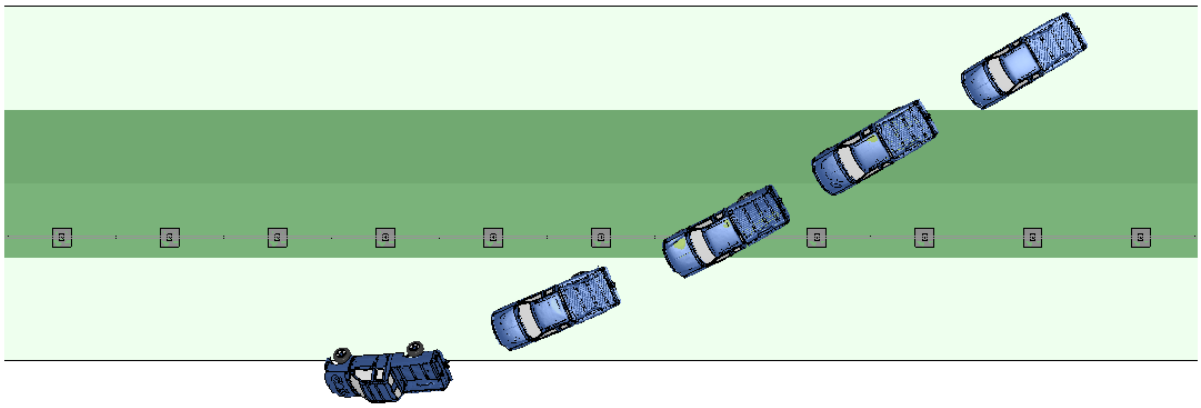

Fig. 4.181: Backside impact on CMB at 70 mph and 30°.

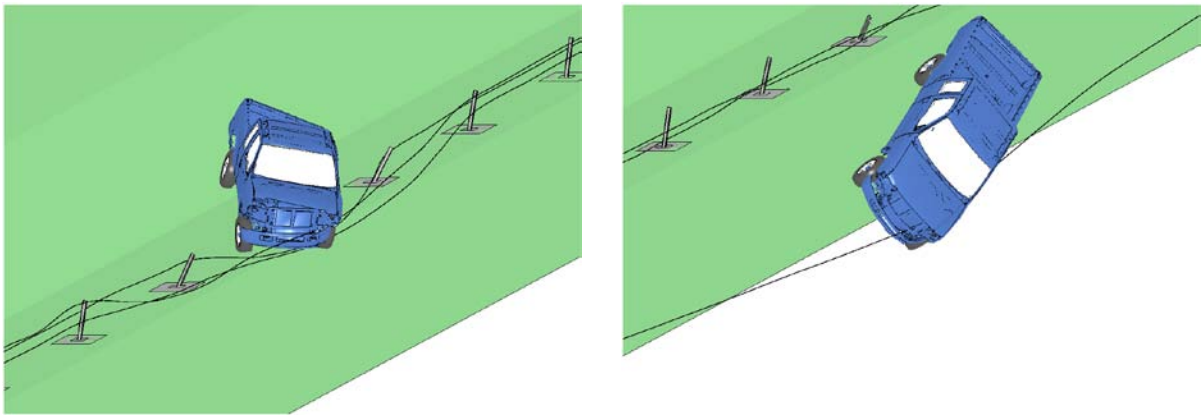

Fig. 4.182: Two instances of vehicle impacting CMB from backside at 70 mph and 30°.

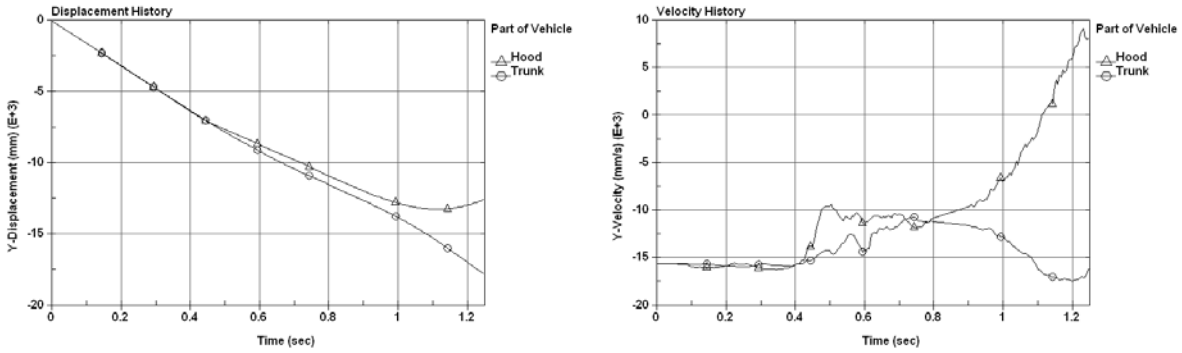


Traversal displacements Traversal velocities

Fig. 4.183: Time histories of traversal displacements and velocities of the vehicle impacting the CMB from backside at 70 mph and 30° ('trunk' means 'bed' on the truck).

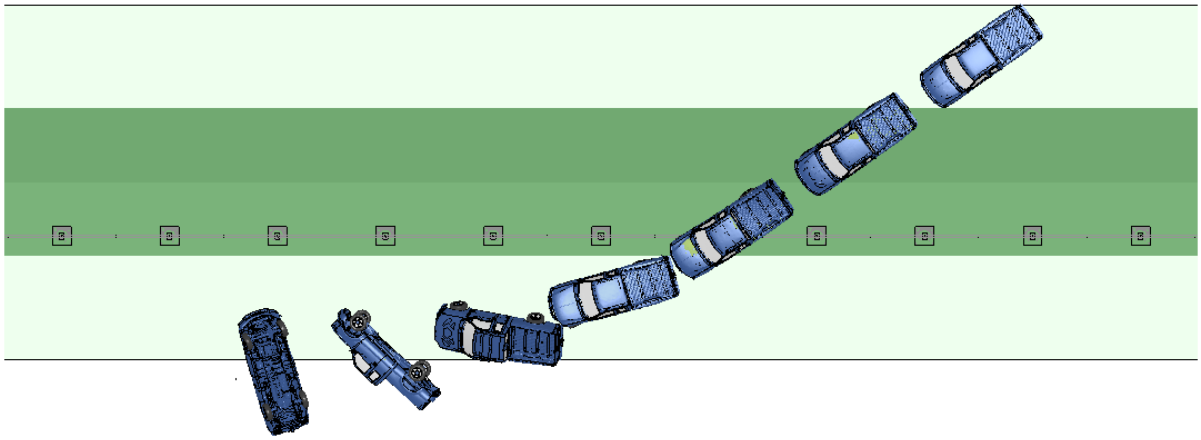

Fig. 4.184: Backside impact on CMB at 70 mph and 35°.

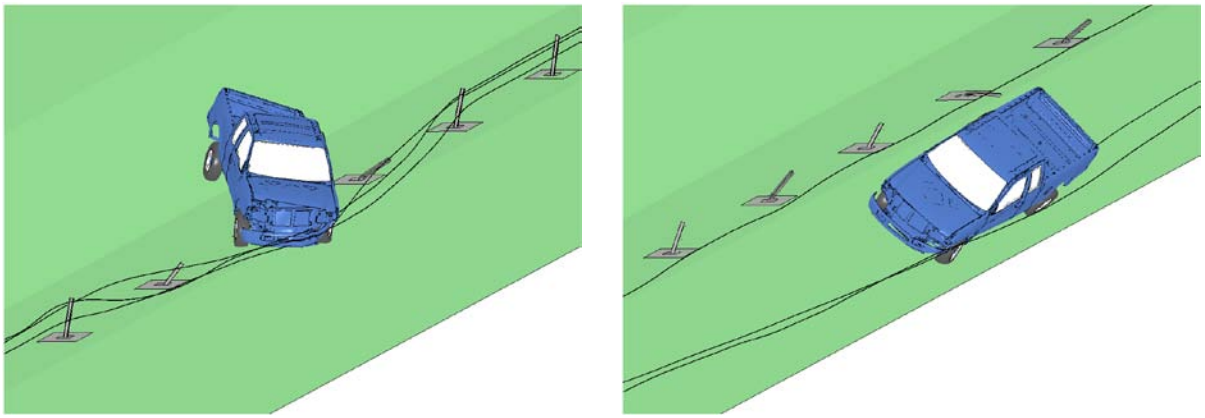

Fig. 4.185: Two instances of vehicle impacting CMB from backside at 70 mph and 35°.

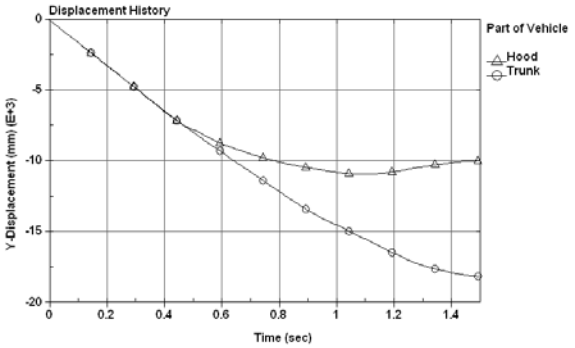


Traversal displacements

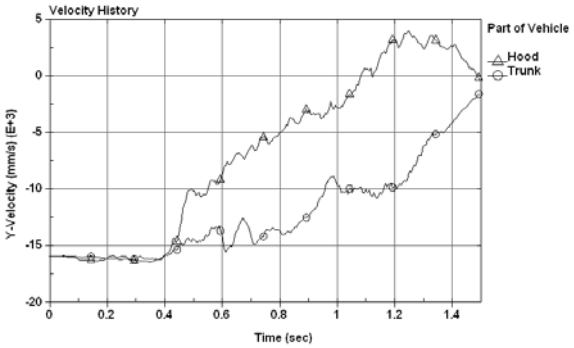


Traversal velocities

Fig. 4.186: Time histories of traversal displacements and velocities of the vehicle impacting the CMB from backside at 70 mph and 35° (‘trunk’ means ‘bed’ on the truck).

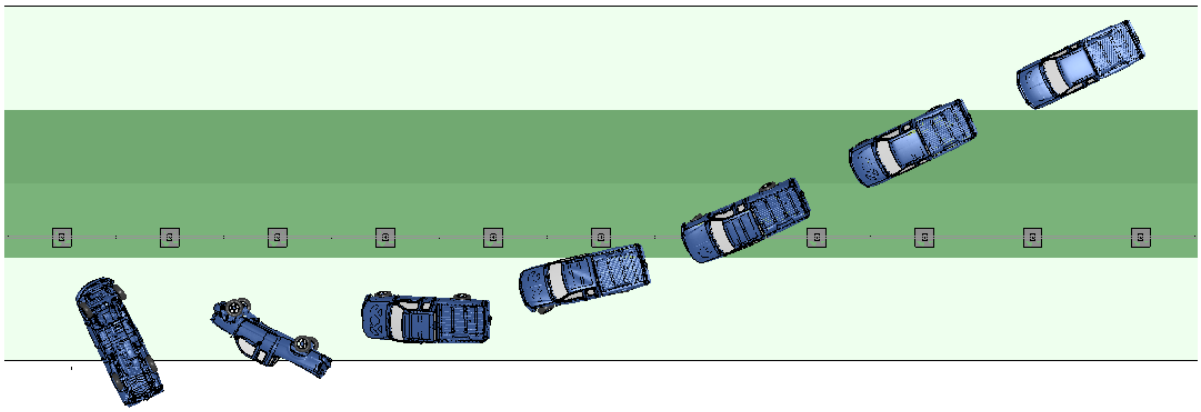

Fig. 4.187: Backside impact on CMB at 75 mph and 25°.

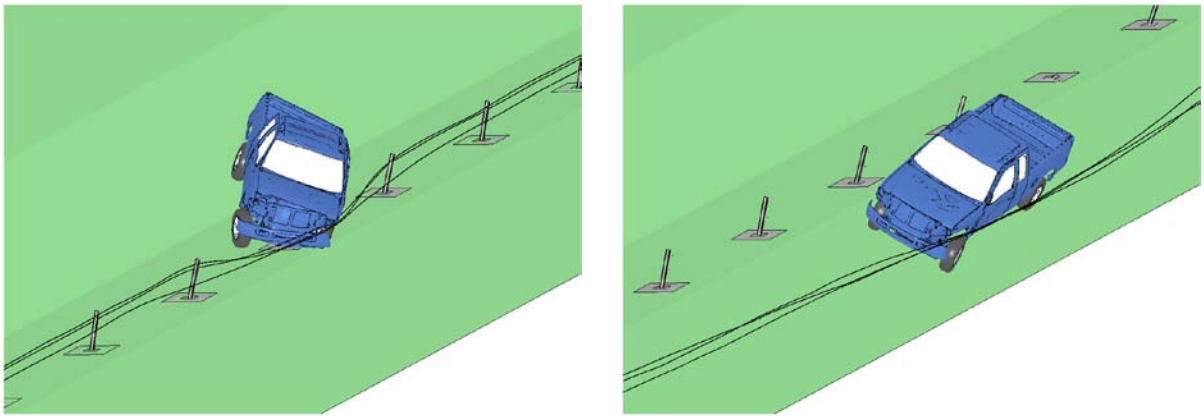

Fig. 4.188: Two instances of vehicle impacting CMB from backside at 75 mph and 25°.

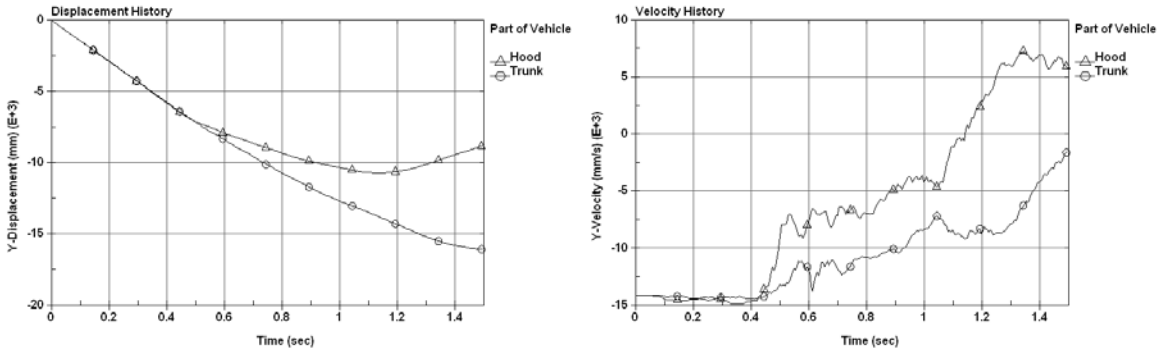


Traversal displacements Traversal velocities

Fig. 4.189: Time histories of traversal displacements and velocities of the vehicle impacting the CMB from backside at 75 mph and 25° ('trunk' means 'bed' on the truck).

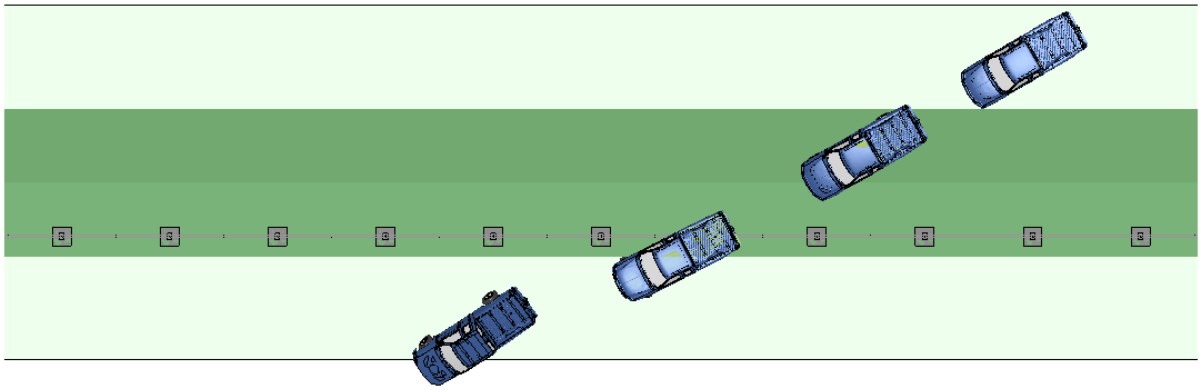

Fig. 4.190: Backside impact on CMB at 75 mph and 30°.

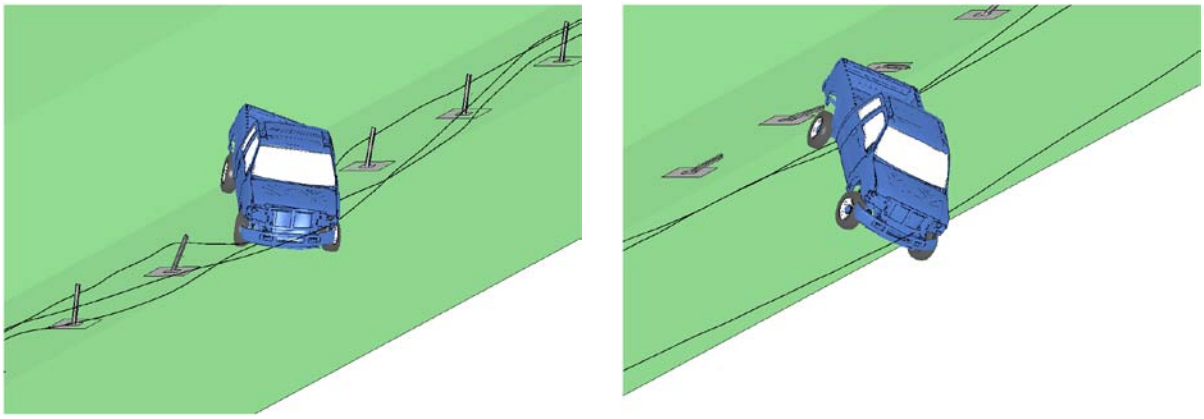

Fig. 4.191: Two instances of vehicle impacting CMB from backside at 75 mph and 30°.

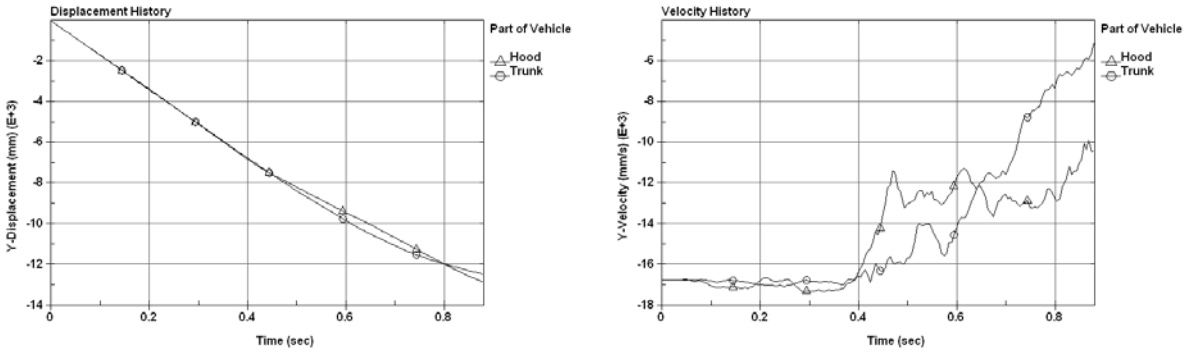


Traversal displacements Traversal velocities

Fig. 4.192: Time histories of traversal displacements and velocities of the vehicle impacting the CMB from backside at 75 mph and 30° (‘trunk’ means ‘bed’ on the truck).

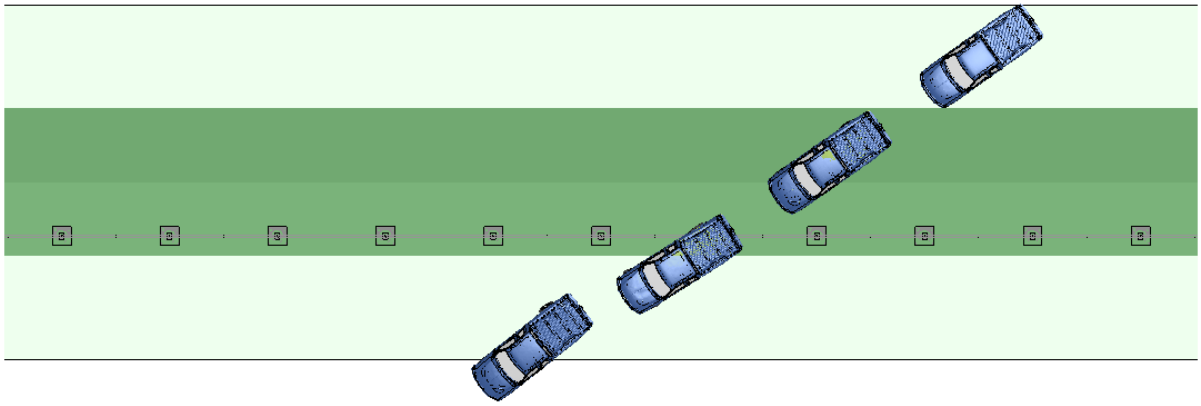

Fig. 4.193: Backside impact on CMB at 75 mph and 35°.

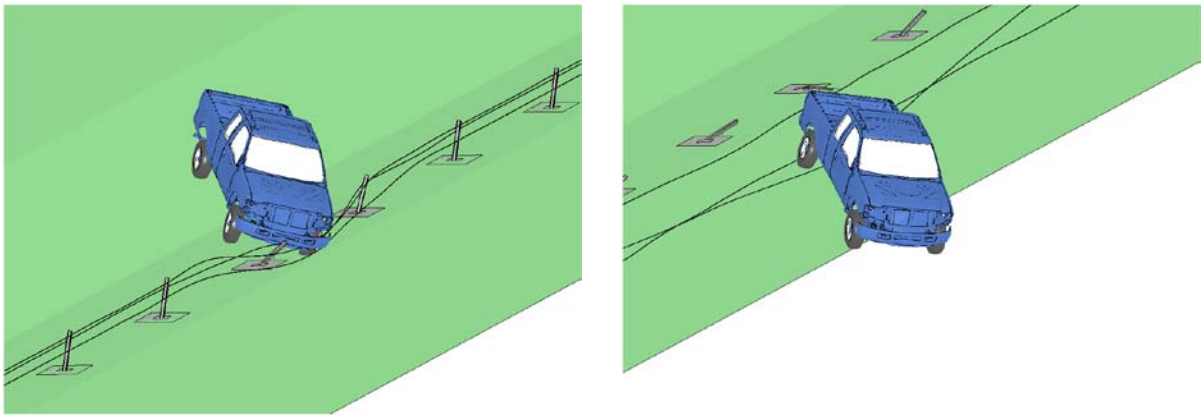

Fig. 4.194: Two instances of vehicle impacting CMB from backside at 75 mph and 35°.

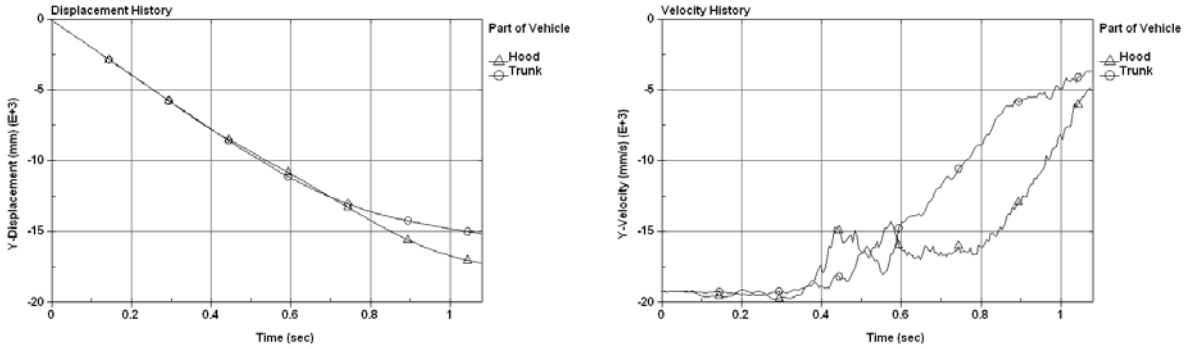


Traversal displacements Traversal velocities

Fig. 4.195: Time histories of traversal displacements and velocities of the vehicle impacting the CMB from backside at 75 mph and 35° (‘trunk’ means ‘bed’ on the truck).

# 5. Findings and Conclusions

In this project, finite element simulations were performed to study the performance of the single-face W-beam guardrail, two designs of the double-face W-beam guardrail, and the generic low-tension cable median barrier (CMB) under impacts of a 2006 Ford F250 passenger truck. The simulation results gave a significant insight into the crash mechanisms of vehicle impacts with W-beams and CMBs. Some of the major research findings are summarized as follows.

- The single-face W-beam guardrail performed effectively under the vehicle's impact at 25° and 62 mph (100 km/hr), which was the standard Test Level 3 (TL-3) impact angle and speed of the NCHRP Report 350. It should be noted that the single-face W-beam was installed on the borderline between a median slope and its adjacent shoulder, which represented a more severe test condition than the flat terrain used in all tests by NCHRP Report 350. In addition, the 2006 Ford F250 had a larger mass and size than the TL-3 vehicle, and thus increased the intensity of the crashes. Given the above mentioned reasons, the single-face W-beam guardrail can be said to outperform the TL-3 requirements. Under impacts at larger speeds and/or angles, the vehicle was found to either roll over or exhibit a strong tendency of rollover towards the median.

- The two designs of the double-face W-beam guardrail had similar performance to the single-face W-beam in a front-side impact under the standard TL-3 impact speed and angle, i.e., 62 mph (100 km/hr) and 25°. In all other front-side impacts, the double-face W-beam was found to reduce the tendency of vehicle rollovers compared to the single-face W-beam.

  For backside impacts, both designs of the double-face W-beam performed much better than in front-side impacts. The vehicle was successfully redirected and/or retained in the ditch without rollover or the tendency of rollover in all backside impacts. If the double-face W-beam guardrail were to replace the two lines of the single-face W-beam, half of the impacts on the single-face W-beam would become backside hits on the double-face W-beam, assuming the numbers of crashes on the two lines of the single-face W-beam are the same. This means that half of the vehicle rollovers would be prevented even at large impact speeds and/or angles.

- It was also observed that there was no significant difference between the two designs of the double-face W-beam under the impacts of a Ford F250; this was true for both front-side and backside impacts. The simulation results showed that the single-face W-beam was less rollover-prone on the 4:1 slope than on the 2.5:1 slope. The same is expected for the double-face W-beam but requires further investigation before a conclusion can be drawn.

- The CMB was found to be able to redirect the vehicle in all cases except for the 30° and 35° backside impacts at 75 mph (120.7 km/hr). However, vehicle rollovers also occurred in most cases. The 25° backside impact at 62 mph (100 km/hr) was the only case without vehicle rollover. Considering the fact that larger (or higher) vehicles are more likely to roll over than smaller vehicles, it is expected to see a reduced number of rollovers on a TL-3 vehicle that would also be redirected.

- It was observed from simulation results of all cases that the vehicle did not land on top of the CMB on the 4:1 slope and cause a straight-through penetration. To this end, the current placement of the CMB is effective in preventing vehicle penetrations. The rollover issues on the current placement deserve further investigation to identify a better solution for improving safety.

The simulation results suggested that the effectiveness of the W-beam and CMB could be reduced on sloped medians compared to their performance on flat terrain as in the NCHRP Report 350. A common issue on sloped medians was the increased potential of vehicle rollovers, particularly for large-size vehicles. It was observed that the tendency and/or severity of vehicle rollover increased with the increase of impact angles while keeping other conditions the same. This was shown to be true for the single-face W-beam, double-face W-beam, and CMB. Nevertheless, the performance of the barriers investigated in this project exceeded the TL-3 requirements of the NCHRP Report 350.

The simulation results of this project should be used to interpret the performance trends of W-beam guardrails and CMBs. They should not be used to draw definitive conclusions about their performance for a specific crash event, because many factors that could affect the performance were not considered in the simulations of this project. These factors included, but were not limited to, impact locations along the longitudinal axes of the barriers, soil conditions, and driver behaviors. Nevertheless, finite element analysis was demonstrated to be a useful tool in crash analysis and could be used in future investigations of other research issues.

# 6. Recommendations

The finite element simulation results of this project showed that, for the combinations of impact conditions, the double-face W-beam guardrail had similar performance to the single-face W-beam in front-side impacts, but with a reduced tendency of vehicle rollover following the impacts. Both designs of the double-face W-beam were found to successfully redirect/retain vehicles in backside impacts without rollovers. The two designs of the double-face W-beam could be used to replace the two lines of the single-face W-beam without performance degradation. Based on the observation that W-beams placed on the 4:1 slope reduced the tendency of vehicle rollovers than on the 2.5:1 slope, it is recommended to place the double-face W-beam on the 4:1 slope after validation.

The simulation results showed that the vehicle would not land on top of the CMB in backside impacts even though it entered the ditch from the shoulder of the high-side slope. Given the high potential of vehicle rollovers on the CMB, it is recommended that further research be conducted on the placement of CMBs on medians with large slopes (e.g., 4:1 and 2.5:1).

# 7. Implementation and Technology Transfer Plan

In this project, two designs of the double-face W-beam guardrail were evaluated and compared to the single-face W-beam. All simulation results will be submitted to NCDOT for consideration in future installation or retrofitting the current single-face W-beam guardrails when allowed by site conditions and deemed necessary by NCDOT officials. The results and analysis of the CMB performance on a 4:1 slope will also be submitted to NCDOT for consideration of further improvement.

The research results of this project will be distributed to the public through this report, which will be made available by NCDOT. The research finding will also be circulated to and shared with state and local agencies through the NCDOT Guardrail Committee, Traffic Engineering Roundtables, Operations meetings, and possible Webinars.

The modeling and simulation work along with research findings will be presented at national and international conferences such as the Transportation Research Board Annual Meetings, the U.S. National Congress on Computational Mechanics, and the World Congress on Computational Mechanics. The results of this research will also be submitted for publication in technical journals such as the Transportation Research Records and Finite Elements in Analysis and Design.

# References


1. AASHTO (2006). *Roadside Design Guide*, 3rd edition, American Association of State Highway and Transportation Officials, Washington, D.C.
2. Alberson, D. C., Bligh, R. P., Buth, C. E., and Bullard, D. L., Jr. (2003). "Cable and wire rope barrier design considerations: review." *Transportation Research Record*, 1851, 95-104.
3. Alberson, D. C., Sheikh, N. M., and Chatham, L. S. (2007). "Guidelines for the Selection of Cable Barrier Systems." *NCHRP 20-7 (210) Final Report*, Transportation Research Board, National Research Council, Washington, D.C.
4. Albin, R. B., Bullard, D. L., and Menges, W. L. (2001). "Washington State cable median barrier." *Transportation Research Record*, 1743, 71-79.
5. Atahan, A. O. (2002). "Finite Element Simulation of a Strong-Post W-Beam Guardrail System." *Simulation*, 78(10), 587-599.
6. Atahan, A. O. (2003). "Impact behaviour of G2 steel weak-post W-beam guardrail on nonlevel terrain." *International Journal of Heavy Vehicle Systems*, 10(3), 209-223.
7. Atahan, A. O. (2007). "Crashworthiness analysis of a bridge rail-to-guardrail transition." *Accident Analysis and Prevention*, in press.
8. Atahan, A. O., and Cansiz, O. F. (2005). "Crashworthiness analysis of a bridge rail-to-guardrail transition." *Finite Elements in Analysis and Design*, 41, 371-396.
9. Bligh, R. P., Abu-Odeh, A. Y., Hamilton, M. E., and Seckinger, N. R. (2004). "Evaluation of Roadside Safety Devices using Finite Element Analysis." *Report 0-1816-1*, Texas Transportation Institute, College Station, TX.
10. Bligh, R. P., and Mak, K. K. (1999). "Crashworthiness of roadside features across vehicle platforms." *Transportation Research Record*, 1690, 68-77.
11. Bligh, R., Miaou, S.-P., Lord, D., and Cooner, S. (2006). "Median Barrier Guidelines for Texas." *Report 0-4254-1*, Texas Transportation Institute, College Station, TX.
12. BMI-SG. (2004). "Improved Guidelines for Median Safety." *NCHRP 17-14(2) Draft Report of Analysis Findings*, Transportation Research Board, National Research Council, Vienne, VA.
13. Bullard, D. L., and Menges, W. L. (1996). "Crash Testing and Evaluation of the WSDOT Three Strand Cable Rail System." Texas Transportation Institute, College Station, TX.
14. Bullard, D. L., and Menges, W. L. (2000). "NCHRP Report 350 Test 3-11 of the Washington Three-strand Cable Barrier with New York Cable Terminal." Texas Transportation Institute, College Station, TX.
15. Donnell, E. T., Harwood, D. W., Bauer, K. M., Mason, J. M., and Pietrucha, M. T. (2002). "Cross-median collisions on Pennsylvania interstates and expressways." *Transportation Research Record*, 1784, 91-99.
16. ESI (2003). *PAM-CRASH Solver Reference Manual, v2003.1*, ESI Group.
17. Gabler, H. C., Gabauer, D. J., and Bowen, D. (2005). "Evaluation of Cross Median Crashes." *Final Report FHWA-NJ-2005-004*, Rowan University, Glassboro, NJ.
18. Hiser, N. R., and Reid, J. D. (2005). "Modeling slip base mechanisms." *International Journal of Crashworthiness*, 10(5), 463-472.
19. Hiss, J. G. F., Jr., and Bryden, J. E. (1992). "Traffic Barrier Performance." *Report 155*, New York State Department of Transportation, Albany, NY.

20. Hunter, W. W., Stewart, J. R., Eccles, K. A., Huang, H. F., Council, F. M., and Harkey, D. L. (2001). "Three-strand cable median barrier in North Carolina: in-service evaluation." *Transportation Research Record*, 1743, 97-103.

21. Kan, C.-D., Marzougui, D., Bahouth, G. T., and Bedewi, N. E. (2001). "Crashworthiness evaluation using integrated vehicle and occupant finite element models." *International Journal of Crashworthiness*, 6, 387-398.

22. Lewis, B. A. (2004). "Manual for LS-DYNA Soil Material Model 147." *FHWA-HRT-04-095*, U.S. Department of Transportation, Federal Highway Administration, McLean, VA.

23. LSTC (2007). *LS-DYNA Keyword User's Manual, version 971*, Livermore Software Technology Corporation (LSTC), Livermore, CA.

24. Lynch, J. M., Crowe, N. C., and Rosendahl, J. F. (1993). "Interstate across median accident study: a comprehensive study of traffic accidents involving errant vehicles which cross the median divider strips on North Carolina interstate highways." In: 1993 AASHTO Annual Meeting Proceedings, Publisher American Association of State Highway and Transportation Officials, 125-133.

25. MacDonald, D. B., and Batiste, J. R. (2007). "Cable Median Barrier - Reassessment and Recommendations." *WSDOT Report*, Washington State Department of Transportation, Olympia, WA.

26. Mackerle, J. (2003). "Finite element crash simulations and impact-induced injuries: an addendum. a bibliography (1998–2002)." *The Shock and Vibration Digest*, 35(4), 273-280.

27. Marzougui, D., Bahouth, G., Eskandarian, A., Meczkowski, L., and Taylor, H. (2000). "Evaluation of portable concrete barriers using finite element simulation." *Transportation Research Record*, 1720, 1-6.

28. Marzougui, D., Mohan, P., Kan, C.-D., and Opiela, K. S. (2007a). "Performance evaluation of low-tension three-strand cable median barriers." *Transportation Research Record*, to be published.

29. Marzougui, D., Mohan, P., Kan, C.-D., and Opiela, K. S. (2007b). "Evaluation of rail height effects on the safety performance of W-beam barriers." *2007 TRB Annual Meeting*, Washington, D.C.

30. Marzougui, D., Zink, M., Zaouk, A. K., Kan, C.-D., and Bedewi, N. E. (2004). "Development and validation of a vehicle suspension finite element model for use in crash simulations." *International Journal of Crashworthiness*, 9(6), 565-576.

31. MASH (2009). *Manual for Assessing Safety Hardware*, 1st ed., American Association of State and Highway Transportation Officials, Washington, D.C.

32. Miaou, S.-P., Bligh, R. P., and Lord, D. (2005). "Developing guidelines for median barrier installation: benefit-cost analysis with Texas data " *Transportation Research Record*, 1904, 3-19.

33. Mohan, P., Marzougui, D., and Kan, C.-D. (2007). "Validation of a single unit truck model for roadside hardware impact." *International Journal of Vehicle Systems Modelling and Testing*, 2(1), 1-15.

34. Mohan, P., Marzougui, D., Meczkowski, L., and Bedewi, N. (2005). "Finite element modeling and validation of a 3-strand cable guardrail system." *International Journal of Crashworthiness*, 10, 267-273.

35. Murphy, B. (2006). "Cable Median Barrier/Rumble Strips in North Carolina." In: 57th Annual Traffic and Safety Conference, Missouri Department of Transportation, Columbia, MO.

36. Murray, Y. D. (2007). "Users Manual for LS-DYNA Concrete Material Model 159." *FHWA-HRT-05-062*, U.S. Department of Transportation, Federal Highway Administration, McLean, VA.

37. Murray, Y. D., Reid, J. D., Faller, R. K., Bielenberg, B. W., and Paulsen, T. J. (2005). "Evaluation of LS-DYNA Wood Material Model 143." *FHWA-HRT-04-096*, U.S. Department of Transportation, Federal Highway Administration, McLean, VA.

38. NCAC (web1). "NCAC Finite Element Models." <*http://www.ncac.gwu.edu/vml/models.html*>.

39. NCAC. (web2). "NCAC Publications." <*http://www.ncac.gwu.edu/filmlibrary/publications.html*>.

40. NCDOT (2002). *Roadway design manual*, North Carolina Department of Transportation, Raleigh, NC.

41. NCDOT (2005). “Median Barriers in North Carolina – Long Term Evaluation,” *NCDOT Safety Evaluation Group*, Traffic Safety Systems Management Section, AASHTO TIG Initiative for “Cable Median Barrier” (TIG-CMB), Raleigh, NC.

42. NCDOT (2006). *Roadway Standard Drawings*, North Carolina Department of Transportation, Raleigh, NC.

43. NCHRP (ongoing). “*Project 22-21: Median Cross-Section Design for Rural Divided Highways,”* Project Page: http://www4.trb.org/trb/crp.nsf/All+Projects/NCHRP+22-21.

44. NCHRP (pending). “*Project 22-22: Placement of Traffic Barriers on Roadside and Median Slopes,”* Project Page: http://www4.trb.org/trb/crp.nsf/All+Projects/NCHRP+22-22.

45. Orengo, F., Ray, M. H., and Plaxico, C. A. (2003). “Modeling tire blow-out in roadside hardware simulations using LS-DYNA.” In: *2003 ASME International Mechanical Engineering Congress & Exposition*, Washington, D.C., IMECE2003-55057.

46. Patzner, G. S., PLAXICO, C. A., and RAY, M. H. (1999). “Effects of post and soil strength on performance of modified eccentric loader breakaway cable terminal.” *Transportation Research Record*, 1690, 78-83.

47. Plaxico, C. A., Hackett, R. M., and Uddin, W. (1997). “Simulation of a vehicle impacting a modified thrie-beam guardrail.” *Transportation Research Record*, 1599, 1-10.

48. Plaxico, C. A., Mozzarelli, F., and Ray, M. H. (2003). “Tests and simulation of a w-beam rail-to-post connection.” *International Journal of Crashworthiness*, 8(6), 543-551.

49. Plaxico, C. A., Patzner, G. S., and Ray, M. H. (1998). “Finite element modeling of guardrail timber posts and the post-soil interaction.” *Transportation Research Record*, 1647, 139-146.

50. Plaxico, C. A., Ray, M. H., and Hiranmayee, K. (2000). “Impact Performance of the G4(1W) and G4(2W) guardrail systems: comparison under NCHRP Report 350 Test 3-11 conditions.” *Transportation Research Record*, 1720, 7-18.

51. Ray, M. H. (1996a). “Repeatability of full-scale crash tests and criteria for validating simulation results.” *Transportation Research Record*, 1528, 155-160.

52. Ray, M. H. (1996b). “Use of finite element analysis in roadside hardware design.” *Transportation Research Circular*, 453, 61-71.

53. Ray, M. H., and McGinnis, R. G. (1997). “NCHRP Synthesis of Highway Practice 244: Guardrail and Median Barrier Crashworthiness.” Transportation Research Board, National Research Council, Washington, D.C.

54. Ray, M. H., and Patzner, G. S. (1997). “Finite element model of modified eccentric loader terminal (MELT).” *Transportation Research Record*, 1599, 11-21.

55. Ray, M. H., and Weir, J. A. (2001). “Unreported collisions with post-and-beam guardrails in Connecticut, Iowa, and North Carolina.” *Transportation Research Record*, 1743, 111-119.

56. Ray, M. H., Oldani, E., and Plaxico, C. A. (2004). “Design and analysis of an aluminum F-shape bridge railing.” *International Journal of Crashworthiness*, 9(4), 349-363.

57. Ray, M. H., Weir, J., and Hopp, J. (2003). “In-Service Performance of Traffic Barriers.” *NCHRP Report 490*, Transportation Research Board, National Research Council, Washington, D.C.

58. Reid, J. D. (1996). “Towards the understanding of material property influence on automotive crash structures.” *Thin-Walled Structures*, 24, 285-313.

59. Reid, J. D. (1998). “Admissible modeling errors or modeling simplifications?” *Finite Elements in Analysis and Design*, 29, 49-63.

60. Reid, J. D. (2004). “LS-DYNA simulation influence on roadside hardware.” *Transportation Research Record*, 1890, 34-41.

61. Reid, J. D., and Bielenberg, B. W. (1999). “Using LS-DYNA simulation to solve a design problem: bullnose guardrail example “ *Transportation Research Record*, 1690, 95-102.

62. Reid, J. D., and Coon, B. A. (2002). “Finite element modeling of cable hook bolts.” In: *7th International LS-DYNA User Conference*, Dearborn, MI.

63. Reid, J. D., and Hiser, N. R. (2004). “Friction modelling between solid elements.” *International Journal of Crashworthiness*, 9(1), 65-72.

64. Reid, J. D., and Hiser, N. R. (2005). “Detailed modeling of bolted joints with slippage.” *Finite Elements in Analysis and Design*, 41, 547-562.

65. Reid, J. D., and Marzougui, D. (2002). “Improved truck model for roadside safety simulations: Part I - structural modeling.” *Transportation Research Record*, 1797, 53-62.

66. Reid, J. D., Coon, B. A., Lewis, B. A., Sutherland, S. H., and Murray, Y. D. (2004). “Evaluation of LS-DYNA Soil Material Model 147.” *FHWA-HRT-04-094*, U.S. Department of Transportation, Federal Highway Administration, McLean, VA.

67. Reid, J. D., Kuipers, B. D., Sicking, D. L., and Faller, R. K. (2009). “Impact performance of W-beam guardrail installed at various flare rates.” *International Journal of Impact Engineering*, 36, 476-485.

68. Ross Jr, H. E., and Sicking, D. L. (1984). “Guidelines for placement of longitudinal barriers on slopes.” *Transportation Research Record*, 970, 3-9.

69. Ross, H. E., Jr., Sicking, D. L., Zimmer, R. A., and Michie, J. D. (1993). “Recommended Procedures for the Safety Performance Evaluation of Highway Features.” *NCHRP Report 350*, Transportation Research Board, National Research Council, Washington, D.C.

70. Sposito, B., and Johnston, S. (1999). “Three-cable Median barrier.” *Final Report OR-RD-99-03*, Oregon Department of Transportation, Salem, OR.

71. Stasburg, G., and Crawley, L. C. (2005). “Keeping Traffic on the Right Side of the Road.” In: *Public Road*.

72. Tiso, P., Plaxico, C., and Ray, M. (2002). “Improved truck model for roadside safety simulations: Part II - suspension modeling.” *Transportation Research Record*, 1797, 63-71.

73. Troy, S. A. (2007). “Median Barriers in North Carolina.” In: *TRB-AFB20 Committee Summer Meeting*, Rapid City, SD.

74. Whitworth, H. A., Bendidi, R., Marzougui, D., and Reiss, R. (2004). “Finite element modeling of the crash performance of roadside barriers.” *International Journal of Crashworthiness*, 9(1), 35-43.

75. WSDOT. (2006). “I-5 Marysville Cable Median Barrier.” *WSDOT Report*, Washington State Department of Transportation, Olympia, WA.

76. Zaouk, A. K., Bedewi, N. E., Kan, C.-D., and Marzouigui, D. (1997). “Development and Evaluation of a C-1500 Pickup Truck Model for Roadside Hardware Impact Simulation.” *FHWA-RD-96-212*, Federal Highway Administration, Washington, D.C.

77. Zaouk, A. K., Marzougui, D., and Bedewi, N. E. (2000a). “Development of a detailed vehicle finite element model, Part I: methodology.” *International Journal of Crashworthiness*, 5(1), 25-36.

78. Zaouk, A. K., Marzougui, D., and Kan, C.-D. (2000b). “Development of a detailed vehicle finite element model, Part II: material characterization and component testing.” *International Journal of Crashworthiness*, 5(1), 37-50.

79. Zweden, J. V., and Bryden, J. E. (1977). “In-service Performance of Highway Barriers.” *Report NYSDOT-ERD-77-RR51*, New York State Department of Transportation, Albany, NY.